Chapter III

Result and Discussion

3.1 Purities of the dyes

Purities of Azorubine, Sunset Yellow FCF, Orange G, Orange RN, Tartrazine and Green S were examined by paper chromatographic technique, ultraviolet-visible and infrared spectrophotometric techniques before they were used for the study of complex formations with metal ions.

3.1.1 Paper chromatography

Three solvent systems were used for testing purities of the dyes. There are system I, the mixture of 1-butanol, water and acetic acid in the ratio of 20:12:5, respectively; system II, the mixture of water and ammonia solution (specific gravity 0.91) in the ratio of 99:1, respectively; and system III is the solution of 2.5% NaCl aqueous solution. The paper chromatogram of each dye in every solvent system studied showed a well defined spot except Orange RN whose chromatogram illustrated two spots (see Figures 3A-3C). The Rf value of each dye in every solvent system was determined and compared to its literature one. The values were listed in Table 1. Some experimental Rf values are slightly different from the literature values (31, 32) owing to the difference in experimental conditions, such as the water content in the paper used, the concentration of the dye solution, the temperature and the vapor pressure of the solvent in chromatographic chamber.

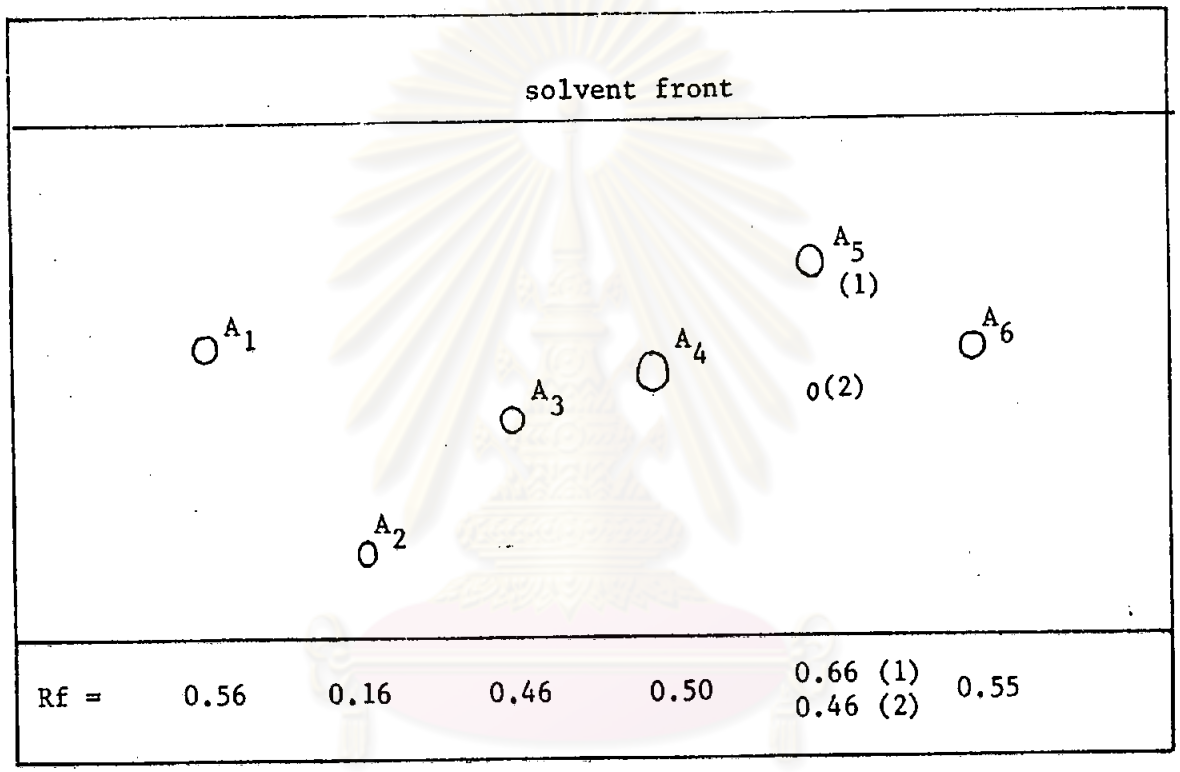

Figure 3A Paper chromatogram of the following dyes by the solvent system I, A_1) Azorubine, A_2) Tartrazine, A_3) Sunset Yellow FCF, A_4) Orange G, A_5) Orange RN, A_6) Green S

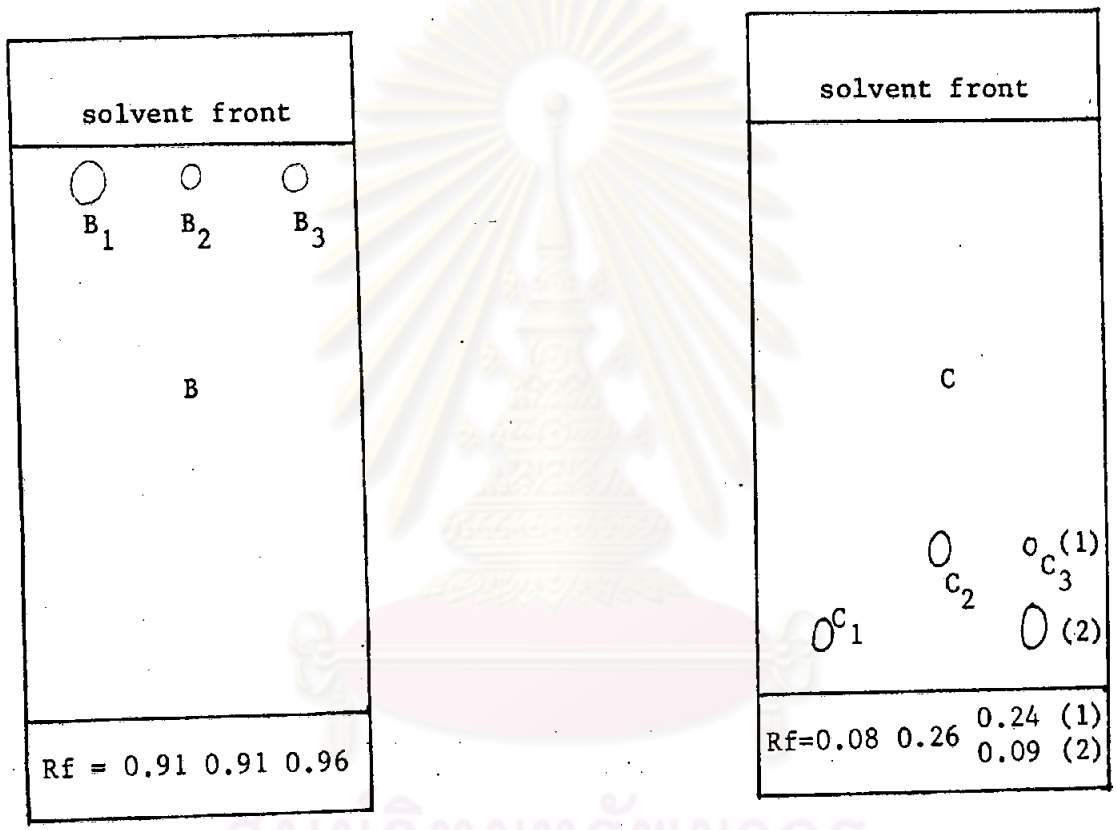

Figure 3B and 3C Paper chromatograms of the following dyes by the solvent system II (B) and the solvent system III (C)

B_1) Orange G
B_2) Tartrazine
B_3) Green S

C_1) Azorubine
C_2) Sunset Yellow FCF
C_3) Orange RN

Table 1 Rf values of Azorubine, Sunset Yellow FCF, Orange G, Orange RN, Tartrazine and Green S by the solvent systems I, II and III

Dye	solvent system I		solvent system II		solvent system III	
	Rf	Rf[31]	Rf	Rf[32]	Rf	Rf[32]
Azorubine	0.56	0.56			0.08	0.08
Sunset Yellow FCF	0.46	0.45			0.26	0.29
Orange G	0.50	0.52	0.91	0.91		
Orange RN	0.66, 0.46	0.68			0.09, 0.24	0.08
Tartrazine	0.16	0.18	0.91	0.91		
Green S	0.55	0.57	0.94	0.96		

3.1.2 Spectrophotometric techniques

3.1.2.1 The ultraviolet-visible spectra of Azorubine, Sunset Yellow FCF, Orange G, Orange RN, Tartrazine and Green S in 0.1 N HCl, and 0.1 N NaOH were performed and compared to the ones obtained from the literature (33) as shown in Figure 4A-4F. The spectrum of each dye indicated an insignificant difference from the literature one. The wavelength at the maximum absorption of the dyes (λmax) in acidic and alkali solution were measured (see Table 2).

3.1.2.2 IR spectra

The IR spectra of Azorubine, Sunset Yellow FCF, Tartrazine, Green S in solid KBr pellets and Orange G, Orange RN in nujol mull were shown in Figures 5A-5F. The spectra of Tartrazine and Orange G indicated insignificant differences from the literature ones (34, 35). No IR spectra of Azorubine, Sunset Yellow FCF, and Green S were reported in the literature. The spectrum of Tartrazine showed the phenolic OH (3450 cm^{-1}), -N=N- (1640 cm^{-1}), aromatic (1390 cm^{-1} and 1490 cm^{-1}-skeleton carbon stretching, and 700-780 cm^{-1}-aromatic out of plane bending) and ionic sulfonate (1190 cm^{-1} and 1040 cm^{-1}) characters (see Figure 5E). The spectrum of Orange G showed the azo -N=N- (1622 cm^{-1}), phenolic OH (3400 cm^{-1}), aromatic (1460 cm^{-1}, 1540 cm^{-1}-skeleton carbon stretching, and 700-800-aromatic out of plane bending) and ionic sulfonate (1200 cm^{-1} and 1040 cm^{-1}) characters (see Figure 5C). The spectrum of Azorubine showed the azo -N=N- (1610 cm^{-1}), phenolic OH (3450 cm^{-1}), aromatic (1480 cm^{-1} and 1510 cm^{-1}-skeleton carbon stretching, and 760 cm^{-1}-aromatic out of plane bending) and ionic sulfonate (1190 cm^{-1} and 1050 cm^{-1}) characters (see

Figure 5A). The spectrum of Sunset Yellow FCF showed the azo -N=N- (1622 cm^{-1}), phenolic OH (3450 cm^{-1}), aromatic (1510 cm^{-1} and 1558 cm^{-1}-skeleton carbon stretching, and 700-800 cm^{-1}-aromatic out of plane bending) and ionic sulfonate (1190 cm^{-1} and 1040 cm^{-1}) characters (see Figure 5B). The spectrum of Green S showed the >C=N (1620 cm^{-1}), phenolic OH (3450 cm^{-1}), aromatic (1370 cm^{-1}-skeleton carbon stretching, and 700-800 cm^{-1}-aromatic out of plane bending) and ionic sulfonate (1170 cm^{-1} and 1040 cm^{-1}) characters (see Figure 5F). The spectrum of Orange RN showed the difference from the literature (36) in the range of 1100-1300 cm^{-1} (see Figure 5D).

The evidences from paper chromatographic behavior as well as the absorption spectrophotometric characteristics of the certified grade dyes indicated that the purities of Azorubine, Sunset Yellow FCF, Orange G, Tartrazine and Green S are high enough for use in the study of complex formations with metal ions except Orange RN. Although the ultraviolet-visible spectrum of the certified grade Orange RN indicated an insignificant difference from the literature (see Figure 4D), the two spots in paper chromatogram of Orange RN showed that it was contaminated and the IR spectrum indicated the difference from the literature (see Figure 5D). Thus, the certified grade Orange RN had to be purified before use in the complex formation study and the column chromatographic technique was selected for this separation.

3.2 Separation of Orange RN

3.2.1 Thin layer chromatography

Thin layer chromatographic technique was used for determining the suitable eluent to purify Orange RN by column chromato-

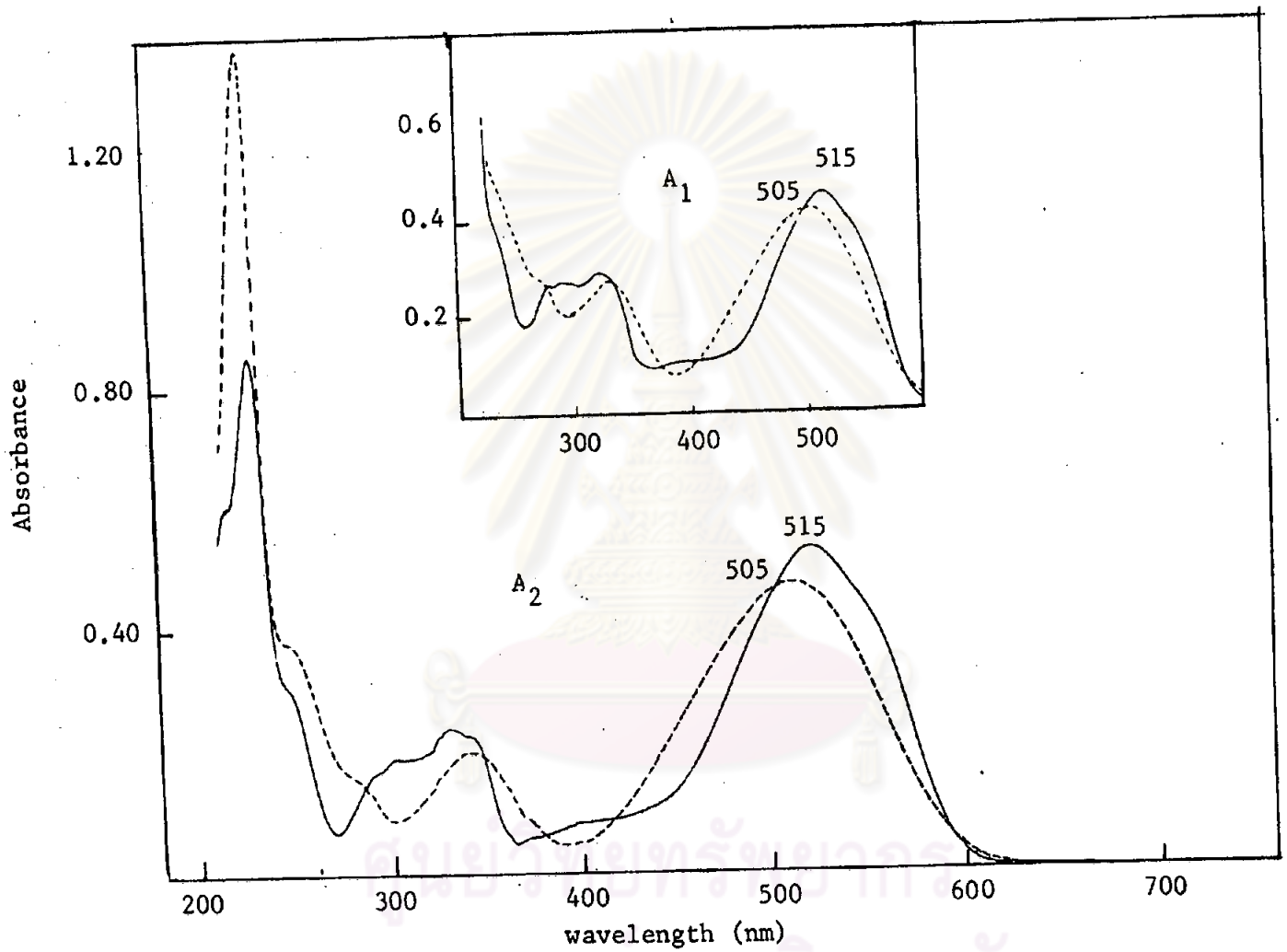

Figure 4A Comparison of UV-visible spectra of Azorubine, —— in 0.1 M HCl and --- in 0.1 M NaOH

A_1) literature (33), A_2) experiment

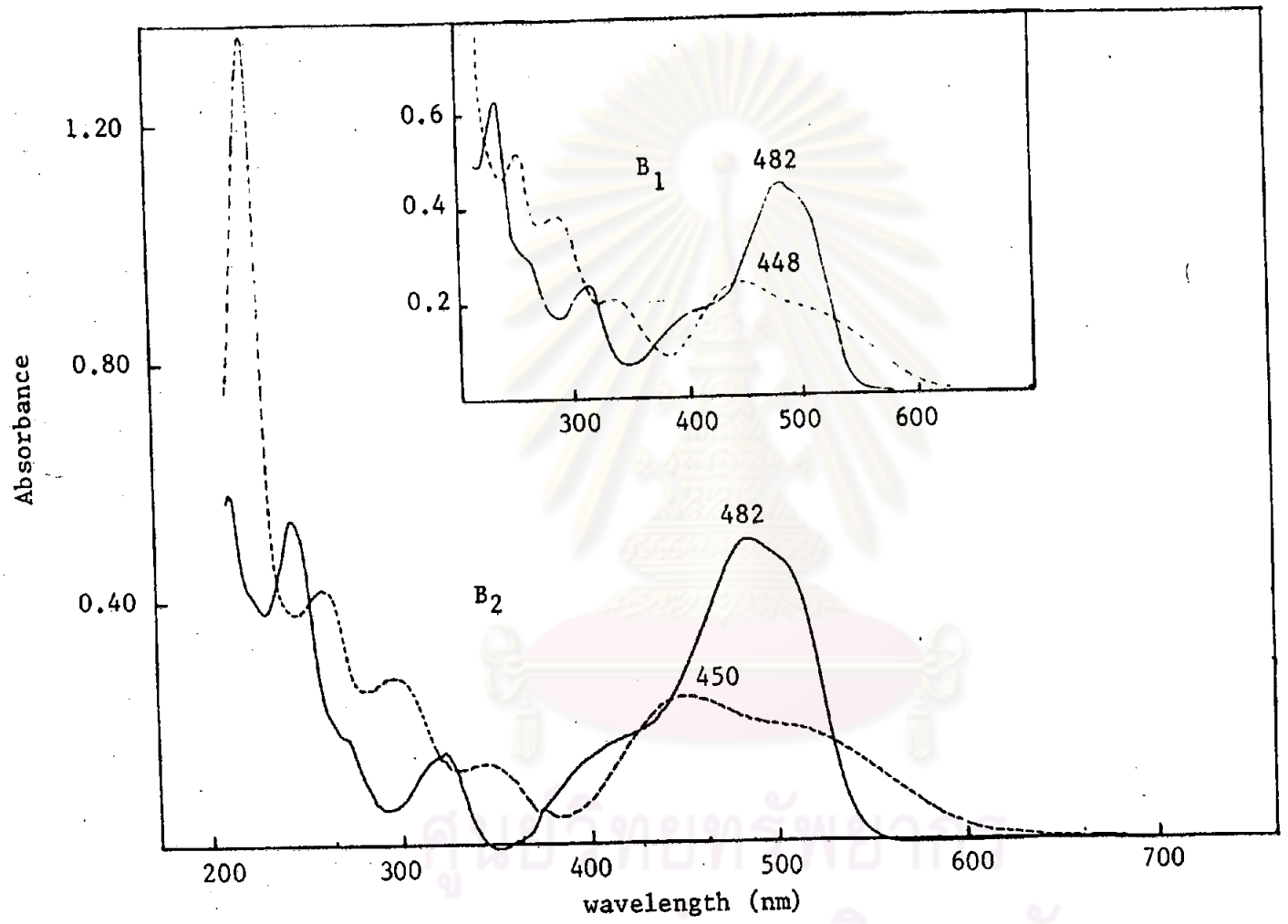

Figure 4B Comparison of UV-visible spectra of Sunset Yellow FCF, —— in 0.1 M HCl and --- in 0.1 M NaOH B_1) literature (33) and B_2) experiment

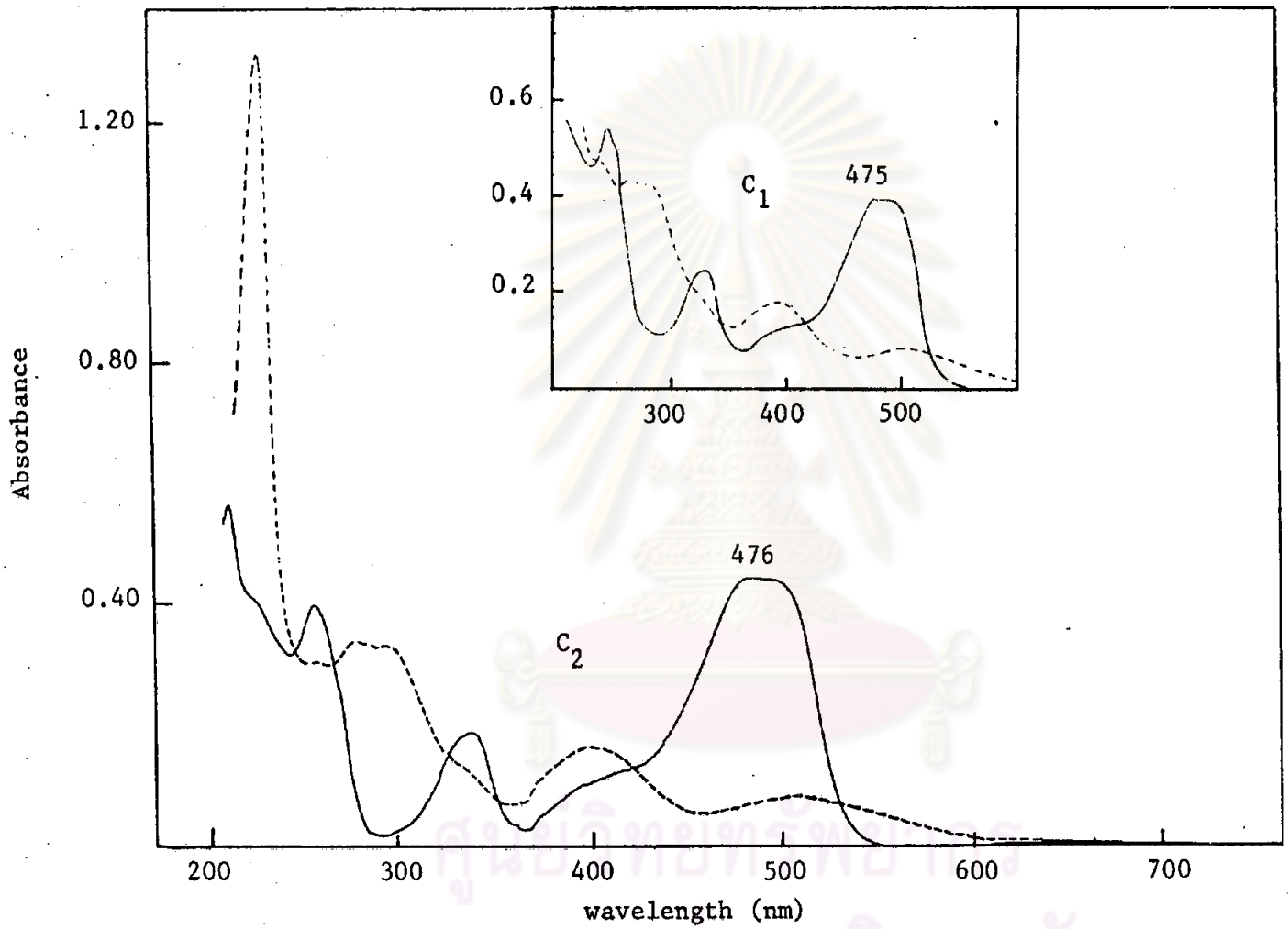

Figure 4C Comparison of UV-visible spectra of Orange G, —— in 0.1 M HCl and --- in 0.1 M NaOH C_1) literature (33) and C_2) experiment

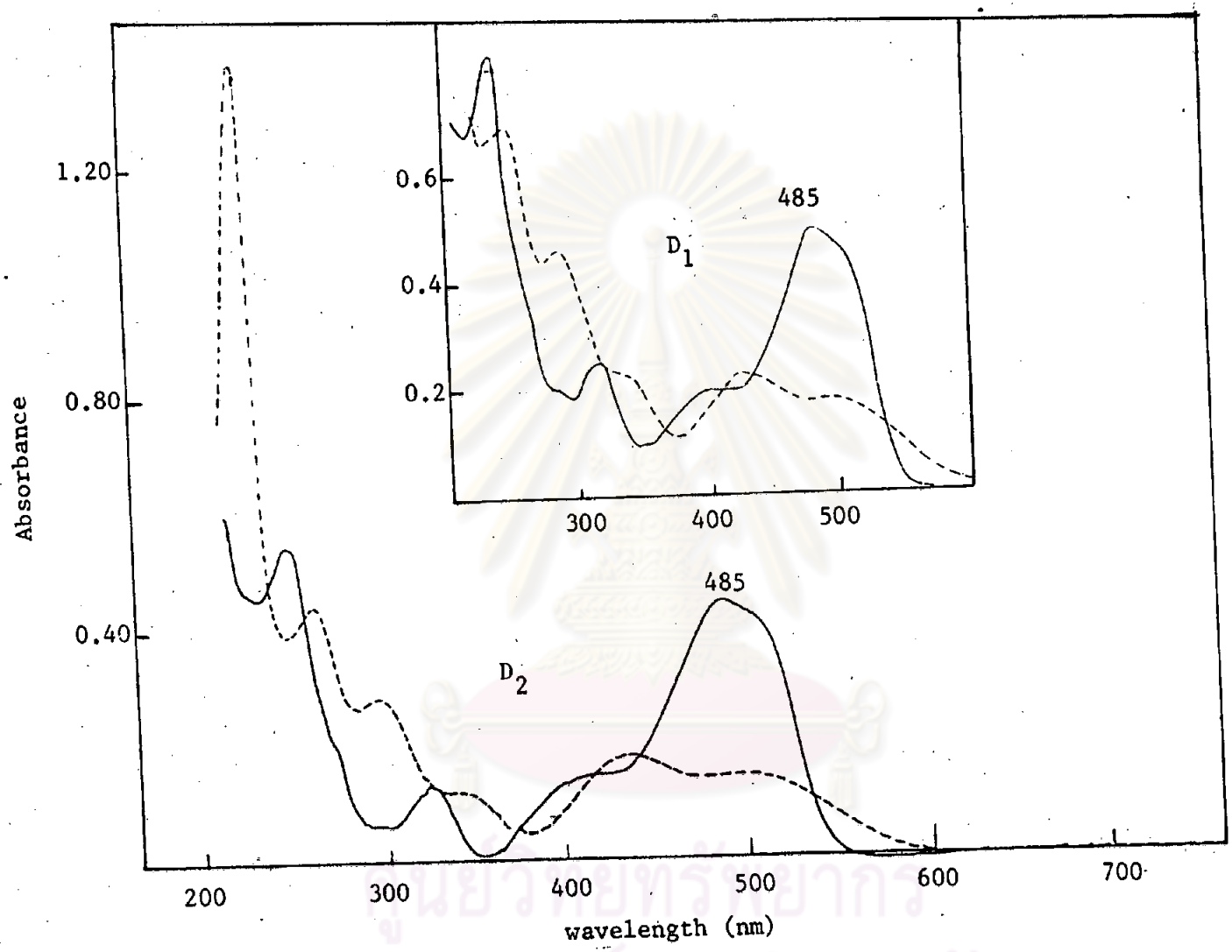

Figure 4D Comparison of UV-visible spectra of Orange RN, —— in 0.1 M HCl and --- in 0.1 M NaOH
D_1) literature (33), D_2) experiment

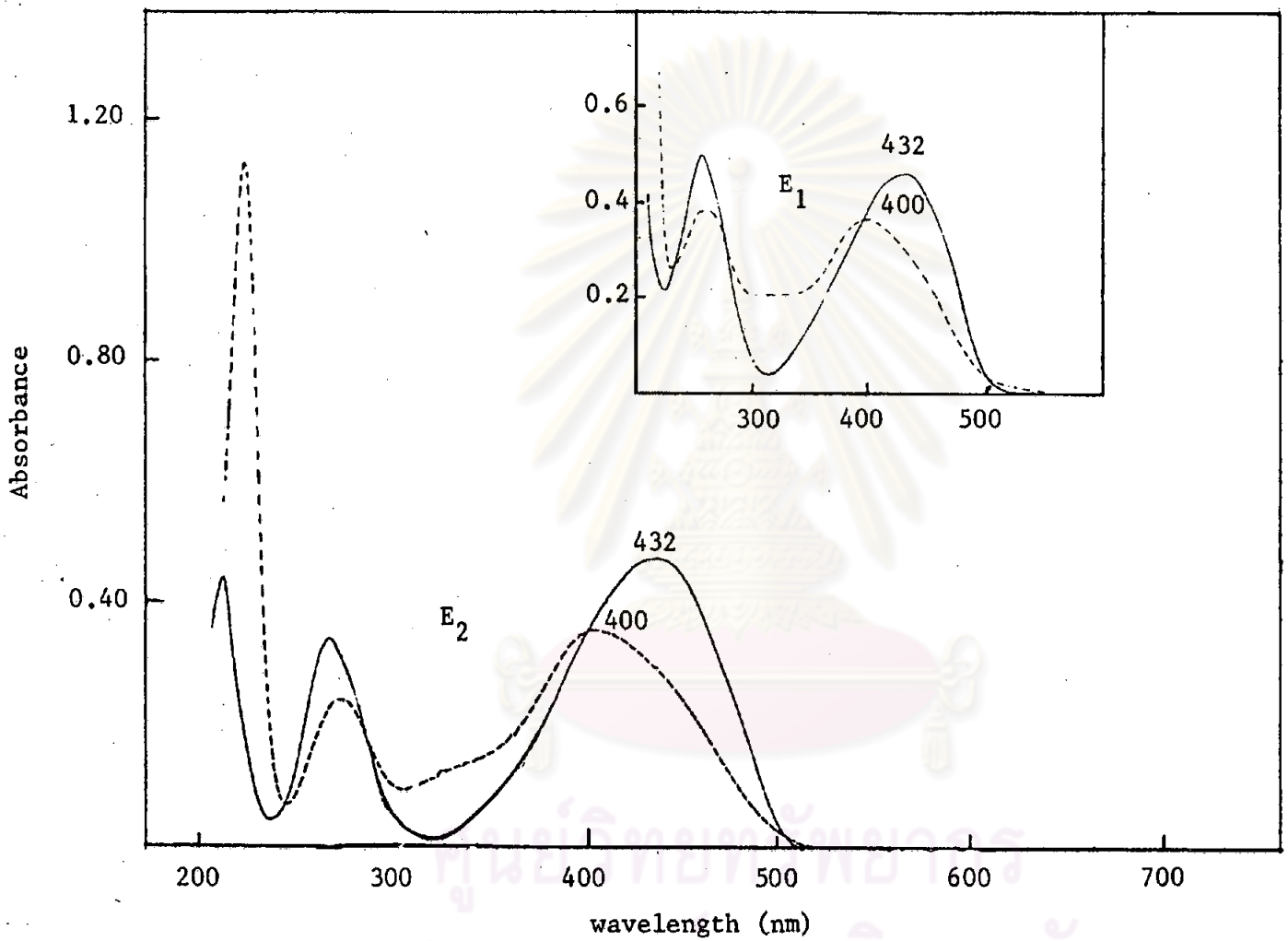

Figure 4E Comparison of UV-visible spectra of Tartrazine, —— in 0.1 M HCl and --- in 0.1 M NaOH E_1) literature (33) and E_2) experiment

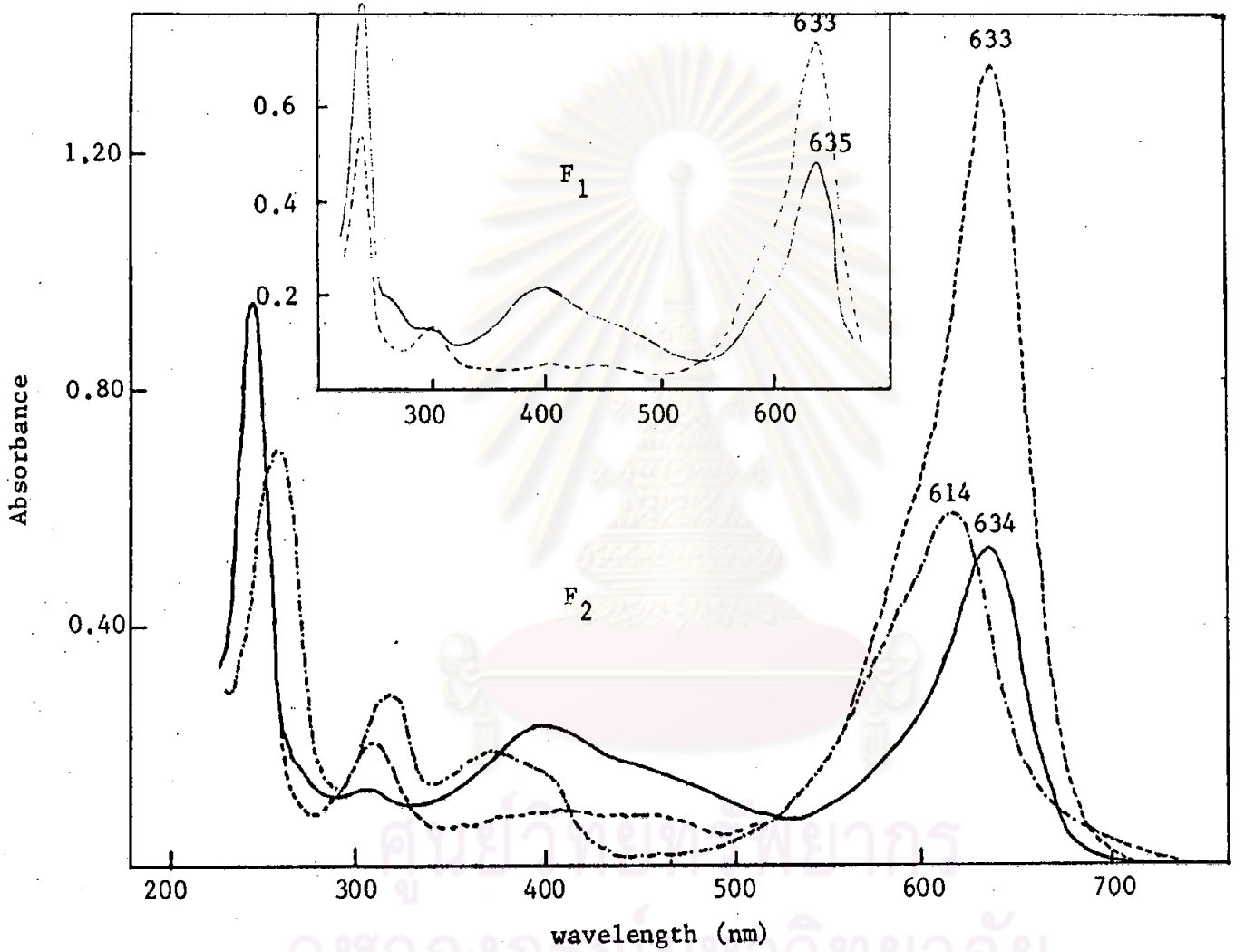

Figure 4F Comparison of UV-visible spectra of Green S, —— in 0.1 M HCl, -·-·-· in 0.1 M NaOH and --- in water F_1) literature (33) and F_2) experiment

Table 2 Absorption characteristics of dyes in the visible region

Dye	λmax, nm	
	in acid sol^{n}	in alkali sol^{n}
Azorubine	515	505
Sunset Yellow FCF	482	450
Orange G	476	-
Orange RN	485	-
Tartrazine	432	400
Green S	634	614

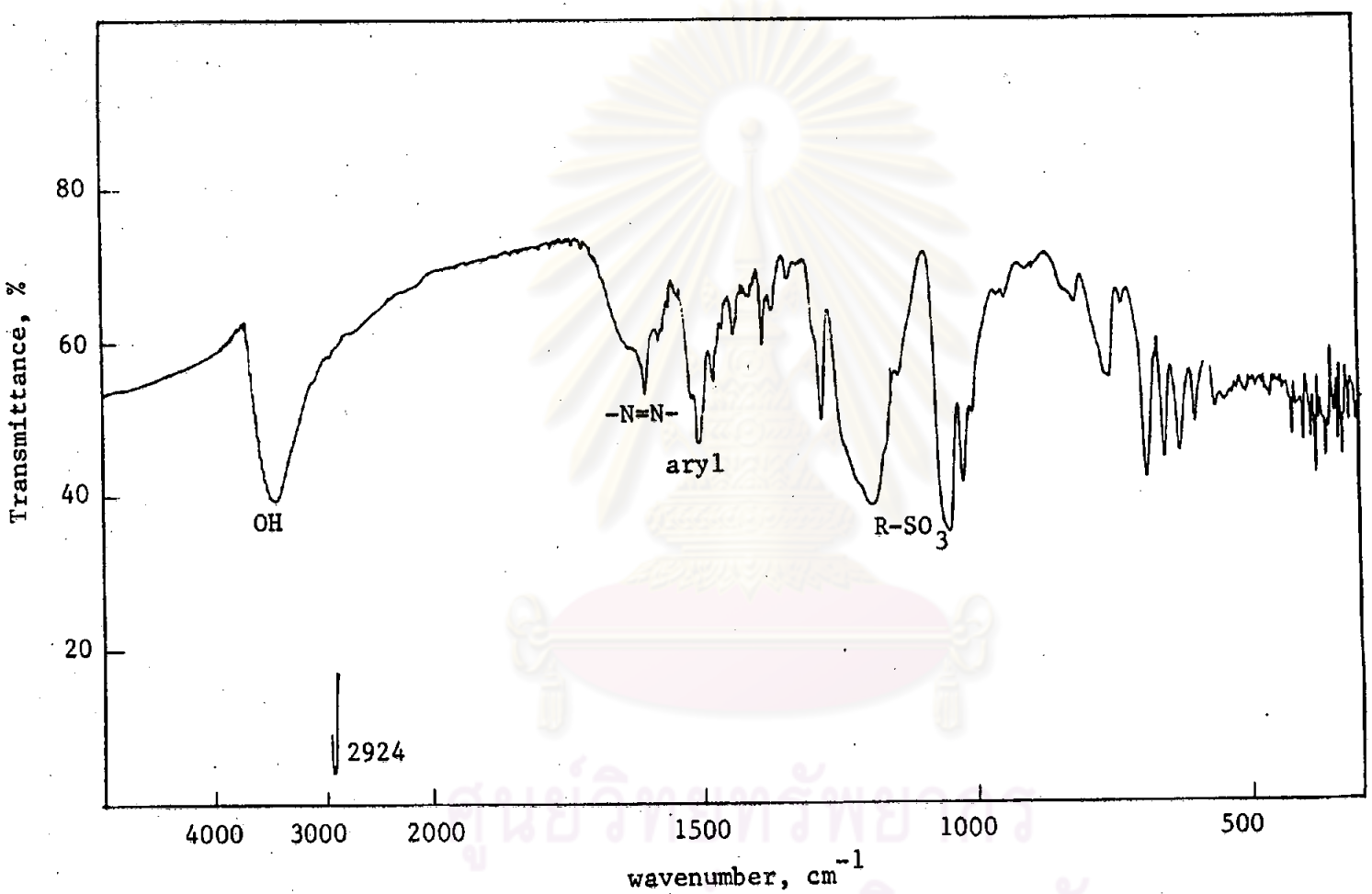

Figure 5A IR spectrum of Azorubine in a solid KBr pellet

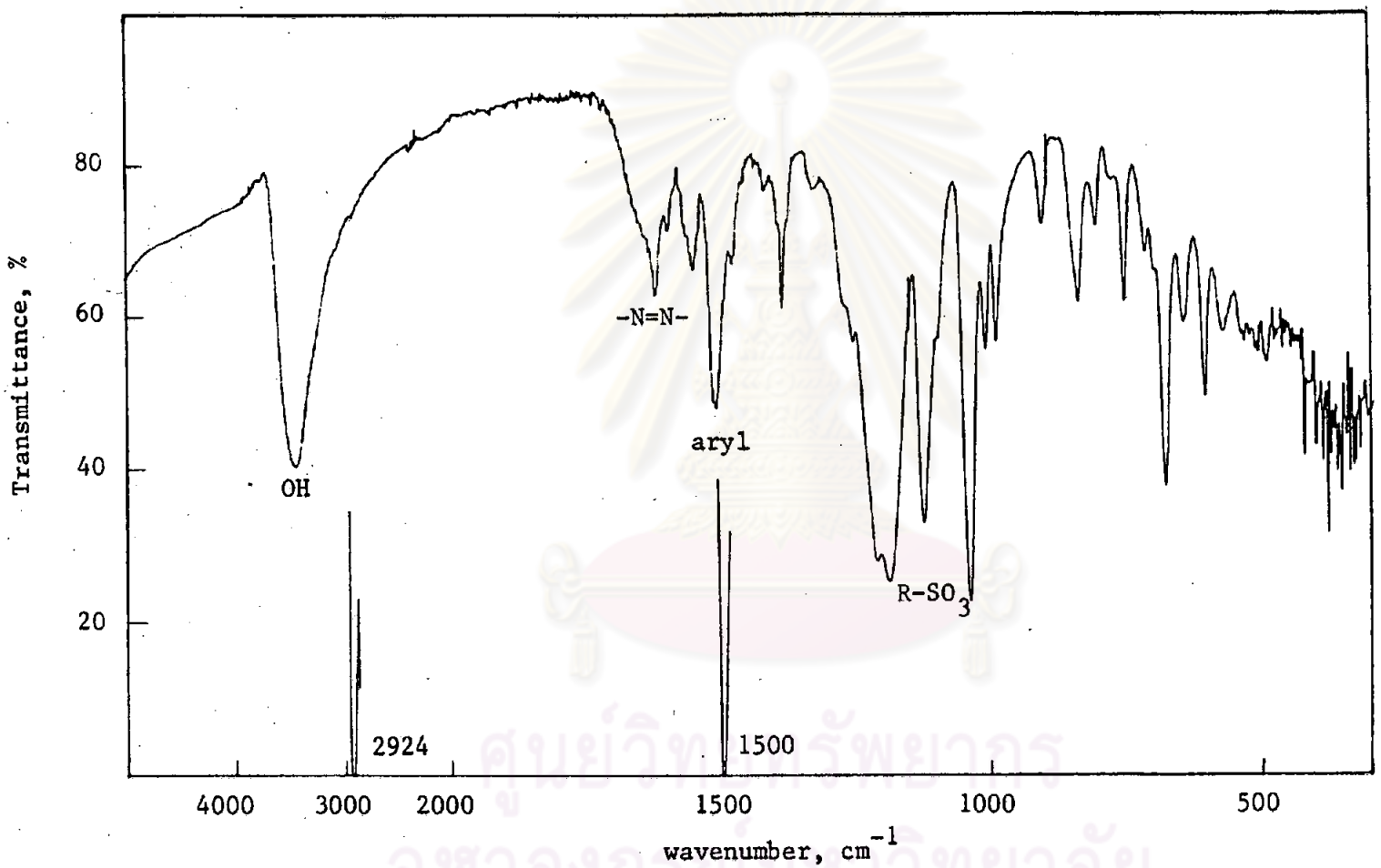

Figure 5B IR spectrum of Sunset Yellow FCF in a solid KBr pellet

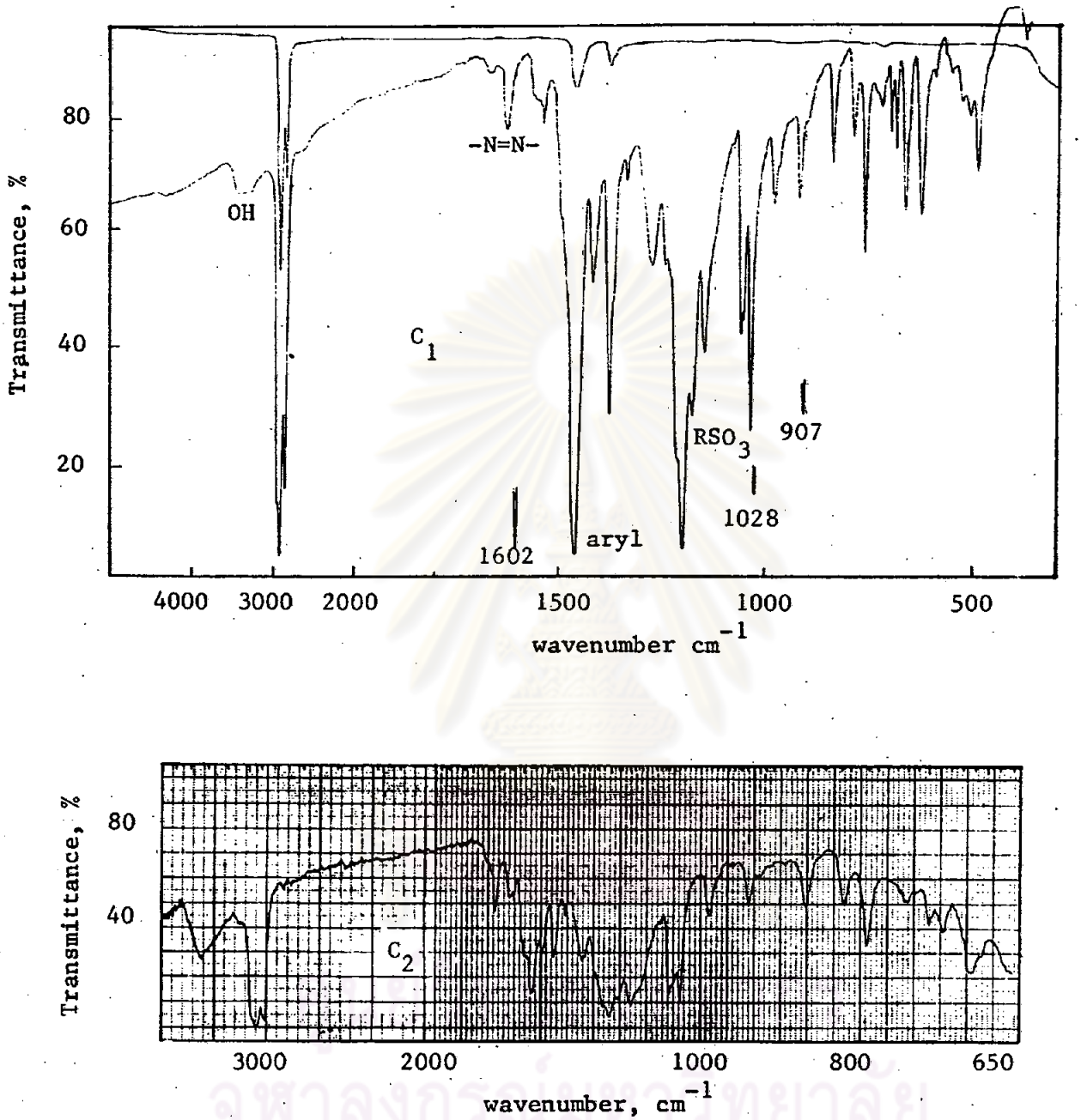

Figure 5C Comparison of IR spectra of Orange G in nujol mull

C_1) experiment

C_2) literature (34)

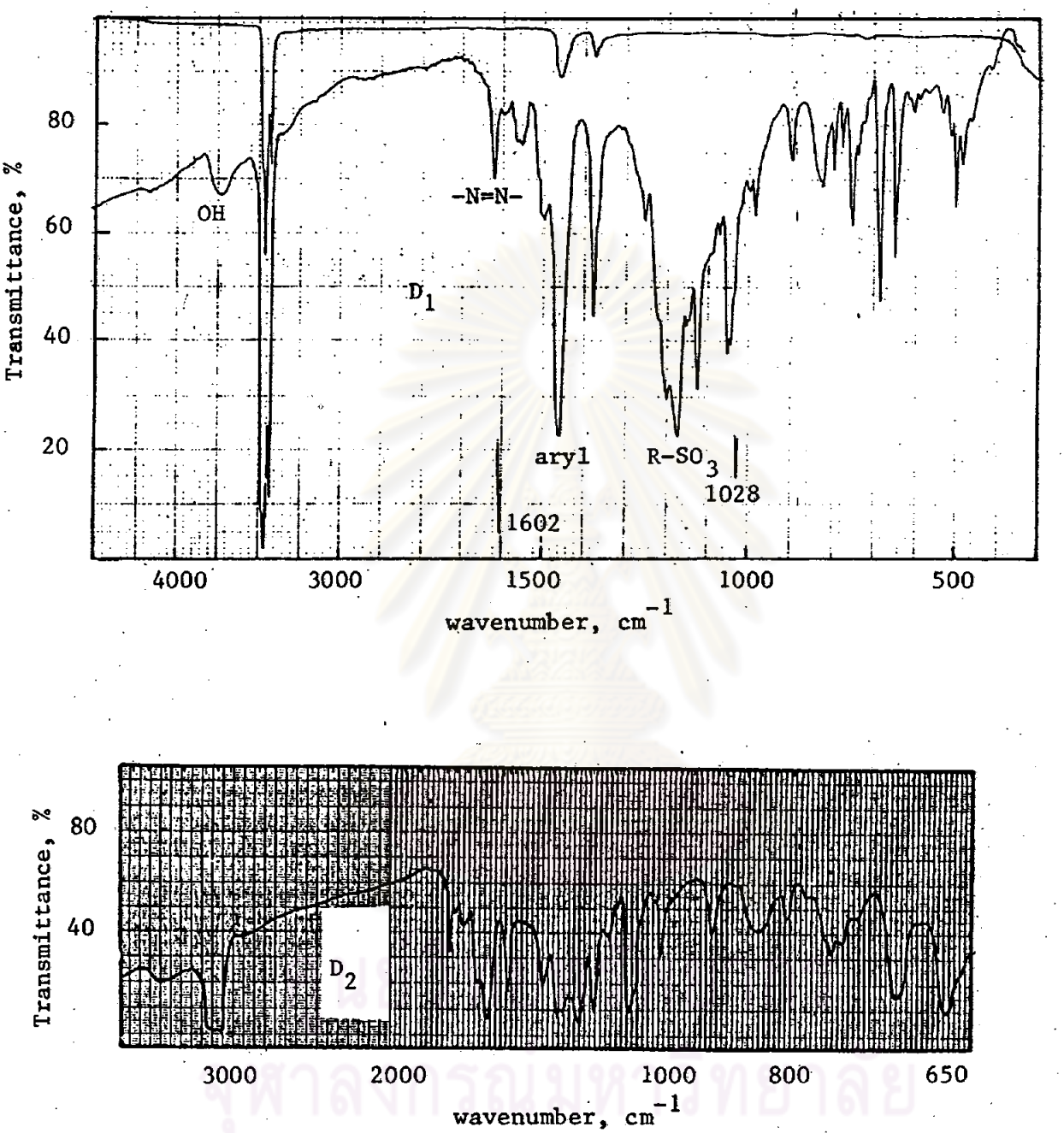

Figure 5D Comparison of IR spectra of Orange RN in nujol mull

D_1) experiment

D_2) literature (36)

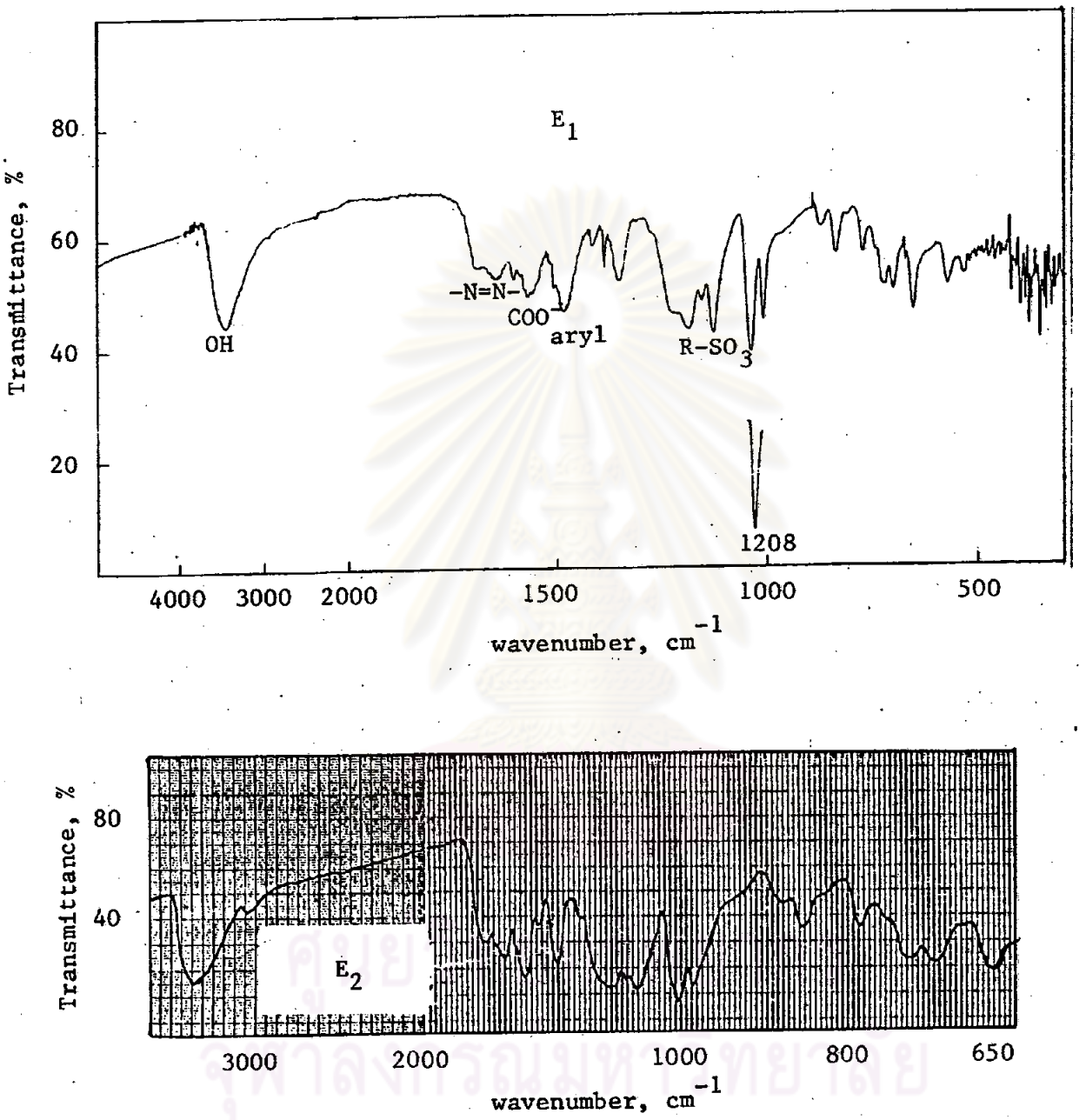

Figure 5E IR spectra of Tartrazine in solid KBr pellets

E_1) experiment

E_2) literature (35)

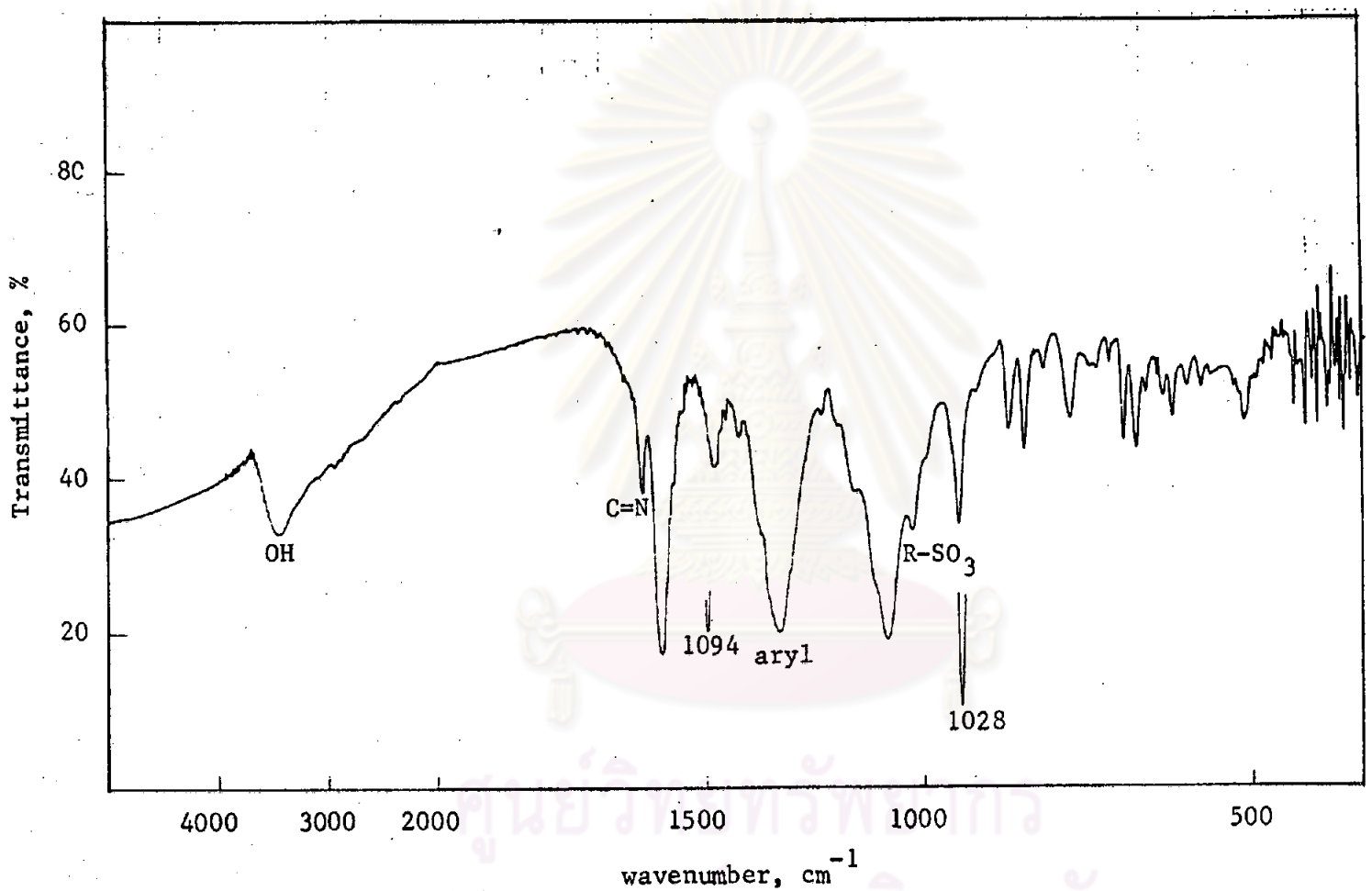

Figure 5F IR spectrum of Green S in a solid KBr pellet

graphy. Five mixed solvent systems of various compositions were investigated. Solvent system I is the mixture of 2-propanol, ammonia solution and water in the ratio of 7:2:1, respectively. System II is the mixture of 2-propanol, ammonia solution and water in the ratio of 10:1:1, respectively. System III is the mixture of 2-propanol and ammonia solution in the ratio of 4:1, respectively. System IV is the mixture of 2-butanol, ethanol, water and ammonia solution in the ratio of 10:20:10:1, respectively. System V is the mixture of 1-butanol, acetic acid and water in the ratio of 10:5:6, respectively. The Rf values of the certified grade Orange RN in these solvent systems are listed in Table 3 and their chromatograms were shown in Figure 6. It can be seen that, the solvent system I showed the biggest difference of the Rf values between Orange RN and the contaminate.

3.2.2 Column chromatography

A 1.0 gm of the certified grade of Orange RN was chromatographed on silica gel column with 2-propanol-ammonia-water. The fraction that was eluted with 2-propanol-ammonia-water (7:2:1) gave a pure Orange Rn of 0.8 gm.

The purity of the separated Orange RN was tested by paper chromatography, ultraviolet-visible and infrared spectrophotometric techniques (see Figure 7, 8 and 9), respectively.

The paper chromatogram of separated Orange RN in the solvent system I or III revealed a single spot whose Rf value was found to be 0.66 or 0.08, respectively. These Rf values are slightly different from the literature values (0.68 for solvent system I, 0.08 for solvent system III) owing to the slight difference in experimental conditions.

The trace impurity in the contaminated Orange RN might has the same absorption characteristics as the pure Orange RN, thus the

ultraviolet-visible spectra of the contaminated Orange RN and the separated Orange RN were identical (see Figure 4D and Figure 8).

Infrared spectra of the separated Orange RN indicated an insignificant difference from the literature one (36), it showed the phenolic OH (3200-3450 cm^{-1}), -N=N- (1620 cm^{-1}), aromatic (1460 cm^{-1} and 1500 cm^{-1}-skeleton carbon stretching, and 700-800 cm^{-1} aromatic out of plane bending) and ionic sulfonate (1200 cm^{-1} and 1160 cm^{-1}) characters (see Figure 9).

The paper chromatogram, infrared, ultraviolet-visible spectra of Orange RN revealed that the purified Orange RN was pure enough for using in the study of complex formations with metal ions.

3.3 Dye content

Titanium trichloride method, spectrophotometric method and Kjeldahl method were used for determining the dye content. Azorubine, Sunset Yellow FCF, Orange G, Tartrazine and Green S were titrated with 0.1185 M standard titanium trichloride solution. The percentage of dye contents of Azorubine, Sunset Yellow FCF, Orange G, Tartrazine and Green S were 85.23, 88.73, 95.43, 89.20, 94.74, respectively (see Table 4). By spectrophotometric method, the dye contents of Sunset Yellow FCF and Tartrazine were 87.79% and 88.92%, respectively. From nitrogen content (Kjeldahl method), the percentage of Orange RN was 85.65. It was seen that the dye contents of the dyes studied were not less than 85%. These evidences indicated that the dyes had high purity.

3.4 The effect of pH on solubilities of dyes, metal ions and their mixtures

Azorubine, Sunset Yellow FCF, Orange G, Orange RN, Tartrazine and Green S are very soluble in many buffer systems such as phosphoric

Table 3 Solvent systems and the corresponding Rf values by thin layer chromatography

solvent system	Rf of Orange RN	
	experiment	literature[37]
I	0.80, 0.54	0.83
II	0.81, 0.58	-
III	0.70, 0.50	0.64
IV	0.82, 0.67	0.88
V	0.81, 0.75	0.82

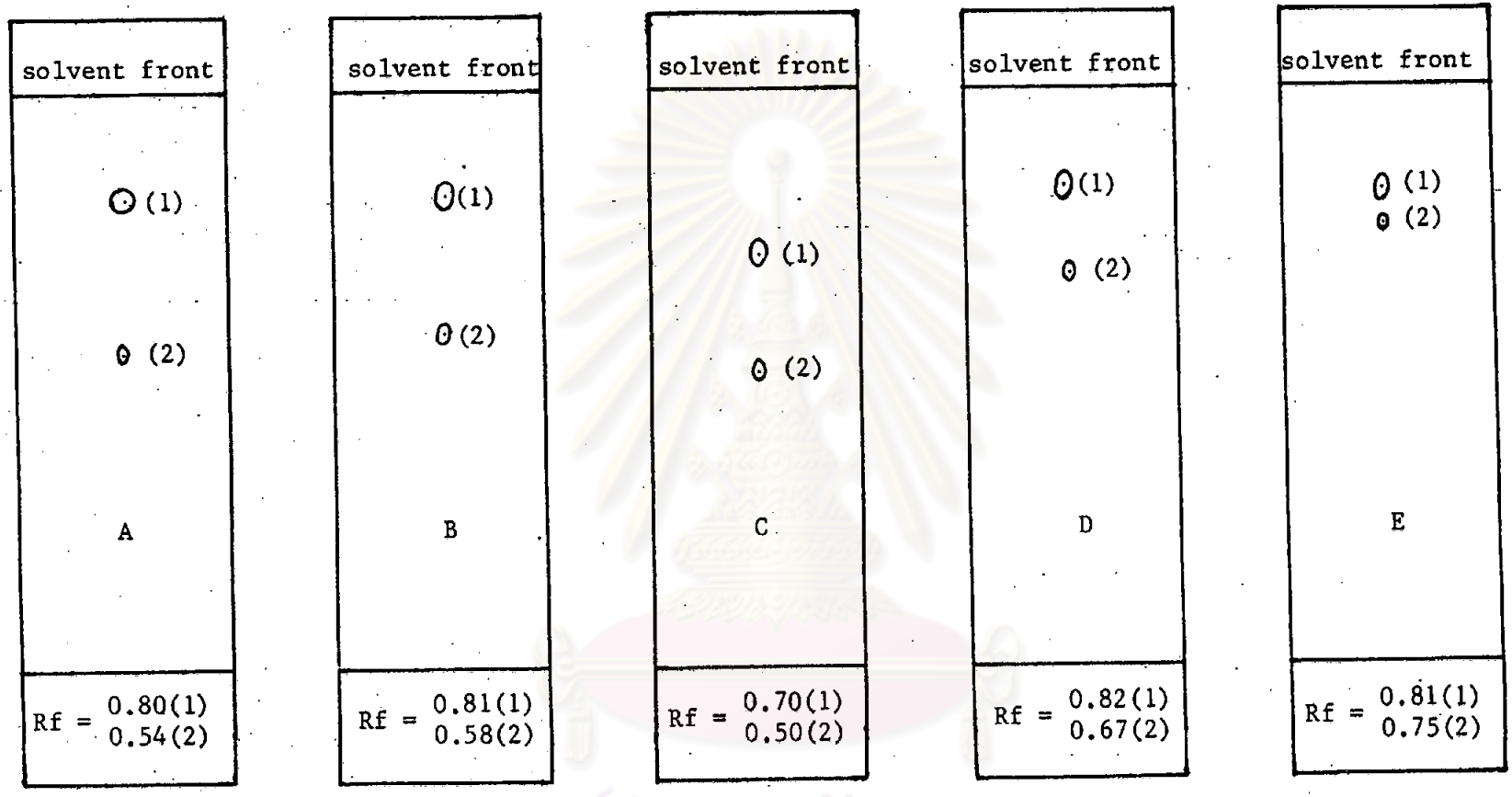

Figure 6 Thin layer chromatograms of Orange RN by A) solvent system I, B) solvent system II, C) solvent system III, D) solvent system IV, E) solvent system V

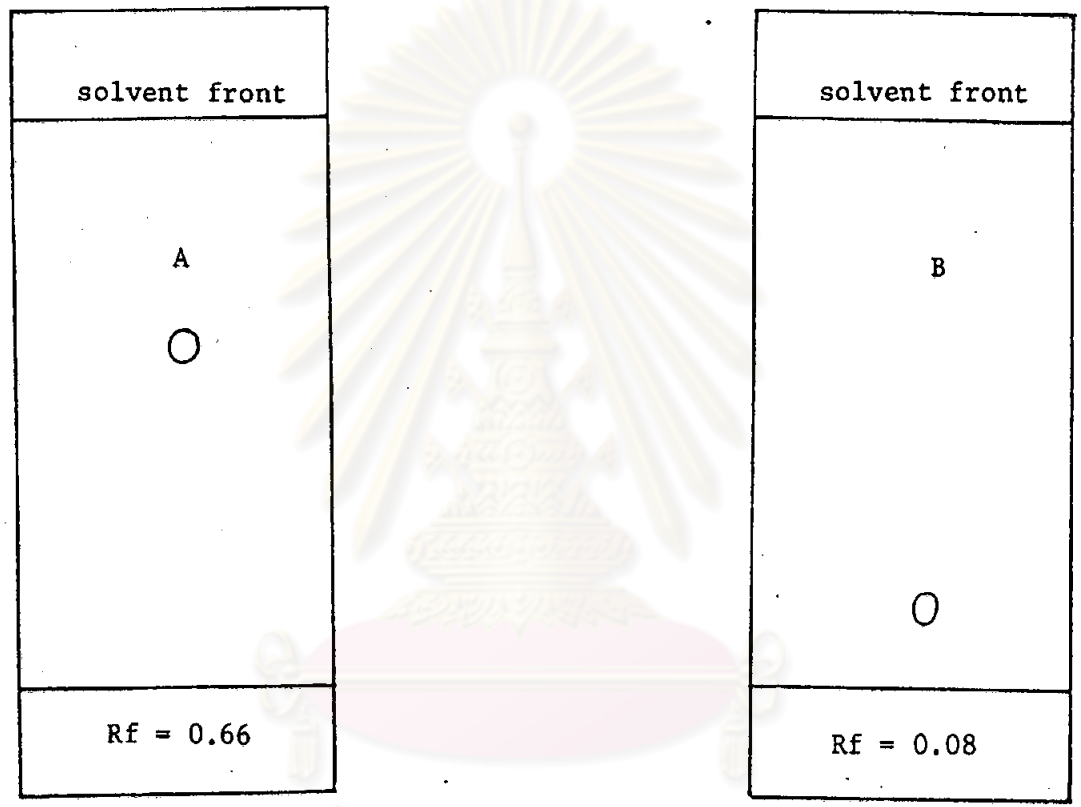

Figure 7 Paper chromatograms of Orange RN after purification by column chromatography in

A) solvent system I

B) solvent system III

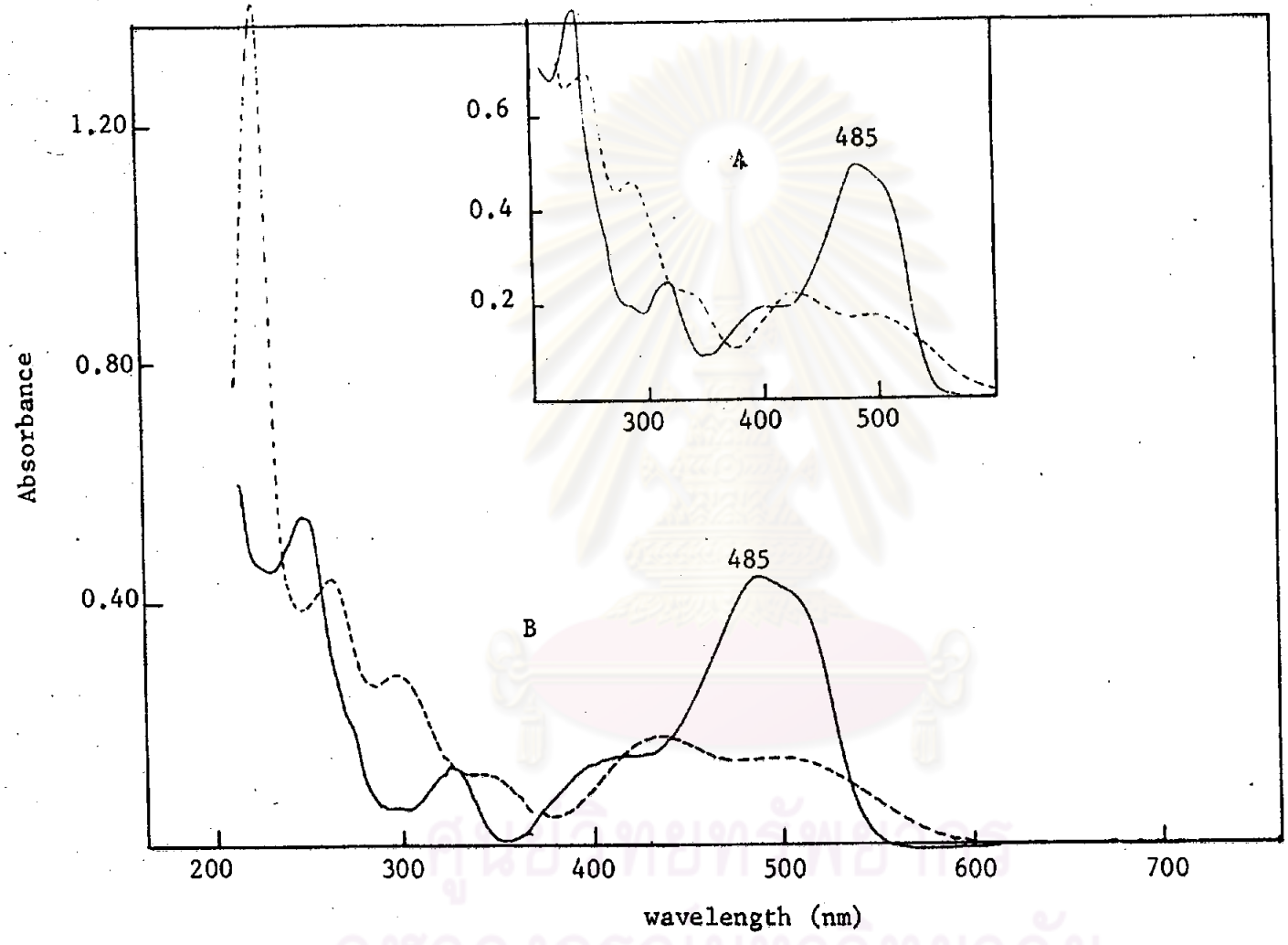

Figure 8 Comparision of UV-visible spectra of Orange RN after purification by column chromatography —— in 0.1 M HCl and --- in 0.1 M NaOH
A) literature (33) and B) experiment

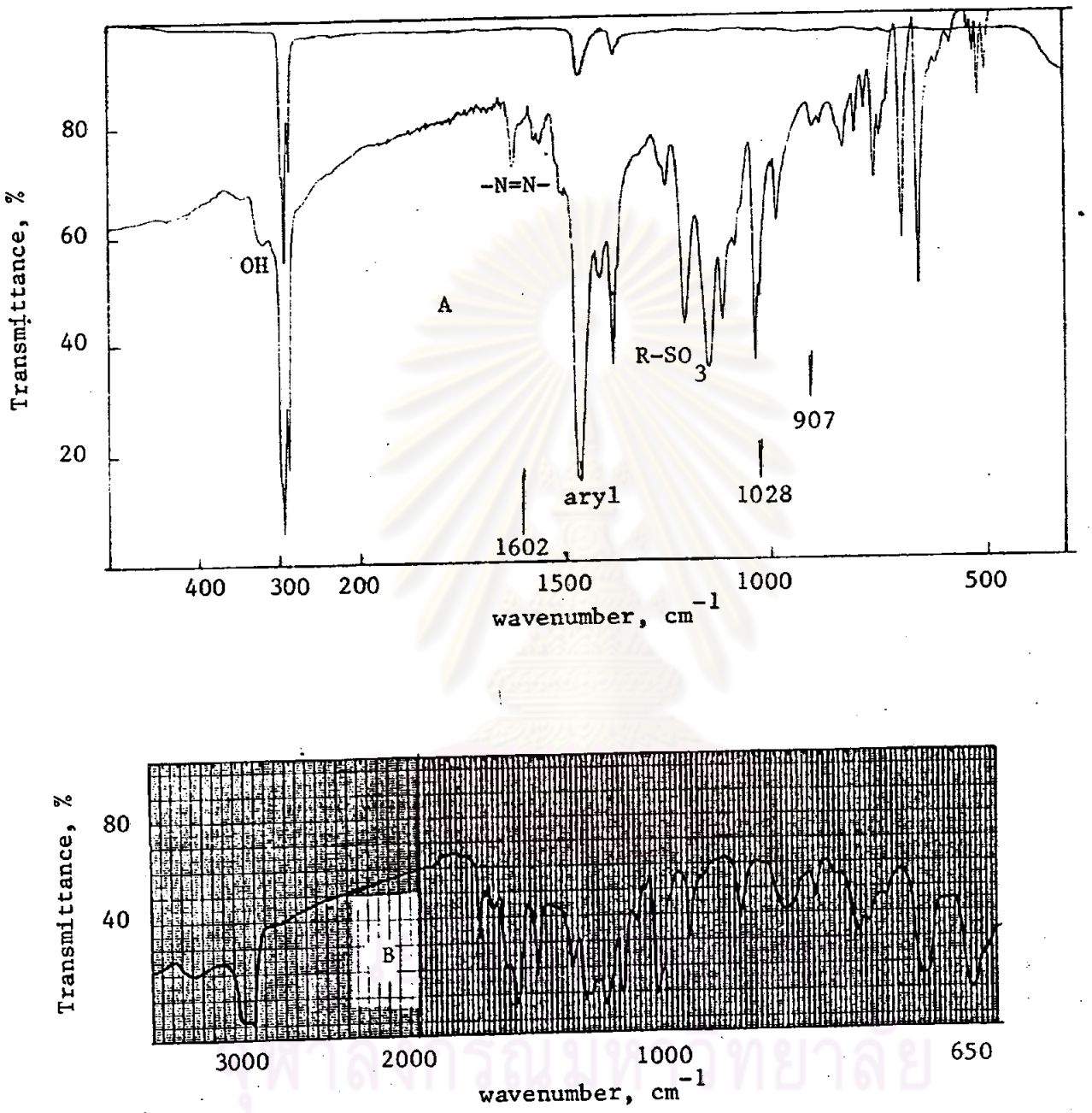

Figure 9 Comparison of IR spectra of Orange RN in nujol mull after purification by column chromatography

A) experiment

B) literature (36)

Table 4 Dye contents of Azorubine, Sunset Yellow FCF, Orange G, Tartrazine and Green S by titanium trichloride method

Dye	$TiCl_3$ titration factor		Volume (cm^3) $TiCl_3$ 0.1185 M	% Pure dye
	gm color/cm^3 (3) 0.1000 M $TiCl_3$	gm color/cm^3 0.1185 M $TiCl_3$		
Azorubine	0.01256	0.01488	4.32	85.23
Sunset Yellow FCF	0.01131	0.01134	4.49	88.73
Orange G	0.01131	0.01134	4.83	95.43
Tartrazine	0.01336	0.01583	4.52	89.20
Green S	0.02883	0.03416	2.40	94.79

acid, acetic acid, McIlvaine buffer, phosphate buffer, acetate buffer and diethylamine.

Metal ions such as, Ti (IV), Cr (III), Mn (II), Co (II), Fe (II), Fe (III), Ni (II), Cu (II) and Zn (II) are soluble in phosphoric acid, acetic acid, McIlvaine buffer, acetate buffer and phosphate buffer. However, precipitation of Mn (II), Co (II), Fe (II), Ni (II) and Cu (II) ion in the phosphate buffer at pH 7.00 are formed when 1.00 cm^3 of 5.00×10^{-3} M of metal ion are mixed with 1.00 cm^3 buffer solution. In diethylamine, at pH 12.5, Cr (III), Mn (II), Co (II), Fe (II), Fe (III), Ni (II) and Cu (II) ion are insoluble (see Table 5).

No physical change or precipitation of the mixture solution of metal ions and the dye solution was observed. However, in acetate buffer it was found that Azorubine, Sunset Yellow FCF, Orange G, Orange RN reacted with Cu (II) ion since the mixture solution changed from red to orange for Azorubine and from orange to yellow for Sunset Yellow FCF, Orange G or Orange RN. The color of Azorubine also changed from red to orange when Azorubine solution was mixed with Cu (II) ion in the phosphate buffer.

3.5 Ultraviolet-visible spectrophotometric characteristics of dyes

3.5.1 The wavelengths of maximum absorption (λmax) of dyes in ultraviolet-visible region and the molar absorptivity (ε) values.

The wavelengths at the maximum absorption (λmax) of the aqueous solution of Azorubine, Sunset Yellow FCF, Orange G, Orange RN, Tartrazine and Green S in ultraviolet-visible region were measured as shown in Table 6. Their molar absorptivities were determined from the linear ranges of the curve of absorbances of dyes against their concentrations (see Figures 10A-10F) and also listed in Table 6. The molar

ble 5 Solubility of the metal ions in various buffer systems

buffer system	pH	1.00×10^{-4}M metal ion									5.00×10^{-3}M metal ion								
		Ti(IV)	Cr(III)	Mn(II)	Co(II)	Fe(II)	Fe(III)	Ni(II)	Cu(II)	Zn(II)	Ti(IV)	Cr(III)	Mn(II)	Co(II)	Fe(II)	Fe(III)	Ni(II)	Cu(II)	Zn(II)
phosphoric acid	1.00	-	-	-	-	-	-	-	-	-	-	-	-	-	-	-	-	-	-
acetic acid	2.30	-	-	-	-	-	-	-	-	-	-	-	-	-	-	-	-	-	-
	3.10	-	-	-	-	-	-	-	-	-	-	-	-	-	-	-	-	-	-
McIlvaine buffer	5.15	-	-	-	-	-	-	-	-	-	-	-	-	-	-	-	-	-	-
	7.40	-	-	-	-	-	-	-	-	-	-	-	-	-	-	-	-	-	-
	6.10	-	-	-	-	-	-	-	-	-	-	-	-	-	-	-	-	-	-
acetate buffer	5.10	-	-	-	-	-	-	-	-	-	-	-	-	-	-	-	-	-	-
	4.00	-	-	-	-	-	-	-	-	-	-	-	-	-	-	-	-	-	-
	5.85	-	-	-	-	-	-	-	-	-	-	-	↓	↓	-	↓	↓	↓	-
phosphate buffer	7.00	-	-	-	-	-	-	-	-	-	-	-	↓	↓	-	↓	↓	↓	-
diethylamine	12.50	-	-	-	-	-	-	-	-	-	-	↓	↓	↓	↓	↓	↓	↓	-

- soluble

↓ precipitation

Table 6 Absorption characteristics of dyes in aqueous solution in UV-visible region

Dye	λmax (nm) in visible-UV	molar absorptivity ε(calculated) in visible region
Azorubine	515, 315	21,333
Sunset Yellow FCF	482, 307	20,000
Orange G	476, 322	18, 286
Orange RN	485, 314	17,858
Tartrazine	432, 252	25,000
Green S	634 -	80,000

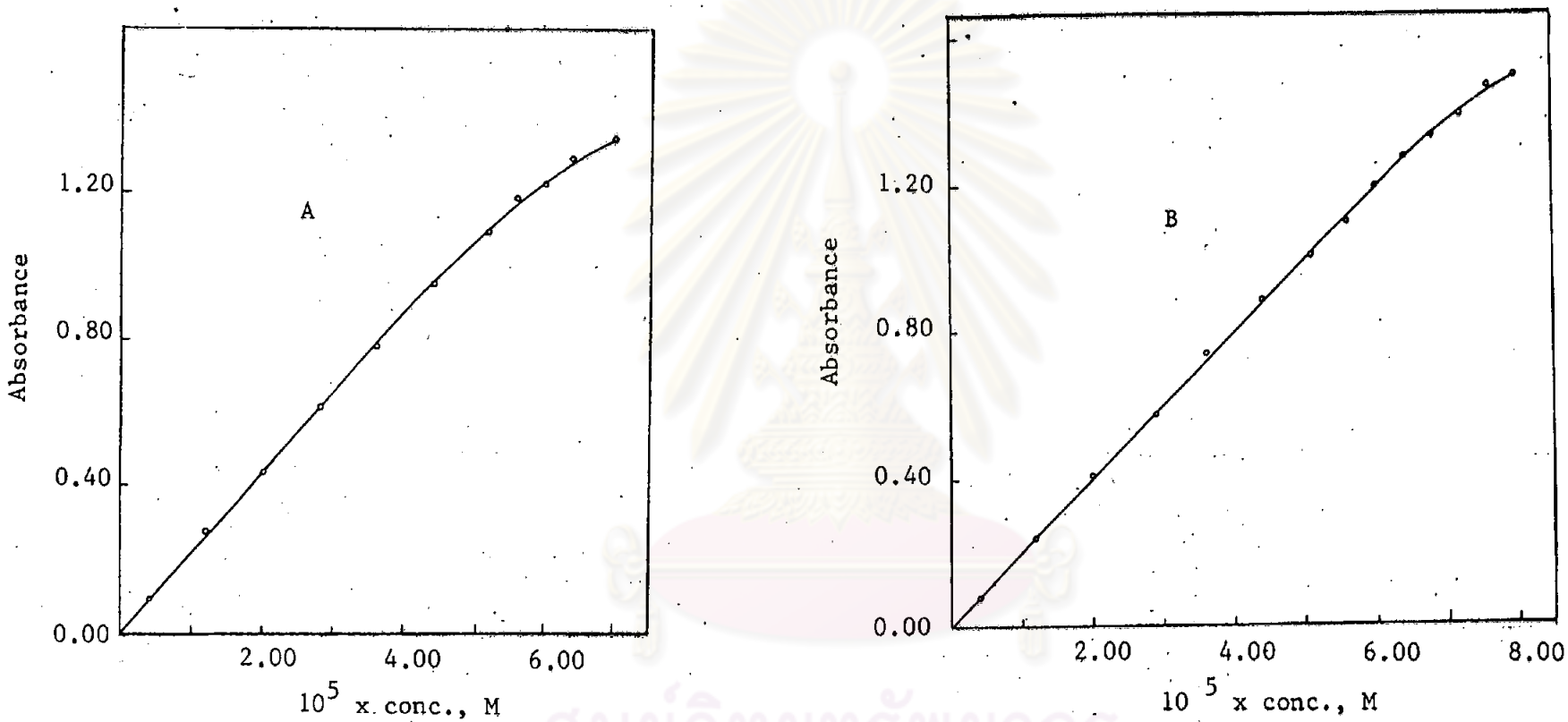

Figure 10A-10B Dependences of absorbances on concentrations of Azorubine (A), and Sunset Yellow FCF (B)

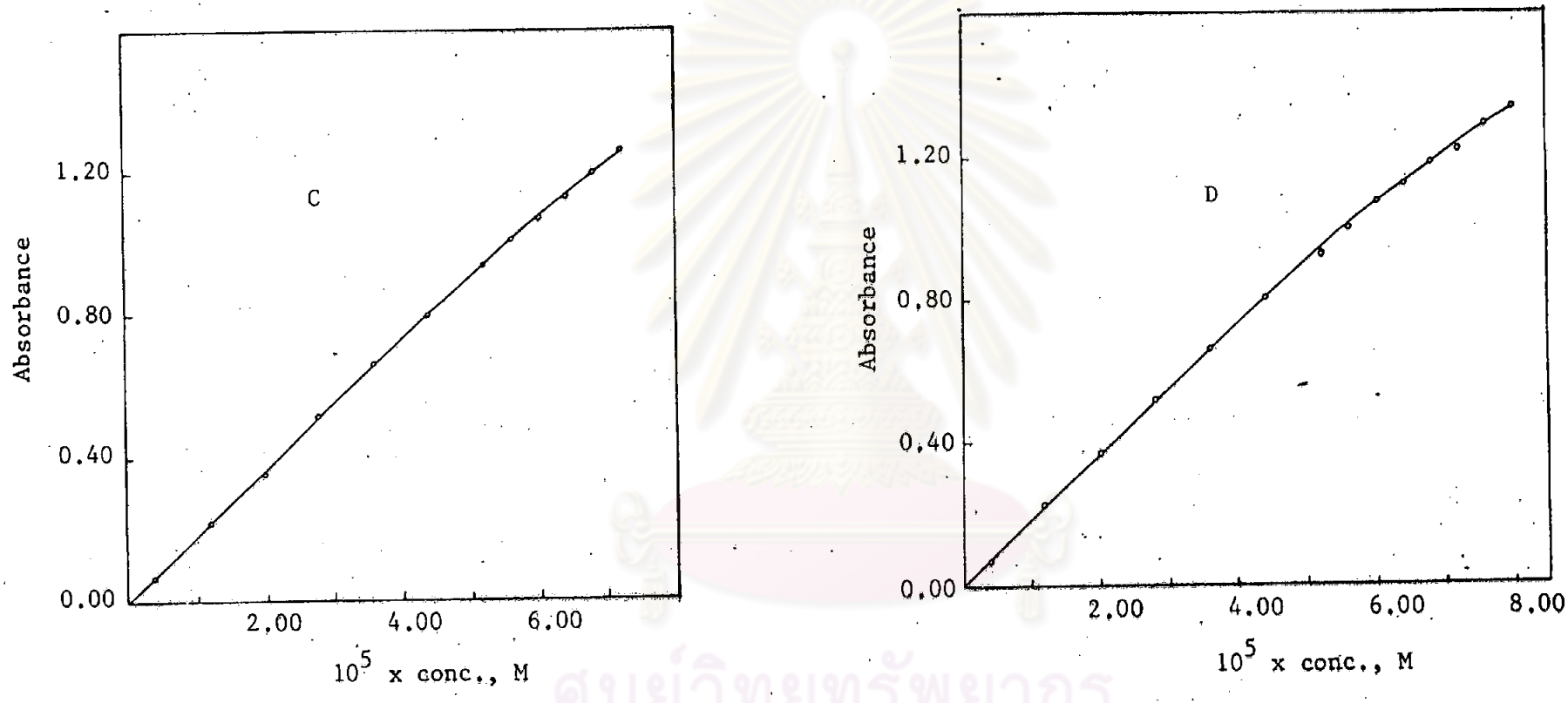

Figure 10C-10D Dependences of absorbances on concentrations of Orange G (C) and Orange RN (D)

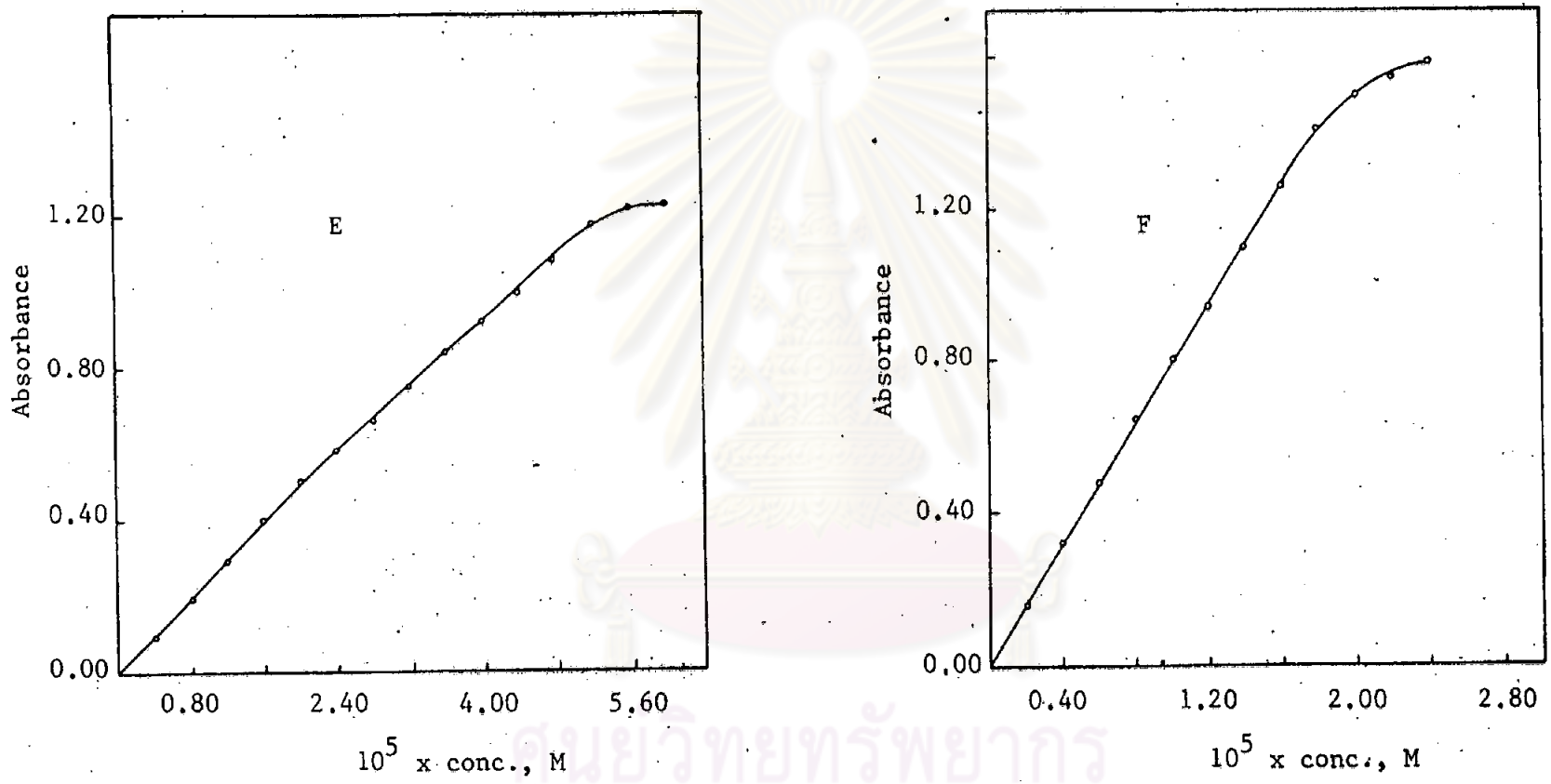

Figure 10E-10F Dependences of absorbances on concentrations of Tartrazine (E) and Green S (F)

absorptivity of each dye was found in the order of 10^4 which indicated the strong absorption of the dye in the visible range. Green S has the highest molar absorptivity and Orange RN gives the lowest molar absorptivity.

3.5.2 Effect of pH on the characteristics of dyes

The absorption spectra of most organic compounds are depended on the pH of a medium. Thus, the absorption spectra of Azorubine, Sunset Yellow FCF, Orange G, Orange RN, Tartrazine and Green S in phosphoric acid, acetic acid, McIlvaine buffer or diethylamine at various pH values were recorded in the range of 220-760 nm. In every buffer system when pH of the solution was higher than 7.00, the wavelengths at the maximum absorption (λmax) of dyes gradually shifted to lower wavelengths. However, at pH lower than 7.00 they were pH independence except Green S that was pH dependence. The absorbance of the dye studied in any buffer system in the visible region decreased as the pH of the solution increased except Green S at pH 1.00 whose absorbance was obviously decreased and the absorption peak in ultraviolet region shifted to the visible region (see Figures 11A-11F and Tables 7A-7F). At pH 12.5, Sunset Yellow FCF, Orange G, Orange RN, Tartrazine and Green S showed an obvious decrease of an absorbance in visible region and the ultraviolet spectra were slightly changed.

The change in the absorption characteristics of the dye may be ascribed to the change in the structure caused by ionization. At the lower pH, the attachment of a proton to the auxochromic group or on one of the nitrogen atoms of the azo group was reported (38)

$$R\text{-}N{=}N\text{-}R \underset{\text{higher pH}}{\overset{\text{lower pH}}{\rightleftharpoons}} R\text{-}N{=}\overset{+}{N}H\text{-}R$$

and when the pH increased, the process reversed.

The dissociation constant of a dye based on such change in the absorption spectrum with the pH of the medium. Therefore, the dissociation constant of each dye was evaluated by plotting the absorbance (A) or $\frac{\Delta A}{\Delta pH}$ against pH of the solution. The curves of $\frac{\Delta A}{\Delta pH}$ of Azorubine, Sunset Yellow FCF, Orange G, Orange RN and Tartrazine showed the inflection points at pH 7.00, 6.00, 10.20, 10.30 and 9.80 respectively (see Tables 8A-8E and Figures 12A-12E). Thus, the pKa of Azorubine, Sunset Yellow FCF, Orange G, Orange RN and Tartrazine are 7.00, 6.00, 10.20, 10.30 and 9.80, respectively. The pKa of Green S was not determined since it decomposed in hydrochloric acid and sodium hydroxide (39).

3.5.3 Dependence of absorbances on concentrations of the dye solutions

Since the absorption spectra of the dyes indicated the strong absorption in the visible range (see Figures 4A-4F), the absorbances of the dye solution were measured in the visible region at the wavelength of 515 nm for Azorubine, 482 nm for Sunset Yellow FCF, 476 nm for Orange G, 485 nm for Orange RN and 634 nm for Green S. The relationships of absorbances and concentrations of the dye in aqueous solution without any buffer are shown in Tables 9A-9B and Figures 10A-10F. A linearity was obtained in the range of concentrations of 0.50×10^{-5} M - 5.00×10^{-5} M for Azorubin, 0.40×10^{-5} M - 3.20×10^{-5} M for Tartrazine, 0.40×10^{-5} M - 6.40×10^{-5} M for Sunset Yellow FCF, 0.40×10^{-5} M - 5.50×10^{-5} M for Orange G, 0.40×10^{-5} M - 5.00×10^{-5} M for Orange RN, or 0.20×10^{-5} M - 1.80×10^{-5} M for Green S.

Since the color changes of the mixture solutions of Cu (II) ion and Sunset Yellow FCF, Orange G or Orange RN in the acetate buffer pH 6.10, 5.10 or 4.00 and of Azorubine with Cu (II) ion in the phosphate buffer pH 7.00, 5.85 or in the acetate buffer pH 6.10 or 5.10 were

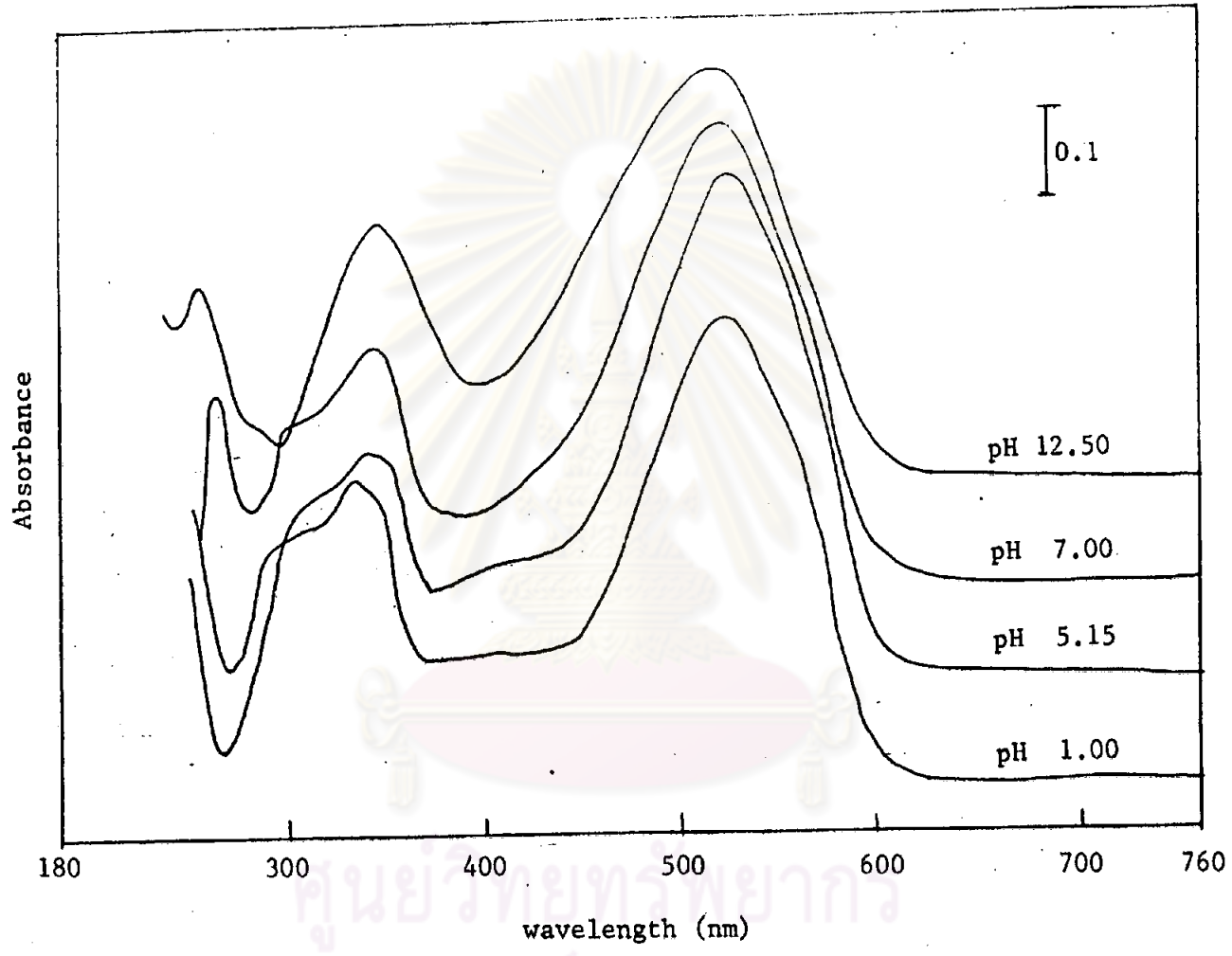

Figure 11A Absorption spectra of Azorubine at various pH values.

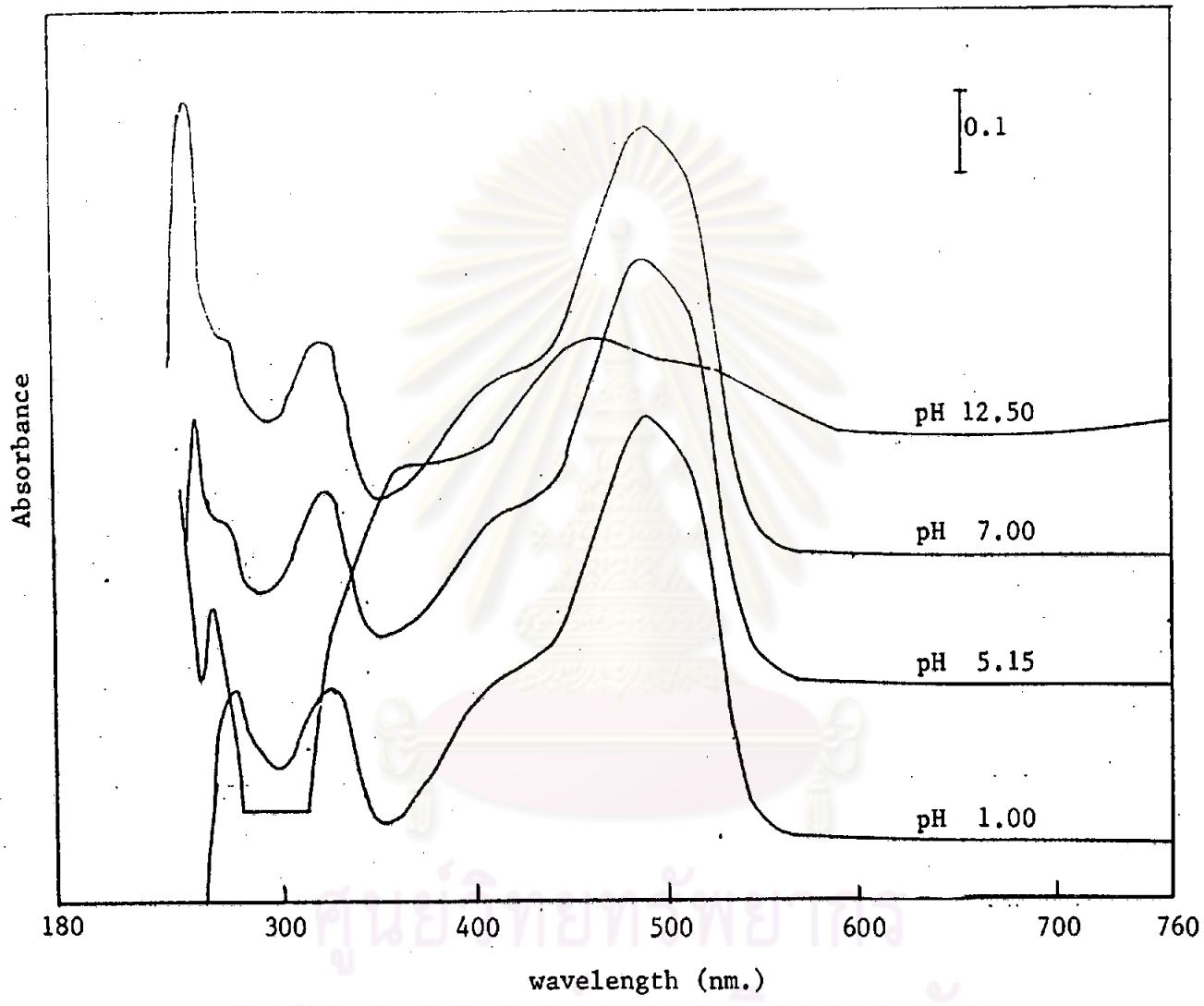

Figure 11B Absorption spectra of Sunset Yellow FCF at various pH values.

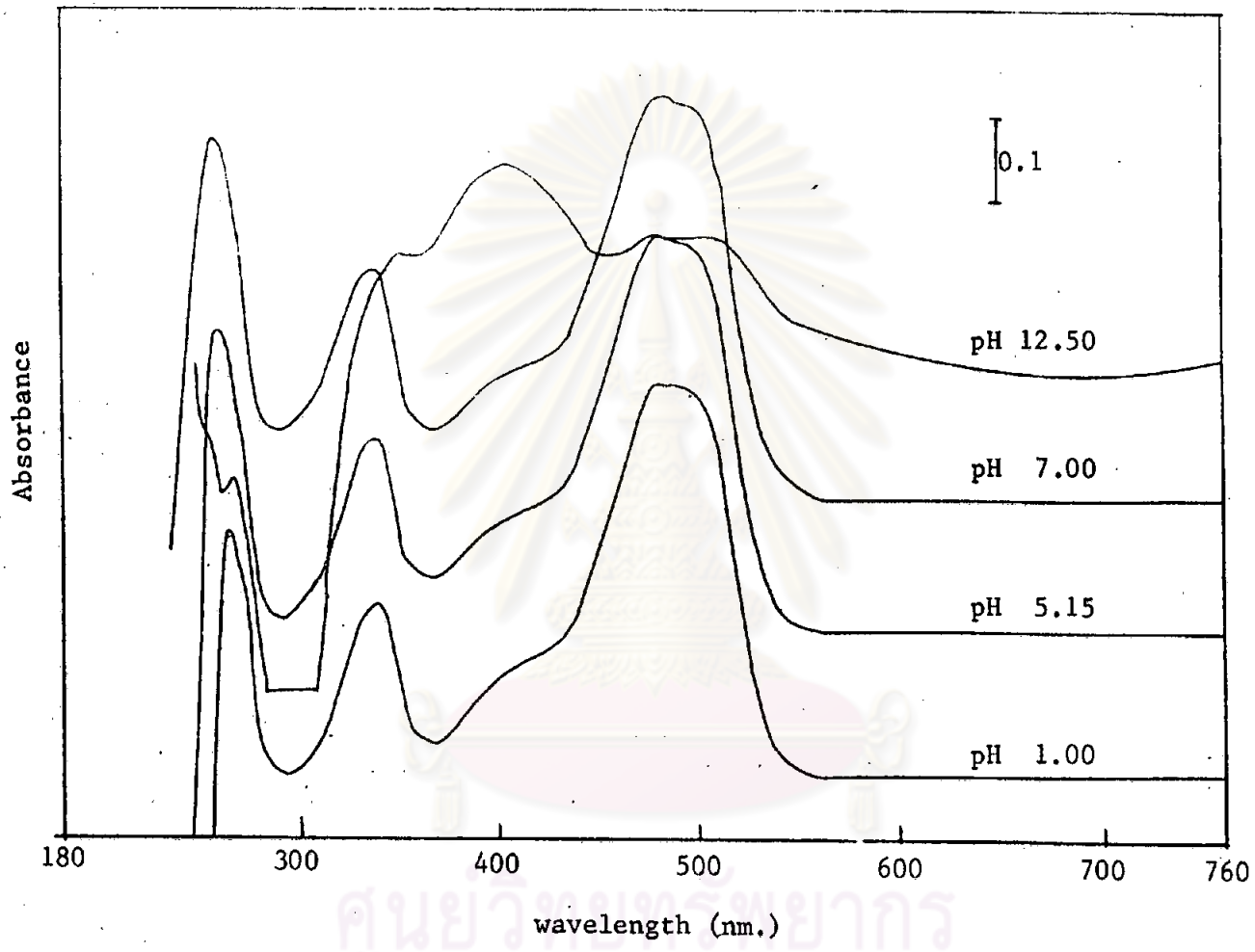

Figure 11C Absorption spectra of Orange G at various pH values.

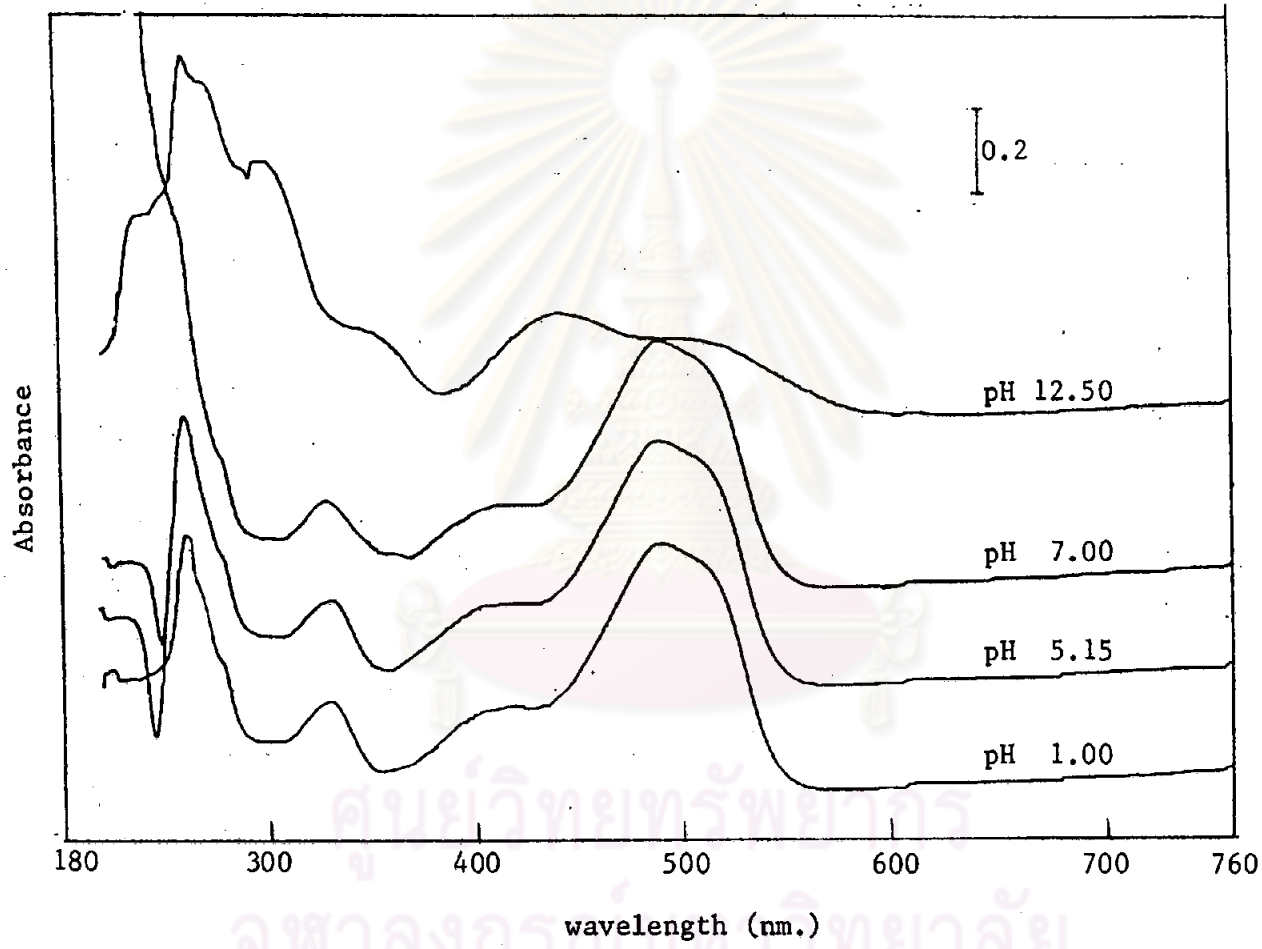

Figure 11D Absorption spectra of Orange RN at various pH values.

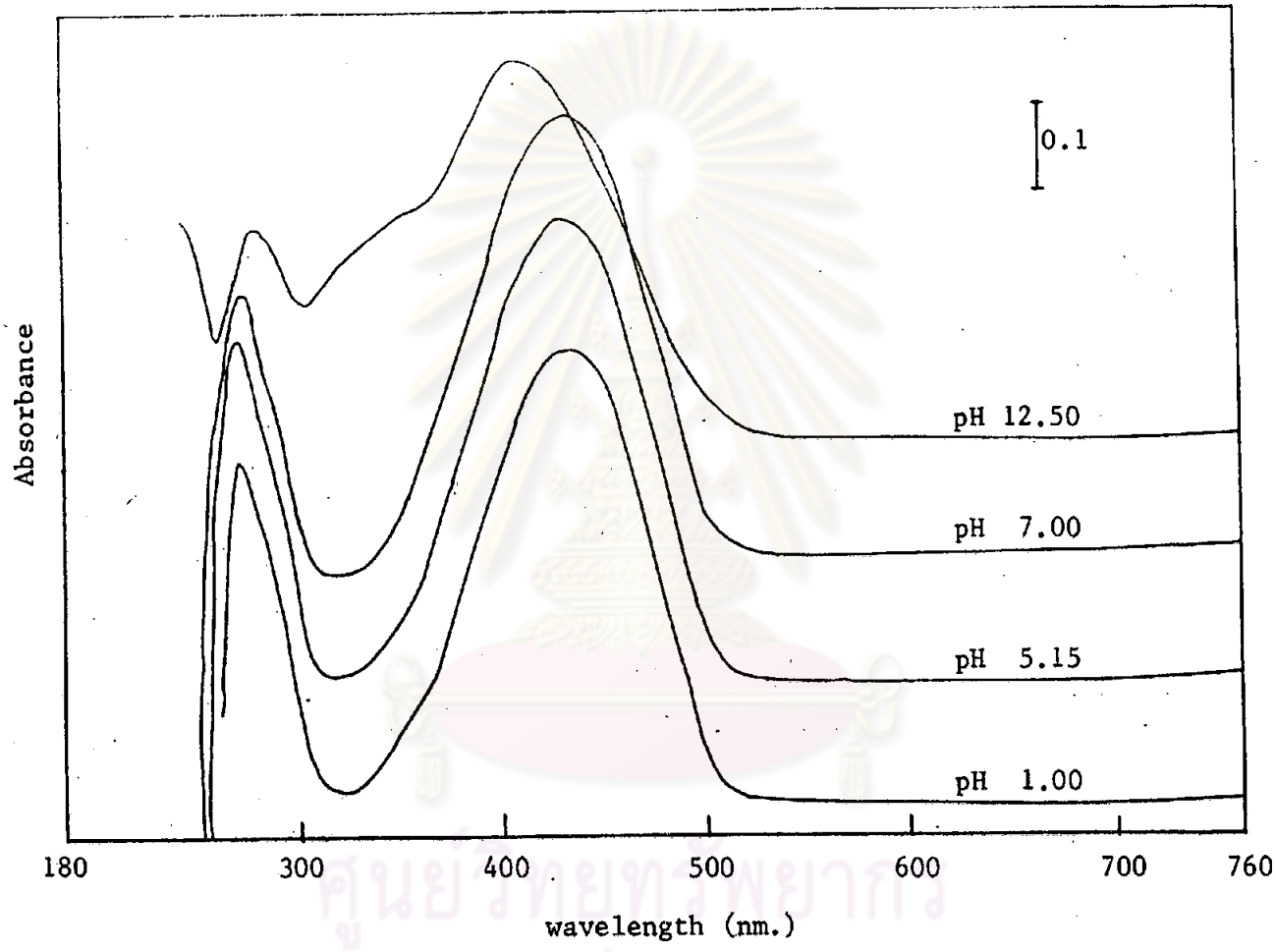

Figure 11E Absorption spectra of Tartrazine at various pH values.

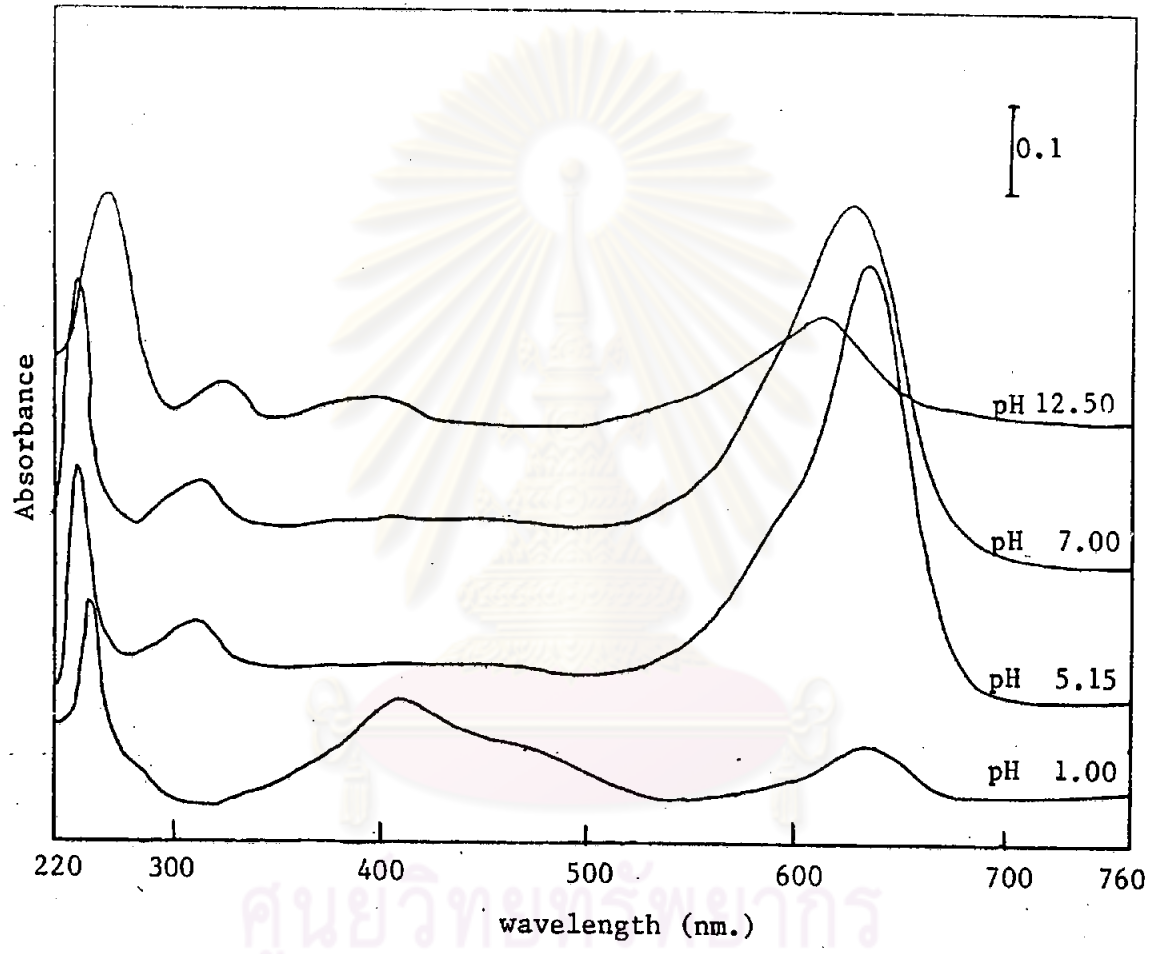

Figure 11F Absorption spectra of Green S at various pH values.

Table 7A Dependence of absorbances on concentrations of Azorubine at various pH values

10^5 x conc., M	Absorbance at 515 nm				
	pH 1.00	pH 3.10	pH 5.15	pH 7.00	pH 12.50
7.20	1.591	1.590	1.588	1.570	1.444
6.40	1.416	1.416	1.414	1.408	1.276
5.60	1.250	1.241	1.233	1.220	1.112
4.80	1.080	1.058	1.053	1.045	0.946
4.00	0.915	0.894	0.892	0.836	0.785
3.20	0.746	0.727	0.723	0.650	0.628
2.40	0.582	0.547	0.538	0.474	0.468
1.60	0.405	0.367	0.363	0.306	0.300
0.80	0.221	0.183	0.182	0.150	0.142

Table 7B Dependence of absorbances on concentrations of Tartrazine at various pH values

10^5 x conc., M	Absorbance at 432 nm				
	pH 1.00	pH 3.10	pH 5.15	pH 7.00	pH 12.50
4.50	1.060	1.039	1.029	1.029	0.807
4.00	0.940	0.929	0.919	0.916	0.722
3.50	0.823	0.812	0.800	0.800	0.640
3.00	0.720	0.700	0.687	0.685	0.560
2.50	0.595	0.583	0.564	0.562	0.477
2.00	0.468	0.464	0.450	0.448	0.385
1.50	0.360	0.350	0.343	0.340	0.303
1.00	0.240	0.235	0.228	0.226	0.222
0.50	0.122	0.120	0.117	0.113	0.056

Table 7C Dependence of absorbances on concentrations of Sunset Yellow FCF at various pH values

10^5 x conc., M	Absorbance at 482 nm				
	pH 1.00	pH 3.10	pH 5.15	pH 7.00	pH 12.50
5.00	1.053	1.047	1.040	1.030	0.598
4.50	0.970	0.946	0.941	0.930	0.526
4.00	0.840	0.827	0.825	0.801	0.465
3.50	0.756	0.751	0.742	0.735	0.416
3.00	0.611	0.611	0.612	0.600	0.344
2.50	0.532	0.530	0.529	0.526	0.302
2.00	0.431	0.426	0.422	0.420	0.251
1.50	0.320	0.317	0.313	0.310	0.191
1.00	0.212	0.210	0.210	0.202	0.134

Table 7D Dependence of absorbances on concentrations of Orange G at various pH values

10^5 x conc., M	Absorbance at 476 nm				
	pH 1.00	pH 3.10	pH 5.15	pH 7.00	pH 12.50
5.00	0.970	0.964	0.958	0.950	0.292
4.50	0.895	0.882	0.875	0.850	0.250
4.00	0.771	0.765	0.760	0.749	0.226
3.50	0.691	0.683	0.682	0.651	0.196
3.00	0.570	0.566	0.566	0.551	0.164
2.50	0.478	0.478	0.472	0.456	0.135
2.00	0.395	0.393	0.390	0.368	0.107
1.50	0.299	0.296	0.296	0.275	0.078
1.00	0.194	0.192	0.190	0.188	0.050

Table 7E Dependence of absorbances on concentrations of Orange RN at various pH values

10^5 x conc., M	Absorbance at 485 nm				
	pH 1.00	pH 3.10	pH 5.15	pH 7.00	pH 12.50
5.00	0.946	0.934	0.930	0.916	0.440
4.50	0.897	0.870	0.845	0.827	0.395
4.00	0.795	0.750	0.740	0.729	0.356
3.50	0.705	0.650	0.640	0.648	0.309
3.00	0.607	0.560	0.550	0.549	0.265
2.50	0.505	0.450	0.450	0.444	0.215
2.00	0.408	0.359	0.358	0.350	0.176
1.50	0.305	0.275	0.270	0.270	0.129
1.00	0.205	0.173	0.171	0.168	0.089

Table 7F Dependence of absorbances on concentrations of Green S at various pH values

10^5 x conc., M	Absorbance at 634 nm				
	pH 1.00	pH 3.10	pH 5.15	pH 7.00	pH 12.50
2.00	0.361	1.502	1.577	1.480	0.185
1.80	0.312	1.377	1.378	1.312	0.168
1.60	0.278	1.232	1.130	1.166	0.150
1.40	0.239	1.071	1.072	1.022	0.132
1.20	0.204	0.920	0.920	0.875	0.111
1.00	0.172	0.766	0.767	0.724	0.093
0.80	0.138	0.616	0.615	0.584	0.074
0.60	0.103	0.465	0.464	0.434	0.051
0.40	0.070	0.312	0.313	0.293	0.033

Table 8A Dependence of absorbances on pH of Azorubine solutions

pH	Absorbance at λmax = 515 nm	ΔA/ΔpH
12.00	0.584	
10.25	0.584	0.00
9.94	0.590	-0.020
9.73	0.585	-0.020
9.39	0.593	-0.020
7.83	0.628	-0.020
6.93	0.673	-0.050
6.00	0.674	-0.010
5.00	0.678	0.004
4.04	0.682	-0.004
3.00	0.688	-0.006
2.02	0.682	0.006
1.02	0.680	0.002

Table 8B Dependence of absorbances on pH of Sunset Yellow FCF solutions

pH	Absorbance at λmax = 482 nm	ΔA/ΔpH
12.07	0.181	
10.35	0.352	-0.099
10.02	0.382	-0.094
9.52	0.410	-0.054
7.82	0.421	-0.006
6.97	0.425	-0.005
6.02	0.436	-0.012
5.02	0.439	-0.003
4.06	0.439	0.000
3.03	0.431	0.008
2.04	0.430	0.010
1.03	0.422	0.011

Table 8C Dependence of absorbances on pH of Orange G solution.

pH	Absorbance at λmax = 476 nm	ΔA/ΔpH
12.50	0.110	
12.03	0.185	0.159
10.23	0.765	-0.322
10.07	0.768	-0.018
9.50	0.778	-0.017
8.07	0.782	-0.003
6.94	0.785	-0.003
6.02	0.785	0.000
5.02	0.782	0.003
4.07	0.783	0.002
3.04	0.783	0.000
2.04	0.783	0.000
1.18	0.779	0.003

Table 8D Dependence of absorbances on pH of Orange RN solutions.

pH	absorbance at λmax = 485 nm	ΔA/ΔpH
13.93	0.217	
12.16	0.515	-0.168
11.62	0.590	-0.139
10.30	0.639	-0.565
9.90	0.642	-0.007
8.88	0.642	0.000
7.99	0.643	-0.001
7.00	0.640	0.003
6.03	0.635	0.005
5.01	0.635	0.000
4.02	0.635	0.000
3.00	0.635	0.000
2.00	0.635	0.000
1.00	0.635	0.000

Table 8E Dependence of absorbances on pH of Tartrazine solutions

pH	absorbance at λmax = 432 nm	ΔA/ΔpH
12.02	0.544	
10.11	0.648	-0.054
9.75	0.725	-0.214
9.10	0.824	-0.150
9.81	0.880	-0.040
6.95	0.892	-0.014
6.00	0.892	0.000
5.02	0.883	0.009
4.06	0.883	0.000
3.03	0.870	0.013
2.06	0.857	0.013
1.18	0.825	0.036

Table 8F Dependence of absorbances on pH of Green S solutions

pH	absorbance at λmax = 634 nm	ΔA/ΔpH
12.02	0.260	
10.23	0.331	-0.040
9.90	0.335	-0.009
9.20	0.352	-0.024
7.85	0.457	-0.078
6.97	0.586	-0.146
6.04	0.638	-0.056
5.06	0.647	-0.009
4.15	0.651	-0.004
3.16	0.631	0.002
2.20	0.521	0.114
1.32	0.244	0.315

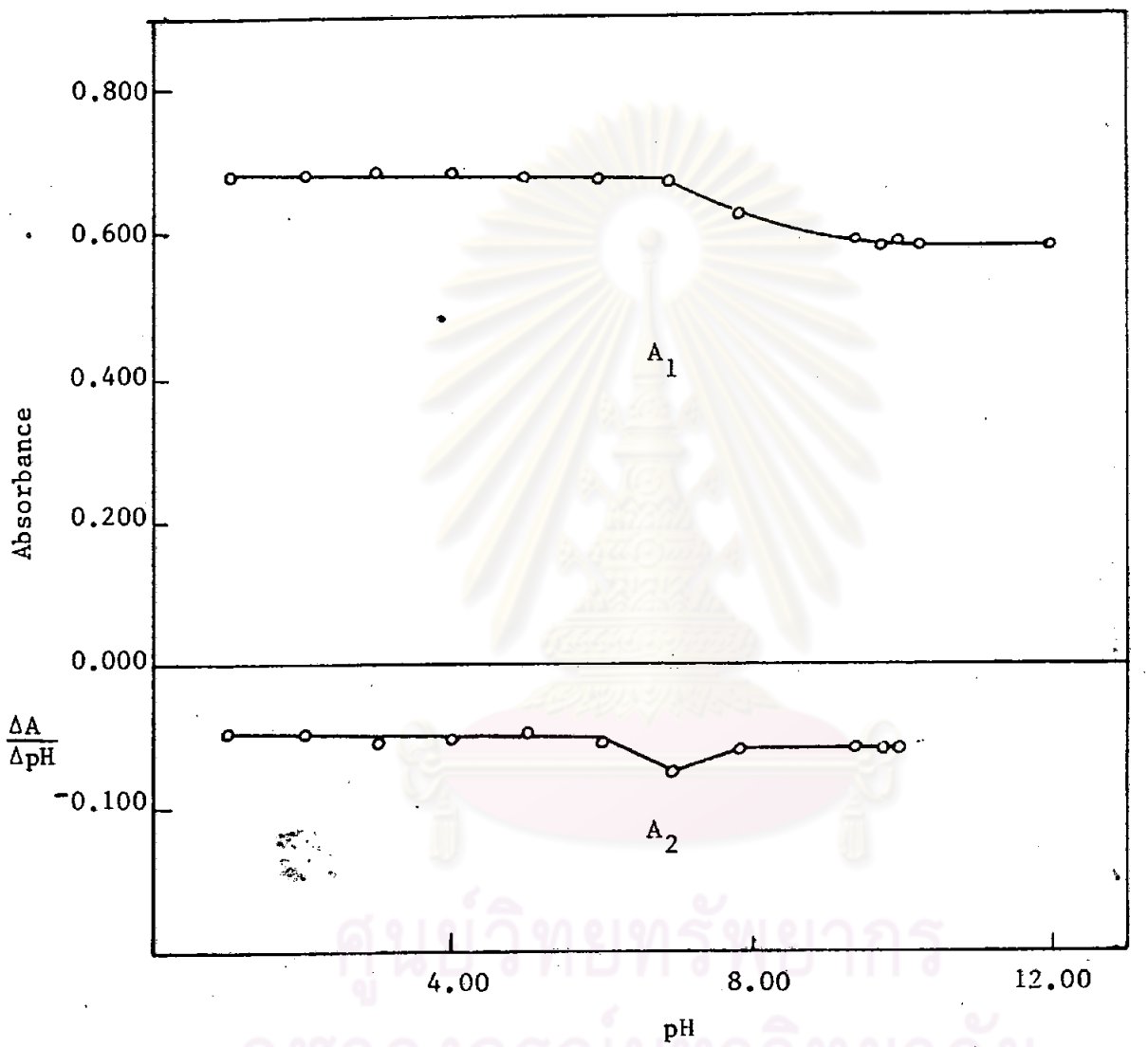

Figure 12A Determination of pKa value for Azorubine by visible spectrophotometric data;

A_1) absorbance VS pH and A_2) $\Delta A/\Delta pH$ VS pH

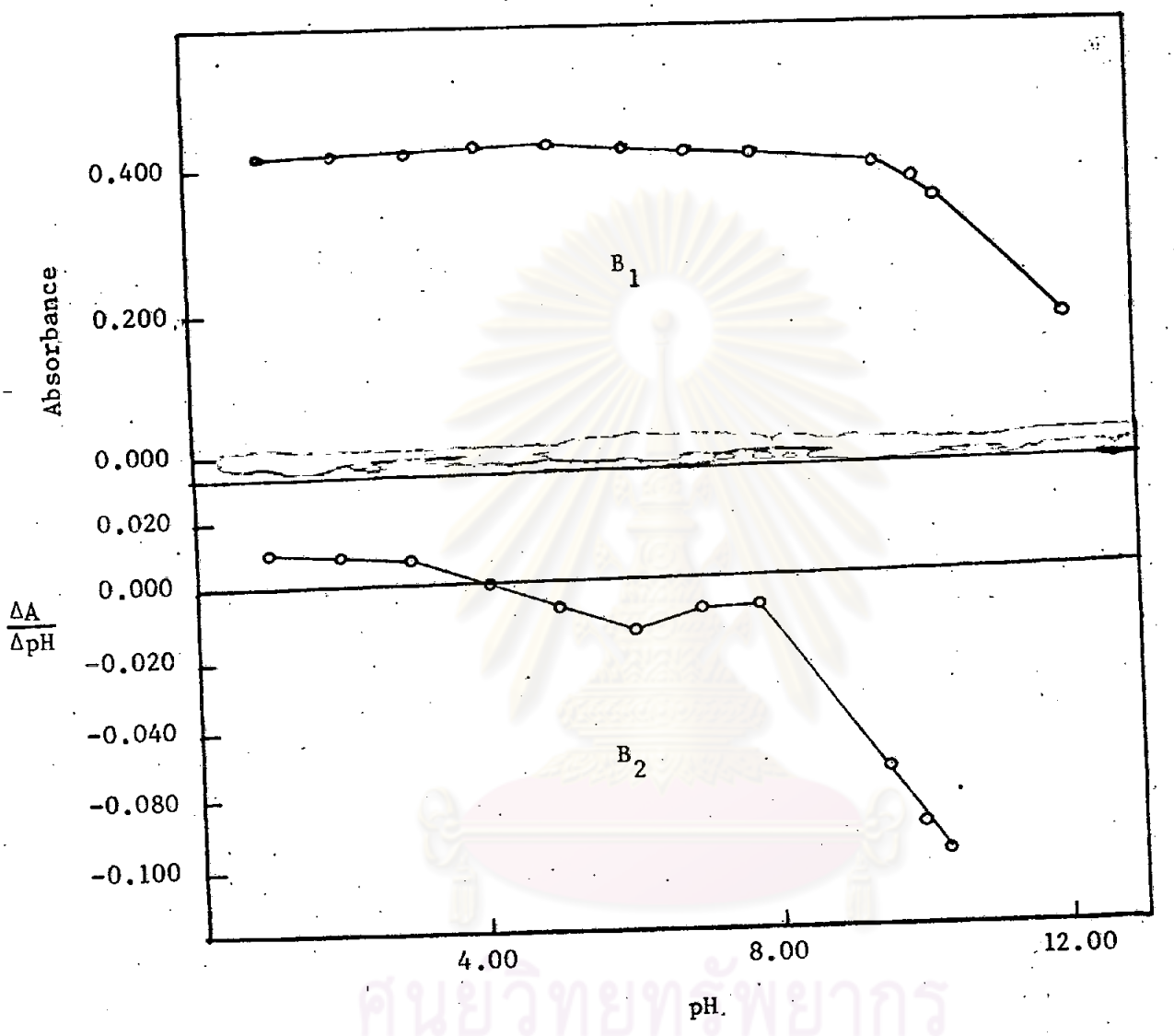

Figure 12B Determination of pKa value for Sunset Yellow FCF by visible spectrophotometric data;

B_1) absorbance VS pH and B_2) $\Delta A/\Delta pH$ VS pH

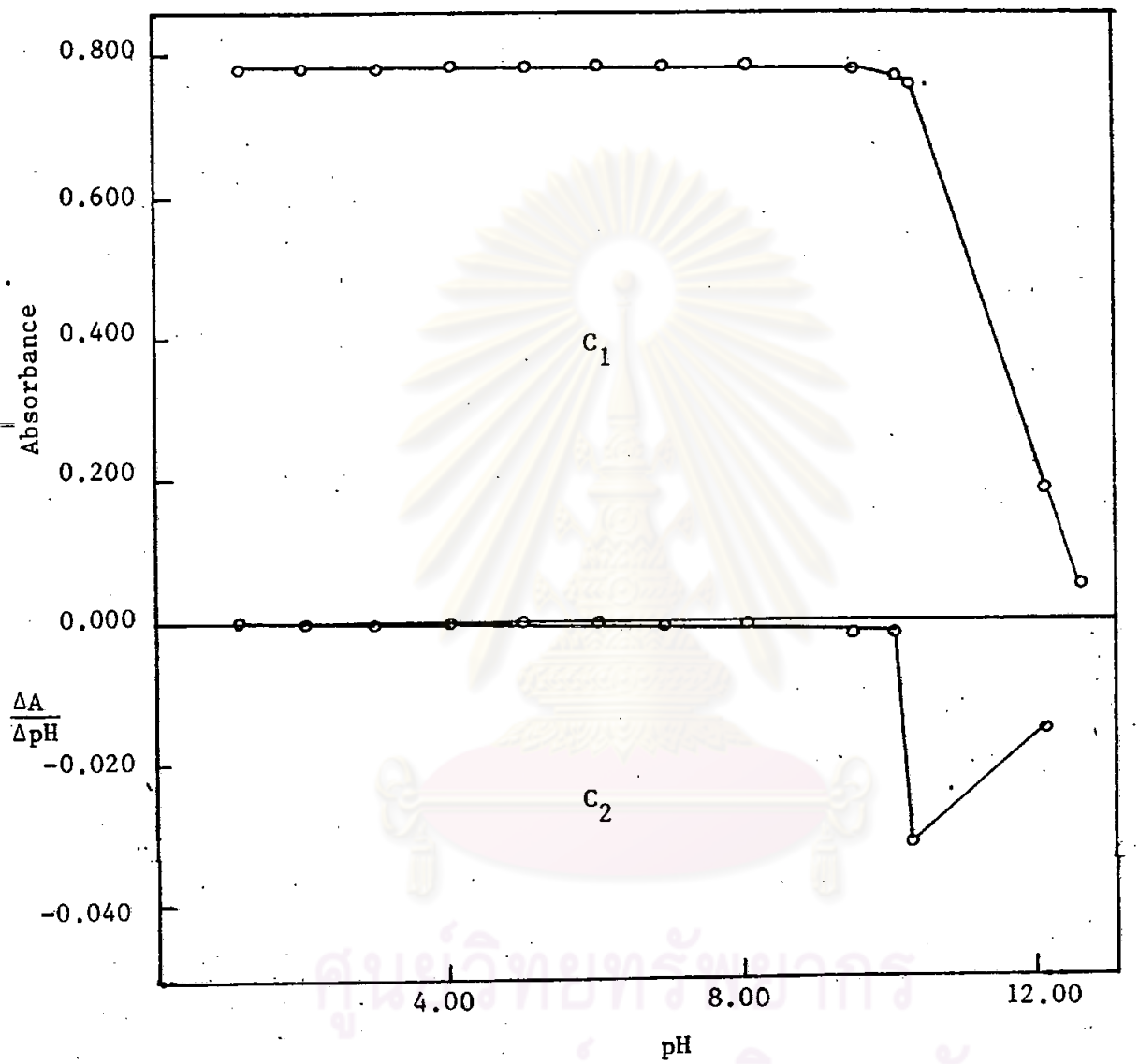

Figure 12C Determination of pKa value for Orange G by visible spectophotometric data;

C_1) absorbance VS pH and C_2) $\Delta A/\Delta pH$ VS pH

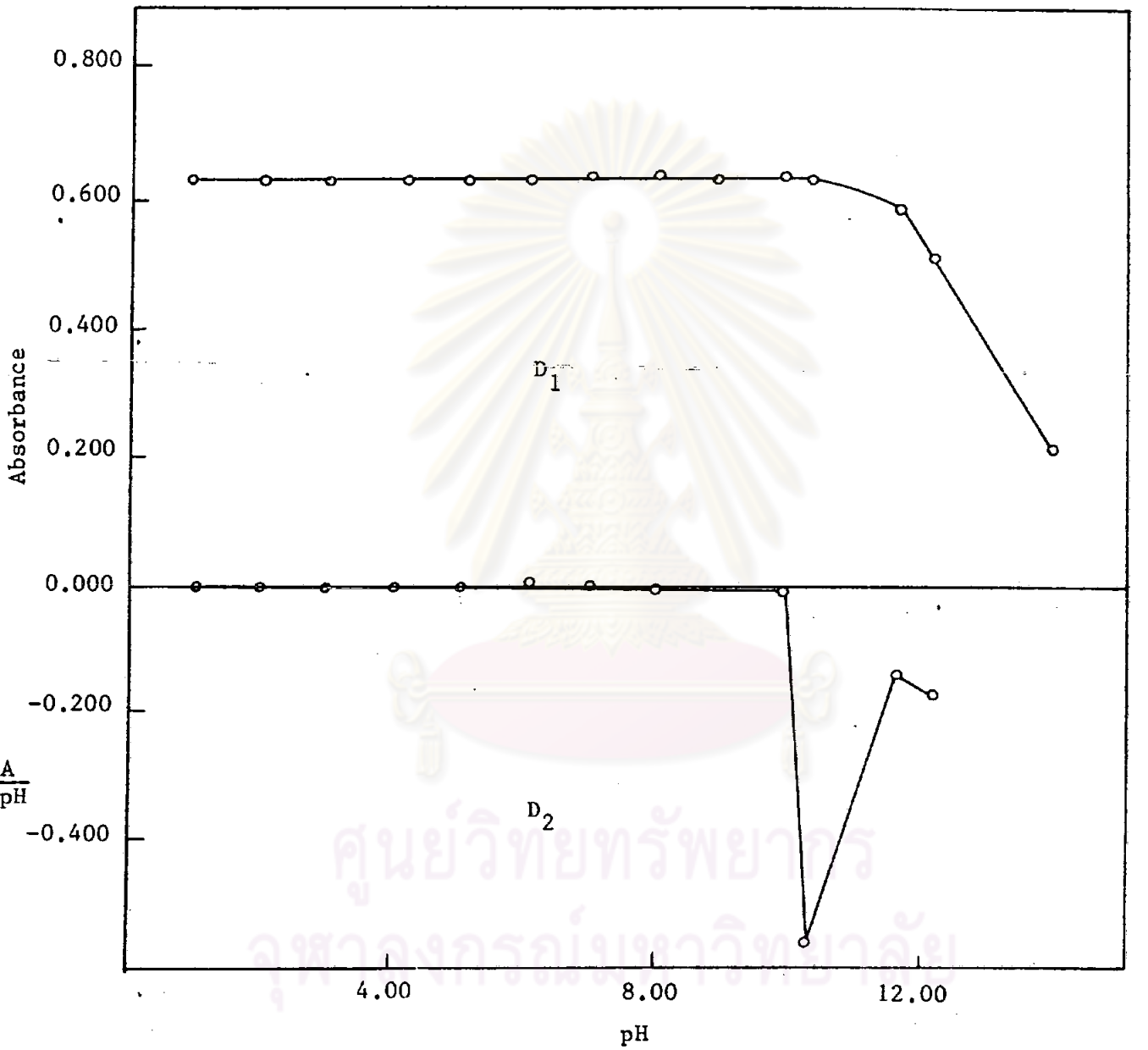

Figure 12D Determination of pKa value for Orange RN by visible spectrophotometric data;

D_1) absorbance VS pH and D_2) $\Delta A/\Delta pH$ VS pH

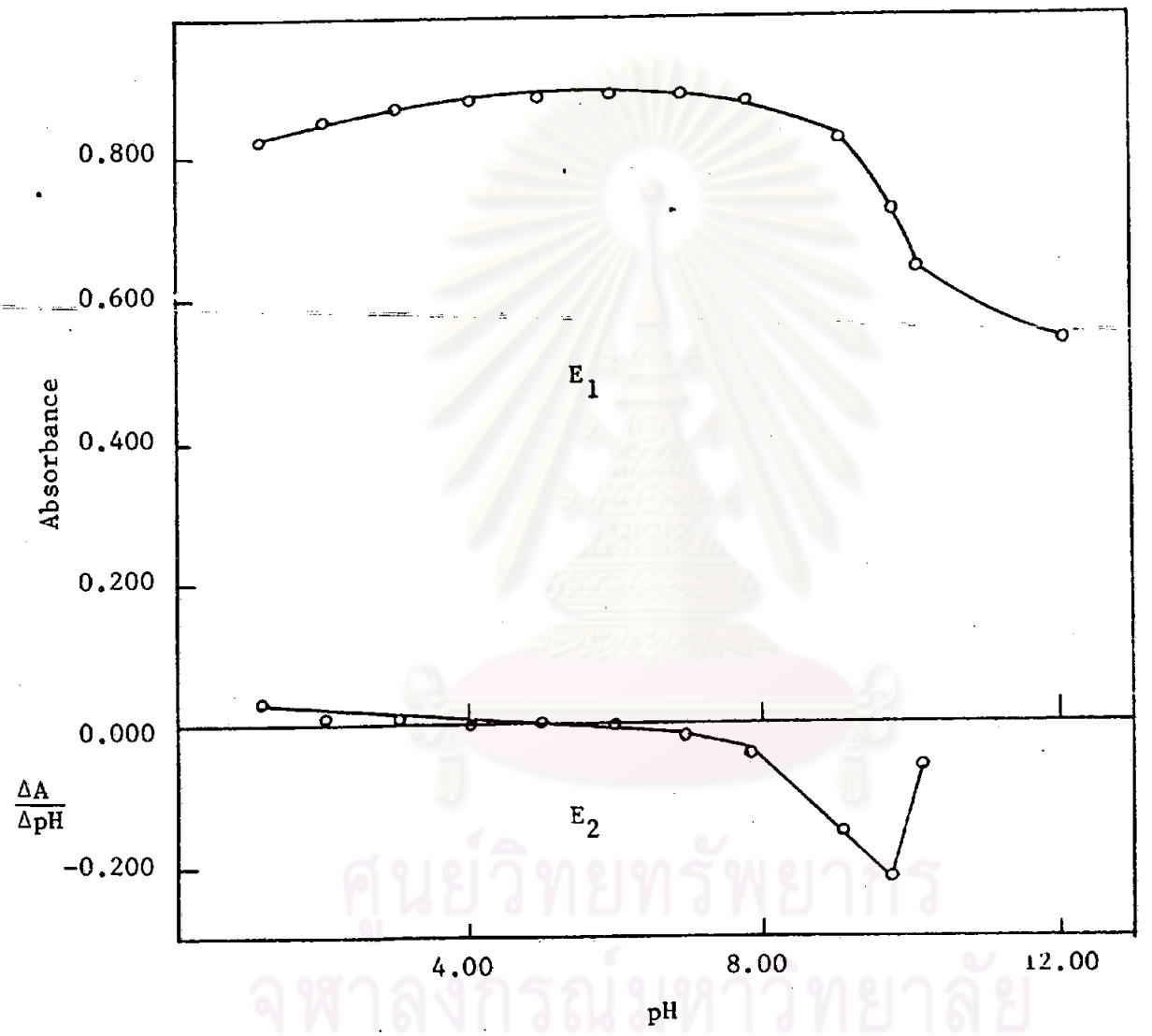

Figure 12E Determination of pKa value for Tartrazine by visible spectrophotometric data;

E_1) absorbance VS pH and E_2) $\Delta A/\Delta pH$ VS pH

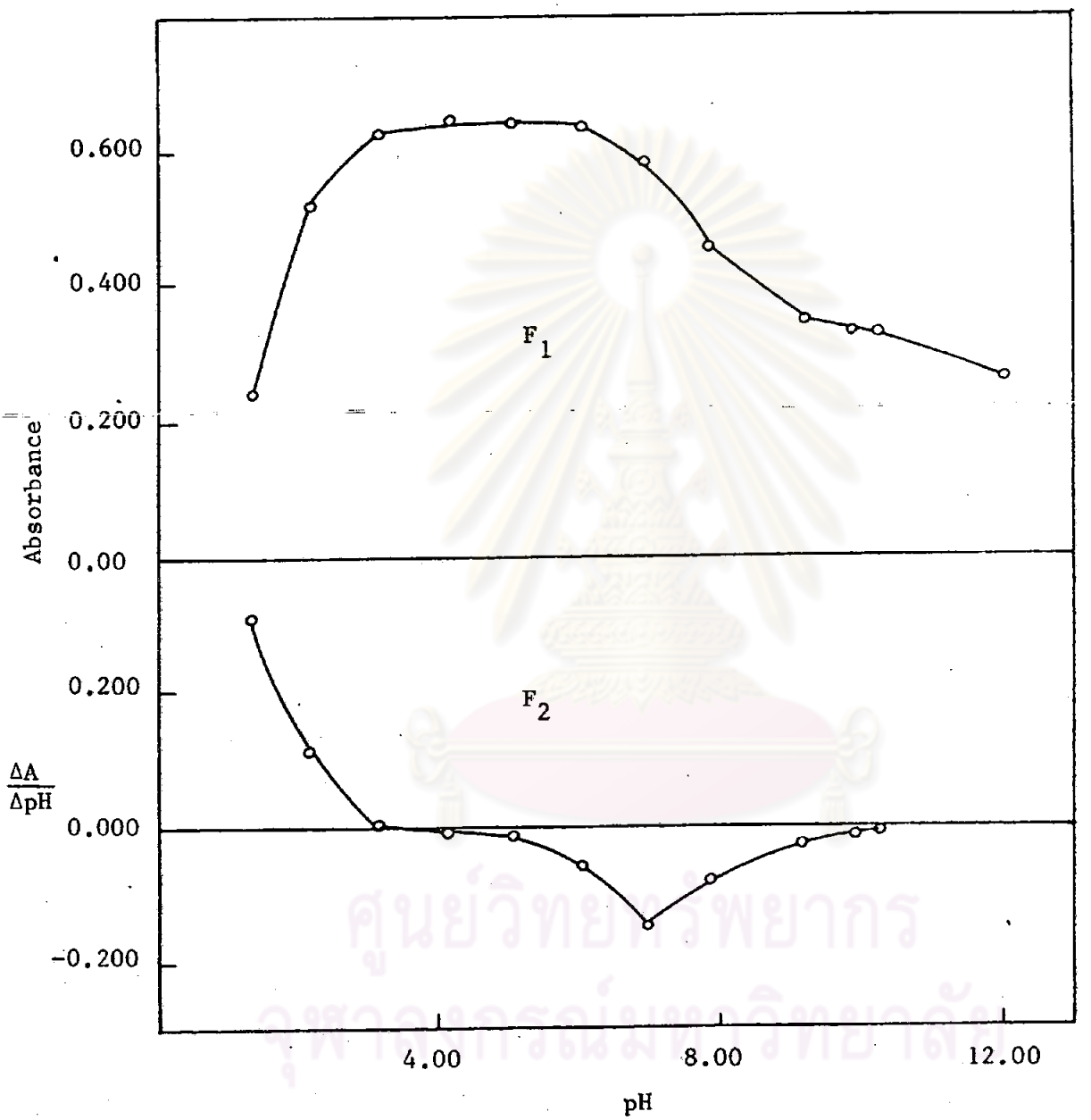

Figure 12F Determination of pKa value of Green S by visible spectrophotometric data;

F_1) absorbance VS pH and F_2) $\Delta A/\Delta pH$ VS pH

Table 9A Dependence of absorbances on concentrations of dyes in aqueous solution

10^5 x conc., M	Absorbance				
	Azorubine	Sunset Yellow FCF	Orange G	Orange RN	Tartrazine
	at λmax 515 nm	at λmax 482 nm	at λmax 476 nm	at λmax 485 nm	at λmax 432 nm
0.40	0.091	0.080	0.070	0.072	0.098
1.20	0.278	0.240	0.220	0.230	0.298
2.00	0.442	0.410	0.365	0.372	0.500
2.80	0.620	0.573	0.518	0.520	0.660
3.60	0.780	0.740	0.660	0.662	0.840
4.40	0.950	0.890	0.800	0.810	1.000
5.20	1.100	1.030	0.940	0.930	1.180
5.60	1.190	1.110	1.010	1.000	1.220
6.00	1.210	1.200	1.070	1.080	1.300
6.40	1.300	1.280	1.130	1.130	-
6.80	1.400	1.310	1.200	1.190	-
7.00	1.350	-	1.270	1.220	-

- not measure

Table 9B Dependence of absorbances on concentrations of Green S in aqueous solution

10^6 x conc., M	absorbance at λmax 634 nm
2.00	0.16
4.00	0.322
6.00	0.480
8.00	0.641
10.00	0.800
12.00	0.940
14.00	1.100
16.00	1.260
18.00	1.450
20.00	1.500
24.00	1.737
26.00	1.922

observed. The dependences of the absorbances on concentrations of Azorubine, Sunset Yellow FCF, Orange G and Orange RN in the acetate buffer and phosphate buffer at the pH mentioned were studied. In the acetate buffer pH 5.10 or 6.10 the absorbance of Azorubine solution is directly proportional to its concentration in the range of 0.80×10^{-5} M - 5.60×10^{-5} M as well as in the phosphate buffer pH 5.85 or 7.00 the absorbance of Azorubine solution is directly proportional to its concentration in the range of 0.80×10^{-5} M - 5.60×10^{-5} M. The absorbances of Sunset Yellow FCF, Orange G, Orange RN in the acetate buffer pH 4.00, 5.10 or 6.10 are directly proportional to the concentrations in the range of 0.80×10^{-5} M - 5.60×10^{-5} M. At higher concentrations, curvatures were shown owing to the deviation from Beer's law (see Tables 10A-10D and Figures 13A-13D).

3.6 Dependence of absorbances on concentrations of the metal ion solutions

Since Azorubine reacted only with Cu (II) ion in the acetate buffer pH 6.10, 5.10 and phosphate buffer pH 7.00, 5.85 and Sunset Yellow FCF, Orange G, Orange RN also reacted only with Cu (II) ion in the acetate buffer pH 6.10, 5.10 or 4.00, the relationship between absorbances and concentrations of Cu (II) ion solution in these buffers and in water were studied. A linear relationship between absorbances and concentrations of Cu (II) ion solutions in every system studied was obtained in the range of concentration 2.00-8.00 $\mu g/cm^3$ (see Table 11 and Figure 14).

3.7 Complex formations between dyes and metal ions

3.7.1 The mixtures of Azorubine and Ti (IV), Cr (III), Mn (II), Co (II), Fe (II), Fe (III), Ni (II), or Zn (II)

The absorption spectra of the mixtures of Azorubine and each metal ion in the buffer systems such as phosphoric acid, acetic acid, McIlvaine buffer, phosphate buffer and diethylamine were recorded in the

Table 10A Dependence of absorbances on concentrations of Azorubine in various buffer system

10^5 x conc., M	A at 515 nm				
	phosphate buffer		acetate buffer		
	pH 7.00	pH 5.85	pH 6.10	pH 5.10	pH 4.00
0.80	0.215	0.220	0.218	0.219	0.219
1.60	0.424	0.441	0.429	0.434	0.442
2.40	0.636	0.643	0.631	0.648	0.652
3.20	0.844	0.868	0.856	0.866	0.872
4.00	1.055	1.079	1.070	1.073	1.084
4.80	1.260	1.290	1.280	1.282	1.294
5.60	1.467	1.480	1.493	1.501	1.507
6.40	1.625	1.640	1.632	1.635	1.638
7.20	1.740	1.752	1.748	1.753	1.764
8.00	1.822	1.835	1.830	1.840	1.847
8.50	1.900	1.940	1.925	1.931	1.934

Table 10B Dependence of absorbances on concentrations of Sunset Yellow FCF in the acetate buffer

10^5 x conc., M	A at 482 nm		
	pH 6.10	pH 5.10	pH 4.00
0.80	0.205	0.204	0.204
1.60	0.403	0.408	0.408
2.40	0.603	0.607	0.612
3.20	0.806	0.808	0.810
4.00	1.007	1.006	1.014
4.80	1.205	1.208	1.211
5.60	1.399	1.406	1.415
6.40	1.498	1.495	1.499
7.20	1.600	1.610	1.616
8.00	1.720	1.724	1.730
8.50	1.753	1.755	1.763

Table 10C Dependence of absorbances on concentrations of Orange G in the acetate buffer

10^5 x conc., M	A at 476 nm		
	pH 6.10	pH 5.10	pH 4.00
0.80	0.176	0.177	0.176
1.60	0.350	0.352	0.350
2.40	0.526	0.525	0.524
3.20	0.701	0.698	0.699
4.00	0.880	0.879	0.879
4.80	1.053	1.060	1.058
5.60	1.224	1.232	1.231
6.40	1.345	1.348	1.347
7.20	1.460	1.465	1.466
8.00	1.564	1.567	1.568
8.50	1.607	1.610	1.612

Table 10D Dependence of absorbances on concentrations of Orange RN in the acetate buffer

10^5 x conc., M	A at 482 nm		
	pH 6.10	pH 5.10	pH 4.00
0.80	0.157	0.161	0.160
1.60	0.312	0.316	0.318
2.40	0.463	0.471	0.474
3.20	0.616	0.630	0.630
4.00	0.765	0.780	0.786
4.80	0.914	0.933	0.940
5.60	1.062	1.087	1.096
6.40	1.200	1.215	1.218
7.20	1.335	1.343	1.346
8.00	1.420	1.428	1.432
8.50	1.476	1.484	1.490

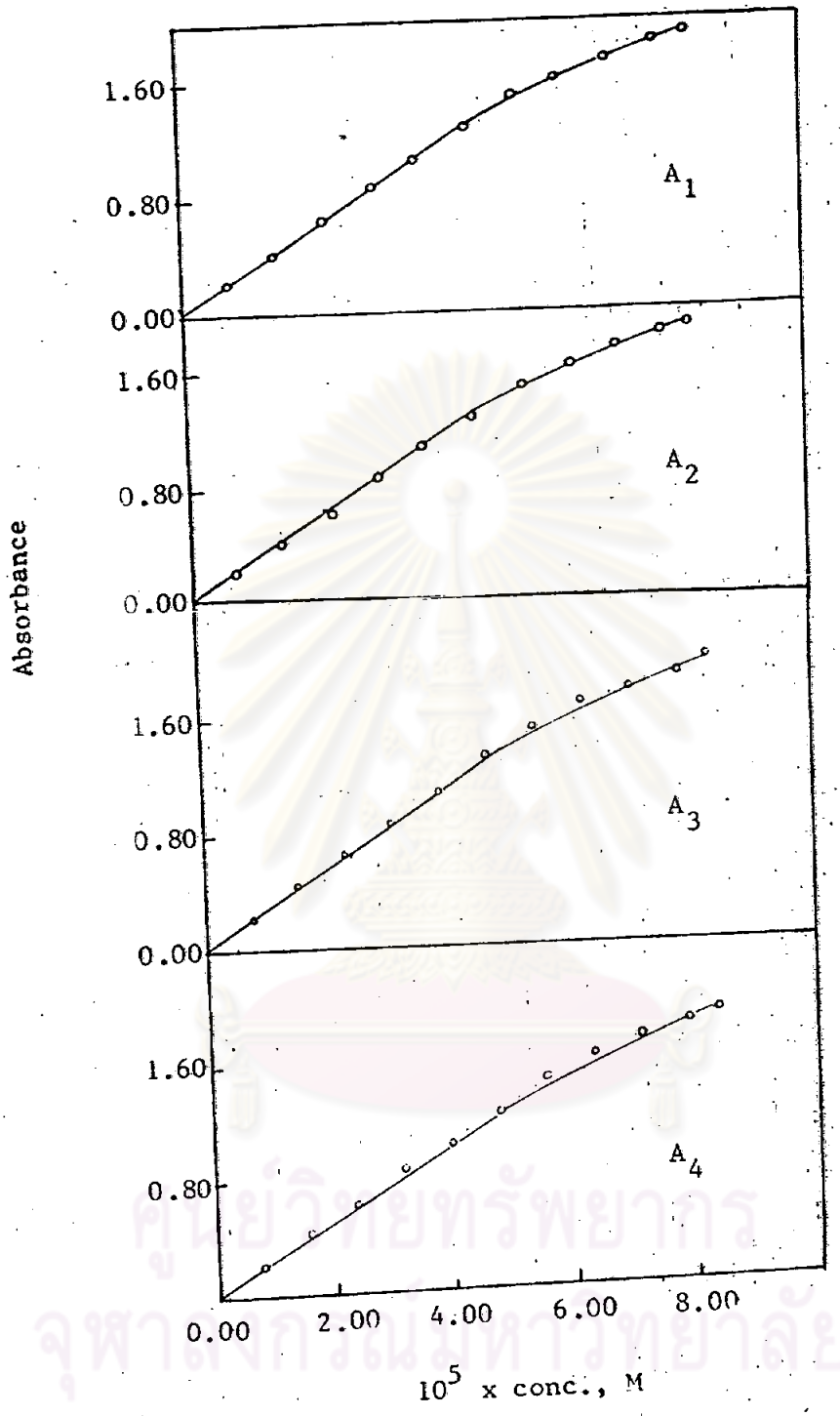

Figure 13A Dependences of absorbances on concentrations of Azorubine in the acetate buffer and phosphate buffer at pH A_1) 5.10, A_2) 6.10, A_3) 5.85 and A_4) 7.00

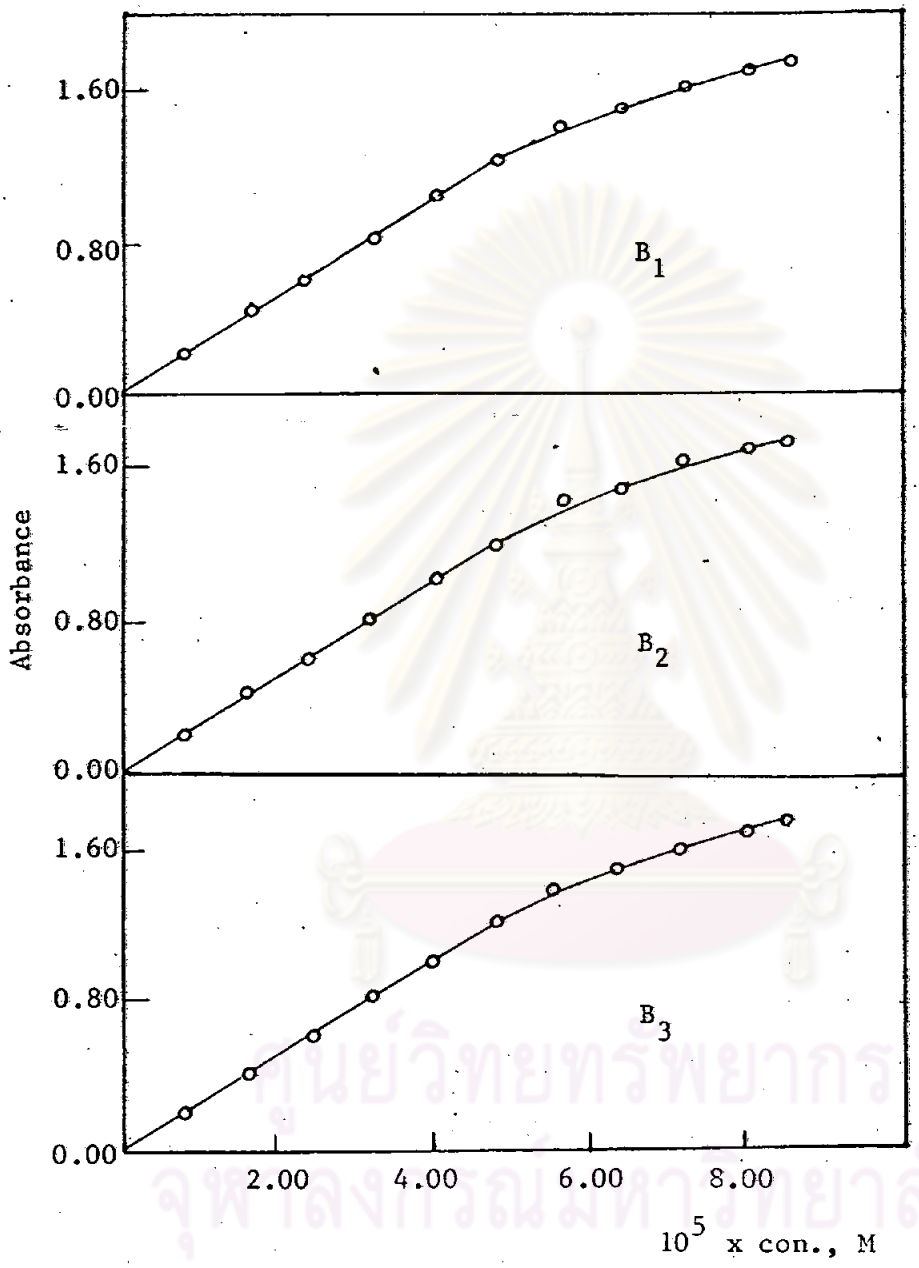

Figure 13B Dependences of absorbances on concentrations of Sunset Yellow FCF in the acetate buffer at pH B_1) 4.00, B_2) 5.10 and B_3) 6.10

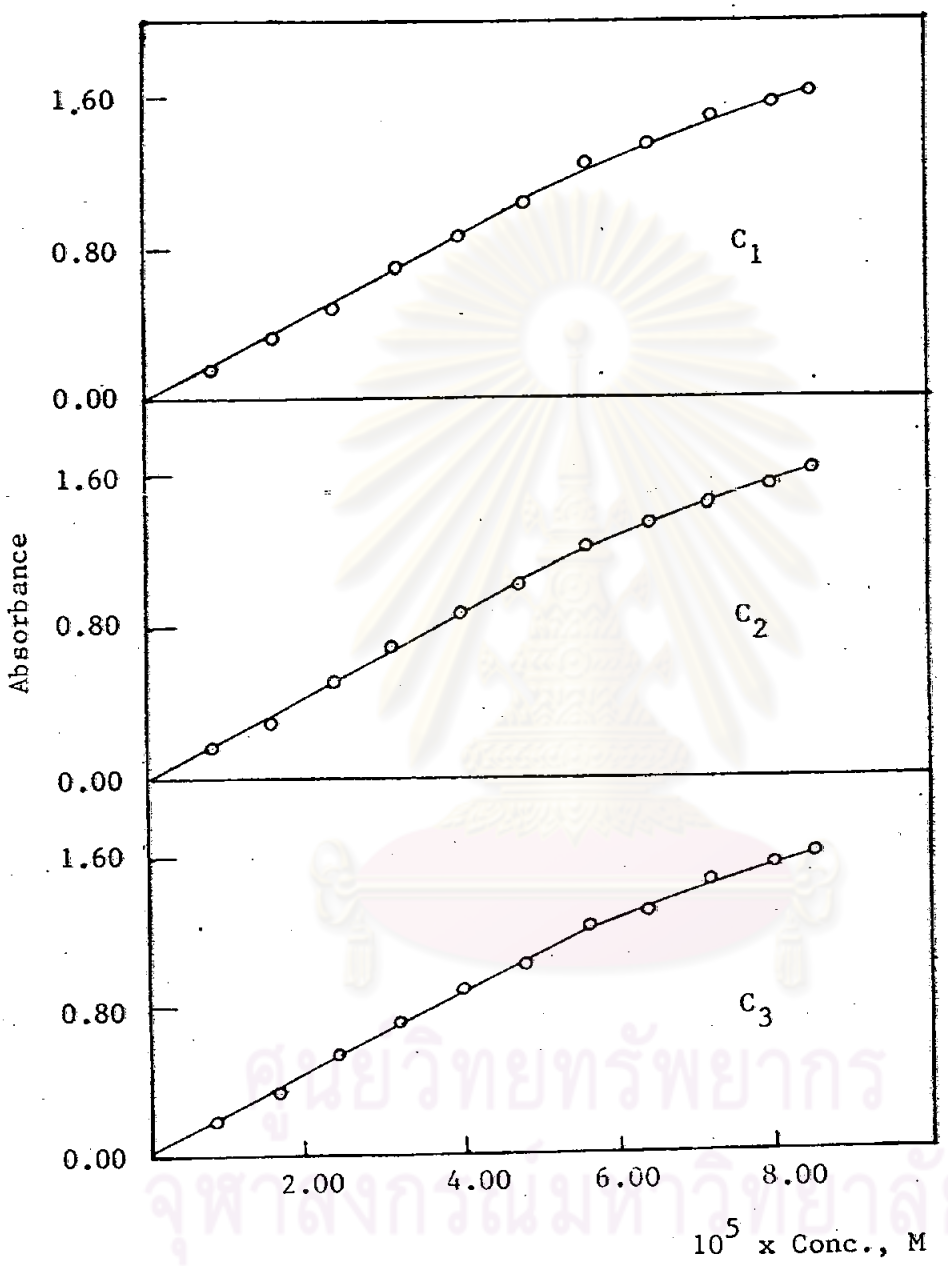

Figure 13C Dependences of absorbances on concentrations of Orange G in the acetate buffer at pH C_1) 4.00, C_2) 5.10 and C_3) 6.10.

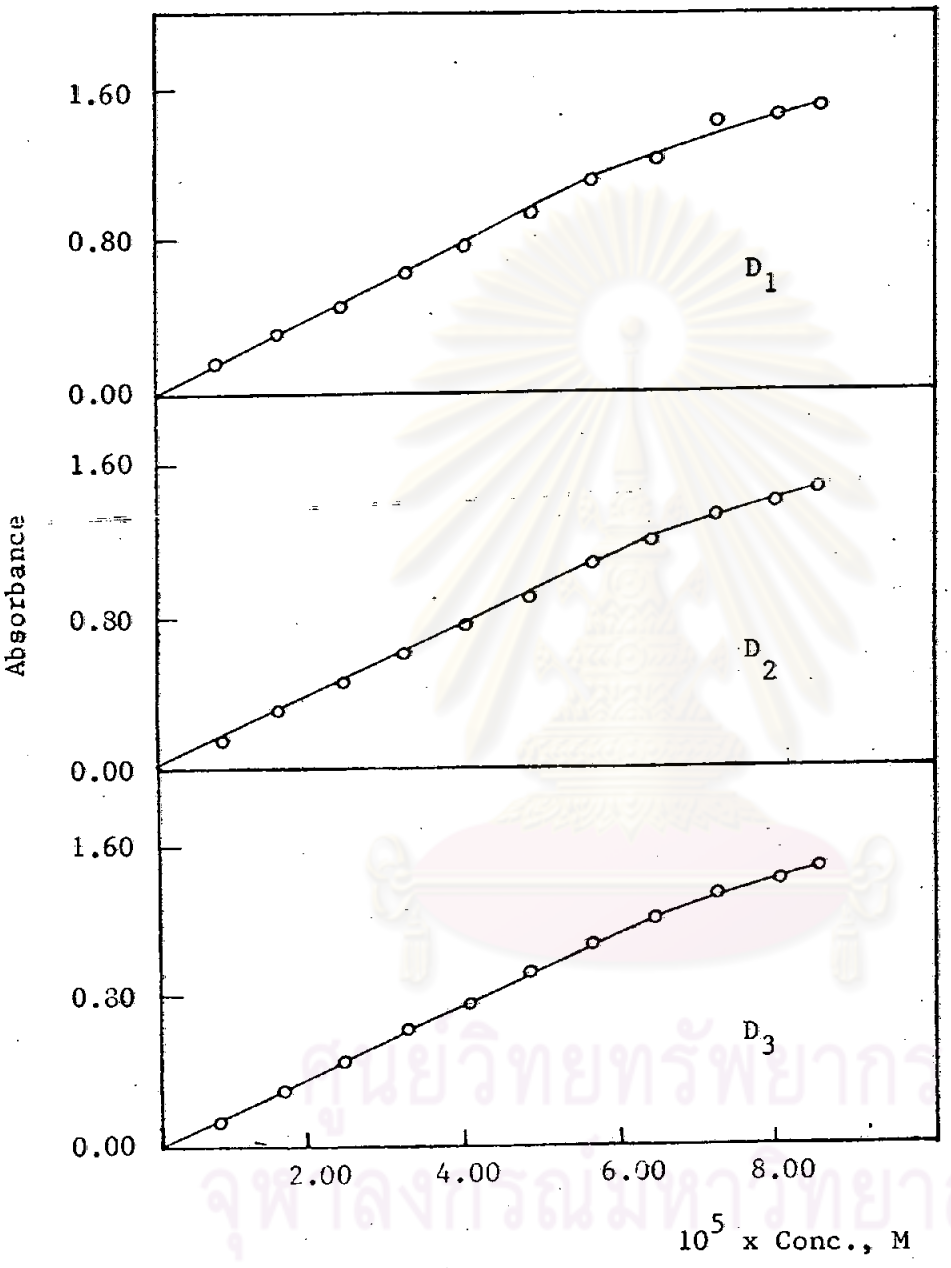

Figure 13D Dependences of absorbances on concentrations of Orange RN in the acetate buffer at pH D_1) 4.00, D_2) 5.10 and D_3) 6.10.

Table 11 Dependences of absorbances on concentrations of Cu (II) ion in the phosphate and the acetate buffer

conc., $\mu g/cm^3$	in water	Absorbance at 324.7 nm				
		phosphate buffer		acetate buffer		
		pH 7.00	pH 5.85	pH 6.10	pH 5.10	pH 4.00
2.00	0.117	0.118	0.118	0.117	0.117	0.118
4.00	0.229	0.235	0.235	0.232	0.230	0.232
6.00	0.339	0.348	0.343	0.340	0.343	0.343
8.00	0.453	0.461	0.461	0.458	0.460	0.460
10.00	0.562	0.586	0.566	0.562	0.568	0.570
12.00	0.660	0.665	0.667	0.663	0.662	0.665
14.00	0.772	0.774	0.775	0.772	0.778	0.780
15.00	0.812	0.815	0.816	0.813	0.817	0.822
18.00	0.853	0.856	0.858	0.854	0.852	0.860

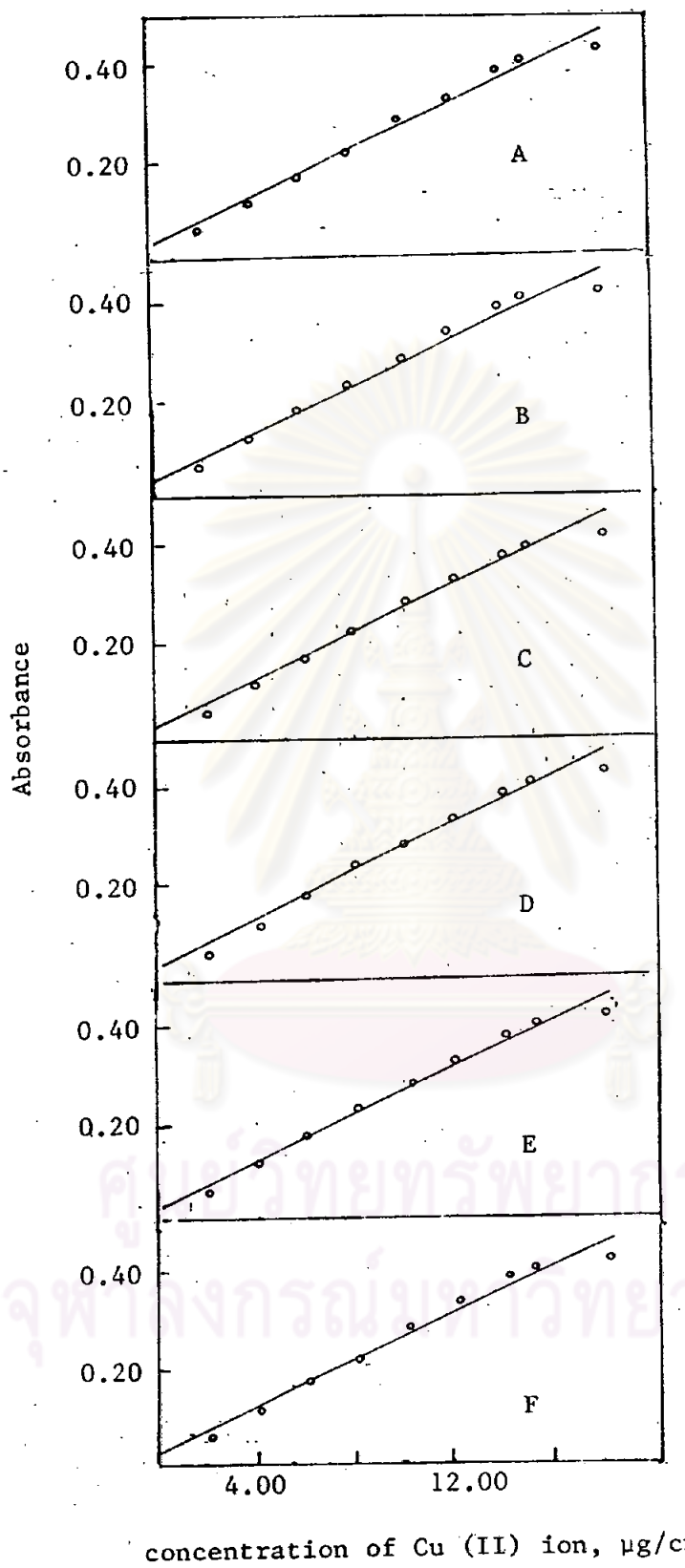

Figure 14 Dependences of absorbances on concentrations of Cu (II) ion A) in water, B) in phosphate buffer pH 7.00, C) in phosphate buffer pH 5.85, D) in acetate buffer pH 6.10, E) in acetate buffer pH 5.10 and F) in acetate buffer pH 4.00

range of wavelengths between 220-760 nm as shown in Figures 15A-15H. The spectra of the metal ion-Azorubine mixtures were not different from that of the dye solution and no physical change in each mixture was observed. This meant that no reaction between Azorubine and Ti (IV), Cr (III), Mn (II), Co (II), Fe (II), Fe (III), Ni (II), or Zn (II) ion occurred in each mixture system. Thus, no complex formed in the solution mixtures of Azorubine and Ti (IV), Cr (III), Mn (II), Co (II), Fe (II), Fe (III), Ni (II), or Zn (II) ion in the buffer systems such as phosphoric acid, acetic acid, McIlvaine buffer, phosphate buffer, diethylamine.

3.7.2 The mixtures of Azorubine and Cu (II) ion

The absorption spectra of the mixtures of Azorubine and Cu (II) ion in phosphoric acid, acetic acid, McIlvaine buffer, phosphate buffer, acetate buffer and diethylamine were recorded in the range of wavelengths between 220-760 nm as shown in Figures 15A-15J. The spectra of Cu (II) ion-Azorubine mixtures in the buffer solutions such as phosphoric acid, acetic acid, McIlvaine buffer, diethylamine were not different from that of the dye solution and no physical change in each mixture was observed. This meant that no reaction between Azorubine and Cu (II) ion occurred and no complex formed in the buffer solutions such as phosphoric acid, acetic acid, McIlvaine buffer and diethylamine. However, in the phosphate buffer pH 7.00, 5.85 and the acetate buffer pH 6.10, 5.10 it was found that Azorubine reacted with Cu (II) ion since the color of the mixture solutions changed from red to orange, the absorption peak shifted to the lower wavelength and the strong absorption of Cu (II) ion-Azorubine mixture appeared in the ultraviolet region (see Figures 15F-15G and Figures 15I-15J)

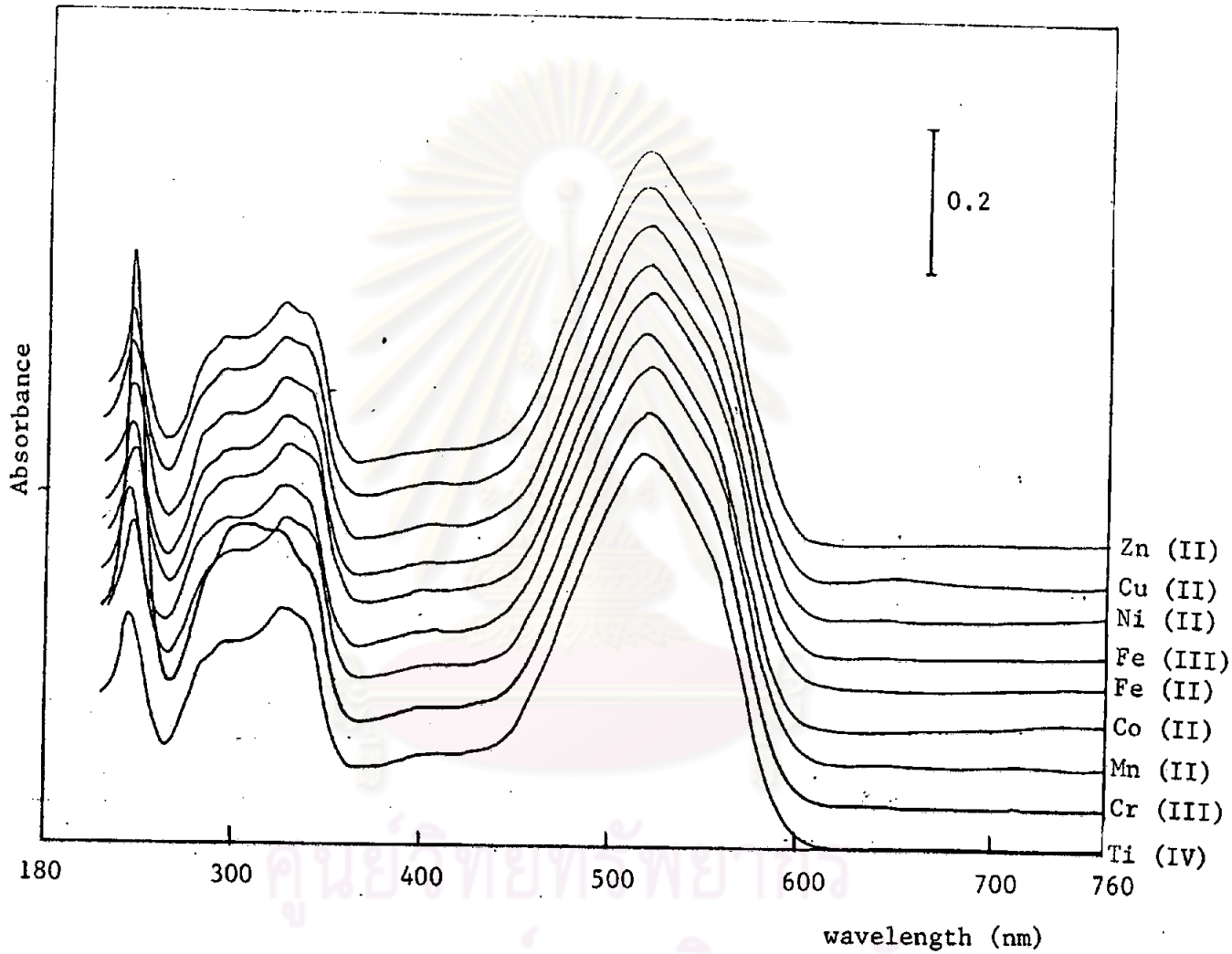

Figure 15A The UV-Visible absorption spectra of the mixture of Azorubine and metal ions in the acetic acid at pH 2.30.

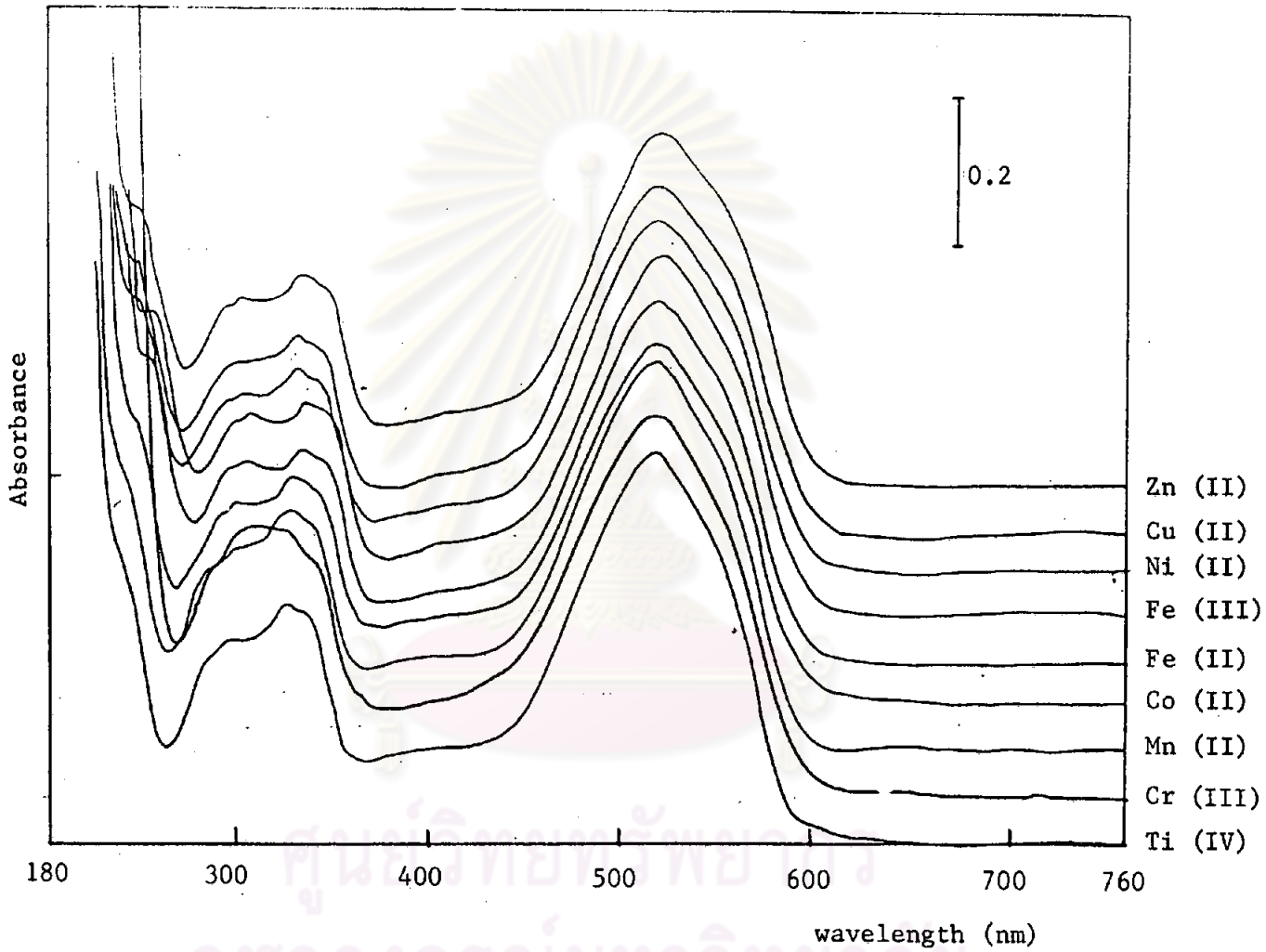

Figure 15B The UV-Visible absorption spectra of the mixture of Azorubine and metal ions in the phosphoric acid at pH 1.00.

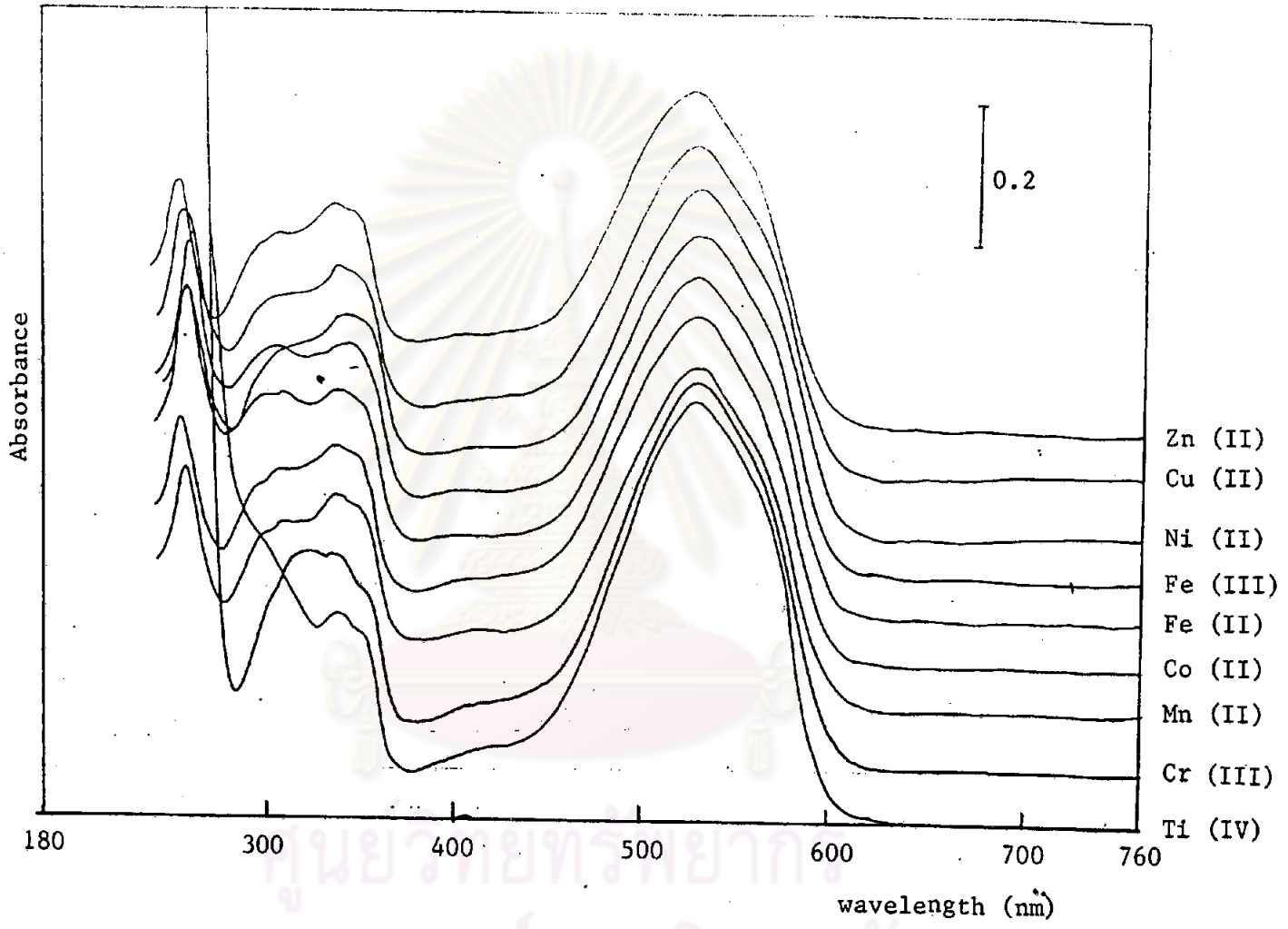

Figure 15C The UV-Visible absorption spectra of the mixture of Azorubine and metal ions in the McIlvaine buffer at pH 3.10.

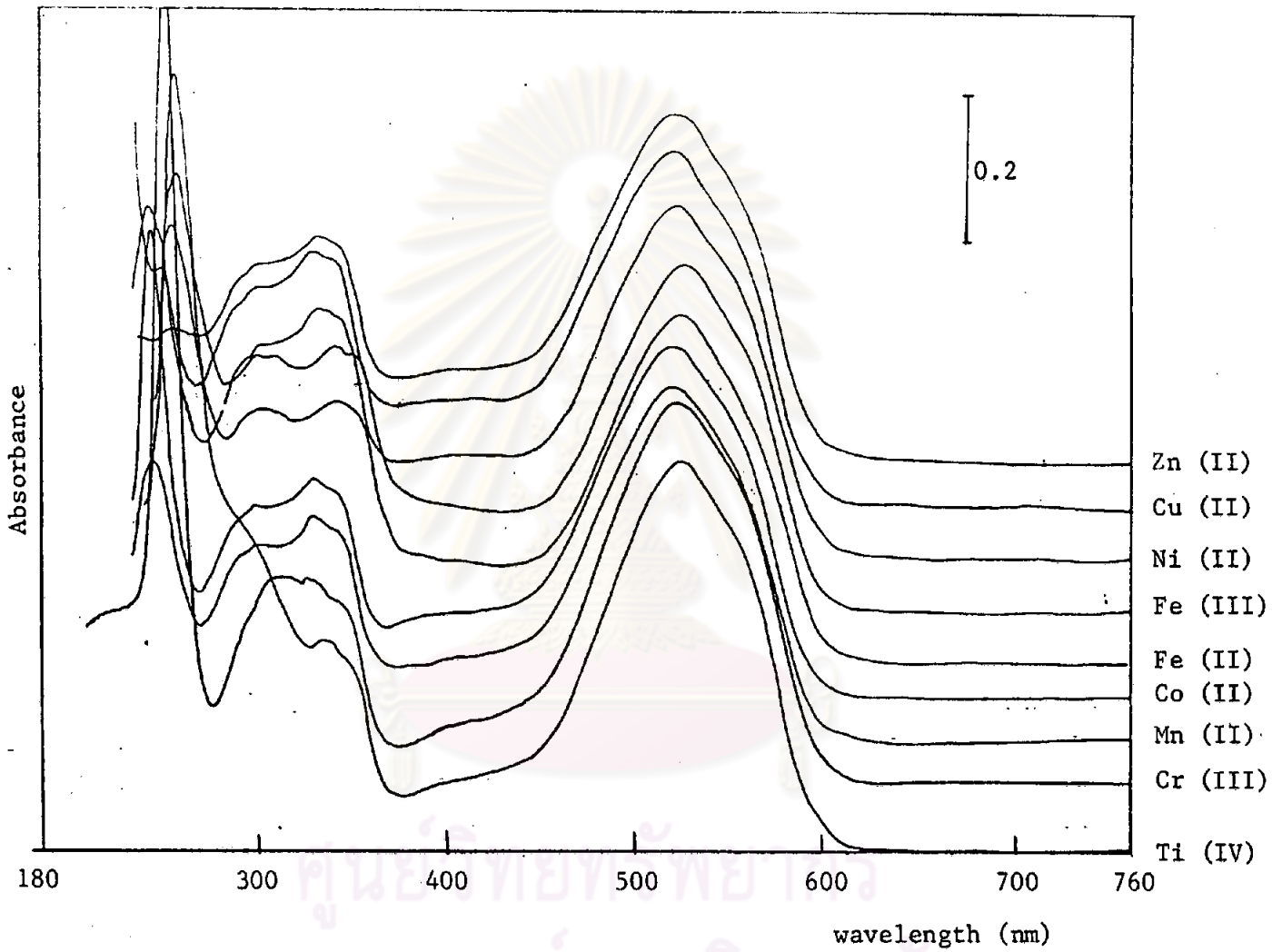

Figure 15D The UV-Visible absorptions spectra of the mixture of Azorubine and metal ions in the McIlvaine buffer at pH 5.15.

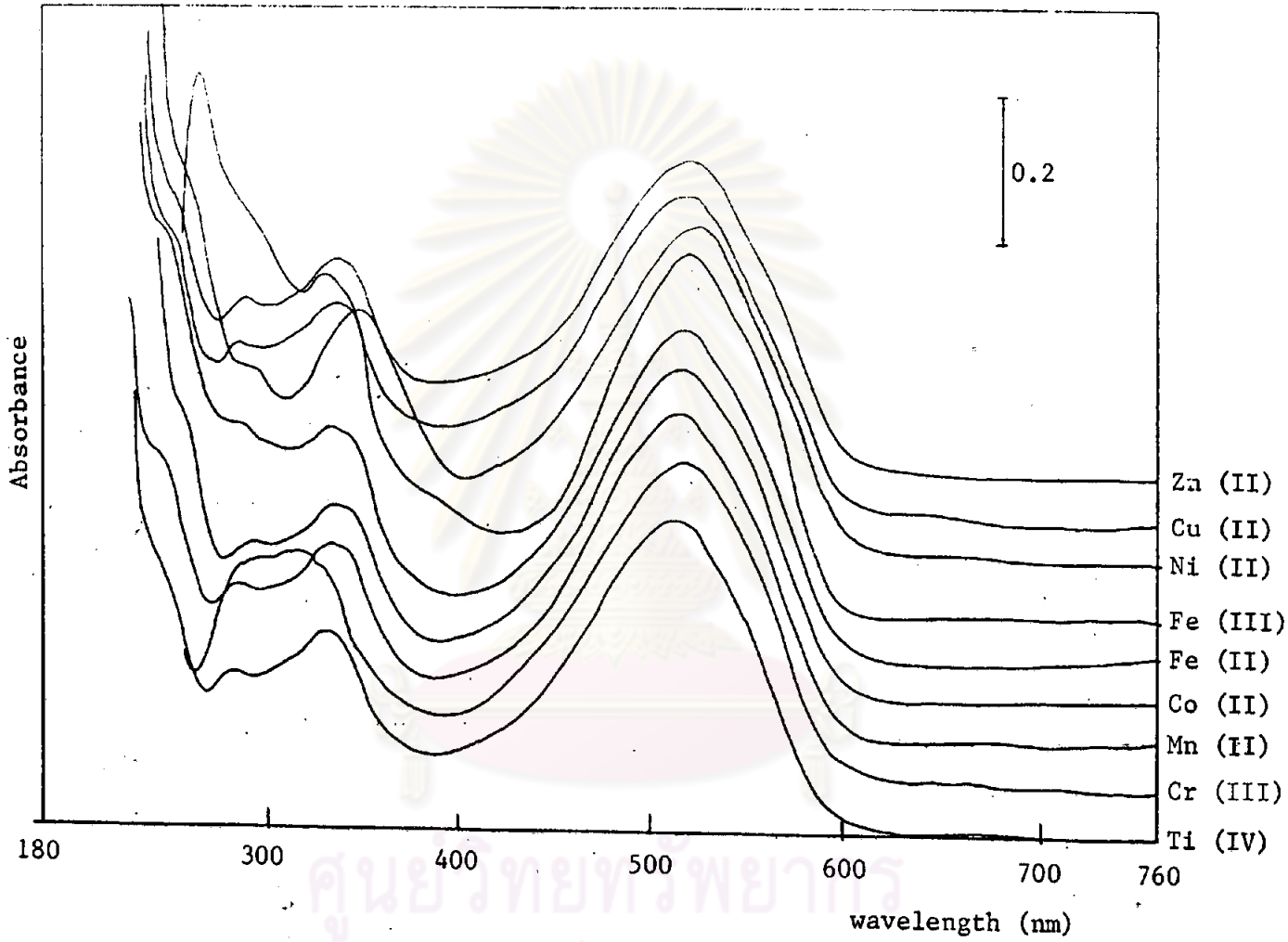

Figure 15E The UV-Visible absorption spectra of the mixture of Azorubine and metal ions in the McIlvaine buffer at pH 7.40.

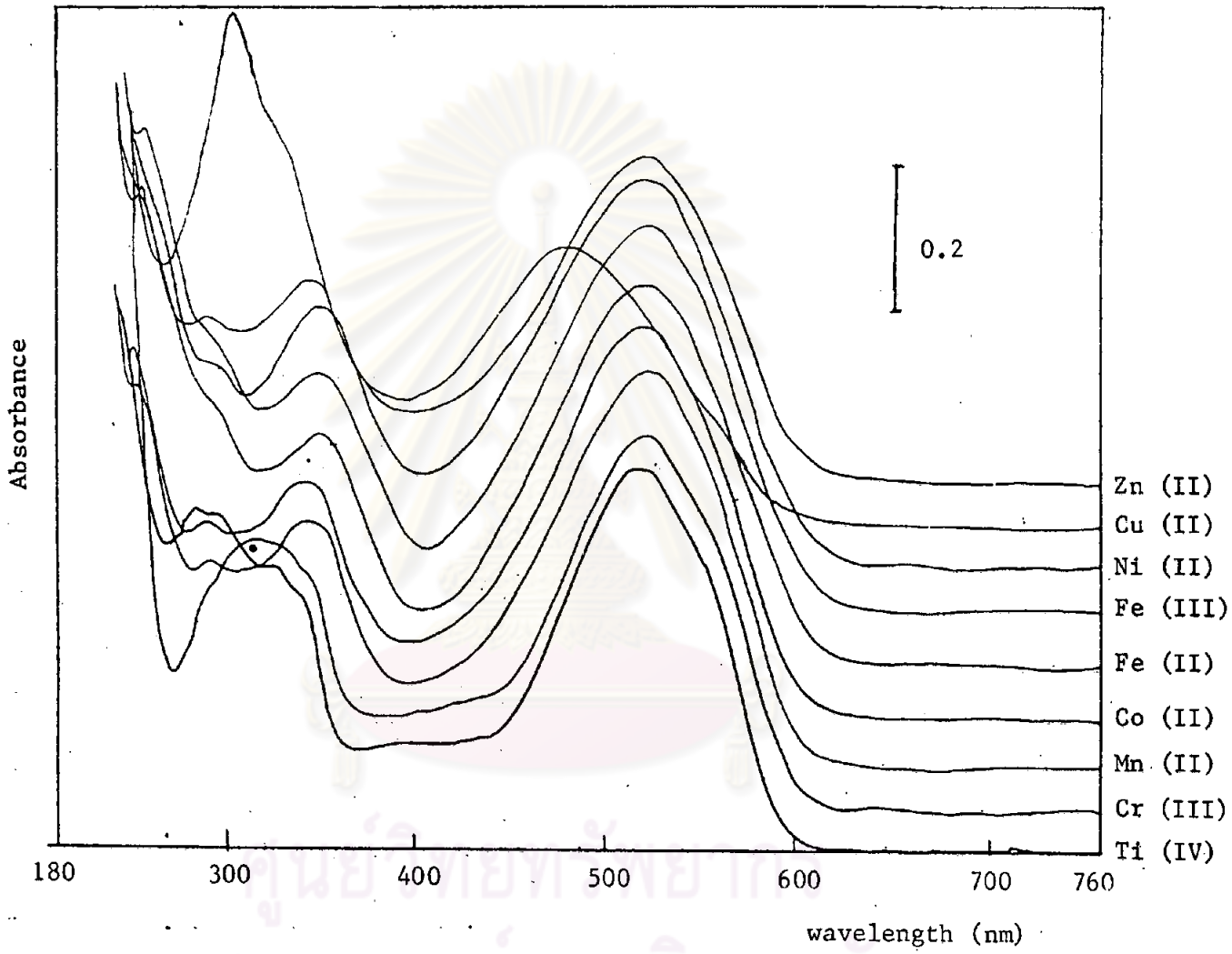

Figure 15F The UV-Visible absorption spectra of the mixture of Azorubine and metal ions in the phosphate buffer at pH 5.85.

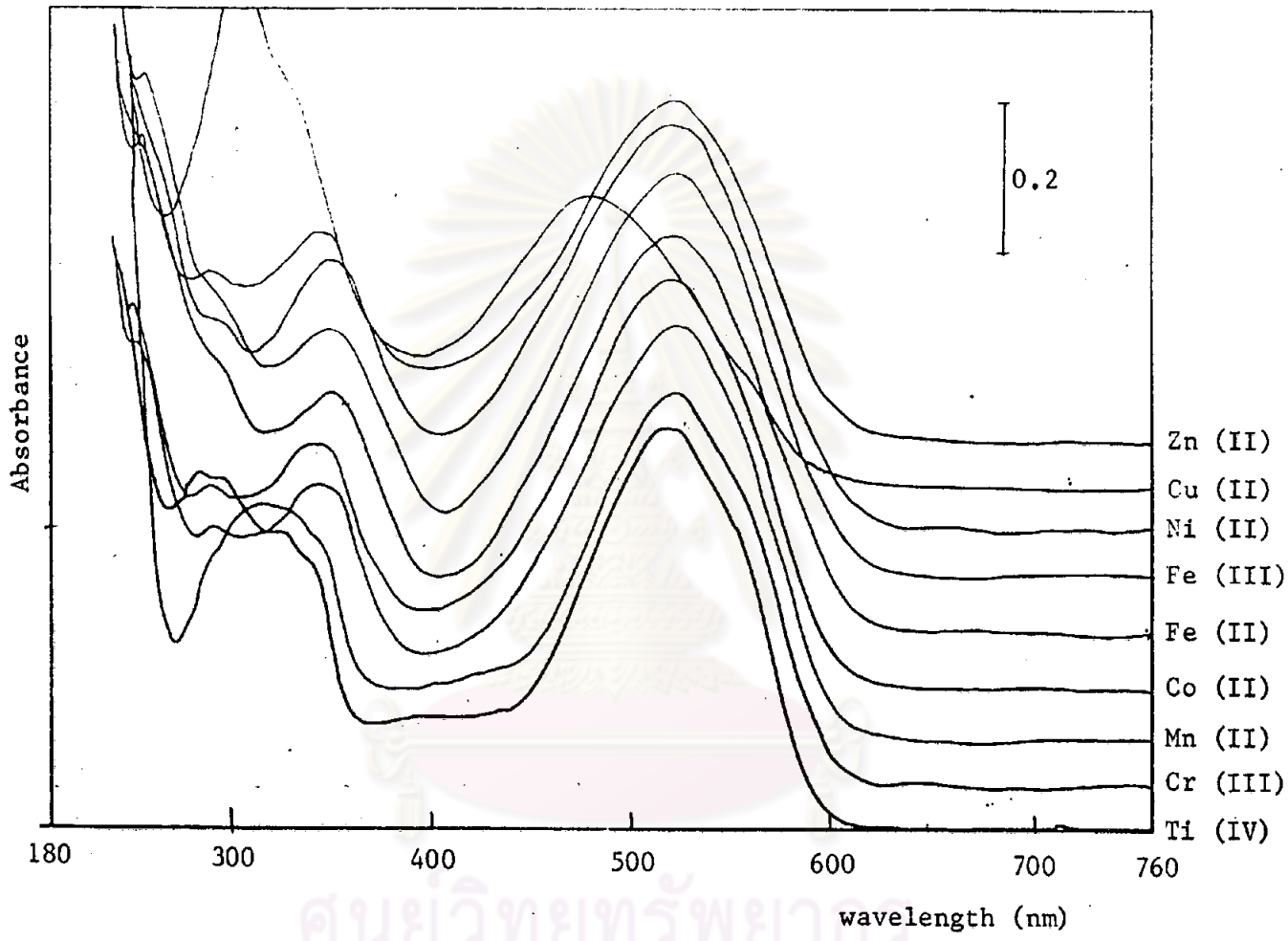

Figure 15G The UV-Visible absorption spectra of the mixture of Azorubine and metal ions in the phosphate buffer at pH 7.00.

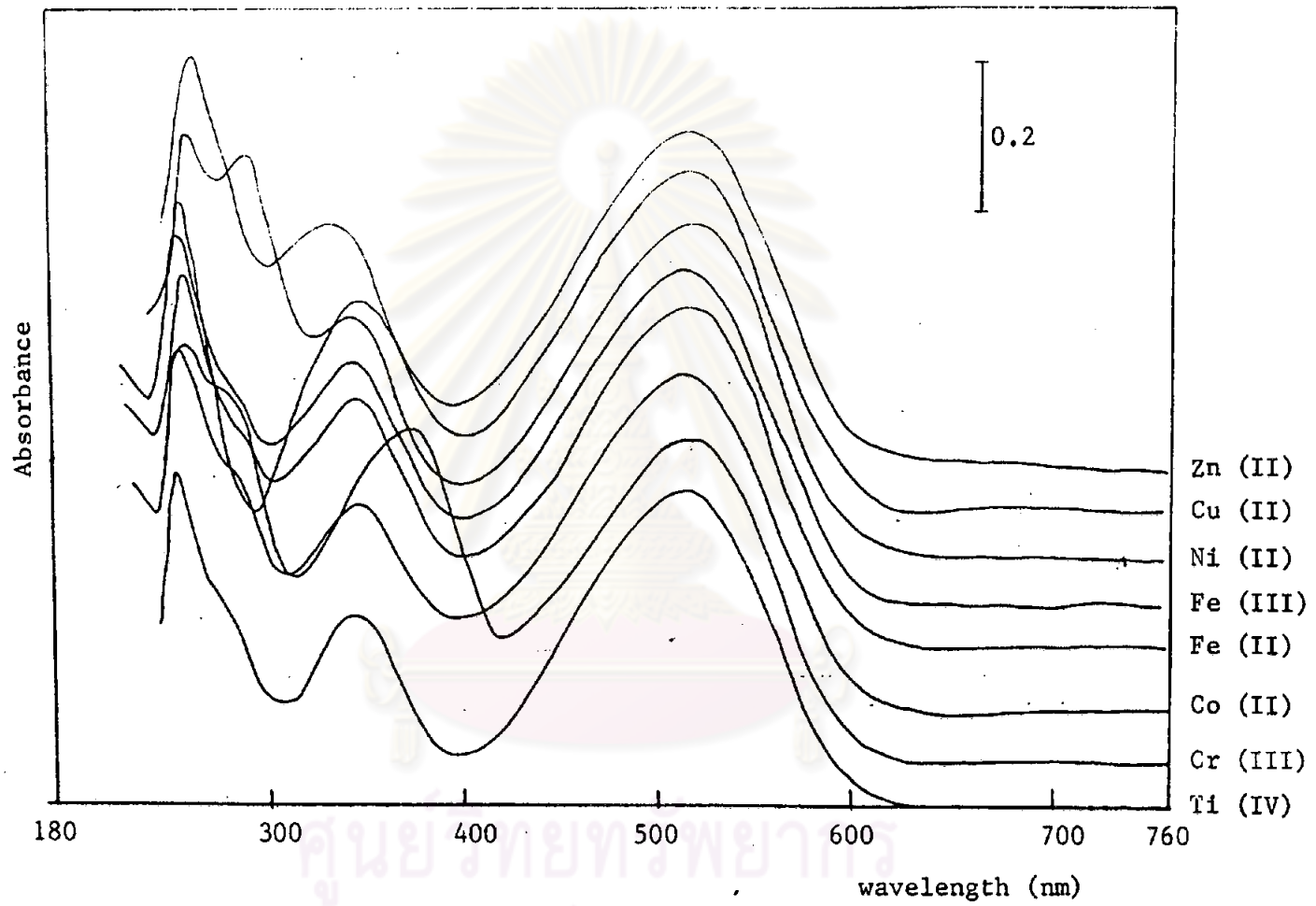

Figure 15H The Uv-Visible absorption spectra of the mixture of Azorubine and metal ions in the diethylamin at pH 12.50.

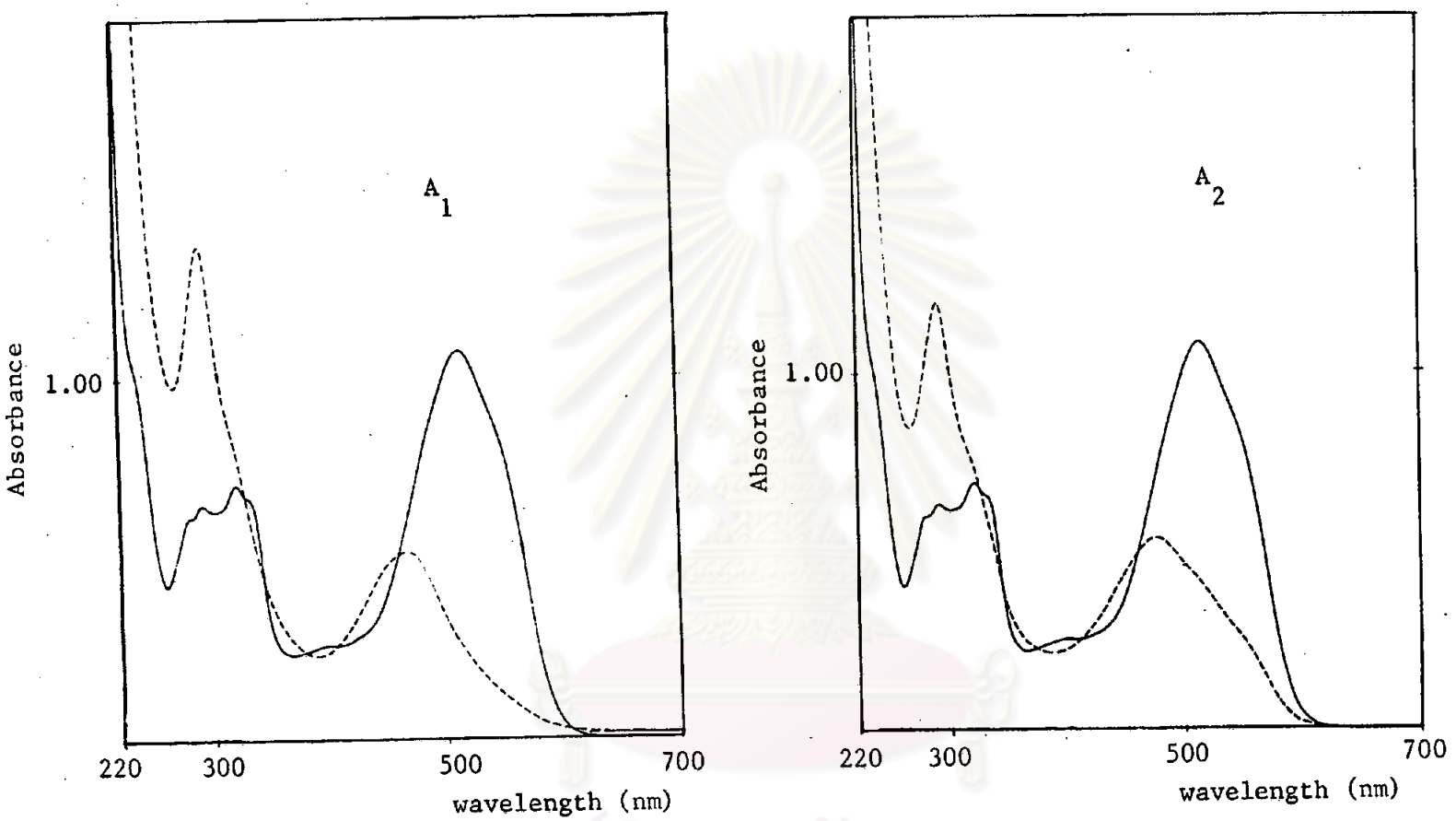

Figure 15I The UV-Visible absorption spectra of the mixture of Azorubine and Cu (II) ion in the acetate buffer at pH A_1) 6.10 and A_2) 5.10

——— Azorubine

----- Cu (II)-Azorubine mixture

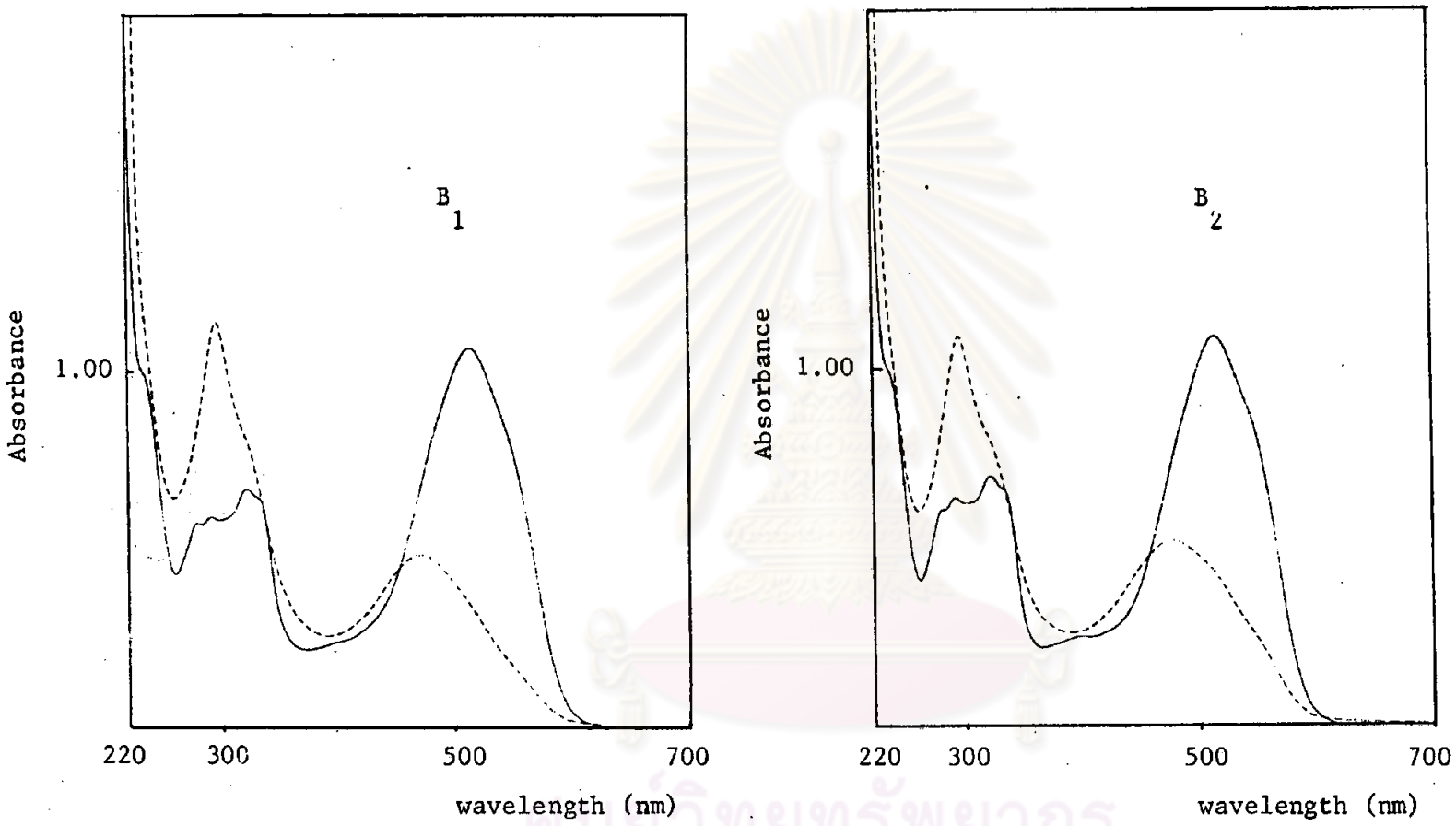

Figure 15J The UV-Visible absorption spectra of the mixture of Azorubine and Cu (II) ion in the phosphate buffer at pH B_1) 7.00 and B_2) 5.85

——— Azorubine

----- Cu (II)-Azorubine mixture

3.7.2.1 Absorption characteristics of the Cu (II)-Azorubine complex

The absorption spectra of Cu (II)-Azorubine complex in the phosphate buffer and acetate buffer illustrated the absorption peak of Cu (II)-Azorubine complex at the wavelengths of 440 nm, 358 nm and 293 nm (see Figures 16A-16B).

Since the strong absorption of the complex occurred at 293 nm and the maximum absorption indicated at 440 nm, the complex was studied at 293 nm in the ultraviolet region and at 440 nm in the visible region.

3.7.2.2 The effect of pH on the absorption spectra of Cu (II) ion-Azorubine mixtures

Ultraviolet-visible spectra of Cu (II) ion-Azorubine mixtures at various pH values were examined as shown in Figure 17. It was seen that the wavelength at the maximum absorption of Cu (II) ion-Azorubine mixture in the range of pH 5.10-7.00 obviously shifted from those of Azorubine to the lower wavelength (see Table 12). The difference between the wavelength at the maximum absorption of Azorubine and Cu (II)-Azorubine mixture was about 38 nm. This shift of the spectra dued to the complex formation of Cu (II) ion with Azorubine. The absorption spectra of Cu (II) ion-Azorubine mixture in the phosphate buffer pH 6.65 and 7.00 were identical. In the acetate buffer pH 4.00, the absorption spectrum of Cu (II) ion-Azorubine mixture was slightly different from its Azorubine spectrum.

The absorption peak of Cu (II) ion-Azorubine mixture in the ultraviolet region was not shifted when pH increased, that was pH independence in the ultraviolet region

(see Table 12).

This result indicated the complex between Cu (II) ion and Azorubine was formed in the acetate buffer pH 5.10-6.10 and in the phosphate buffer pH 5.85-7.00.

3.7.2.3 The influence of time on the color development

The effect of time on the absorbance of the Cu (II)-Azorubine complex in the acetate and the phosphate buffer at 440 nm was shown in Table 13, and Figure 18. It seemed that the absorbance of the complex was time independence. It meant that the complex formed quite rapidly.

3.7.2.4 Composition of Cu (II)-Azorubine complex

The complex formation between Cu (II) ion and Azorubine was performed in the phosphate buffer and the acetate buffer in the pH range of 5.10-7.00. The absorbance of Cu (II)-Azorubine complex was measured 5 minutes after the preparation. Since the absorption spectrum of Cu (II)-Azorubine mixture revealed the same absorption characteristic as Azorubine, the slope ratio method was unsuitable. The method of continuous variation and the molar ratio method were used for determining the composition of the complex formed.

3.7.2.4.1 The method of continuous variation

A series of solutions which contained various mole fractions of Cu (II) ion and Azorubine but the sum of the concentrations of Cu (II) ion and Azorubine was kept constant was prepared. The absorbances of the mixture solutions were measured at 440 nm and 293 nm using its buffer solution as reference. The data were

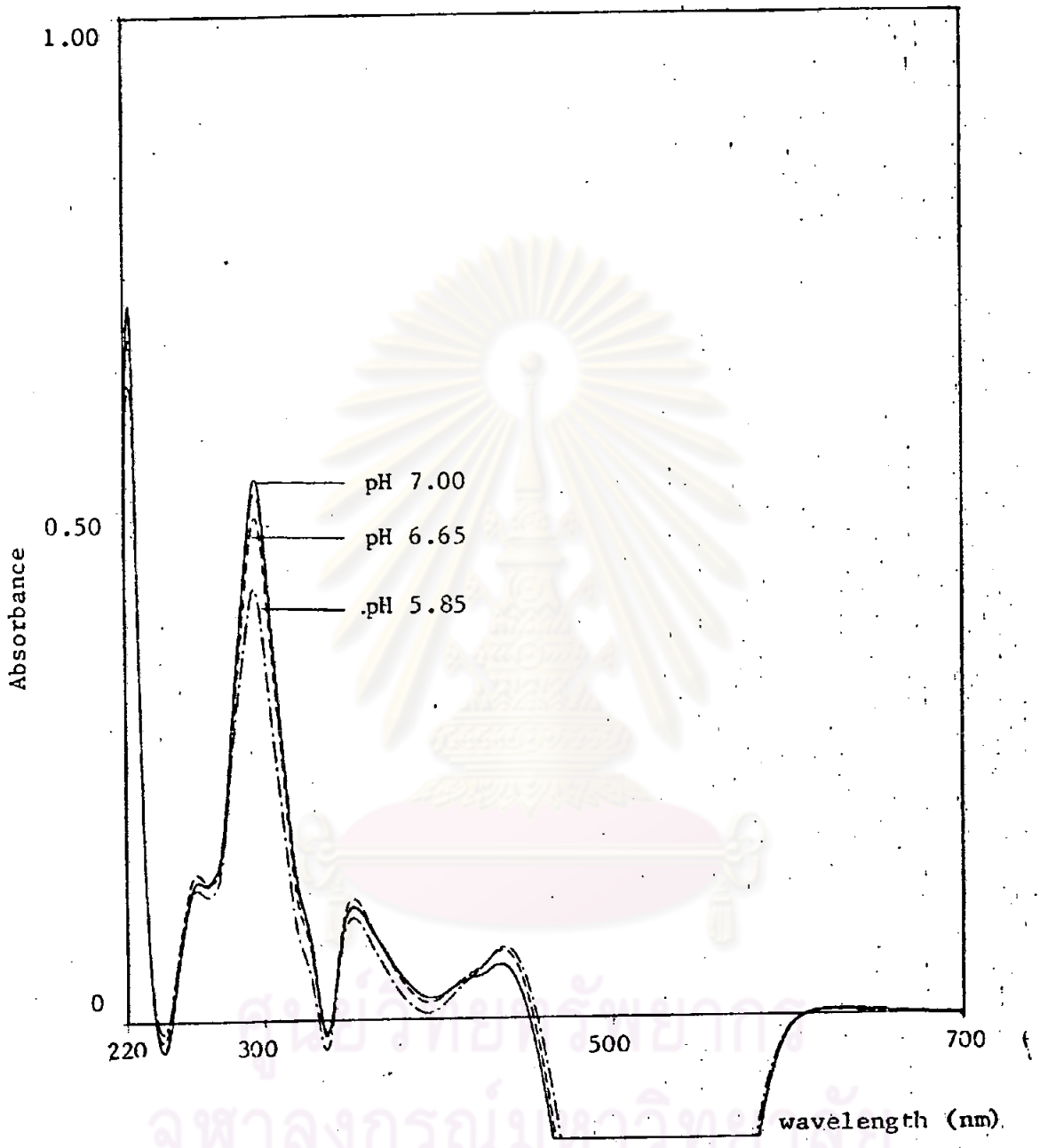

Figure 16A The UV-Visible absorption spectra of Cu (II)-Azorubine complex (2.00×10^{-5} M Cu (II) ion and 2.00×10^{-5} M Azorubine) in the phosphate buffer at various pH values, using 2.00×10^{-5} M Azorubine as reference.

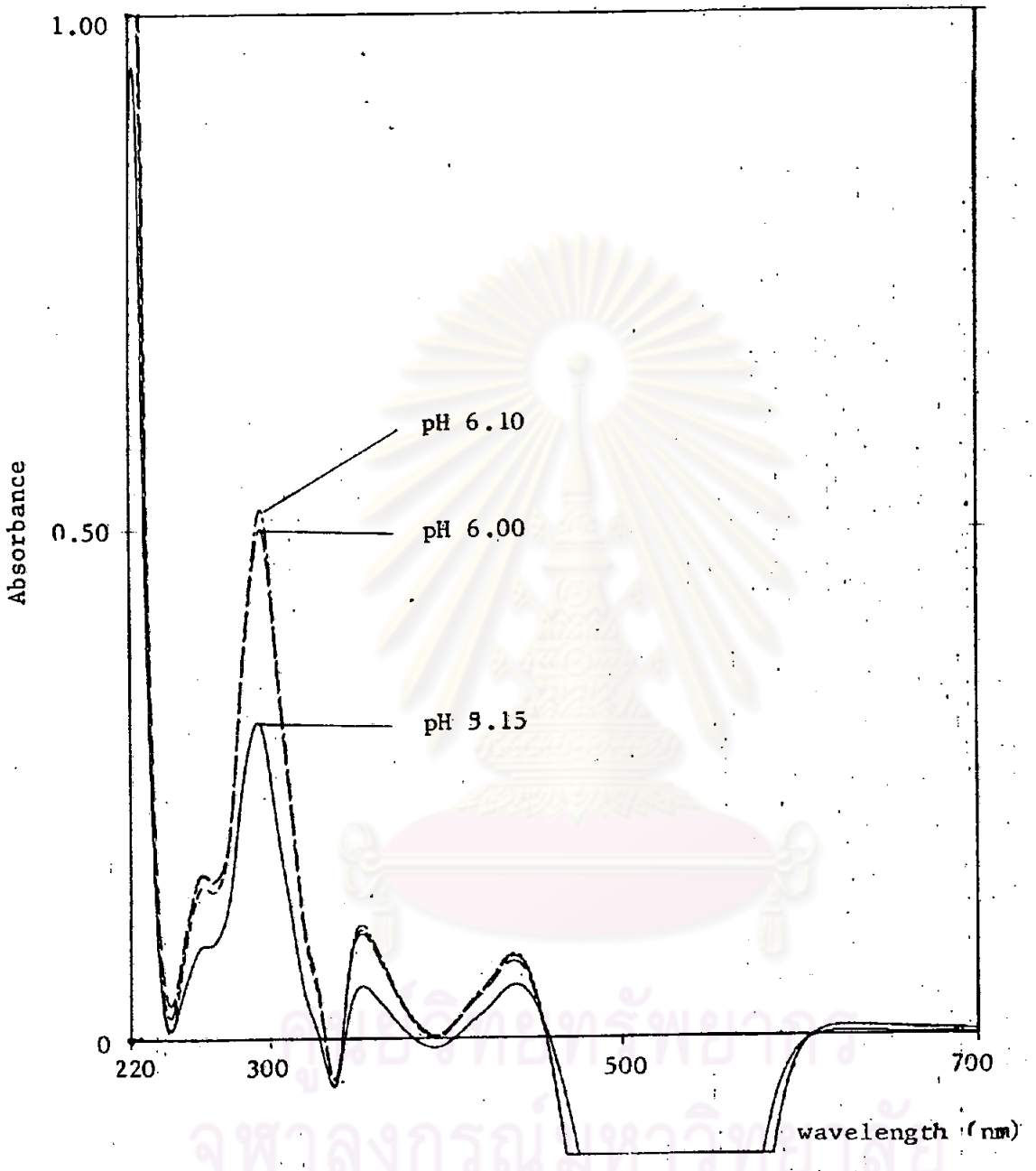

Figure 16B The UV-Visible absorption spectra of Cu (II)-Azorubine complex (2.00×10^{-5} M Cu (II) ion and 2.00×10^{-5} M Azorubine) in the acetate buffer at various pH values, using 2.00×10^{-5} M Azorubine as reference.

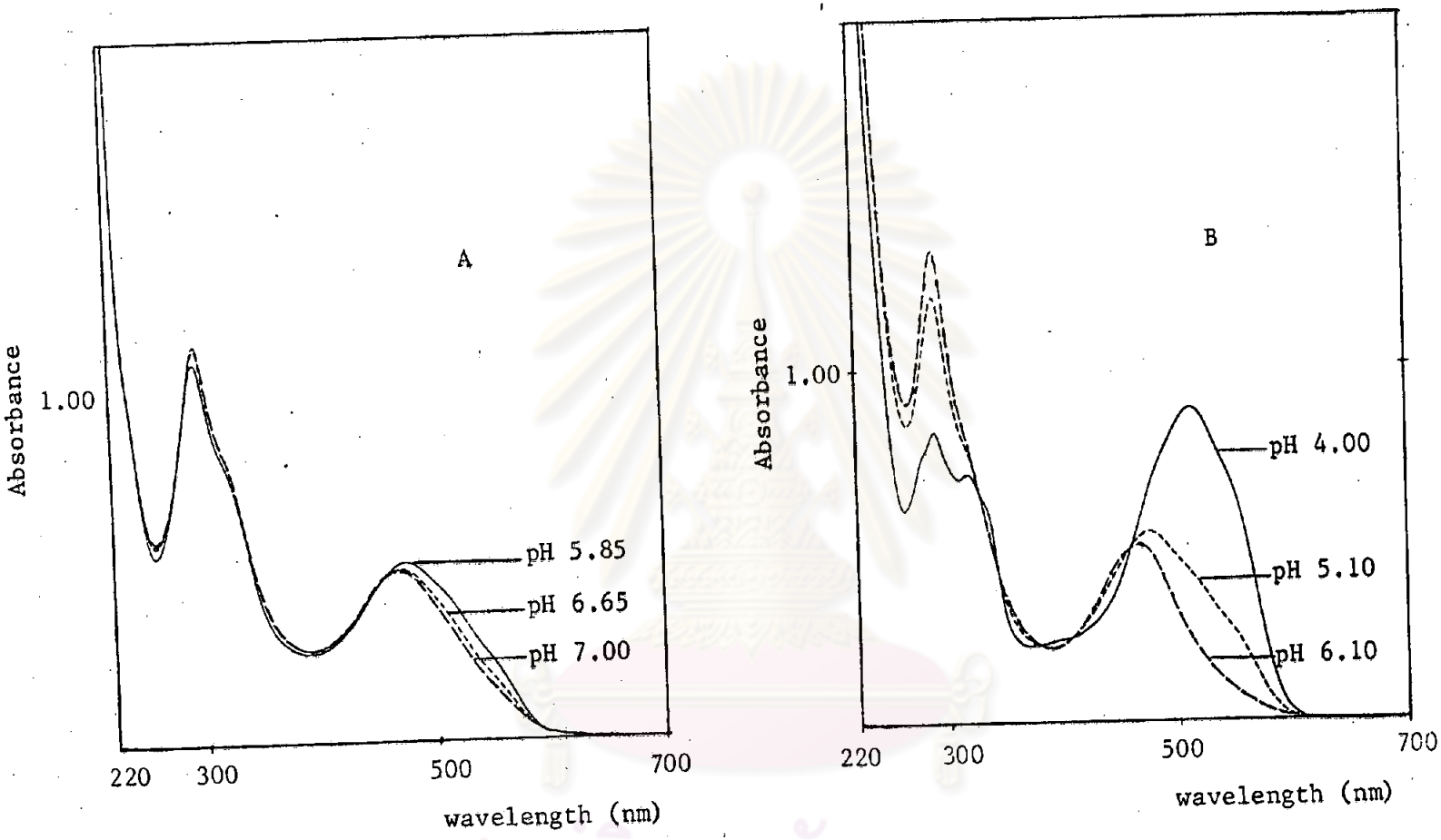

Figure 17 Effects of pH on the absorption spectra of the Cu (II) ion-Azorubine mixture in A) phosphate buffer and B) acetate buffer

Table 12 Absorption characteristics of Azorubine and Cu (II) ion-Azorubine mixtures at various pH values in ultraviolet-visible region.

buffer	pH	λmax in visible region, nm			λmax in ultraviolet region, nm		
		Azorubine	Cu (II) ion-Azorubine mixture	Δ λmax	Azorubine	Cu (II) ion-Azorubine mixture	Δ λmax
acetate	4.00	515	515	0	315	293	22
acetate	5.10	515	480	35	315	293	22
phosphate	5.85	515	478	37	315	293	22
acetate	6.10	515	476	39	315	293	22
phosphate	6.65	515	476	39	315	293	22
phosphate	7.00	515	476	39	315	293	22

Table 13 Effect of time on the color development of the Cu (II)-Azorubine complex in various buffer system.

Time	Absorbance at λ 440 nm			
	phosphate buffer		acetate buffer	
	pH 7.00	pH 5.88	pH 6.10	pH 5.10
0 min.	0.068	0.076	0.085	0.030
5 min.	0.064	0.073	0.082	0.030
15 min.	0.064	0.073	0.082	0.030
30 min.	0.064	0.073	0.082	0.030
1 hr.	0.065	0.073	0.082	0.030
2 hr.	0.064	0.073	0.082	0.030
3 hr.	0.064	0.074	0.082	0.031
6 hr.	0.065	0.074	0.082	0.031
24 hr.	0.065	0.074	0.080	0.031

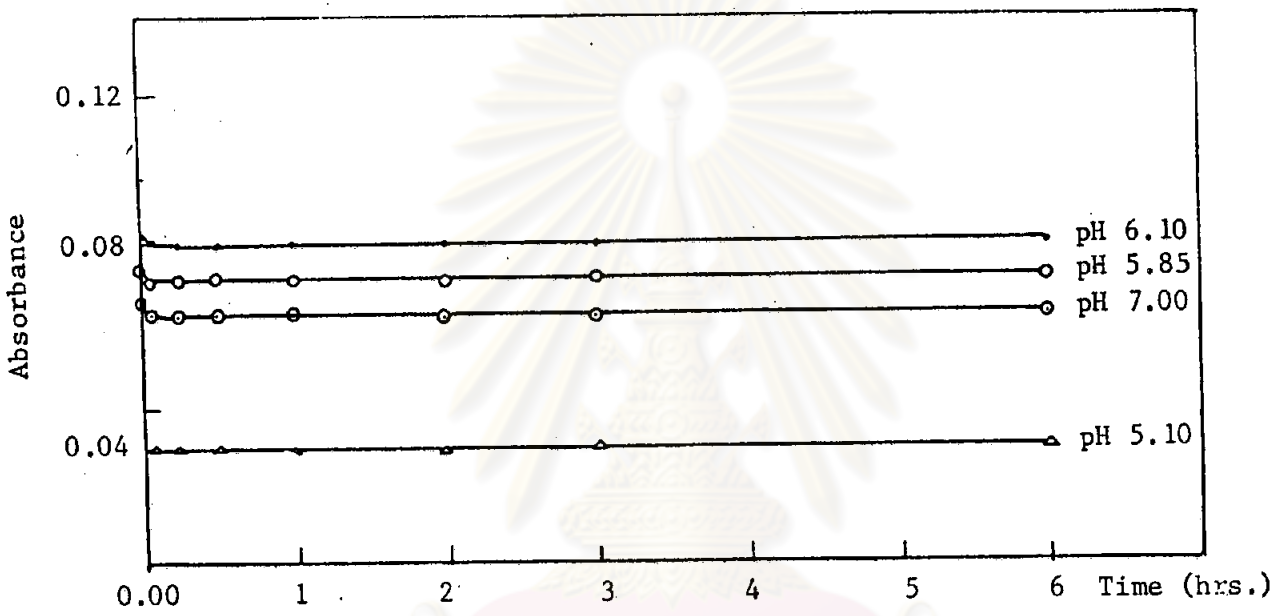

Figure 18 The influence of time on the absorbance of the Cu (II)-Azorubine complex in various pH values.

shown in Tables 14A-14D. The corrected absorbance which was the difference in each absorbance found and the corresponding absorbance for no reaction was calculated (24, 40). Then the absorbances found and the corrected absorbances were plotted VS mole fraction of Cu (II) ion in the same figure. It was seen from Figures 19A-19C that a 1:2 Cu (II)-Azorubine complex formed in the phosphate buffer pH 7.00, 5.85 and in the acetate buffer pH 6.10. However, a 1:1 Cu (II)-Azorubine complex formed in the acetate buffer pH 5.10 (see Figure 19D).

3.7.2.4.2 The molar ratio method

The absorbances of the mixture solutions which contained a constant concentration of Azorubine and a series of concentrations of Cu (II) ion were measured at the wavelength of 440 nm and 293 nm against the reagent blank. Their absorbances are listed in Tables 15A-15D. The plots of the absorbances of the mixture solutions VS their molar ratios were shown in Figures 20A-20D. The curve showed a deflection at the molar ratio of 1:2 Cu (II)-Azorubine complex in the phosphate buffer pH 7.00, 5.85 or in the acetate buffer pH 6.10 (see Figures 20A-20C). In the acetate buffer pH 5.10 the curves showed a 1:1 Cu (II)-Azorubine complex (see Figure 20D).

In the acetate buffer, the ratio of Cu (II): Azorubine depended on pH of the solution. Therefore, the preparation of Cu (II)-Azorubine complex in the acetate buffer must be careful for the pH of the

solution.

From the continuous variation and molar ratio method they revealed that the 1:2 complex (metal:dye) formed in the phosphate buffer pH 7.00, 5.85 or acetate buffer pH 6.10 and the 1:1 complex formed in the acetate buffer pH 5.10. It was reported that the azo dye having hydroxyl group ortho to the azo linkage can form complex with transition metal ions (38). There are one of hydroxyl group and the lone pair electrons of nitrogen atom of the azo group able to take part in bonding with the metal. Therefore, the possible structure of Cu (II)-Azorubine complex can be generalized by the formular

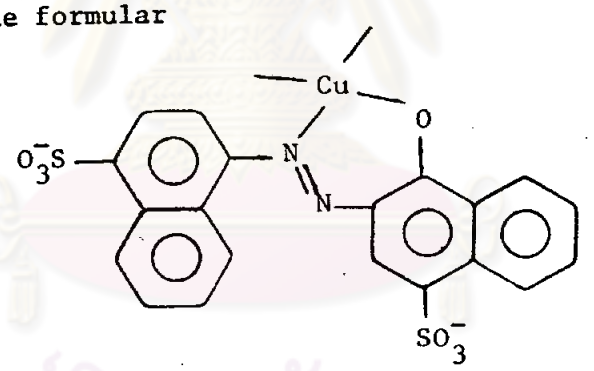

where the unfilled valencies either correspond to another dye molecule attached in the same way as the first, or other molecules that can act as ligands for the metal ion such as water.

3.7.3 The mixtures of Sunset Yellow FCF and Ti (IV), Cr (III), Mn (II), Co (II), Fe (II), Fe (III), Ni (II) or Zn (II)

The absorption spectra of the mixtures of each metal ion and Sunset Yellow FCF in phosphoric acid, acetic acid, McIlvaine buffer, phosphate buffer were shown in Figures 21A-21G. Since the absorption

Table 14A Method of Continuous variation of Azorubine and Cu (II) ion in the phosphate buffer pH 7.00.

10^5 x Conc., M		Mole fraction of Cu (II) ion	Absorbance	
Azorubine	Cu (II) ion		λ 440 nm	λ 293 nm
4.00	0·00	0.00	0.340	0.605
3.80	0.20	0.05	0.325	0.621
3.60	0.40	0.10	0.318	0.641
3.40	0.60	0.15	0.306	0.657
3.20	0.80	0.20	0.295	0.673
2.80	1.20	0.30	0.267	0.661
2.40	1.60	0.40	0.234	0.602
2.00	2.00	0.50	0.196	0.515
1.60	2.40	0.60	0.158	0.420
1.20	2.80	0.70	0.118	0.319
0.80	3.20	0.80	0.078	0.220
0.40	3.60	0.90	0.040	0.120

Table 14B Method of continuous variation of Azorubine and Cu (II) ion in the phosphate buffer pH 5.85.

10^5 x Conc., M		Mole fraction of Cu (II) ion	Absorbance	
Azorubine	Cu (II) ion		λ 440 nm	λ 293 nm
4.00	0.00	0.00	0.320	0.665
3.80	0.20	0.05	0.305	0.657
3.60	0.40	0.10	0.297	0.650
3.40	0.60	0.15	0.285	0.646
3.20	0.80	0.20	0.273	0.637
2.80	1.20	0.30	0.247	0.602
2.40	1.60	0.40	0.217	0.541
2.00	2.00	0.50	0.183	0.463
1.60	2.40	0.60	0.146	0.376
1.20	2.80	0.70	0.110	0.287
0.80	3.20	0.80	0.072	0.194
0.40	3.60	0.90	0.037	0.103

Table 14C Method of Continuous variation of Azorubine and Cu (II) ion in the acetate buffer pH 6.10.

10^5 x Conc., M		Mole fraction of Cu (II) ion	Absorbance	
Azorubine	Cu (II) ion		λ 440 nm	λ 293 nm
4.00	0.00	0.00	0.318	0.640
3.80	0.20	0.05	0.310	0.642
3.60	0.40	0.10	0.295	0.650
3.40	0.60	0.15	0.285	0.651
3.20	0.80	0.20	0.274	0.649
2.80	1.20	0.30	0.250	0.621
2.40	1.60	0.40	0.220	0.565
2.00	2.00	0.50	0.186	0.492
1.60	2.40	0.60	0.151	0.409
1.20	2.80	0.70	0.115	0.316
0.80	3.20	0.80	0.076	0.218
0.40	3.60	0.90	0.040	0.116

Table 14D Method of continuous variation of Azorubine and Cu (II) ion in the acetate buffer pH 5.10.

10^5 x Conc., M		Mole fraction of Cu (II) ion	Absorbance	
Azorubine	Cu (II) ion		440 nm	293 nm
4.00	0.00	0.00	0.253	1.401
3.60	0.40	0.10	0.280	0.953
3.40	0.60	0.15	0.267	0.892
3.20	0.80	0.20	0.251	0.827
2.80	1.20	0.30	0.223	0.713
2.40	1.60	0.40	0.193	0.604
2.00	2.00	0.50	0.161	0.495
1.60	2.40	0.60	0.130	0.394
1.20	2.80	0.70	0.098	0.293
0.80	3.20	0.80	0.066	0.197
0.40	3.60	0.90	0.034	0.099

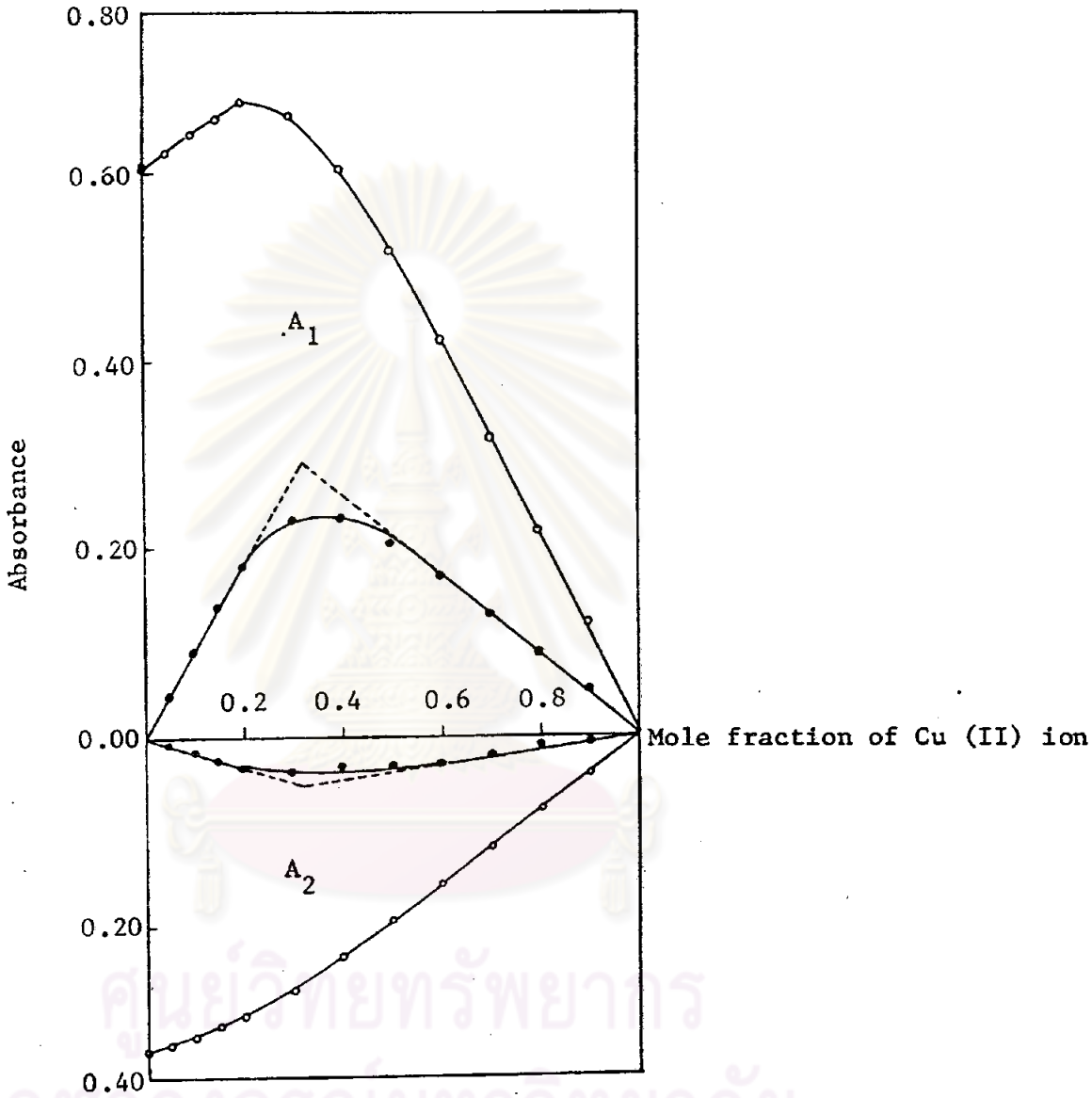

Figure 19A Continuous variation plots for solutions contained various mole fractions of Cu (II) ion in the phosphate buffer pH 7.00 at A_1) 293 nm, A_2) 440 nm

- ∘ The absorbance found
- • The absorbance corrected

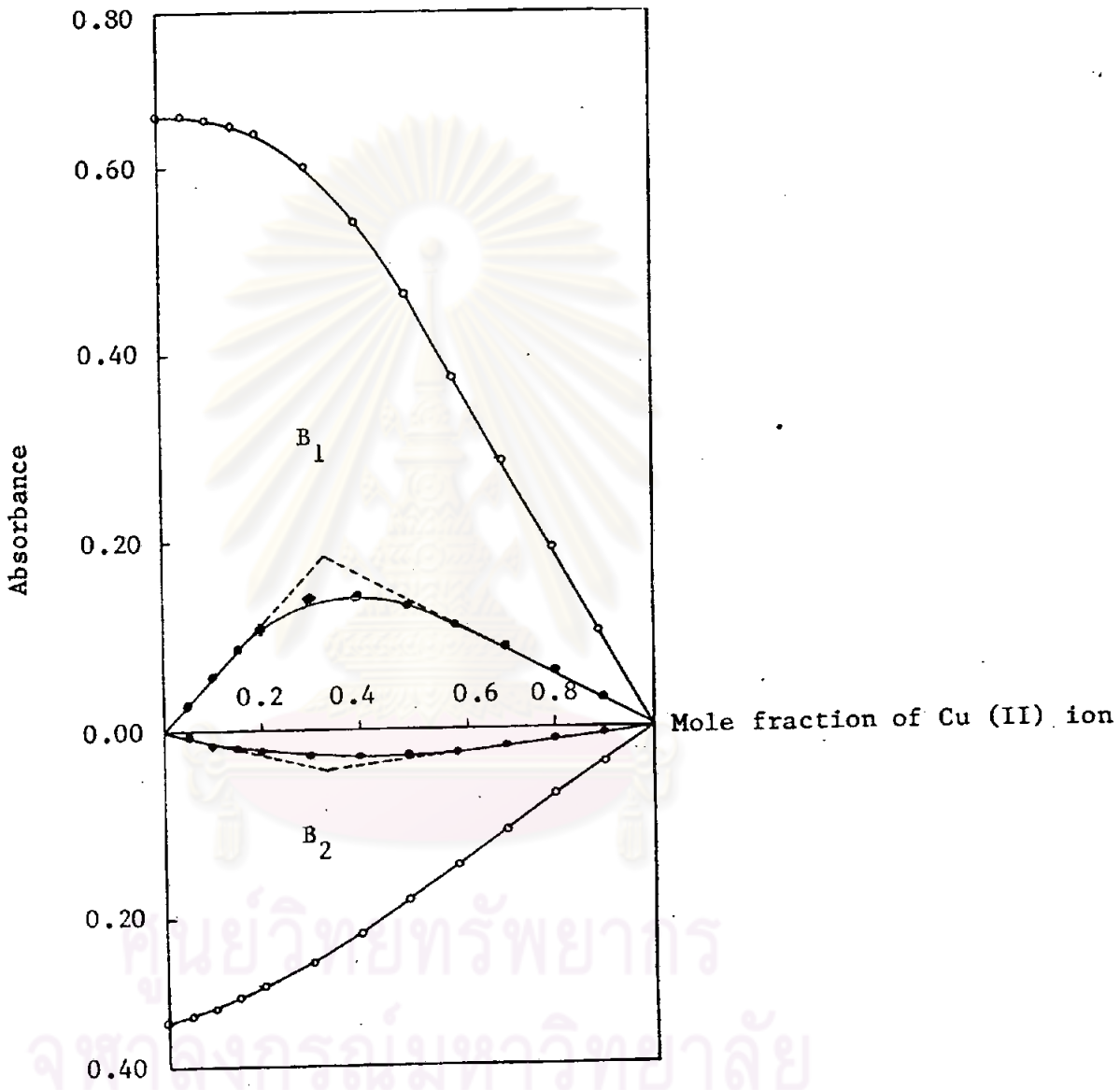

Figure 19B Continuous variation plots for solutions contained various mole fractions of Cu (II) ion in the phosphate buffer pH 5.85 at B_1) 293 nm, B_2) 440 nm.

- ∘ The absorbance found
- • The absorbance corrected

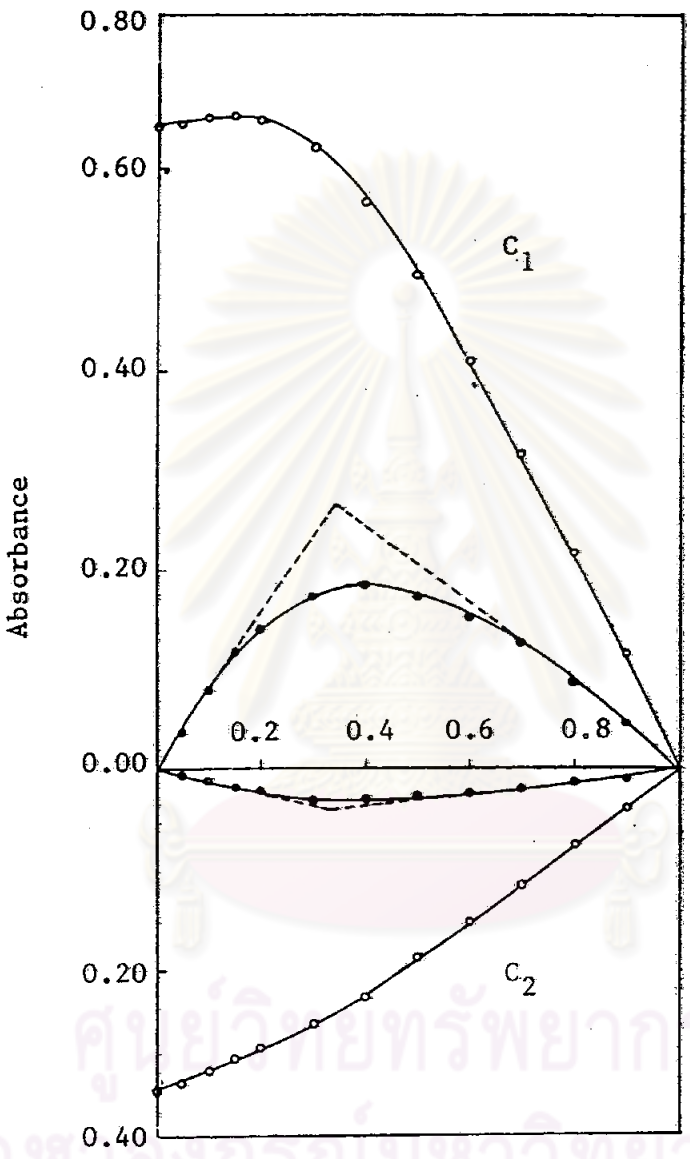

Figure 19C Continuous variation plots for solutions contained various mole fractions of Cu (II) ion in the acetate buffer pH 6.10 at C_1) 293 nm, C_2) 440 nm.

- ∘ The absorbance found
- • The absorbance corrected

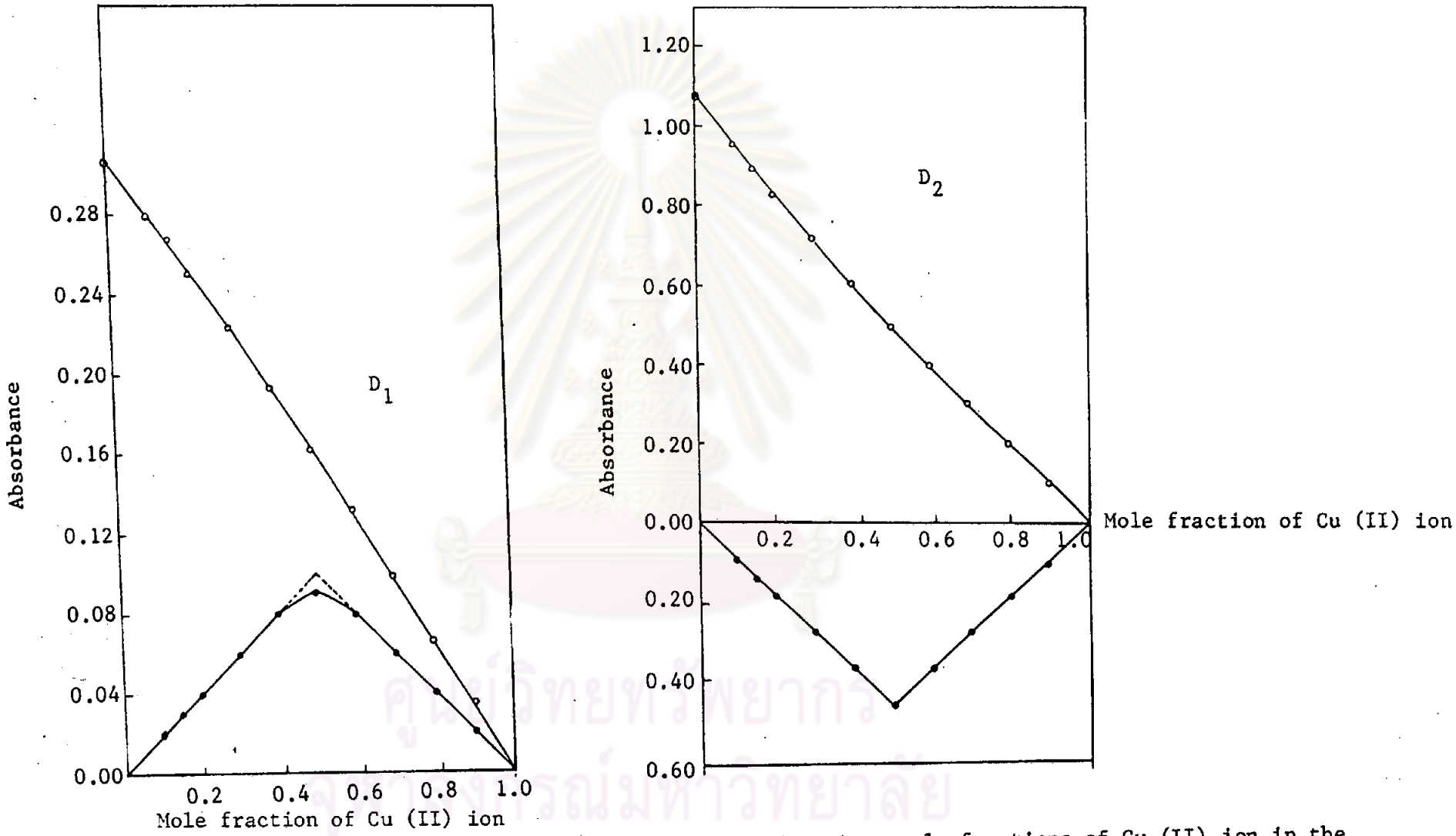

Figure 19D Continuous variation plots for solutions contained various mole fractions of Cu (II) ion in the acetate buffer pH 5.10 at D_1) 440 nm, D_2) 293 nm.

- ∘ The absorbance found
- • The absorbance corrected

Table 15A The Molar ratio study of Azorubine and Cu (II) ion in the phosphate buffer pH 7.00.

Molar ratio, Cu (II) : Azorubine	Absorbance	
	λ 440 nm	λ 293 nm
0.1	0.011	0.111
0.2	0.024	0.224
0.3	0.032	0.316
0.4	0.040	0.390
0.5	0.043	0.432
0.6	0.047	0.462
0.7	0.048	0.479
0.8	0.050	0.493
0.9	0.050	0.498
1.0	0.050	0.504
1.2	0.050	0.511
1.4	0.051	0.518
1.6	0.051	0.522
1.8	0.052	0.535
2.0	0.052	0.540

Table 15B The Molar ratio study of Azorubine and Cu (II) ion in the phosphate buffer pH 5.85.

Molar ratio, Cu (II) : Azorubine	Absorbance	
	λ 440 nm	λ 293 nm
0.1	0.008	0.005
0.2	0.016	0.100
0.3	0.026	0.159
0.4	0.034	0.206
0.5	0.039	0.241
0.6	0.042	0.265
0.7	0.046	0.286
0.8	0.049	0.305
0.9	0.052	0.319
1.0	0.054	0.333
1.2	0.058	0.353
1.4	0.059	0.362
1.6	0.061	0.377
1.8	0.062	0.384
2.0	0.064	0.396

Table 15C The Molar ratio study of Azorubine and Cu (II) ion in the acetate buffer pH 6.10.

Molar ratio, Cu (II) : Azorubine	Absorbance	
	λ 440 nm	λ 293 nm
0.1	0.013	0.126
0.2	0.030	0.218
0.3	0.045	0.297
0.4	0.054	0.357
0.5	0.061	0.399
0.6	0.066	0.433
0.7	0.071	0.462
0.8	0.073	0.480
0.9	0.076	0.497
1.0	0.078	0.513
1.2	0.083	0.540
1.4	0.084	0.553
1.6	0.086	0.568
1.8	0.086	0.577
2.0	0.088	0.588

Table 15D The Molar ratio study of Azorubine and Cu (II) ion in the acetate buffer pH 5.10.

Molar ratio, Cu (II) : Azorubine	Absorbance	
	λ 440 nm	λ 293 nm
0.1	0.003	0.022
0.2	0.008	0.047
0.3	0.013	0.075
0.4	0.015	0.089
0.5	0.018	0.108
0.6	0.020	0.125
0.7	0.023	0.142
0.8	0.026	0.160
0.9	0.028	0.172
1.0	0.030	0.187
1.2	0.035	0.213
1.4	0.038	0.235
1.6	0.042	0.255
1.8	0.045	0.276
2.0	0.048	0.293
2.2	0.048	0.298
2.4	0.050	0.315
2.6	0.052	0.326
2.8	0.054	0.338

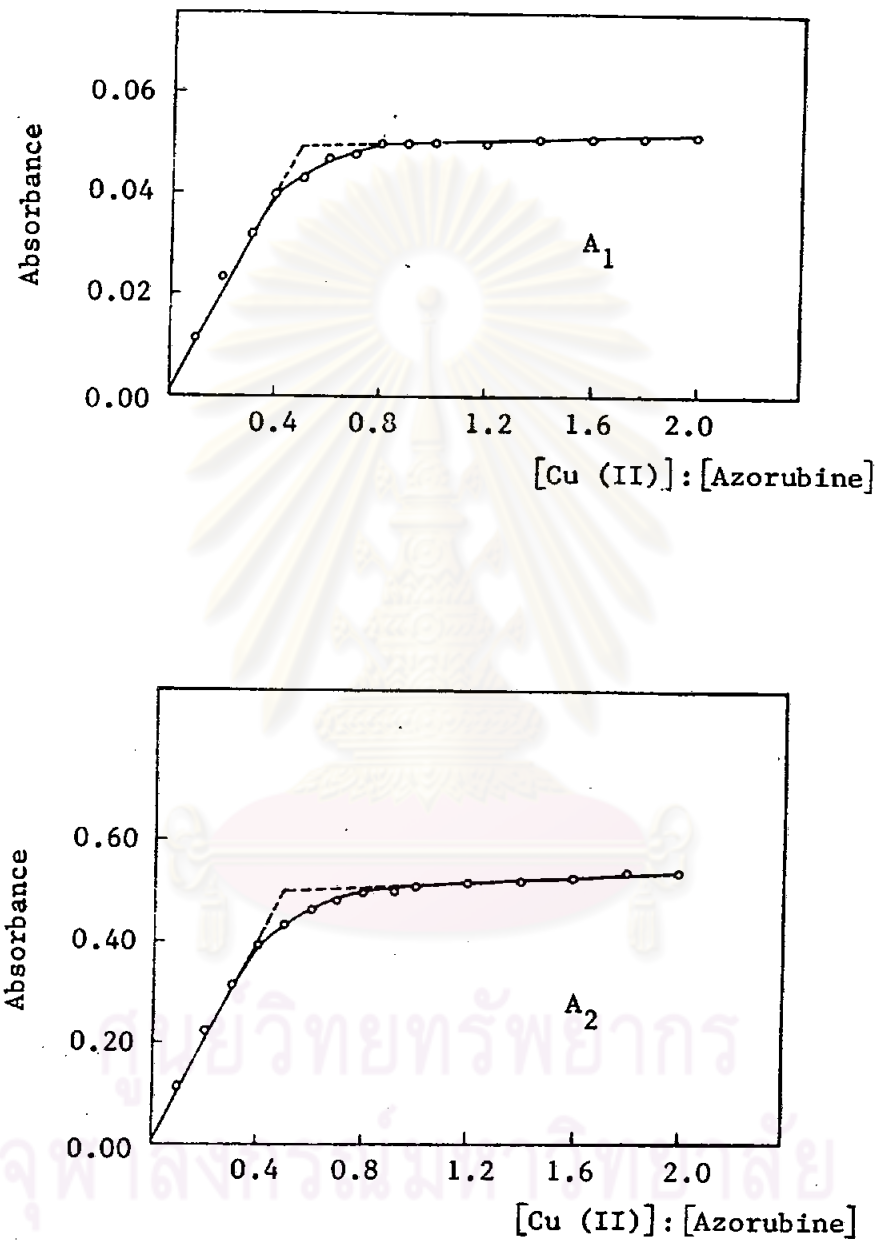

Figure 20A Molar ratio plots for solutions contained 4.00×10^{-5} M Azorubine and various concentrations of Cu (II) ion in the phosphate buffer pH 7.00 at

A_1) 440 nm

A_2) 293 nm

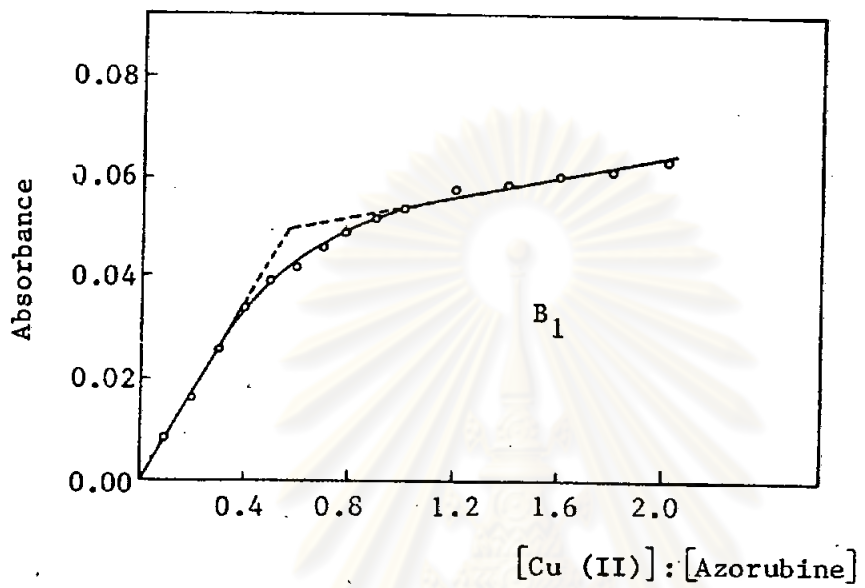

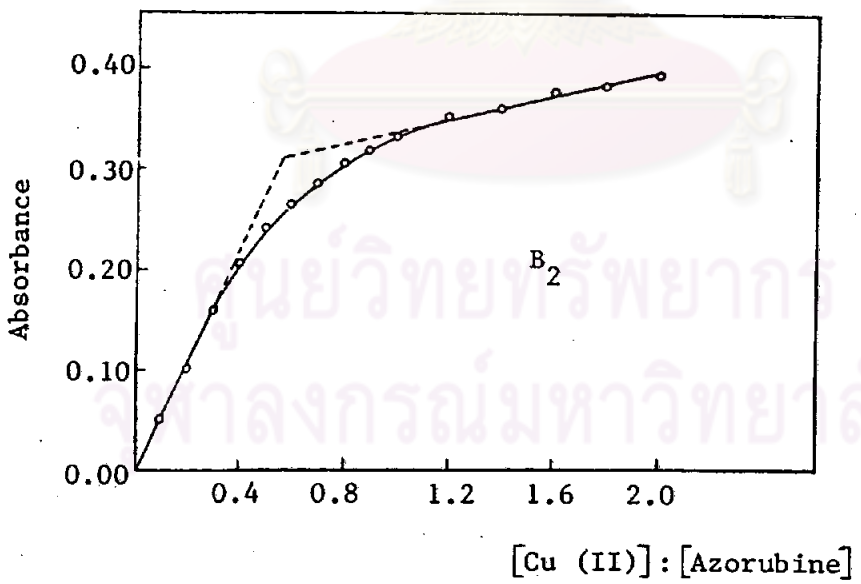

Figure 20B Molar ratio plots for solutions contained 4.00×10^{-5} M Azorubine and various concentrations of Cu (II) ion in the phosphate buffer pH 5.85 at

B_1) 440 nm

B_2) 293 nm

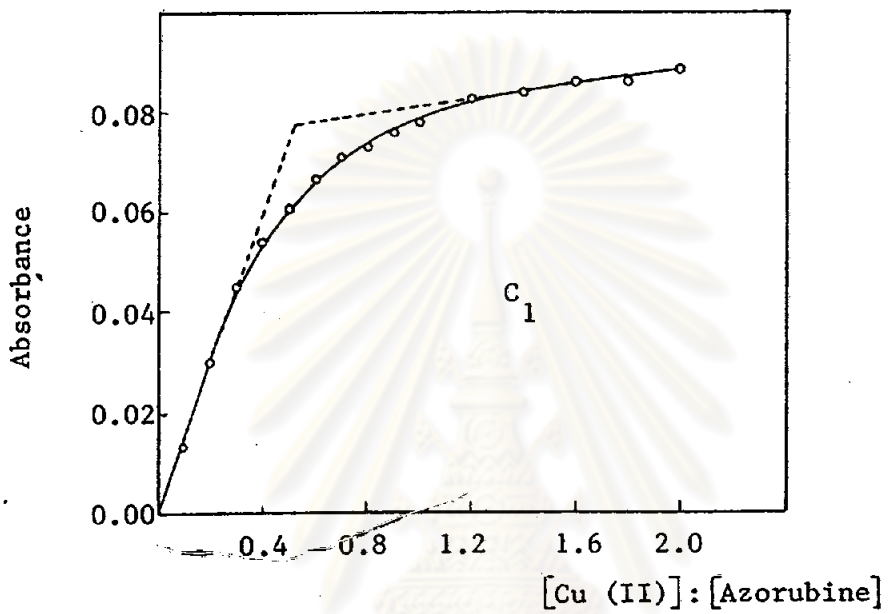

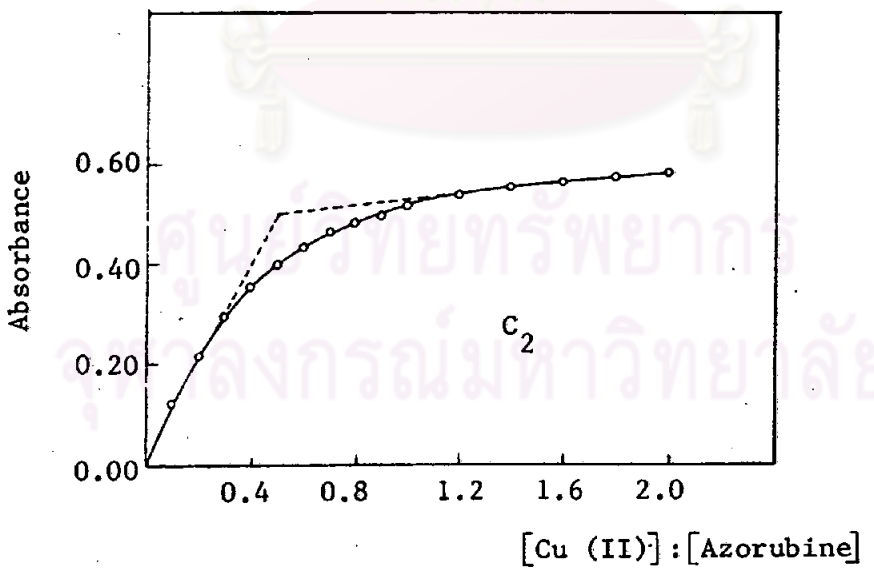

Figure 20C Molar ratio plots for solutions contained 4.00×10^{-5} M Azorubine and various concentrations of Cu (II) ion in the acetate buffer pH 6.10 at

C_1) 440 nm

C_2) 293 nm

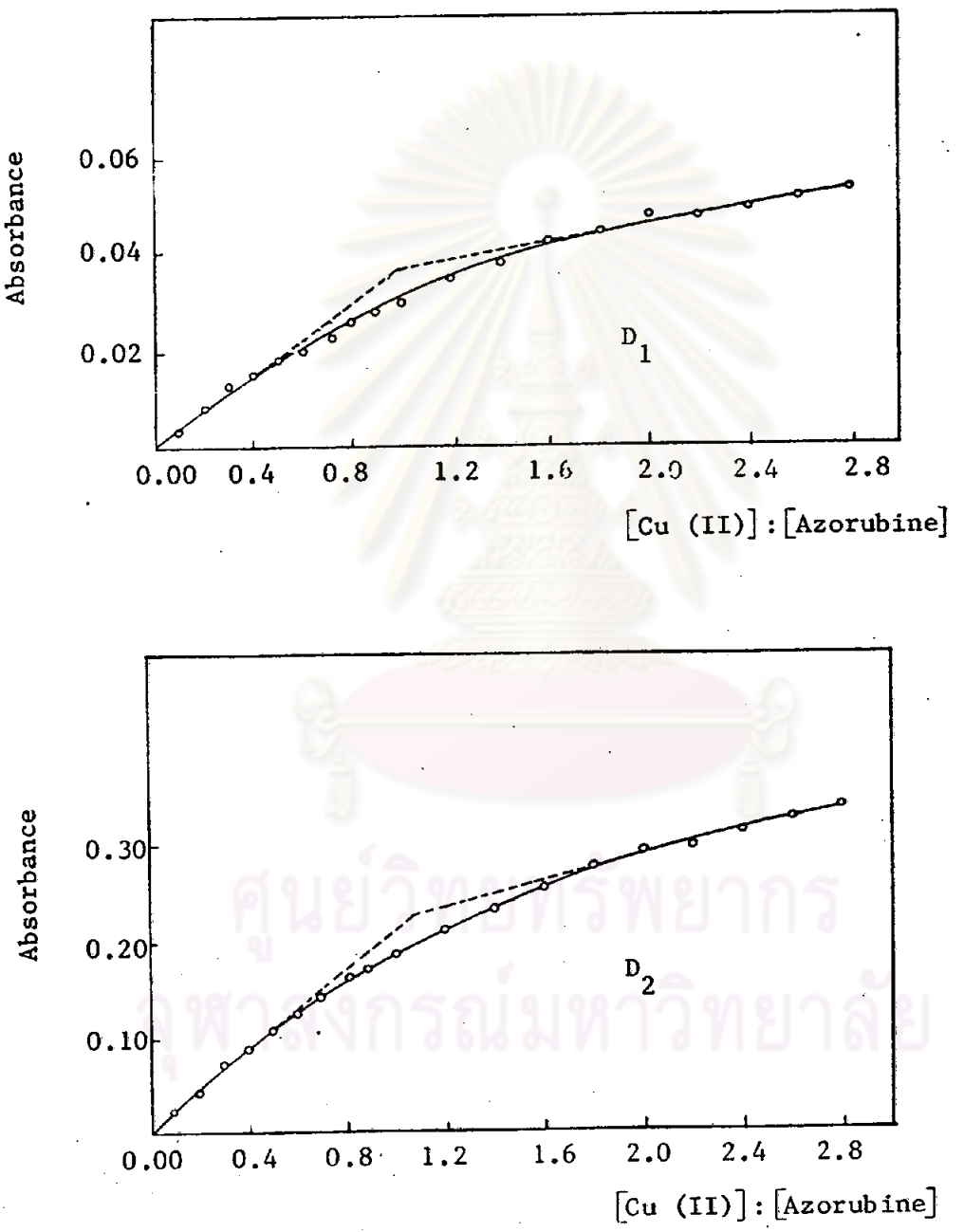

Figure 20D Molar ratio plots for solutions contained 4.00×10^{-5} M Azorubine and various concentrations of Cu (II) ion in the acetate buffer pH 5.10 at

D_1) 440 nm

D_2) 293 nm

spectra of the mixtures between the metal ion and Sunset Yellow FCF were not different from that of Sunset Yellow FCF and no physical change in each mixture system was observed, no complex formed between Sunset Yellow FCF and Ti (IV), Cr (III), Mn (II), Fe (II), Fe (III), Ni (II) or Zn (II) ion in the buffer solutions mentioned above.

3.7.4 The mixtures of Sunset Yellow FCF and Cu (II) ion

The absorption spectra of the mixtures of Sunset Yellow FCF and Cu (II) ion in phosphoric acid, acetic acid, McIlvaine buffer, phosphate buffer and acetate buffer were recorded as shown in Figures 21A-21J. The spectra of Cu (II) ion-Sunset Yellow FCF mixtures in the buffer solutions such as phosphoric acid, acetic acid, McIlvaine buffer and phosphate buffer were not different from its dye spectrum and no physical change in each mixture solution was observed. This meant that no reaction between Sunset Yellow FCF and Cu (II) ion occurred and no complex formed in the buffer solutions such as phosphoric acid, acetic acid, McIlvaine buffer and phosphate buffer. However, in the acetate buffer pH 6.10, 5.10 or 4.00 it was found that Sunset Yellow FCF reacted with Cu (II) ion since the color of the mixture solution changed from orange to yellow-orange. The absorption spectra of Cu (II) ion-Sunset Yellow FCF solutions in the acetate buffer at various pH differed from that of Sunset Yellow FCF (see Figures 21H-21J). A small hypsochromic shifted and a new absorption band at 354 nm occurred at pH 5.10, 6.10 and the absorbance of Sunset Yellow FCF at 482 nm decreased in the presence of Cu (II) ion (see Figures 21H-21J).

3.7.4.1 Absorption characteristics of Cu (II) ion-Sunset Yellow FCF mixture

The absorption spectra of Sunset Yellow FCF, the mixture of Sunset Yellow FCF and Cu (II) ion in the acetate

buffer pH 6.10, 5.10, 4.00 were recorded in the range of wavelengths between 220-700 nm (see Figures 21H-21J). It was seen that the absorption spectra of Cu (II) ion-Sunset Yellow FCF slightly shifted to the lower wavelength and the absorbance of Sunset Yellow FCF decreased in the presence of Cu (II) ion. The strong absorption band of the Cu (II) ion-Sunset Yellow FCF mixture in the acetate buffer pH 6.10, 5.10, 4.00 appeared at 470 nm, 475 nm and 480 nm, respectively. The new absorption peak of the mixture of Cu (II) ion and Sunset Yellow FCF which occurred at 354 nm was weak.

The absorption spectra of Cu (II) ion-Sunset Yellow FCF mixtures are different from that of Sunset Yellow FCF in the ultraviolet region and the absorption peak of Sunset Yellow FCF at 307 nm disappeared (see Figures 21H-21J).

3.7.4.2 The effect of pH on the absorption spectra of Cu (II) ion-Sunset Yellow FCF mixtures

Ultraviolet-visible spectra of Cu (II) ion-Sunset Yellow FCF mixtures at various pH values were shown in Figure 22. It was seen that the color change was enhanced with the increase of pH, while lowering of pH tended to reverse the color change. The wavelength at the maximum absorption of Cu (II) ion-Sunset Yellow FCF mixture gradually shifted to the lower wavelength when the pH of solution increased. At pH 5.10 and 6.10, the new absorption peak appeared at 354 nm but this absorption peak dissappeared at pH 4.00 (see Table 16 and Figure 22). The absorption spectra of the mixture of Cu (II) ion and Sunset Yellow FCF in the acetate buffer pH 6.10, 5.10, 4.00 were slightly different from each other in the ultraviolet

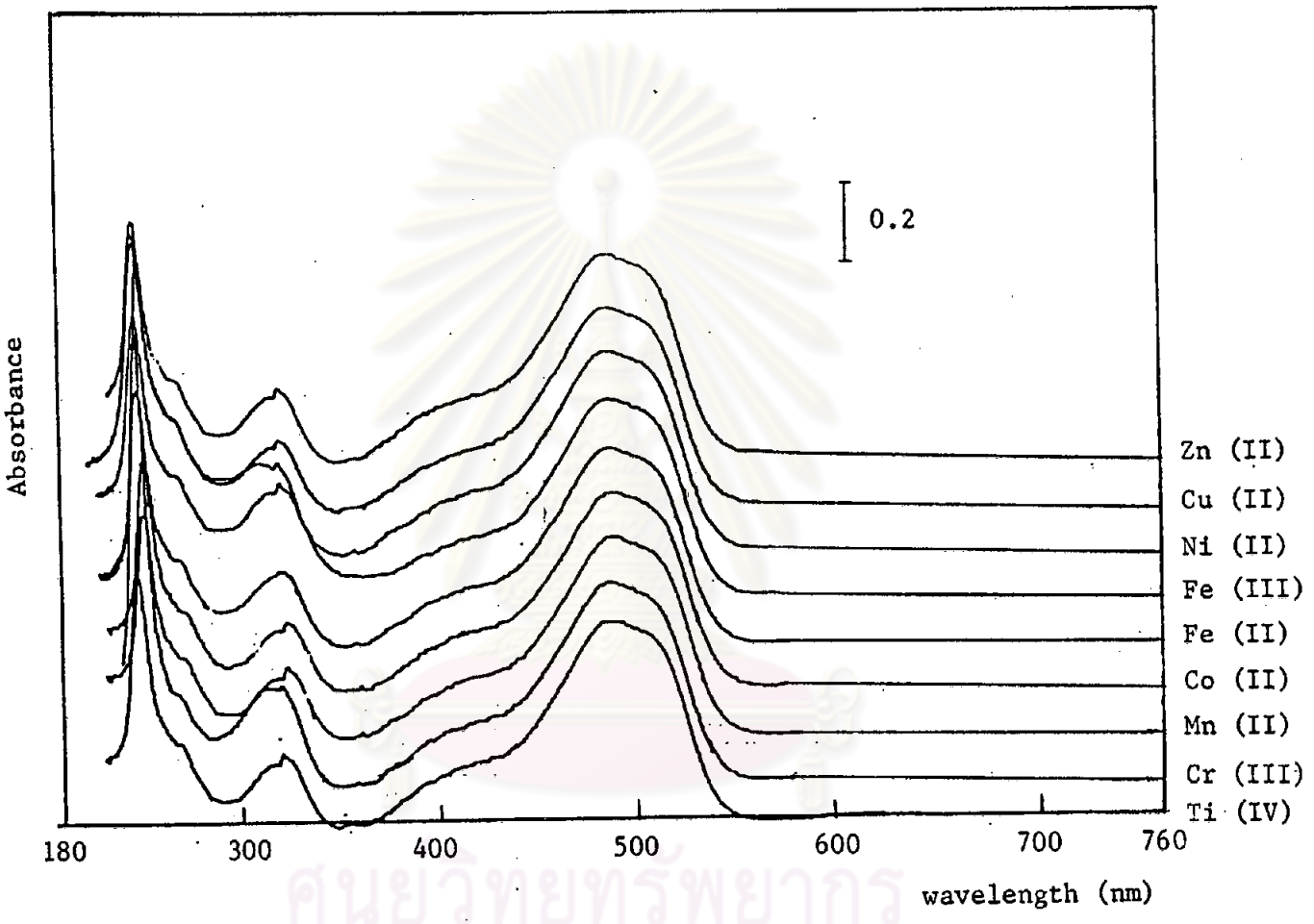

Figure 21A The UV-Visible absorption spectra of the mixture of Sunset Yellow FCF and metal ions in the acetic acid at pH 2.30.

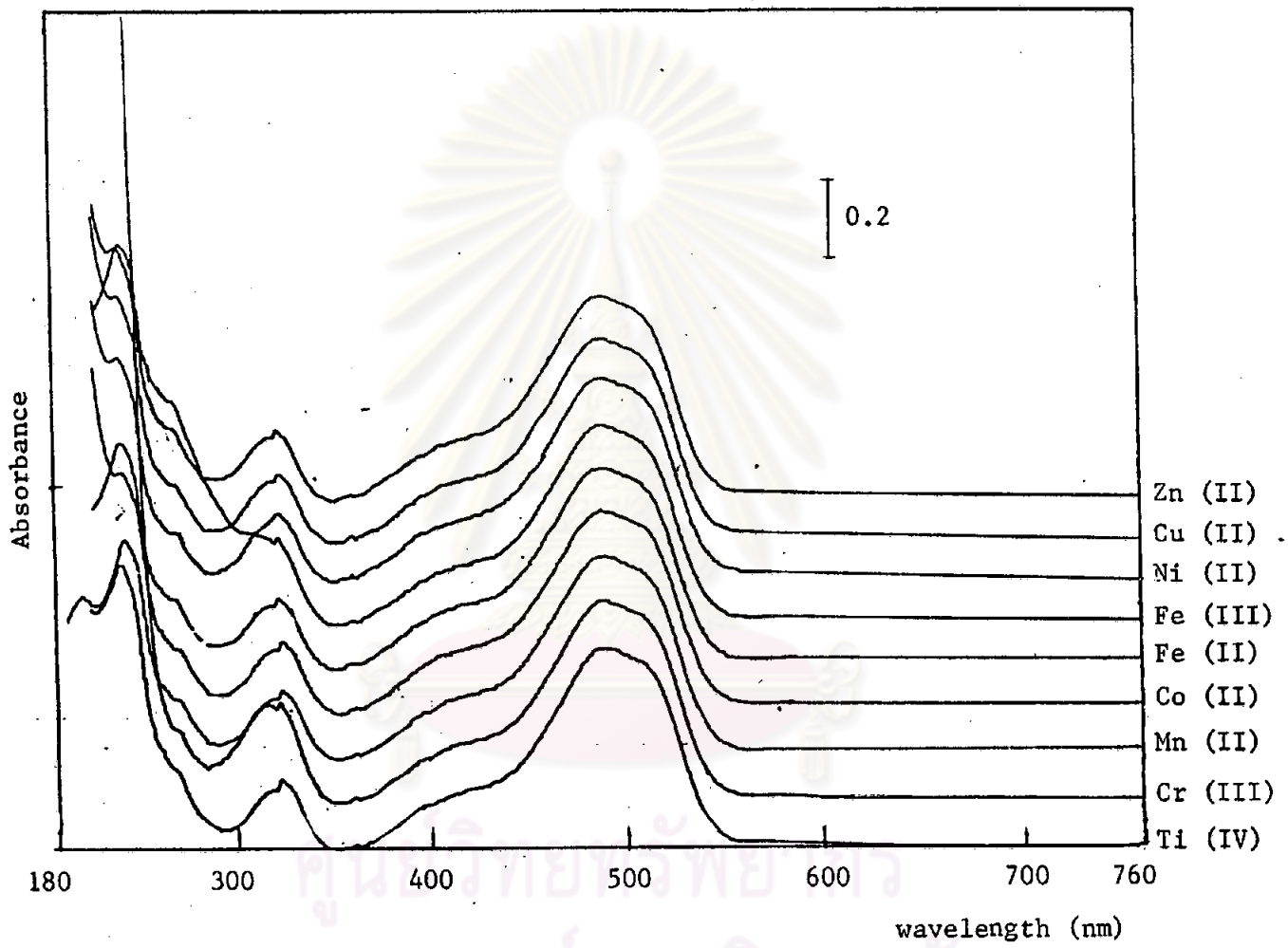

Figure 21B The UV-Visible absorption spectra of the mixture of Sunset Yellow FCF and metal ions in the phosphoric acid at pH 1.00.

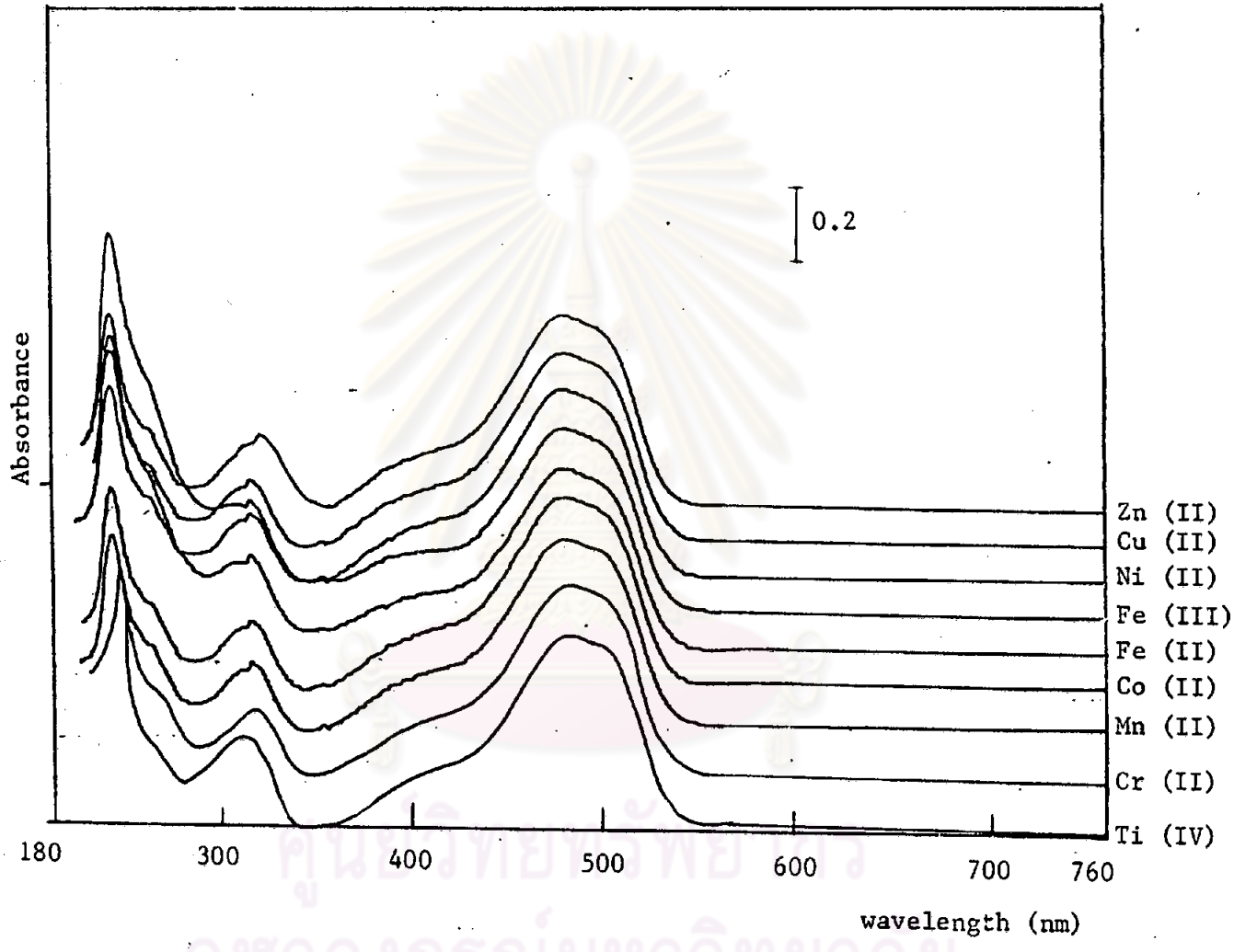

Figure 21C The UV-Visible absorption spectra of the mixture of Sunset Yellow FCF and metal ions in the McIlvaine buffer at pH 3.10.

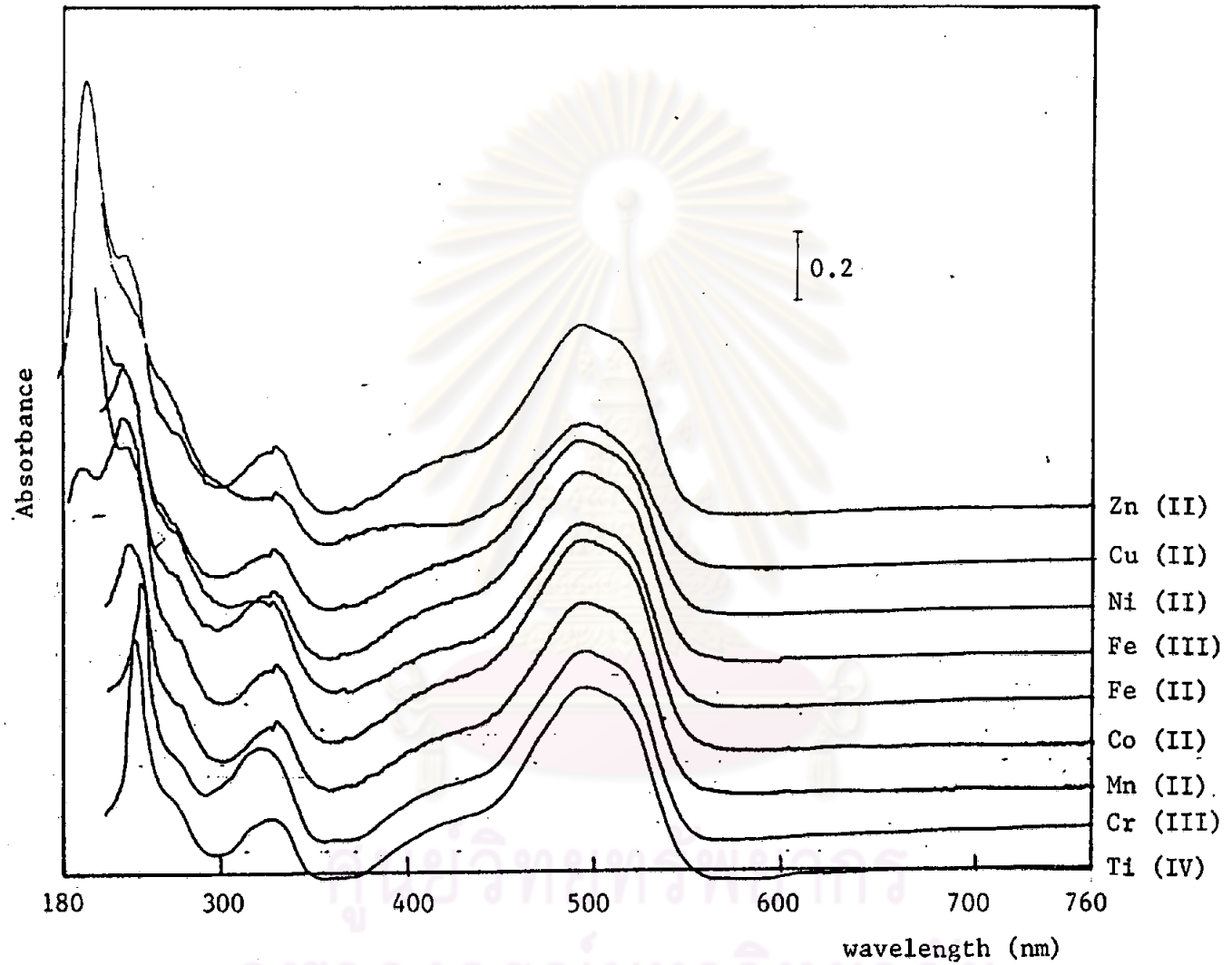

Figure 21D The UV-Visible absorption spectra of the mixture of Sunset Yellow FCF and metal ions in the McIlvaine buffer at pH 5.15.

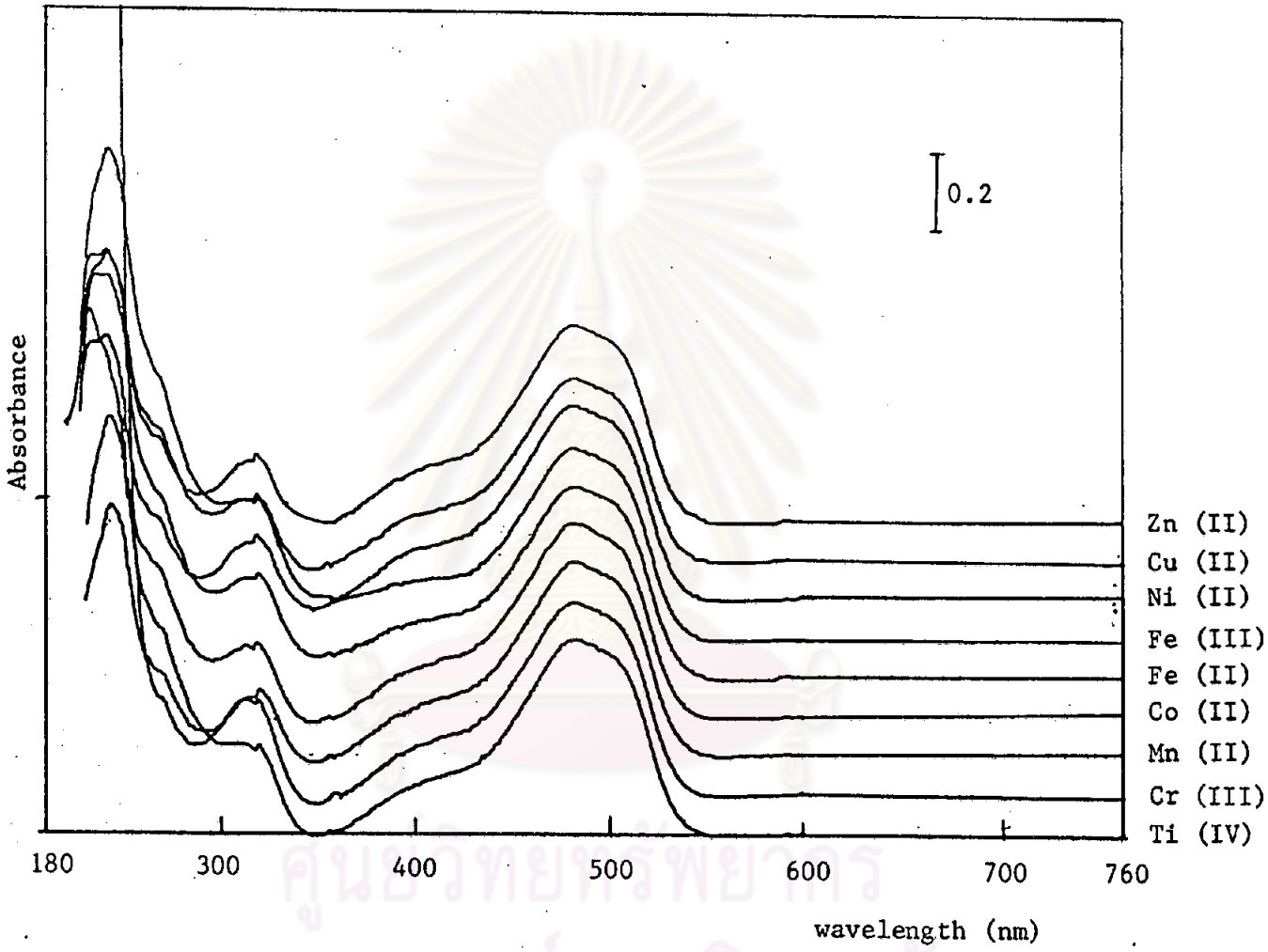

Figure 21E The UV-Visible absorption spectra of the mixture of Sunset Yellow FCF and metal ions in the McIlvaine buffer at pH 7.40.

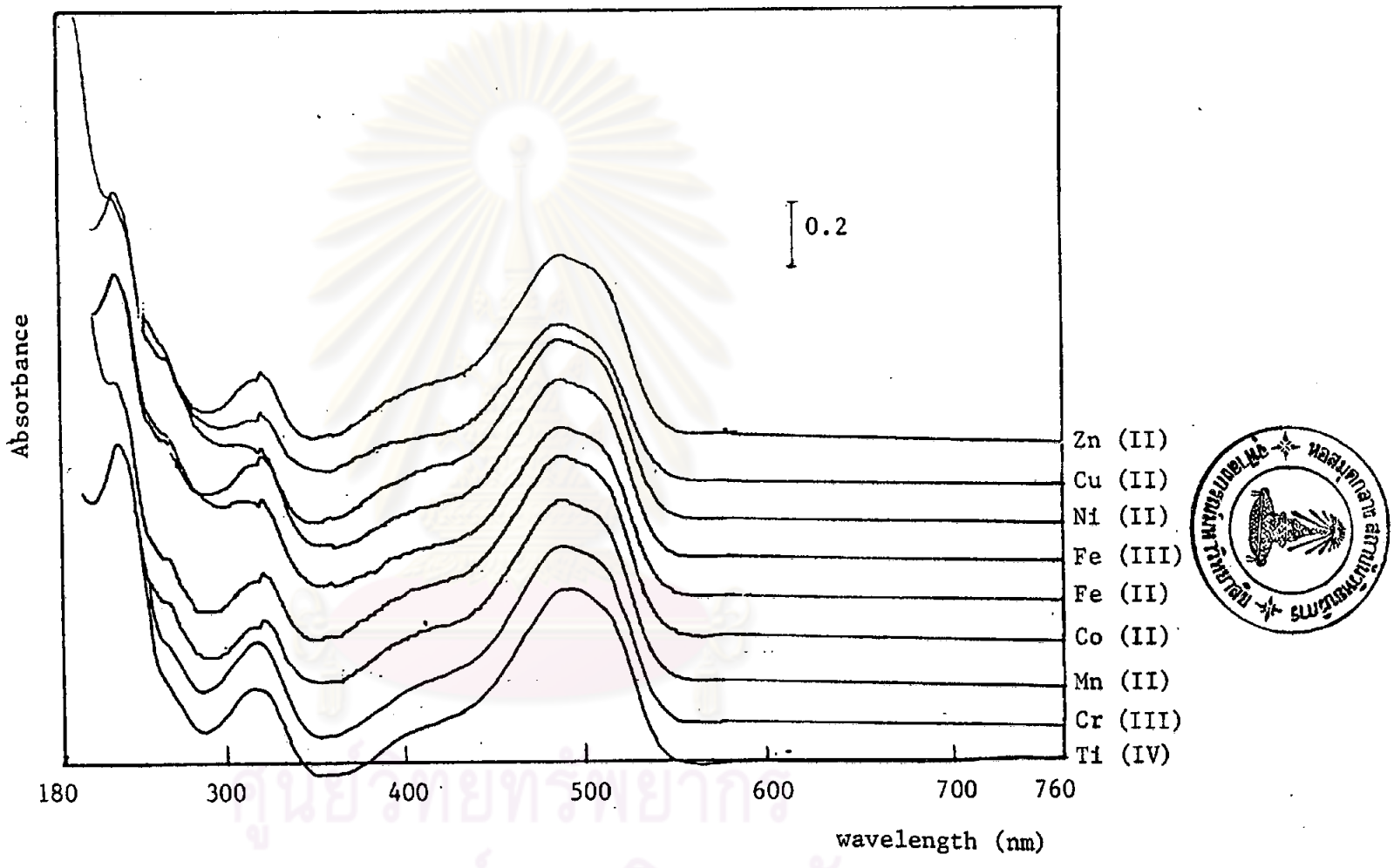

Figure 21F The UV-Visible absorption spectra of the mixture of Sunset Yellow FCF and metal ions in the phosphate buffer at pH 5.85.

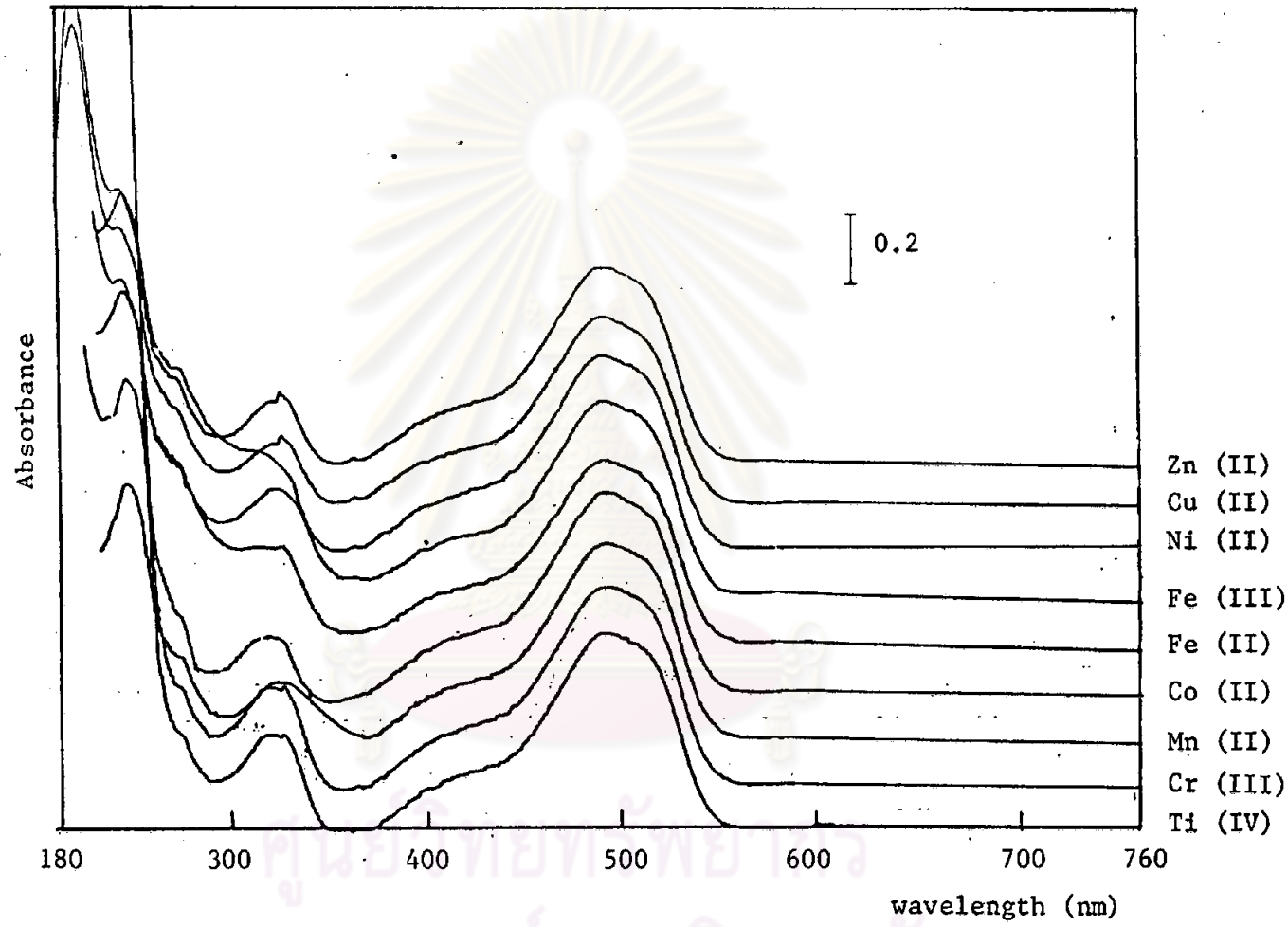

Figure 21G The UV-Visible absorption spectra of the mixture of Sunset Yellow FCF and metal ions in the phosphate buffer at pH 7.00.

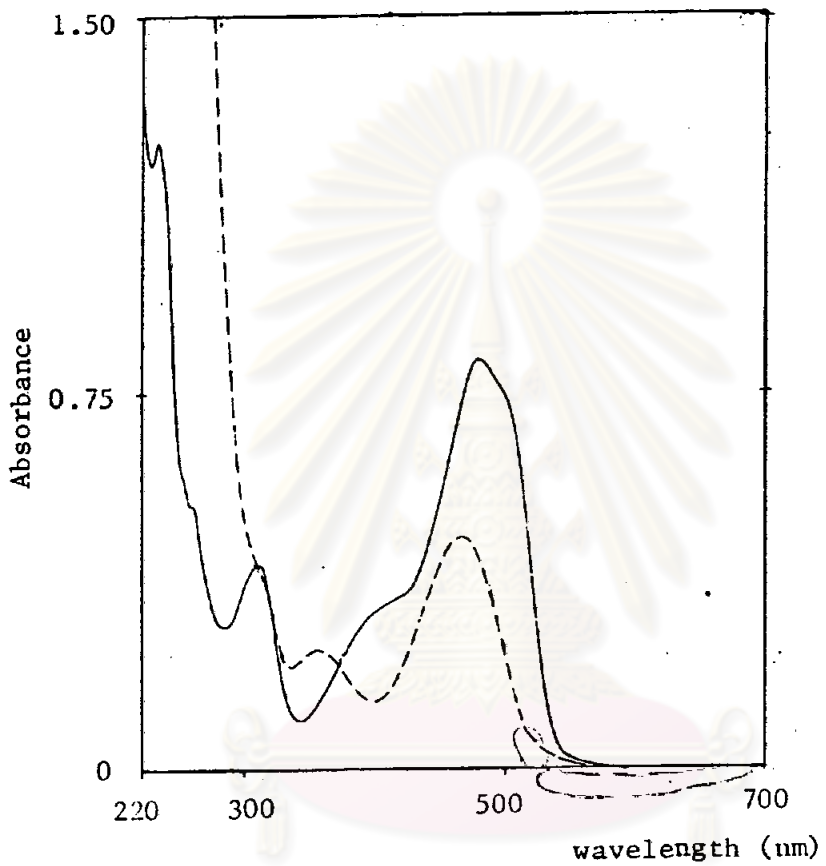

Figure 21H The UV-Visible absorption spectra of Sunset Yellow FCF and Cu (II) ion-Sunset Yellow FCF mixture in the acetate buffer at pH 6.10.

——— Sunset Yellow FCF

----- Cu (II)-Sunset Yellow FCF mixture

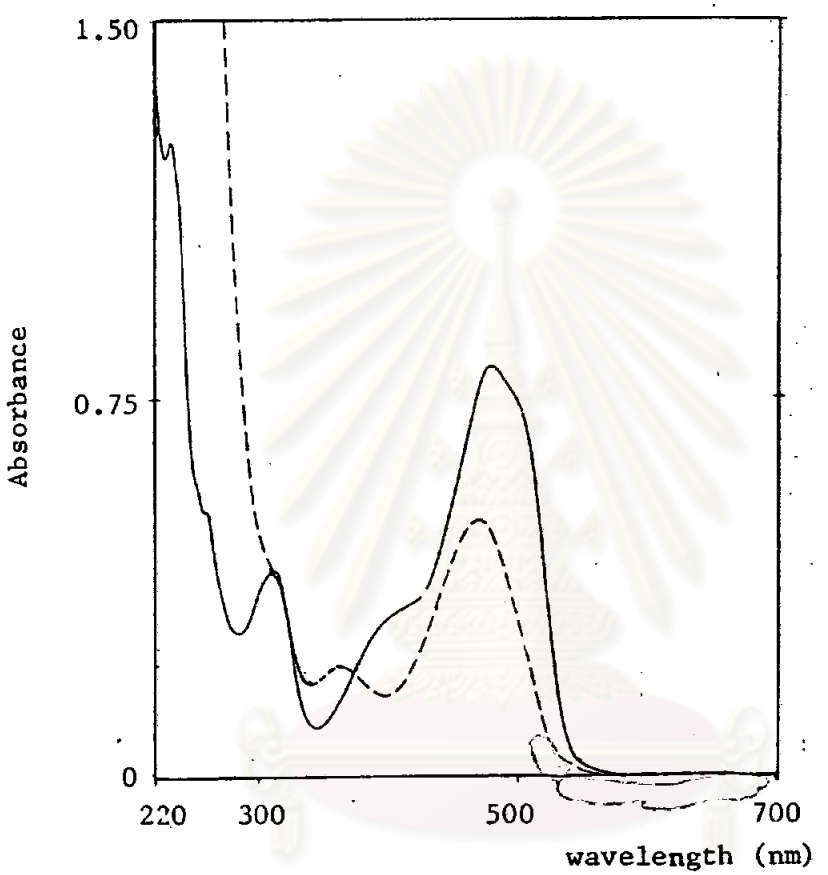

Figure 21I The UV-Visible absorption spectra of Sunset Yellow FCF and Cu (II) ion-Sunset Yellow FCF mixture in the acetate buffer at pH 5.10.

——— Sunset Yellow FCF

----- Cu (II)-Sunset Yellow FCF mixture

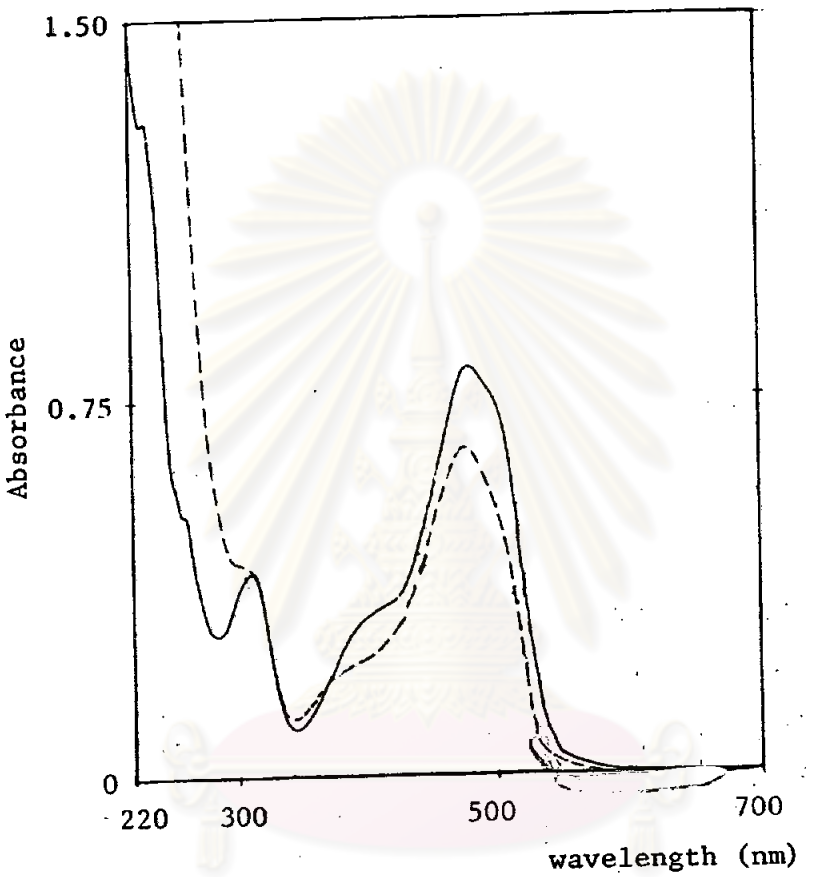

Figure 21J The UV-Visible absorption spectra of Sunset Yellow FCF and Cu (II) ion-Sunset Yellow FCF mixture in the acetate buffer at pH 4.00.

——— Sunset Yellow FCF

----- Cu (II)-Sunset Yellow FCF mixture

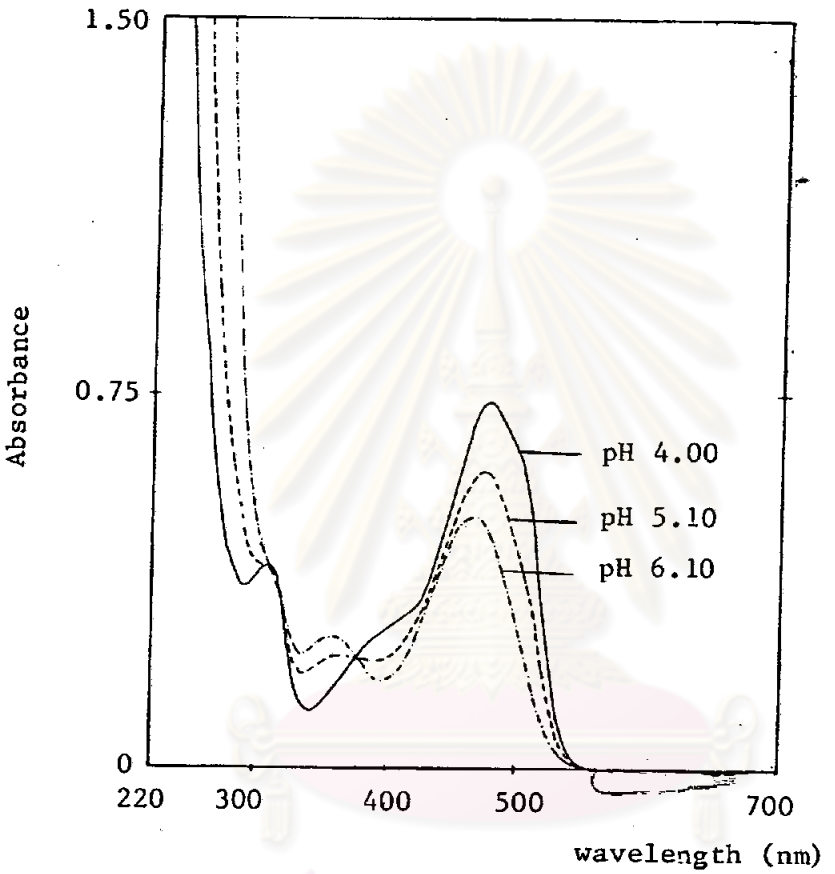

Figure 22 Effect of pH on the absorption spectra of the Cu (II) ion-Sunset Yellow FCF mixture in the acetate buffer.

Table 16 Absorption characteristics of Sunset Yellow FCF and Cu (II) ion-Sunset Yellow FCF mixtures at various pH values in ultraviolet region.

pH	λmax in visible region, nm			λmax in ultraviolet region, nm		
	Sunset Yellow FCF	Cu (II) ion-Sunset Yellow FCF mixture	Δ λmax	Sunset Yellow FCF	Cu (II) ion-Sunset Yellow FCF mixture	Δ λmax
4.00	482	480	2	307	-	-
5.10	482	475	7	307	354	47
6.10	482	470	12	307	354	47

region and they intersected each other at the fixed wavelength. This fix point is the isobestic point.

3.7.4.3 The influence of time on the color development

The effect of time on the absorbance of the Cu (II) ion-Sunset Yellow FCF mixture in the acetate buffer at 482 nm was shown in Table 17 and Figure 23. After the preparation, the absorbance of the mixture increased with time for 2 hours and after that the absorbance was time independence.

3.7.4.4 Composition of Cu (II)-Sunset Yellow FCF complex

The complex formation between Cu (II) ion and Sunset Yellow FCF was performed in the acetate buffer pH 6.10, 5.10 and 4.00. The absorbances of the Cu (II) ion-Sunset Yellow FCF mixtures were measured at 482 nm, 2 hours after the preparation.

Because of the serious overlapping absorption bands between Sunset Yellow FCF and Cu (II) ion-Sunset Yellow FCF mixture, the method of continuous variation was unsuitable for determining the composition of the complex. Similarly, the slope ratio method was also unsuitable since large concentration of Sunset Yellow FCF could not be employed. The molar ratio method was therefore employed for the treatment of the spectro photometric data.

The absorbances of the mixture solutions which contained a constant concentration of Sunset Yellow FCF and a series of concentrations of Cu (II) ion were measured, using its buffer solution as reference at 482 nm. The data were shown in Table 18.

The plots of absorbances of mixture solutions VS their molar ratios are shown in Figures 24A-26A. By graphical method, the compositions of the complex formed between Sunset Yellow FCF and Cu (II) ion are 2:1 in the acetate buffer pH 6.10 and the 1:1 Cu (II)-Sunset Yellow FCF formed in the acetate buffer pH 5.10 or 4.00.

Since the absorption spectra of Cu (II) ion-Sunset Yellow FCF in the acetate buffer pH 6.10, 5.10, 4.00 slightly shifted from Sunset Yellow FCF spectrum and the absorption spectrum of each mixture intersected each other at the same wavelength at 378 nm illustrated a simple equilibrium of Cu (II) ion-Sunset Yellow FCF as followed (21).

$$nCu^{2+} + H_xD \rightleftharpoons [Cu_nD]^{2n-x} + xH^+$$

where; H_xD = formular of Sunset Yellow FCF

$[Cu_nD]^{2n-x}$ = Cu (II)-Sunset Yellow FCF complex

The formular

$$\varepsilon = \varepsilon_x + \frac{1}{K'} \cdot \frac{\varepsilon_D - \varepsilon}{(C_M^o)^n}$$

was used for determining the composition of Cu (II)-Sunset Yellow FCF complex by plotting ε VS $\frac{\varepsilon_D - \varepsilon}{(C_M^o)^n}$

The spectrophotometric data of Cu (II)-Sunset Yellow FCF system in the acetate buffer pH 6.10, 5.10 and 4.00 are shown in Tables 19A-19C. The plots of ε VS $\frac{\varepsilon_D - \varepsilon}{(C_M^o)^n}$ are shown in Figures 24B-26B. At pH 6.10, the plot of ε VS $\frac{\varepsilon_D - \varepsilon}{(C_M^o)^n}$ when n = 1, did not yield a straight line. This meant that the complex

formation between Cu (II) and Sunset Yellow FCF was not 1:1 in the acetate buffer pH 6.10. However, the plots of ε VS $\frac{\varepsilon_D - \varepsilon}{(C_M^o)^n}$ when n = 2 gave a straight line (see Figure 24B). This indicated that the molar absorptivity data, at pH 6.10 could be explained by the reaction of type (I) (see page 11) with n = 2. This result illustrated the formation of 2:1 Cu (II)-Sunset Yellow FCF complex. At pH 5.10 or 4.00, the plots of ε VS $\frac{\varepsilon_D - \varepsilon}{(C_M^o)^n}$ did not yield a straight line. However, the plots of ε VS $\frac{\varepsilon_D - \varepsilon}{C_M^o}$ provided a straight line (see Figures 25B and 26B). This indicated the formation of 1:1 Cu (II)-Sunset Yellow FCF complex occurred in the acetate buffer pH 5.10 and 4.00.

From the molar ratio method it revealed that the 2:1 complex (metal:dye) formed in the acetate buffer pH 6.10 and the 1:1 complex formed in the acetate buffer pH 5.10 or 4.00.

Since complexation involving the replacement of the H atom of OH group together with the coordination by the azo nitrogen atom of Sunset Yellow FCF was reported (21, 38). Thus, the 1:1 Cu (II)-Sunset Yellow FCF complex can be generalized by the formular

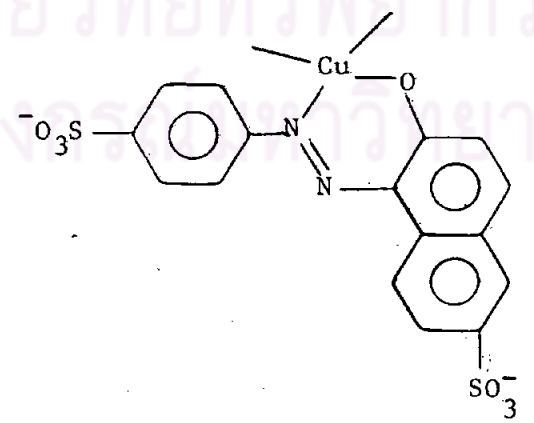

where the unfilled valencies are other molecules that can act as ligands for the metal ion such as water.

Table 17 Effect of time on the color development of the Cu (II) ion-Sunset Yellow FCF mixture in the acetate buffer.

Time	absorbance at λ 482 nm		
	pH 4.00	pH 5.10	pH 6.10
0 min.	0.951	0.814	0 642
5 min.	0.953	0.817	0.643
15 min.	0.956	0.819	0.645
30 min.	0.956	0.820	0.645
1 hr.	0.960	0.824	0.647
2 hr.	0.963	0.827	0.650
3 hr.	0.963	0.827	0.650
6 hr.	0.963	0.827	0.650
24 hr.	0.963	0.826	0.650

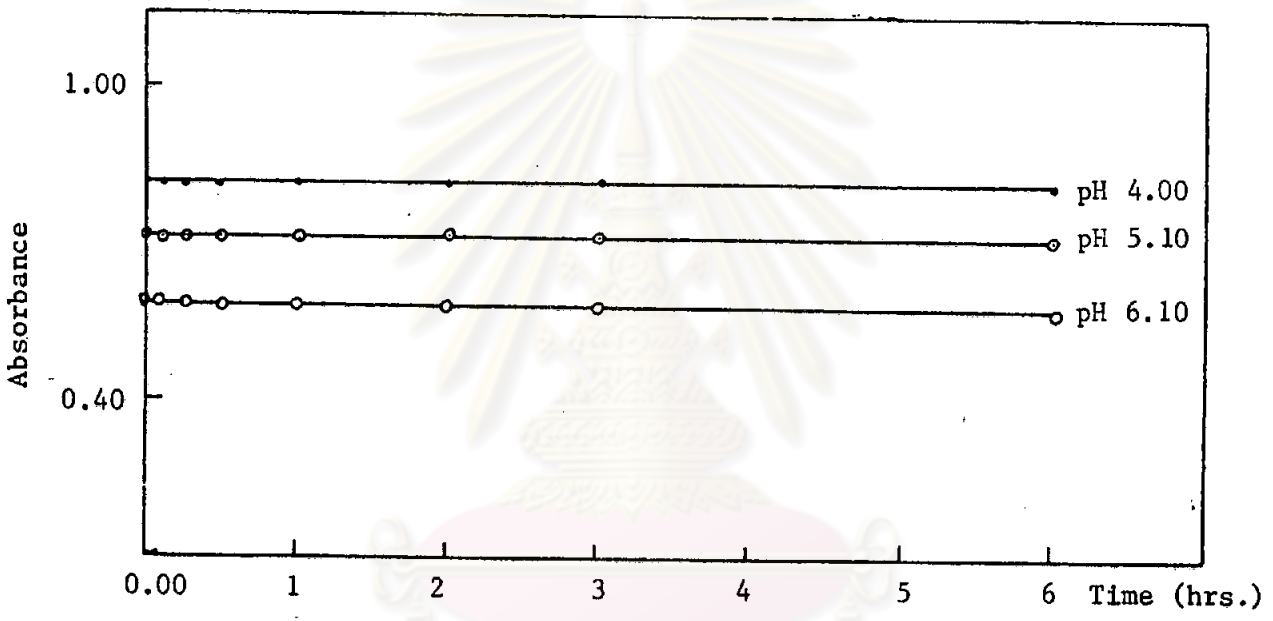

Figure 23 The influence of time on the absorbance of the Cu (II) ion-Sunset Yellow FCF mixture at various pH values.

Table 18 The molar ratio study of Sunset Yellow FCF and Cu (II) ion in the acetate buffer.

Molar ratio, Cu (II) : Sunset Yellow FCF	Absorbance at 482 nm		
	pH 6.10	pH 5.10	pH 4.00
0.00	0.507		0.503
0.20	0.493	0.512	0.502
0.40	0.481	0.510	0.501
0.60	0.473	0.509	0.500
0.80	0.463	0.508	0.500
1.00	0.456	0.506	0.499
1.20	0.450	0.505	0.499
1.40	0.441	0.503	0.498
1.60	0.435	0.502	0.499
1.80	0.430	0.501	0.498
2.00	0.420	0.501	0.498
2.20	0.420	0.500	0.498
2.40	0.418	0.498	0.498
2.60	0.411	0.497	0.498
2.80	0.405	0.497	0.497
3.00	0.406	0.495	0.496
3.20	0.397	0.494	0.496
3.40	0.395	0.494	0.496
3.60	0.391	0.492	0.496
4.00	0.386	0.491	0.495
4.40	0.379	0.489	0.495
4.80	0.374	0.486	0.495
5.20	0.369	0.485	0.495
5.60	0.366	0.484	0.494
6.00	0.367	0.482	0.494
6.40	0.360	0.482	0.496
6.80	0.355	0.481	0.494

Table 19A Spectrophotometric data of the Cu (II)-Sunset Yellow FCF System in the acetate buffer pH 6.10, using 3.2×10^{-5} M Sunset Yellow FCF.

$10^3 \times C_M^o$, M	Absorbance at 482 nm	$\varepsilon \times 10^4$	$\frac{\varepsilon_D - \varepsilon}{(C_M^o)^n} \times 10^{10}$
0.00	0.804	2.5125	
0.40	0.505	1.5780	5.8406
0.80	0.482	1.5063	1.5722
1.20	0.472	1.4750	0.7205
1.60	0.468	1.4625	0.4101
2.40	0.465	1.4531	0.1839
3.20	0.464	1.4500	0.1038
4.00	0.463	1.4469	0.0666

Table 19B Spectrophotometric data of the Cu (II)-Sunset Yellow FCF System in the acetate buffer pH 5.10, using 3.2×10^{-5} M Sunset Yellow FCF.

$10^3 \times C_M^o$, M	Absorbance at 482 nm	$\varepsilon \times 10^4$	$\frac{\varepsilon_D - \varepsilon}{C_M^o} \times 10^7$
0.00	0.805	2.5156	
0.40	0.652	2.0375	1.1953
0.80	0.594	1.8563	0.8241
1.20	0.563	1.7594	0.6302
1.60	0.545	1.7031	0.5078
2.00	0.533	1.6656	0.4250
2.40	0.523	1.6344	0.3672
3.20	0.511	1.5969	0.2871

Table 19C Spectrophotometric data of the Cu (II)-Sunset Yellow FCF System in the acetate buffer pH 4.00, using 3.2×10^{-5} M Sunset Yellow FCF.

$10^3 \times C_M^o$, M	Absorbance at 482 nm	$\varepsilon \times 10^4$	$\frac{\varepsilon_D - \varepsilon}{C_M^o} \times 10^6$
0.00	0.806	2.5187	
0.40	0.767	2.3969	3.045
0.80	0.739	2.3094	2.6163
1.20	0.718	2.2438	2.2908
1.60	0.702	2.1938	2.0306
2.00	0.683	2.1344	1.9215
2.40	0.677	2.1156	1.6796
3.20	0.659	2.0594	1.4325

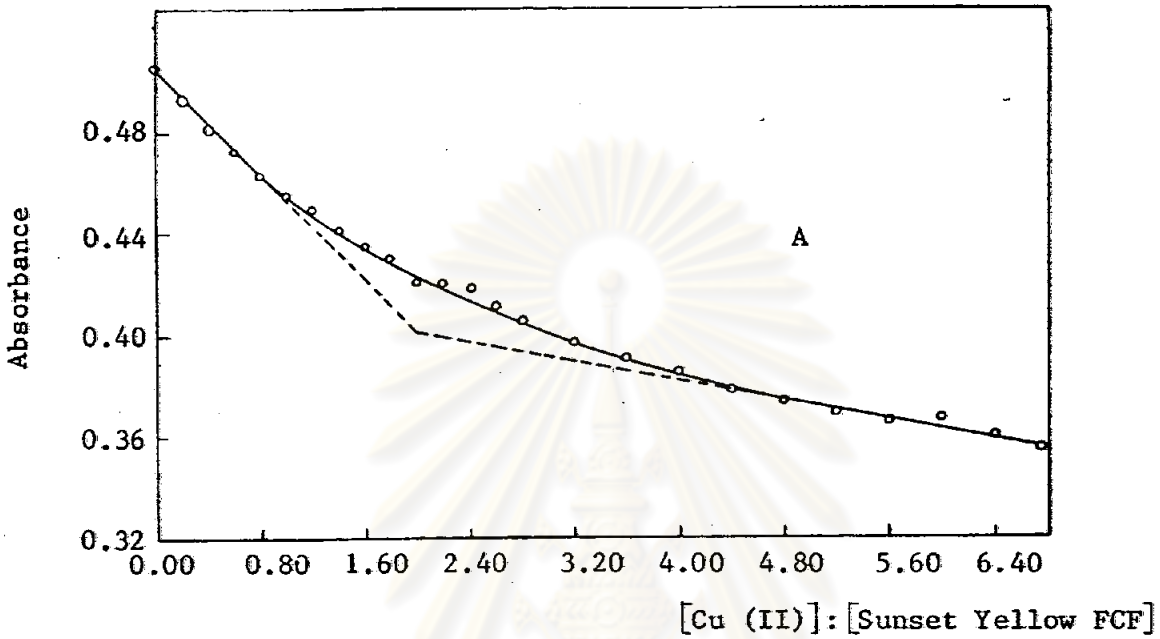

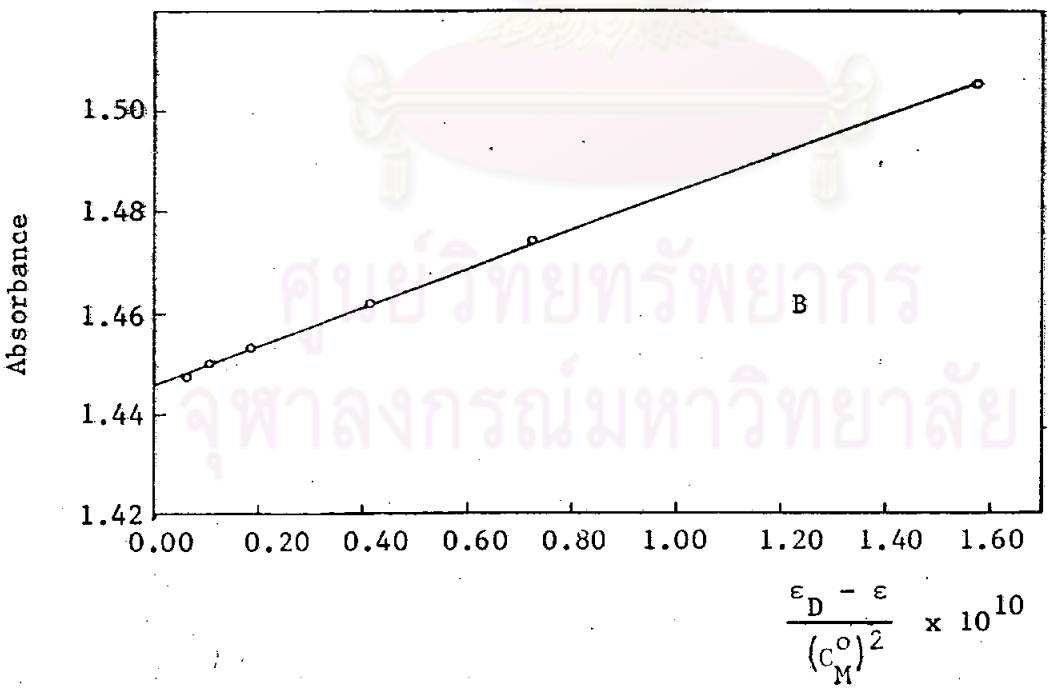

Figure 24 The Cu (II)-Sunset Yellow FCF system at pH 6.10

A) Molar ratio plot for the solution contained 2.00 x 10^{-5} M Sunset Yellow FCF and various concentration of Cu (II) ion

B) plot of ε VS $\frac{\varepsilon_D - \varepsilon}{(C_M^o)^2}$ for the solution contained 3.20 x 10^{-5} M Sunset Yellow FCF and various concentrations of Cu (II) ion

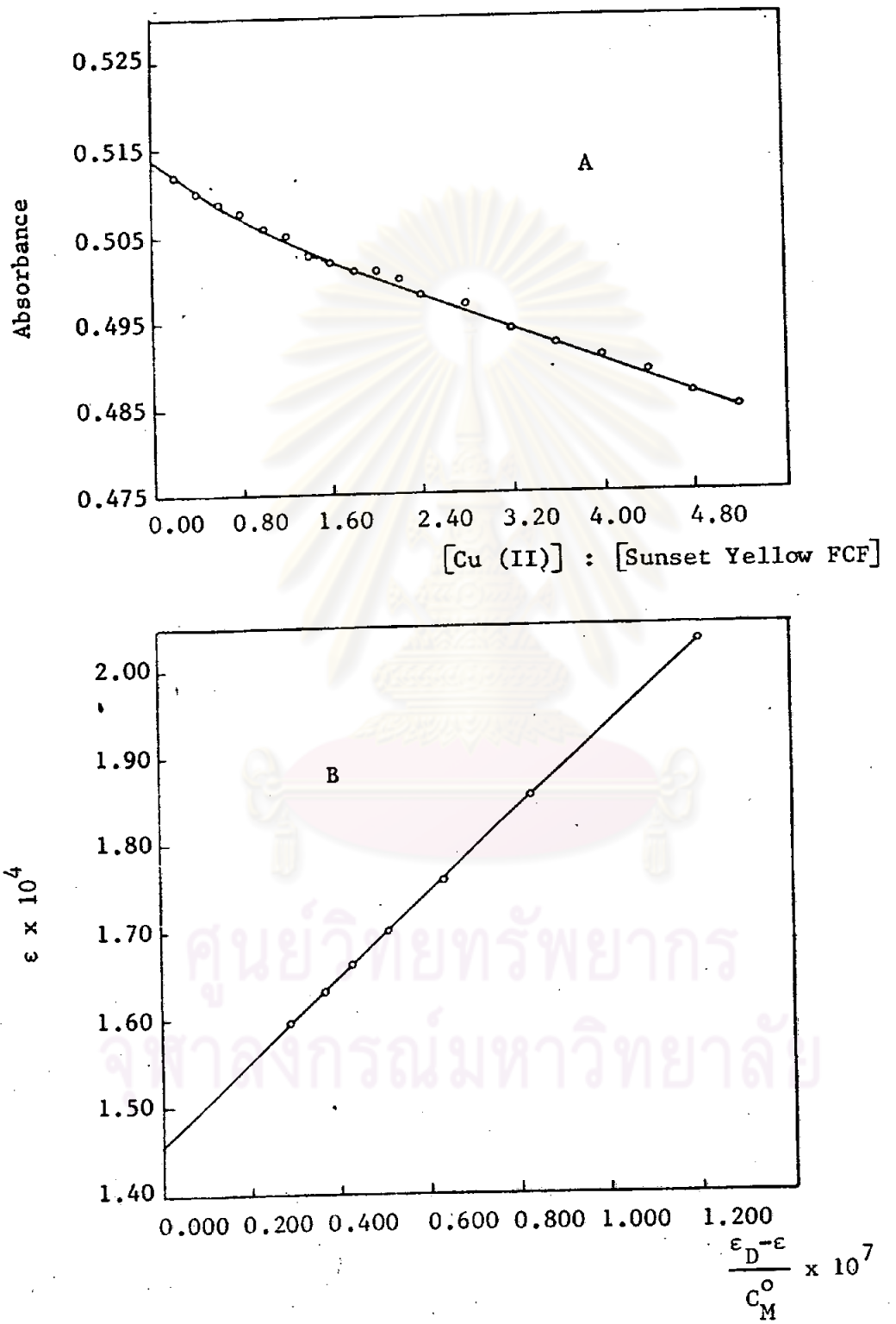

Figure 25 The Cu (II)-Sunset Yellow FCF system at pH 5.10

A) Molar ratio plot for the solution contained 2.00×10^{-5} M Sunset Yellow FCF and various concentrations of Cu (II) ion

B) plot of ε VS $\frac{\varepsilon_D - \varepsilon}{C_M^o}$ for the solution contained 3.20×10^{-5} M Sunset Yellow FCF and various concentrations of Cu (II) ion

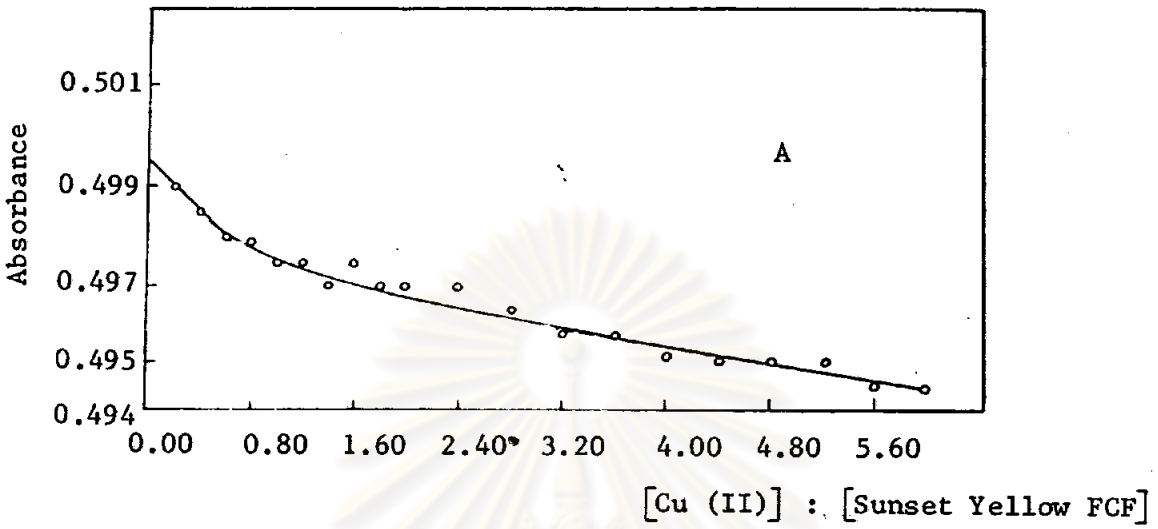

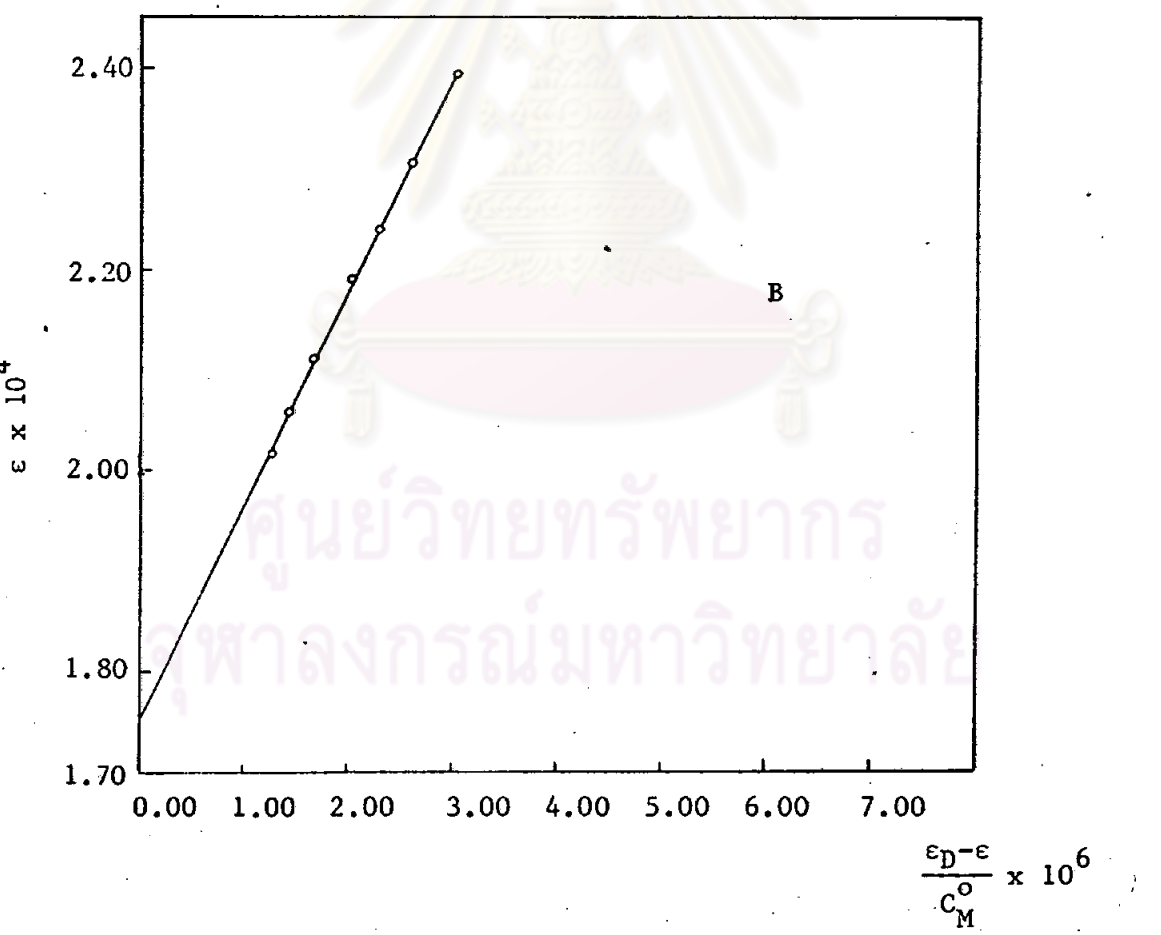

Figure 26 The Cu (II)-Sunset Yellow FCF system at pH 4.00
A) Molar ratio plot for the solution contained 2.00 x 10^{-5} M Sunset Yellow FCF and various concentrations of Cu (II) ion
B) plot of ε VS $\frac{\varepsilon_D-\varepsilon}{C_M^o}$ for the solution contained 3.20 x 10^{-5} M Sunset Yellow FCF and various concentrations of Cu (II) ion

For 2:1 Cu (II)-Sunset Yellow FCF complex, it was proposed as a salt forming Cu (II) ion and a coordinated Cu (II) ion per dye molecule (21). Since the exact location of Cu (II) ion is not known. Thus, the structure of this complex can not be written.

3.7.5 The mixtures of Orange G and Ti (IV), Cr (III), Mn (II), Co (II), Fe (II), Fe (III), Ni (II) or Zn (II)

The absorption spectra of the mixtures of each metal ion and Orange G in phosphoric acid, acetic acid, McIlvaine buffer, phosphate buffer and diethylamine were shown in Figures 27A-27H. Since the absorption spectra of the metal ion-Orange G mixtures were not different from that of the dye solution and no physical change in each mixture system was observed, no complex formed between Orange G and Ti (IV), Cr (III), Mn (II), Co (II), Fe (II), Fe (III), Ni (II), or Zn (II) ion.

3.7.6 The mixtures of Orange G and Cu (II) ion

The absorption spectra of the mixtures of Orange G and Cu (II) ion in phosphoric acid, acetic acid, McIlvaine buffer, phosphate buffer, acetate buffer and diethylamine were recorded as shown in Figures 27A-27K. The spectra of Cu (II) ion-Orange G mixtures in phosphoric acid, acetic acid, McIlvaine buffer, phosphate buffer and diethylamine were not different from that of the dye solution and no physical change in each mixture solution was observed. This meant that no reaction between Orange G and Cu (II) ion occurred and no complex formed in the buffer solutions such as phosphoric acid, acetic acid, McIlvaine buffer, phosphate buffer and diethylamine. However, in the acetate buffer at pH 6.10, 5.10 or 4.00 it was found that Orange G reacted with Cu (II) ion since the color of the mixture solution changed from orange to

yellow-orange. The absorption spectra of Cu (II)-Orange G solution in the acetate buffer differed from those of Orange G. A small hypsochromic shift occurred and the absorption intensity of Orange G at 476 nm decreased in the presence of Cu (II) ion (see Figures 27J-27K).

3.7.6.1 Absorption characteristics of Cu (II) ion-Orange G mixture

The absorption spectra of Orange G, the mixture of Orange G and Cu (II) ion in the acetate buffer pH 6.10, 5.10, 4.00 were recorded in the range of wavelengths between 220-700 nm (see Figures 27I-27K). The absorption spectra of Cu (II) ion-Orange G mixture slightly shifted to the lower wavelength and the absorbance of Orange G decreased in the presence of Cu (II) ion. The strong absorption band of Cu (II) ion-Orange G mixture in the acetate buffer pH 6.10, 5.10, 4.00 appeared at 468 nm, 474 nm and 474 nm, respectively. In the ultraviolet region the absorption spectra of the mixtures of Cu (II) ion and Orange G were slightly different from the spectrum of Orange G by a small peak at 390 nm disappeared.

3.7.6.2 The effect of pH on the absorption spectra of Cu (II) ion-Orange G mixture

Ultraviolet-visible spectra of Cu (II) ion-Orange G mixtures at various pH values were shown in Figure 28. It was seen that the absorbance of Cu (II) ion-Orange G mixture decreased when the pH of the solution increased and the wavelength at the maximum absorption of Cu (II) ion-Orange G mixture gradually shifted to lower wavelength when the pH increased (see Table 20 and Figure 28). The absorption spectra of Cu (II) ion-Orange G mixture in the acetate buffer at pH 6.10, 5.10, 4.00

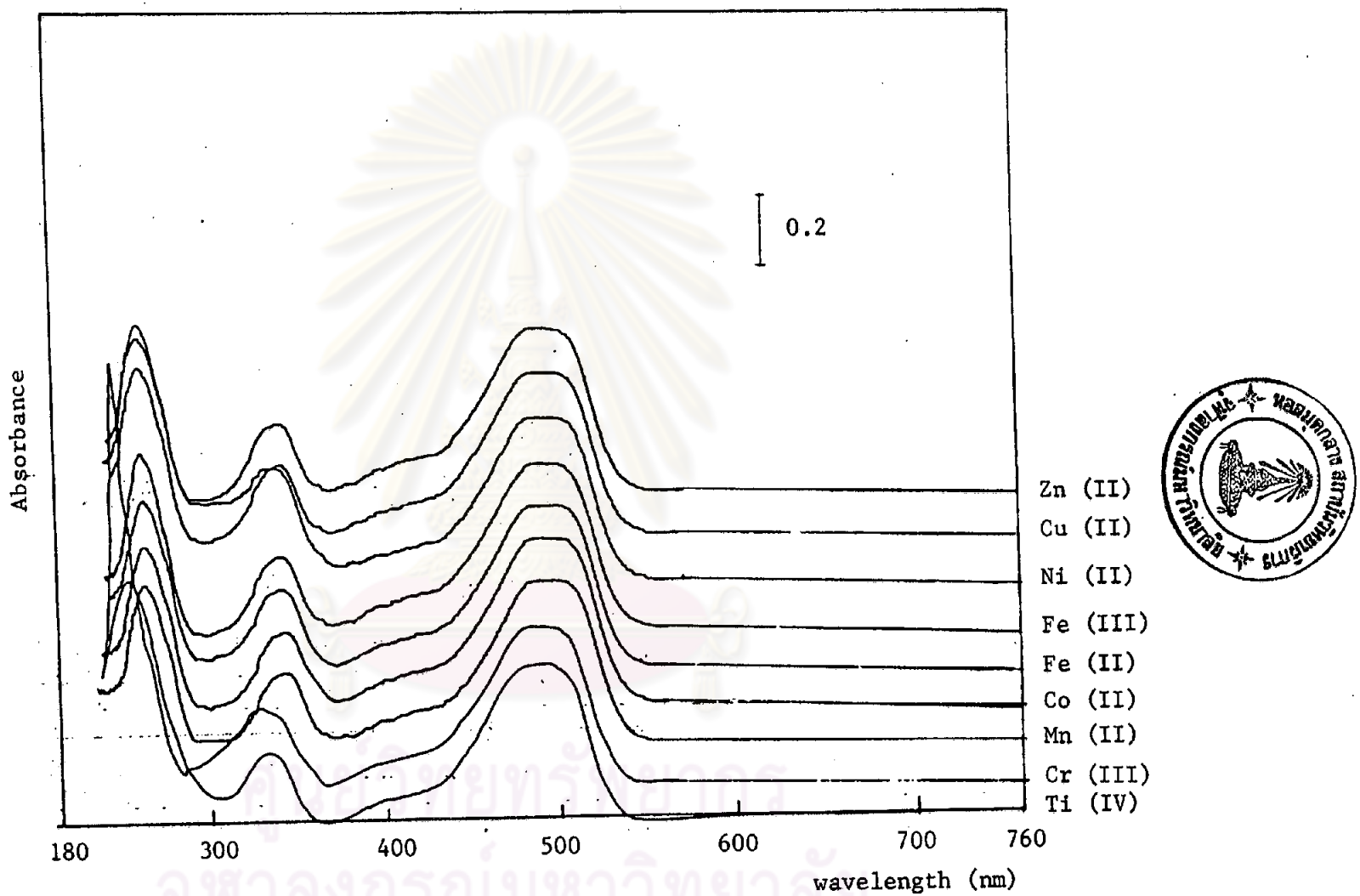

Figure 27A The UV-Visible absorption spectra of the mixture of Orange G and metal ions in acetic acid at pH 2.30.

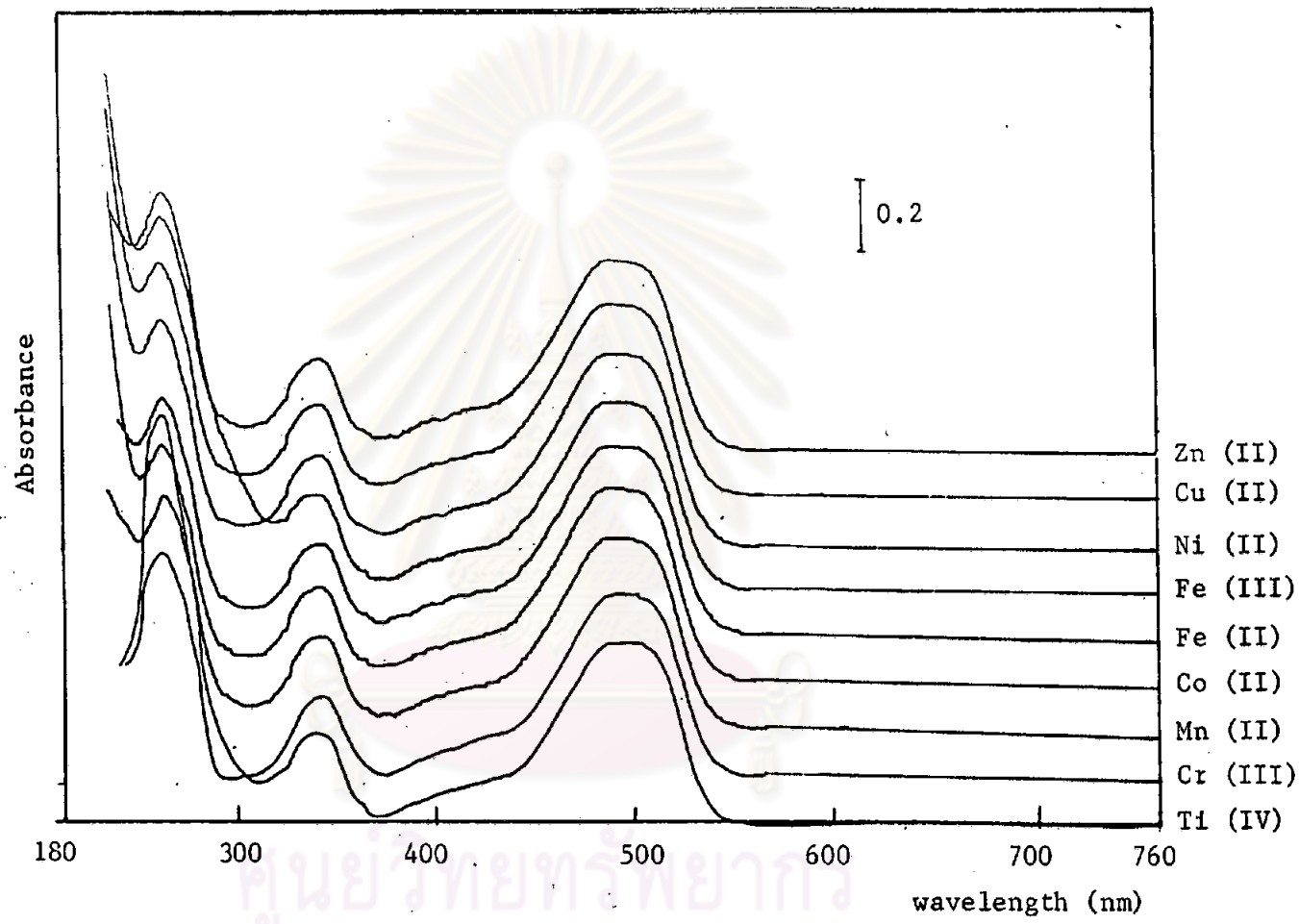

Figure 27B The UV-Visible absorption spectra of the mixture of Orange G and metal ions in phosphoric acid at pH 1.00.

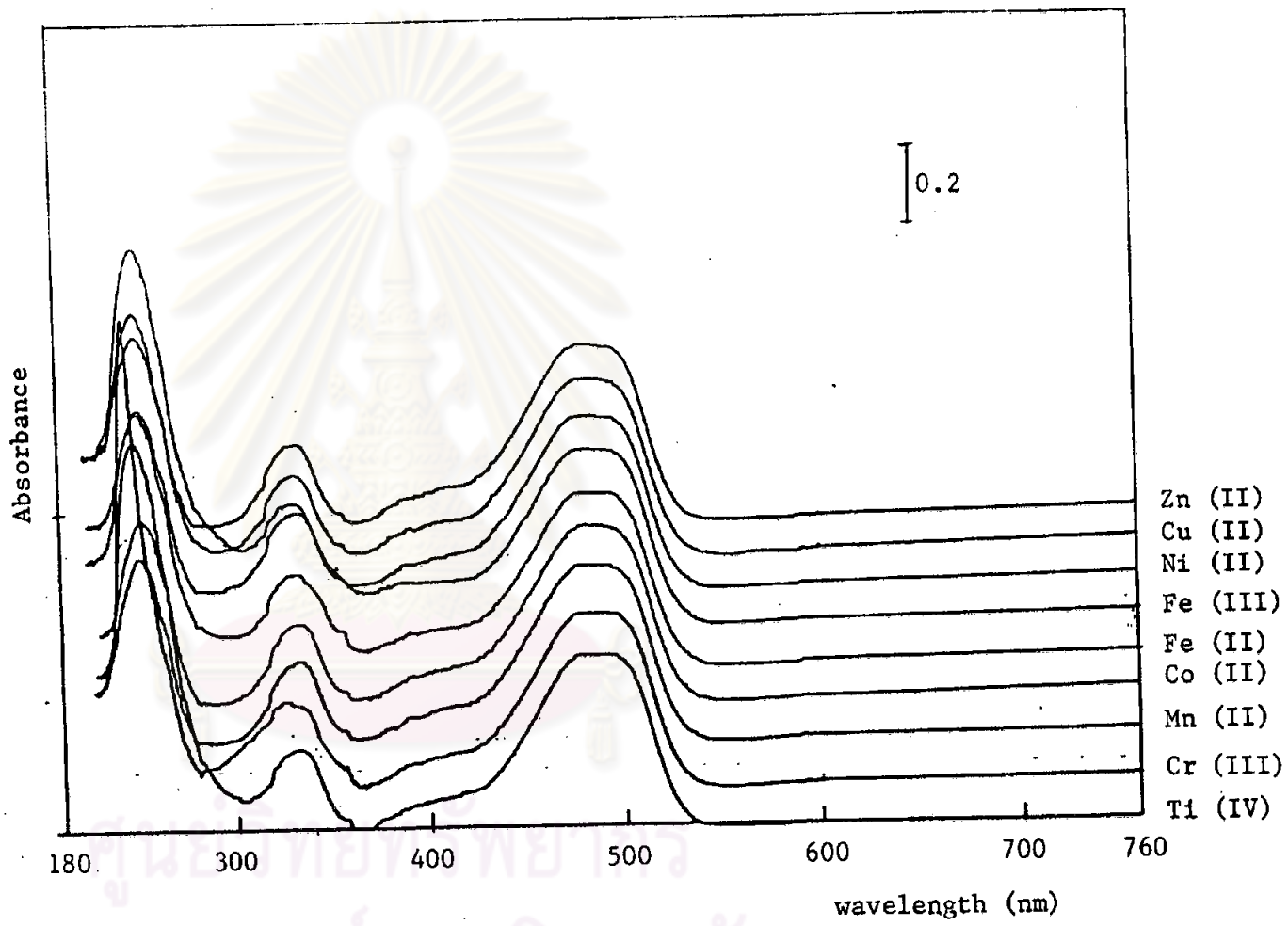

Figure 27C The UV-Visible absorption spectra of the mixture of Orange G and metal ions in the McIlvaine buffer at pH 3.10.

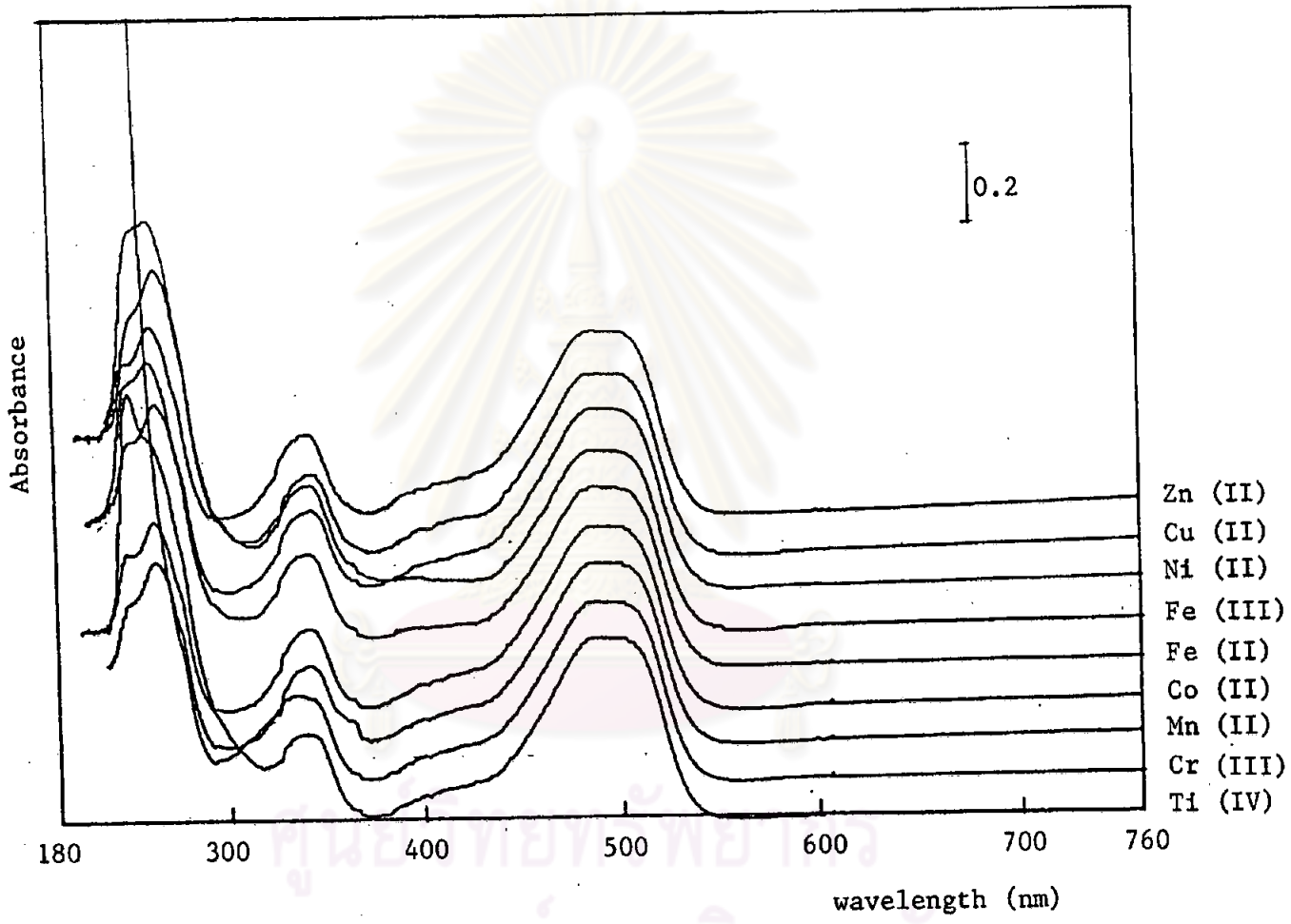

Figure 27D The UV-Visible absorption spectra of the mixture of Orange G and metal ions in the McIlvaine buffer at pH 5.15.

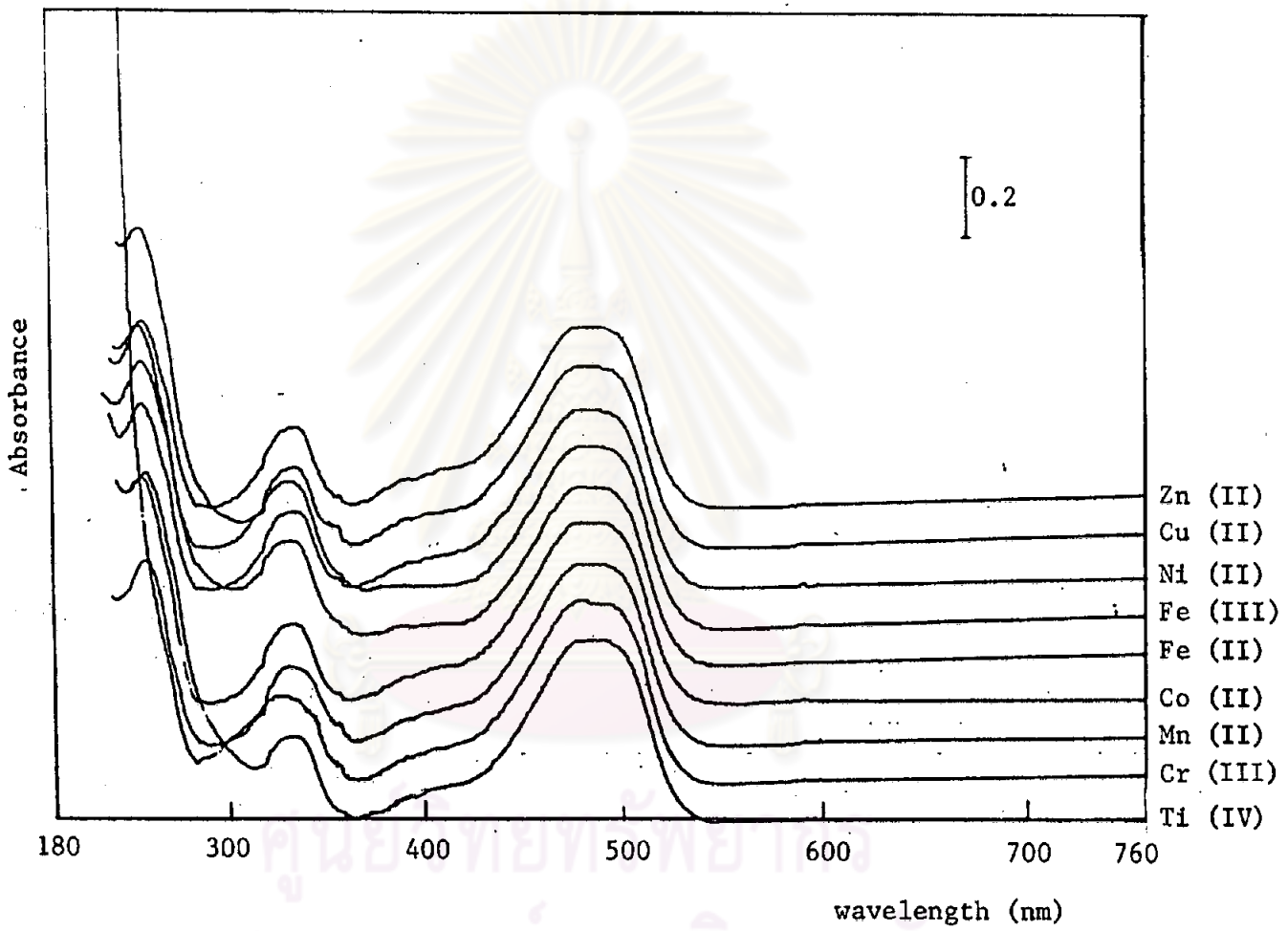

Figure 27E The UV-Visible absorption spectra of the mixture of Orange G and metal ions in the McIlvaine buffer at pH 7.40.

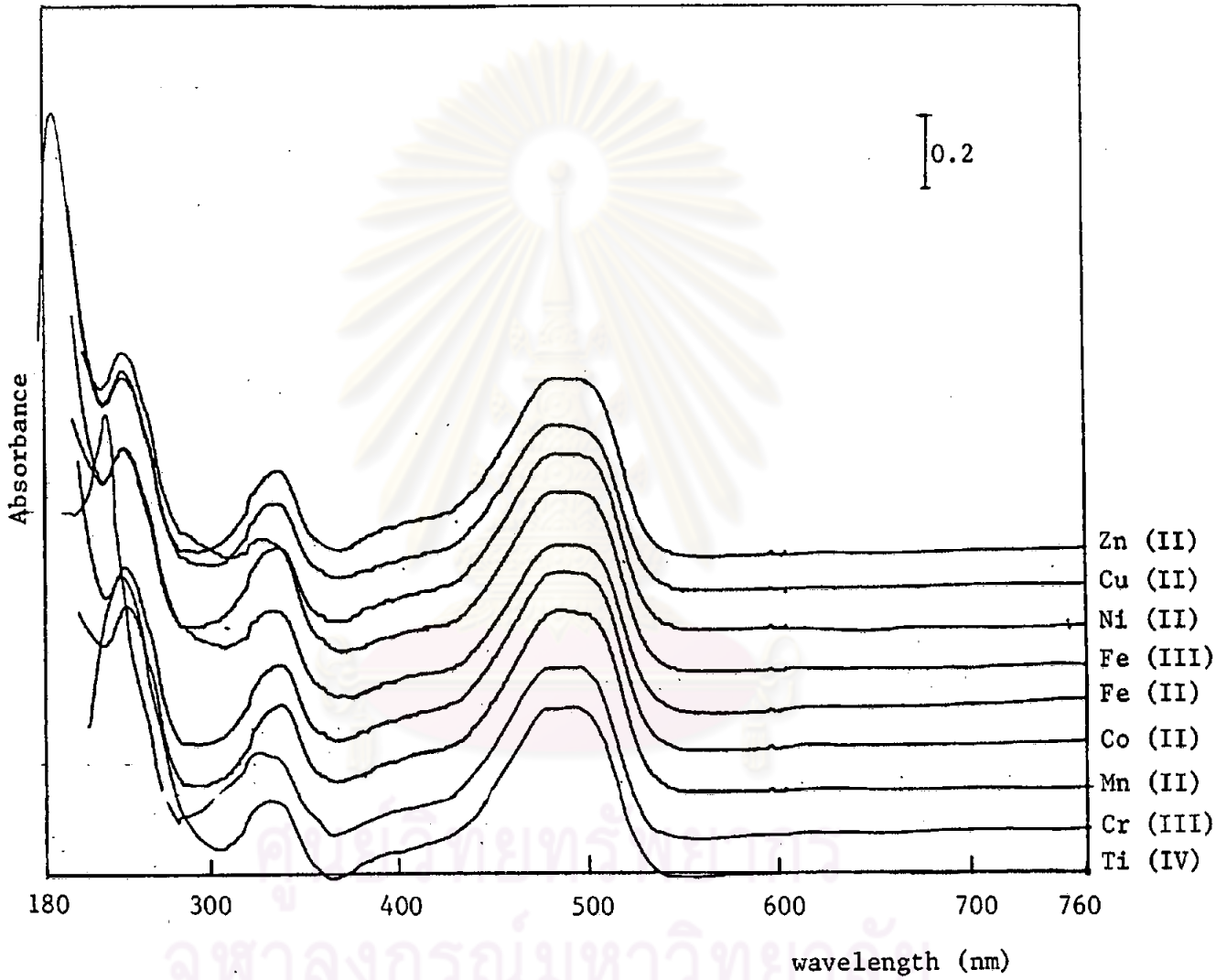

Figure 27F The UV-Visible absorption spectra of the mixture of Orange G and metal ions in the phosphate buffer at pH 5.85.

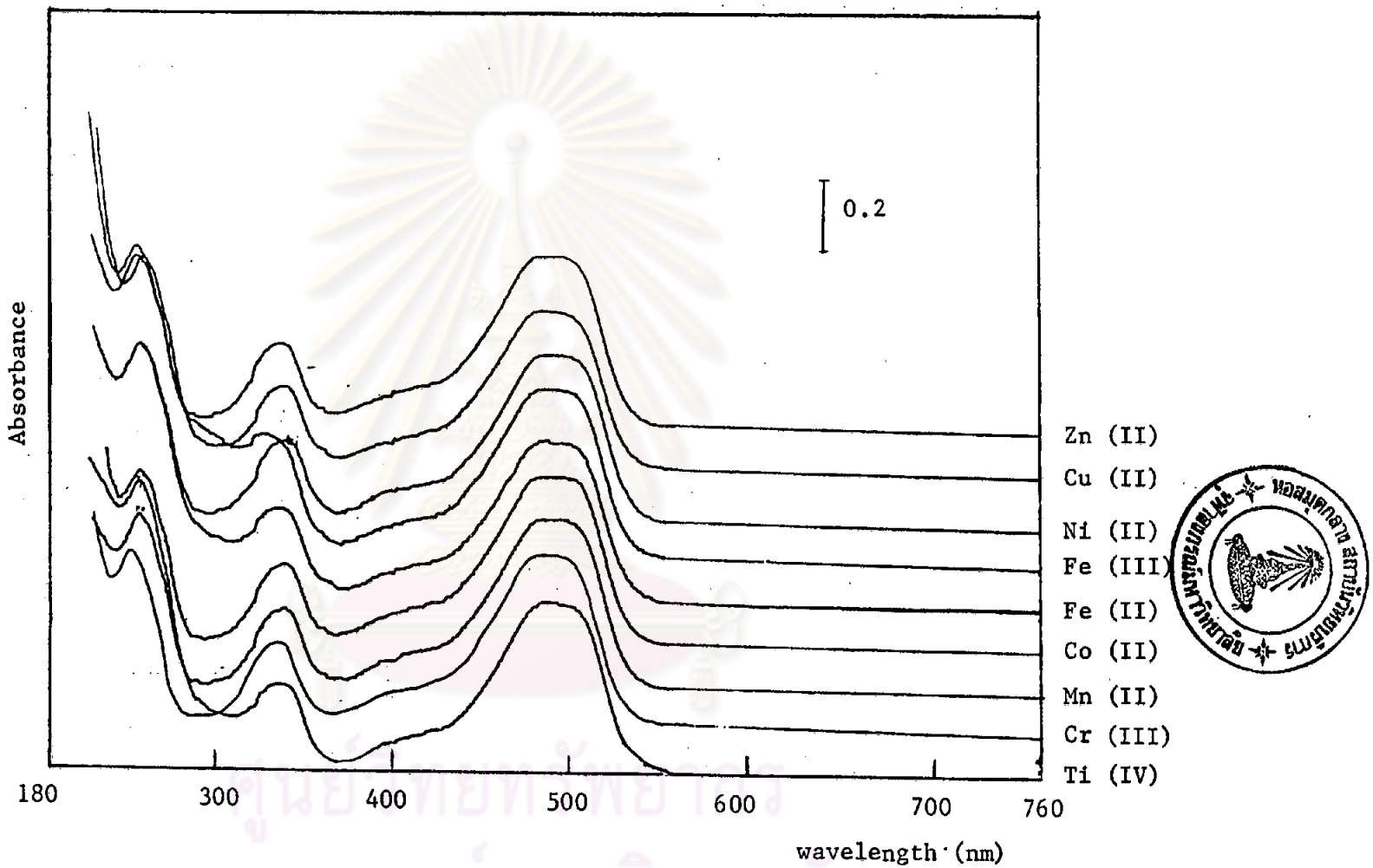

Figure 27G The UV-Visible absorption spectra of the mixture of Orange G and metal ions in the phosphate buffer at pH 7.00.

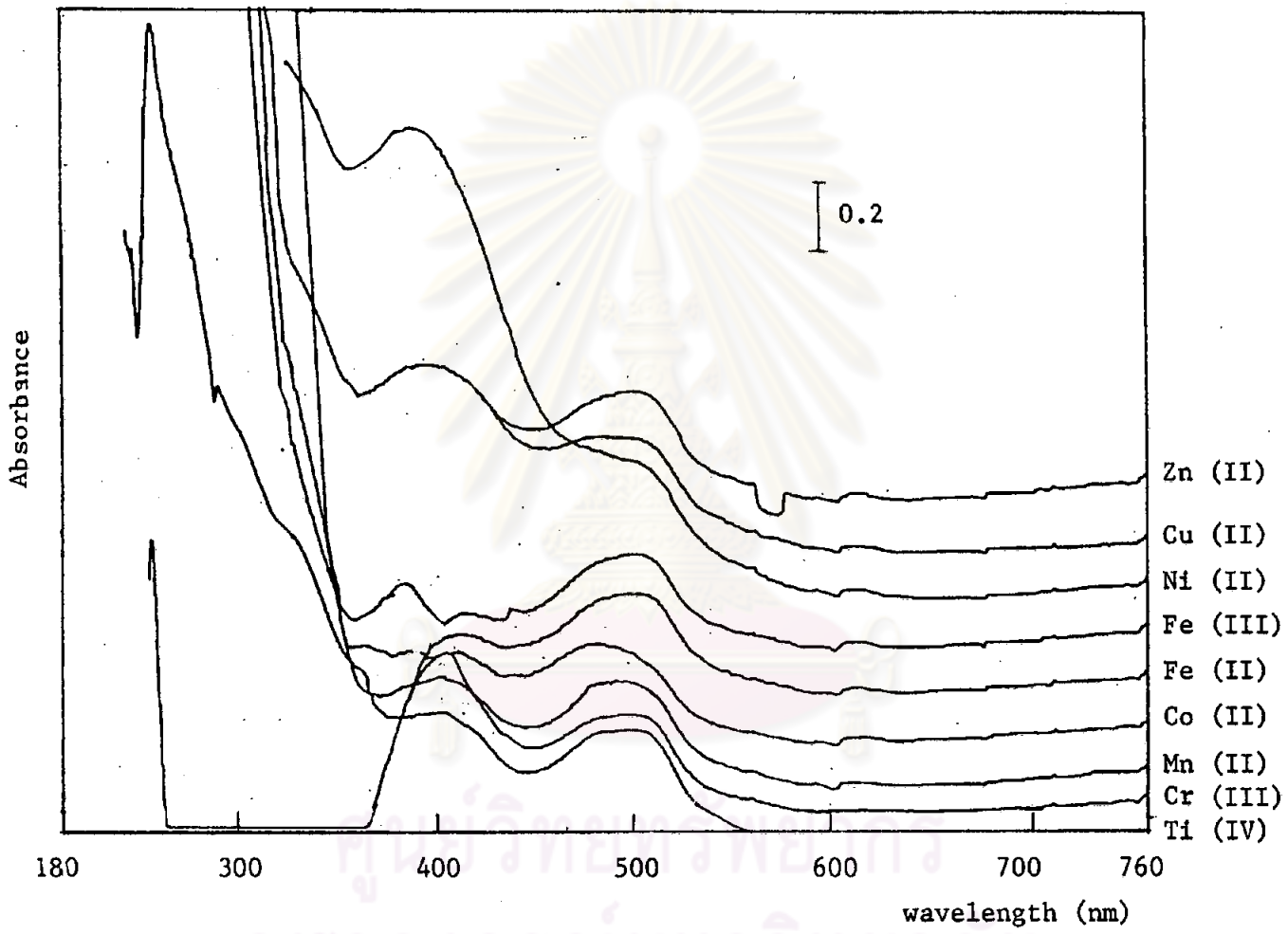

Figure 27H The UV-Visible absorption spectra of the mixture of Orange G and metal ions in diethylamine pH 12.50.

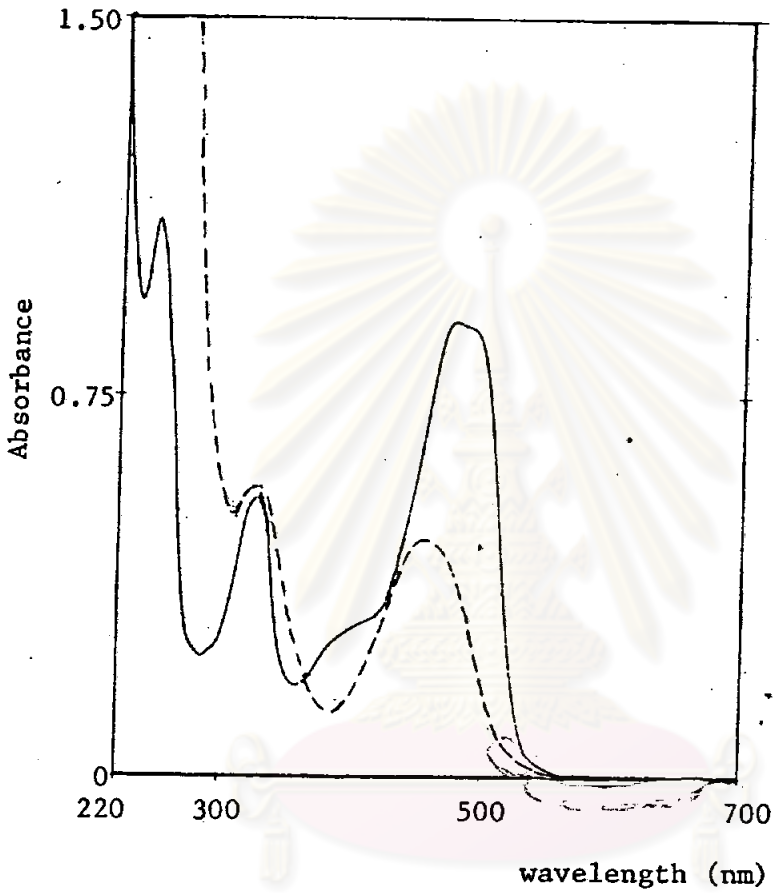

Figure 27I The UV-Visible absorption spectra of Orange G and Cu (II) ion-Orange G mixture in the acetate buffer at pH 6.10.

——— Orange G

----- Cu (II)-Orange G mixture

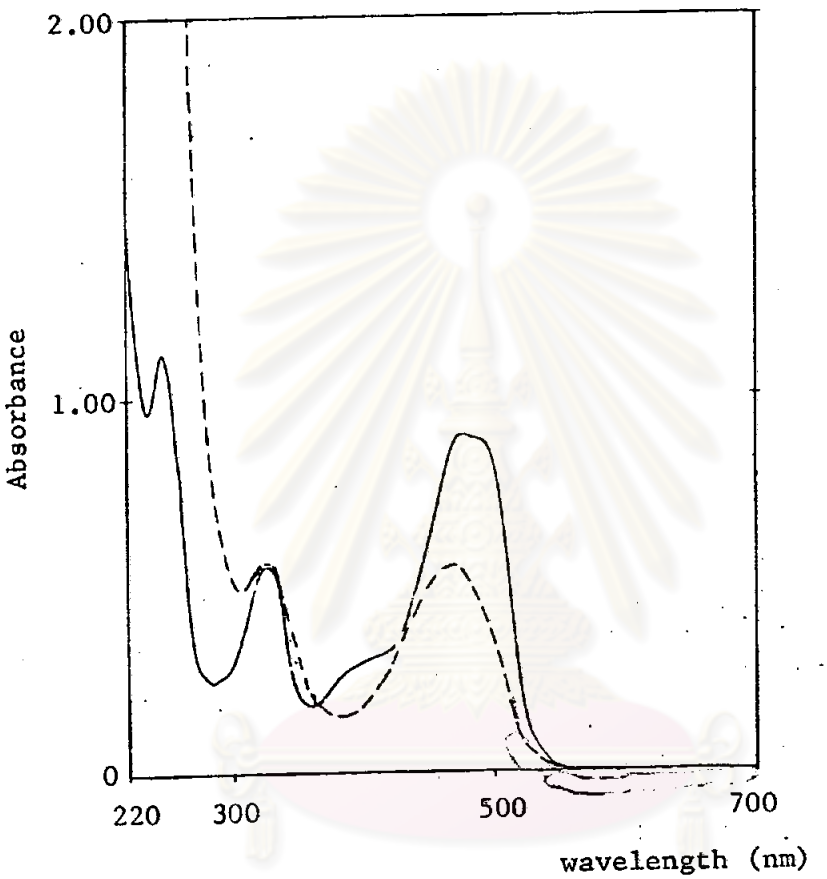

Figure 27J The UV-Visible absorption spectra of Orange G and Cu (II) ion-Orange G mixture in the acetate buffer at pH 5.10.

——— Orange G

----- Cu (II)-Orange G mixture

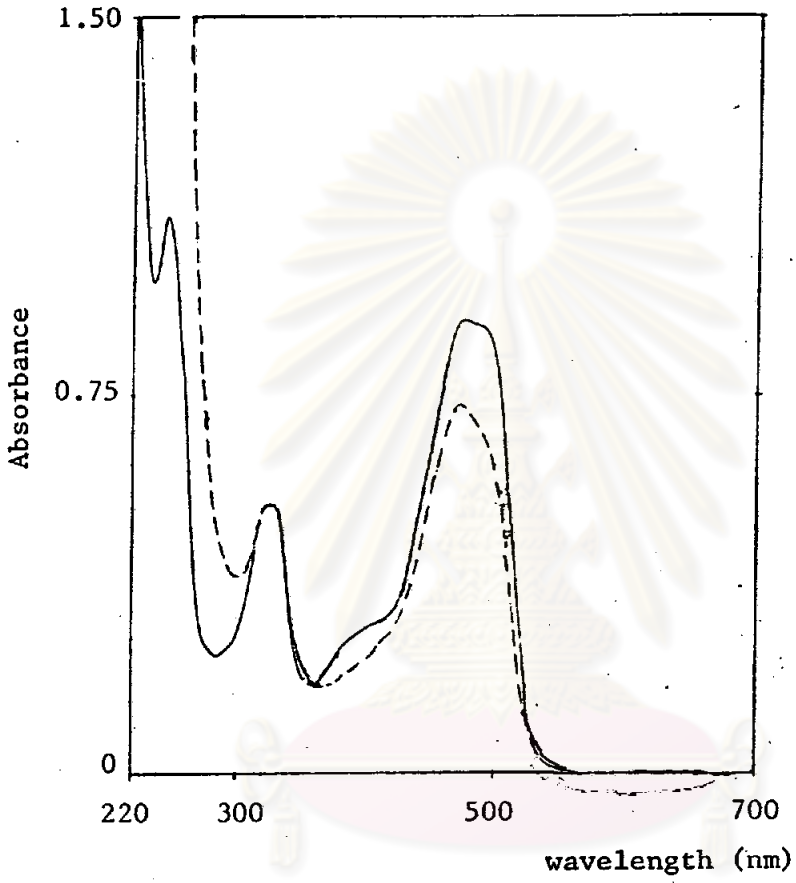

Figure 27K The UV-Visible absorption spectra of Orange G and Cu (II) ion-Orange G mixture in the acetate buffer at pH 4.00.

——— Orange G

----- Cu (II)-Orange G mixture

Table 20 Absorption characteristics of Orange G and Cu (II) ion-Orange G mixtures at various pH values in ultraviolet-visible region.

pH	λmax in visible region, nm			λmax in ultraviolet region, nm		
	Orange G	Cu (II) ion-Orange G mixture	Δ λmax	Orange G	Cu (II) ion-Orange G mixture	Δ λmax
4.00	476	474	2	322	322	0
5.10	476	474	2	322	322	0
6.10	476	468	8	322	322	0

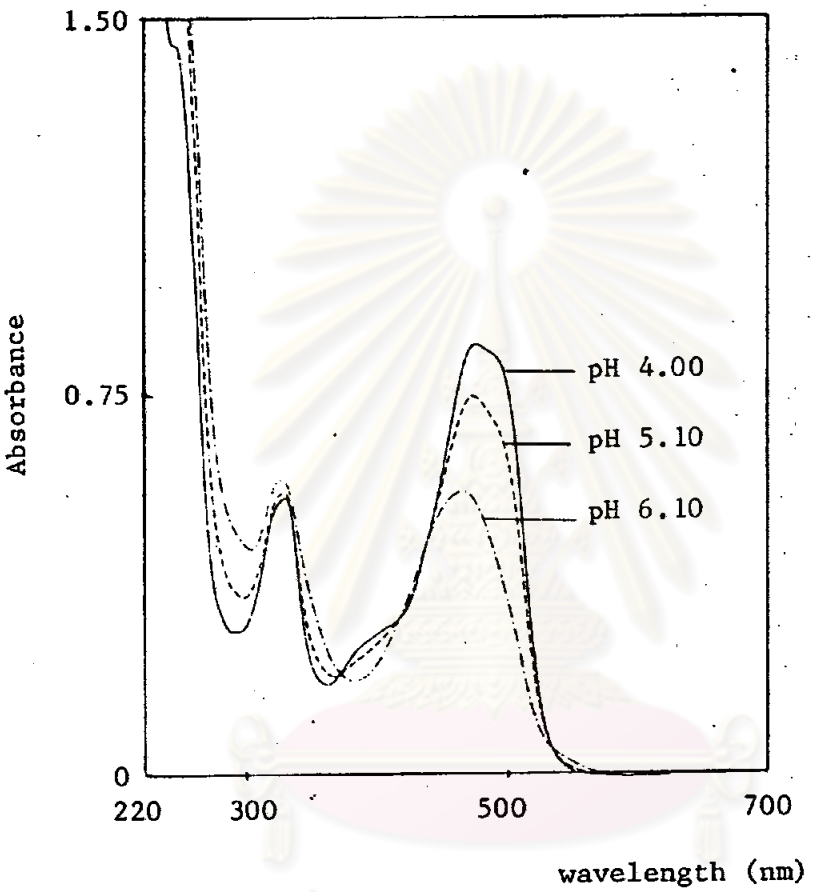

Figure 28 Effect of pH on the absorption spectra of the Cu (II) ion-Orange G mixture in the acetate buffer.

intersected each other at the same wavelength at 370 nm (isobestic point) (see Figures 27I-27K).

3.7.6.3 The influence of time on the color development

The influence of time on the absorbance of Cu (II) ion-Orange G mixture in the acetate buffer at 476 nm was shown in Table 21 and Figure 29. After the preparation, the absorbance of the mixture increased with time for 2 hours and after that the absorbance was time independence.

3.7.6.4 The composition of Cu (II) ion-Orange G complex

The complex formation between Cu (II) ion and Orange G was performed in the acetate buffer pH 6.10, 5.10 and 4.00. The absorbances of Cu (II) ion-Orange G mixtures were measured at 476 nm, 2 hours after the preparation.

Because of the serious overlapping absorption bands between Orange G and Cu (II) ion-Orange G mixture, the molar ratio method was used for determining the composition of the complex formed by plotting the absorbances of the mixture solution VS their molar ratios and plotting ε VS $\frac{\varepsilon_D - \varepsilon}{(C_M^o)^E}$.

The absorbances of the mixture solutions which contained a constant concentration of Orange G and a series of concentrations of Cu (II) ion were measured at 476 nm against the buffer solution. The absorption values are listed in Table 22. The plots of the absorbances of mixture solutions VS their molar ratios are shown in Figures 30A-32A. By graphical method, the composition of the complex formed between Orange G and Cu (II) ion is 1:1 in the acetate buffer pH 6.10, 5.10 or 4.00.

It was found that the plots of ε VS $\frac{\varepsilon_D - \varepsilon}{(C_M^{con})^n}$ when n = 1 obeyed the reaction of type

$$Cu^{2+} + H_xD \rightleftharpoons [CuD]^{(2-x)} + xH^+$$

The results are shown in Tables 23A-23C and Figures 30B-32B. Therefore, the complex formed between Orange G and Cu (II) ion is 1:1 in the acetate buffer pH 6.10, 5.10 or 4.00.

Since Orange G is an ortho hydroxy azo dye which has similar structure as Azorubine and Sunset Yellow FCF. Therefore, the complex formation of the 1:1 Cu (II)-Orange G complex is expected to the replacement of H atom of the OH group together with coordination by the azo N-atom.

3.7.7 The mixtures of Orange RN and Ti (IV), Cr (III), Mn (II), Co (II), Fe (II), Fe (III), Ni (II), or Zn (II)

The absorption spectra of the mixtures of Orange RN and each metal ion in phosphoric acid, acetic acid, McIlvaine buffer, phosphate buffer and diethylamine were shown in Figures 33A-33H. Since the absorption spectra of the metal ion-Orange RN mixtures were not different from that of Orange RN and no physical change in each mixture system was observed, no complex formed between Orange RN and Ti (IV), Cr (III), Mn (II), Co (II), Fe (II), Fe (III), Ni (II), or Zn (II) ion in the buffer solutions mentioned above.

3.7.8 The mixtures of Orange RN and Cu (II) ion

The absorption spectra of the mixtures of Orange RN and Cu (II) ion in phosphoric acid, acetic acid, McIlvaine buffer, phosphate buffer, acetate buffer and diethylamine were recorded as shown in Figures 33A-33K. The spectra of Cu (II) ion-Orange RN mixtures in the buffer

solutions such as phosphoric acid, acetic acid, McIlvaine buffer, phosphate buffer were not different from its dye spectrum and no physical change in each mixture solution was observed. This meant that no reaction between Orange RN and Cu (II) ion occurred and no complex formed in the buffer system such as phosphoric acid, acetic acid, McIlvaine buffer, phosphate buffer and diethylamine. However, in the acetate buffer pH 6.10, 5.10 or 4.00 it was found that Orange RN reacted with Cu (II) ion since the color of the mixture solution changed from orange to yellow-orange. The absorption spectra of Cu (II) ion-Orange RN solutions differed from those of Orange RN. A small hypsochromic shift and a new absorption band at 350 nm occurred at pH 5.10, 6.10 and the absorbance of Orange RN at 485 nm decreased in the presence of Cu (II) ion (see Figures 33I-33K).

3.7.8.1 Absorption characteristics of Cu (II) ion-Orange RN mixture

The absorption spectra of Orange RN, the mixture of Orange RN and Cu (II) ion in the acetate buffer pH 6.10, 5.10, 4.00 were recorded in the range of wavelengths between 220-700 nm (see Figures 33I-33K). It was seen that the absorption spectra of Cu (II) ion-Orange RN slightly shifted to the lower wavelength and the absorbance of Orange RN decreased in the presence of Cu (II) ion. The strong absorption band of the Cu (II) ion-Orange RN mixture in the acetate buffer pH 6.10, 5.10, 4.00 appeared at 467 nm, 478 nm, 480 nm, respectively. The new absorption peak of the mixture of Cu (II) ion and Orange RN which occurred at 350 nm was weak.

The absorption spectra of Cu (II) ion-Orange RN mixtures are different from that of Orange RN in the ultraviolet

Table 21 Effect of time on the color development of the Cu (II) ion-Orange G mixture in the acetate buffer.

Time	absorbance at λ 476 nm		
	pH 6.10	pH 5.10	pH 4.00
0 min.	0.548	0.738	0.830
5 min.	0.550	0.746	0.836
15 min.	0.552	0.746	0.836
30 min.	0.553	0.748	0.839
1 hr.	0.555	0.752	0.843
2 hr.	0.556	0.755	0.845
3 hr.	0.557	0.755	0.845
6 hr.	0.556	0.755	0.845
24 hr.	0.556	0.755	0.844

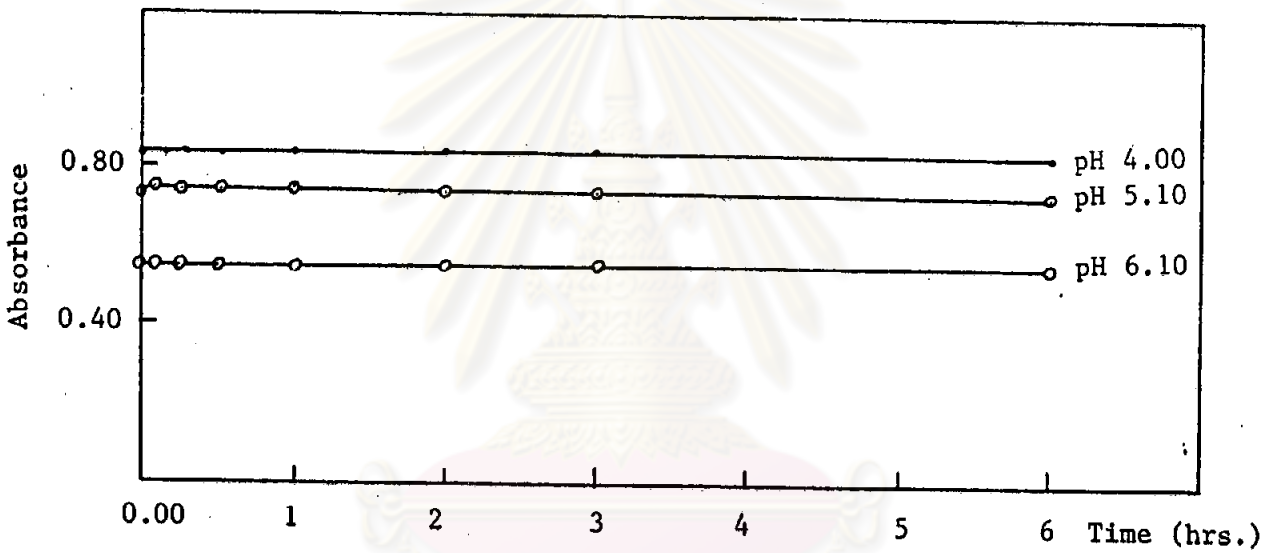

Figure 29 The influence of time on the absorbance of the Cu (II) ion-Orange G mixture at various pH values.

Table 22 The molar ratio study of Orange G and Cu (II) ion in the acetate buffer.

Molar ratio Cu (II) : Orange G	Absorbance at 476 nm		
	pH 6.10	pH 5.10	pH 4.00
0.08	0.867	0.876	0.882
0.16	0.858	0.874	0.881
0.24	0.850	0.874	0.880
0.32	0.847	0.870	0.879
0.40	0.833	0.871	0.878
0.48	0.829	0.869	0.877
0.56	0.818	0.868	0.876
0.64	0.812	0.869	0.875
0.72	0.805	0.866	0.877
0.80	0.803	0.864	0.875
1.00	0.783	0.802	0.877
1.20	0.765	0.855	0.875
1.60	0.739	0.852	0.874
2.00	0.715	0.847	0.873
2.40	0.700	0.842	0.872
2.80	0.682	0.838	0.871
3.20	0.666	0.830	0.871
3.60	0.653	0.826	0.870
4.00	0.639	0.820	0.870

Table 23A Spectrophotometric data of the Cu (II)-Orange G System in the acetate buffer pH 6.10, using 4.00×10^{-5} M Orange G.

$10^3 \times C_M^o$, M	Absorbance at 485 nm	$\varepsilon \times 10^4$	$\frac{\varepsilon_D - \varepsilon}{C_M^o} \times 10^7$
0.00	0.881	2.2025	
0.40	0.546	1.3650	2.0937
0.80	0.501	1.2525	1.1875
1.20	0.484	1.2100	0.8271
1.60	0.473	1.1825	0.6375
2.00	0.467	1.1675	0.5175
2.40	0.462	1.1550	0.4365
3.20	0.457	1.1425	0.3313

Table 23B Spectrophotometric data of the Cu (II)-Orange G System in the acetate buffer pH 5.10, using 4.00×10^{-5} M Orange G.

$10^3 \times C_M^o$, M	Absorbance at 476 nm	$\varepsilon \times 10^4$	$\frac{\varepsilon_D - \varepsilon}{C_M^o} \times 10^6$
0.00	0.884	2.2100	
0.40	0.751	1.8775	8.3125
0.80	0.680	1.700	6.3750
1.20	0.639	1.5975	5.1042
1.60	0.612	1.5300	4.2500
2.00	0.591	1.4775	3.6625
2.40	0.574	1.4350	3.2292
3.20	0.551	1.3775	2.6016

Table 23C Spectrophotometric data of the Cu (II)-Orange G System in the acetate buffer pH 4.00, using 4.00×10^{-5} M Orange G.

$10^3 \times C_M^o$, M	Absorbance at 476 nm	$\varepsilon \times 10^4$	$\frac{\varepsilon_D - \varepsilon}{C_M^o} \times 10^6$
0.00	0.885	2.2125	
0.40	0.845	2.1125	2.5000
0.80	0.815	2.0375	2.1875
1.20	0.792	1.9800	1.9375
1.60	0.775	1.9375	1.7188
2.00	0.760	1.9000	1.5625
2.40	0.748	1.8700	1.4271
3.20	0.726	1.8150	1.2422

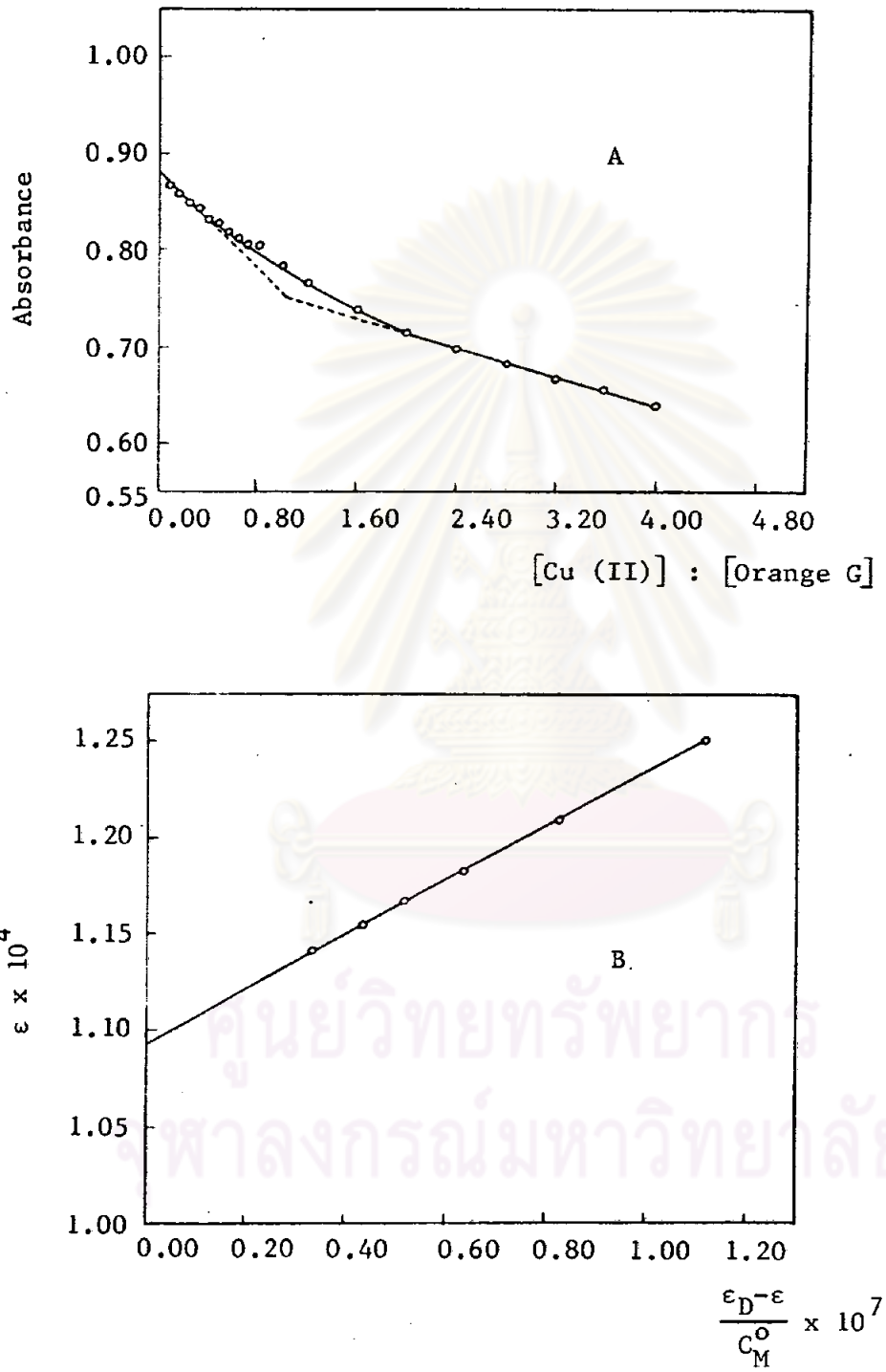

Figure 30 The Cu (II)-Orange G system at pH 6.10

A) Molar ratio plot for the solution contained 4.00×10^{-5} M Orange G and various concentrations of Cu (II) ion

B) plot of ε VS $\frac{\varepsilon_D - \varepsilon}{C_M^o}$ for the solution contained 4.00×10^{-5} M Orange G and various concentrations of Cu (II) ion

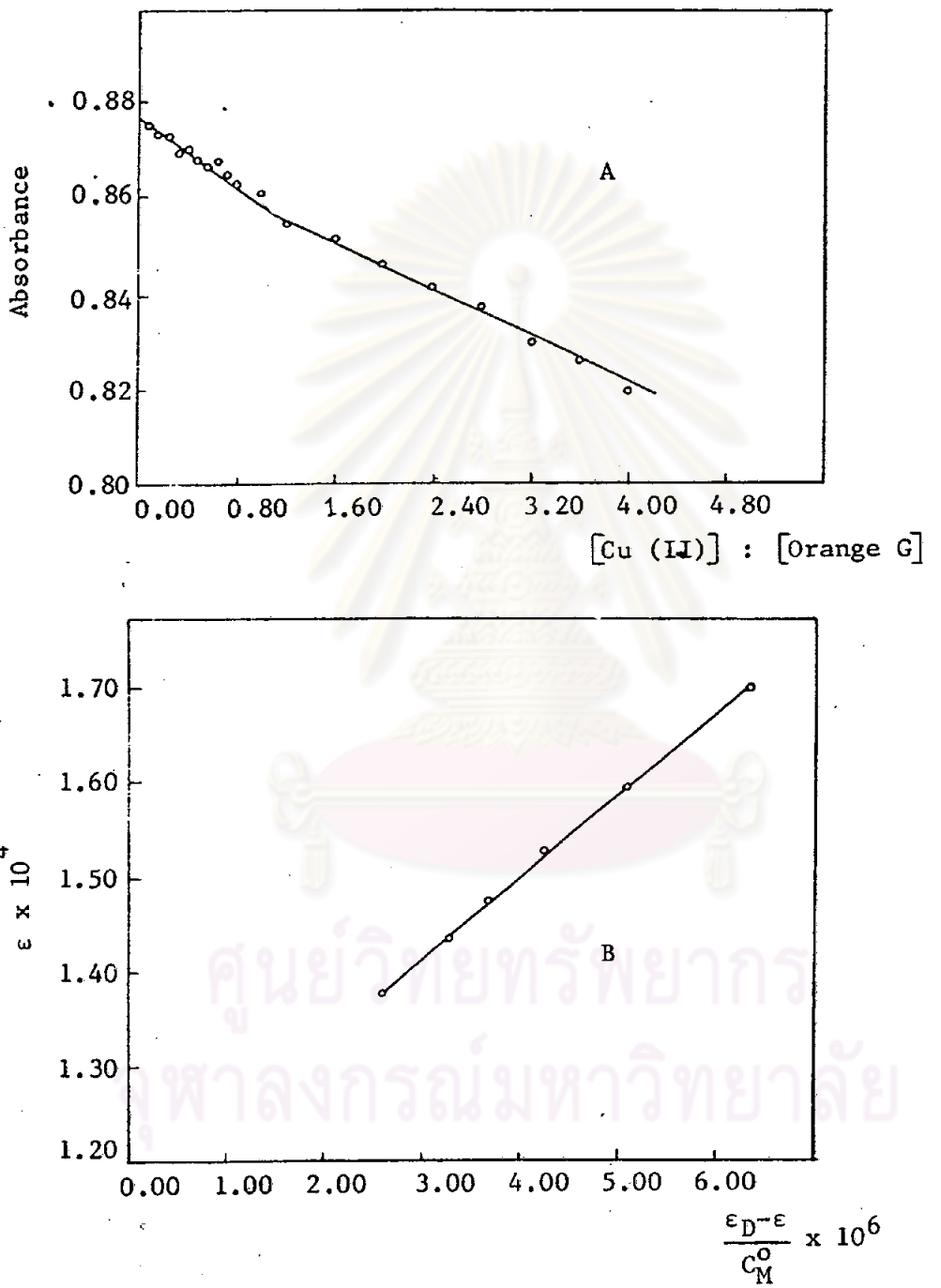

Figure 31 The Cu (II)-Orange G system at pH 5.10

A) Molar ratio plot for the solution contained 4.00×10^{-5} M Orange G and various concentrations of Cu (II) ion

B) plot of ε VS $\frac{\varepsilon_D-\varepsilon}{C_M^o}$ for the solution contained 4.00×10^{-5} M Orange G and various concentrations of Cu (II) ion

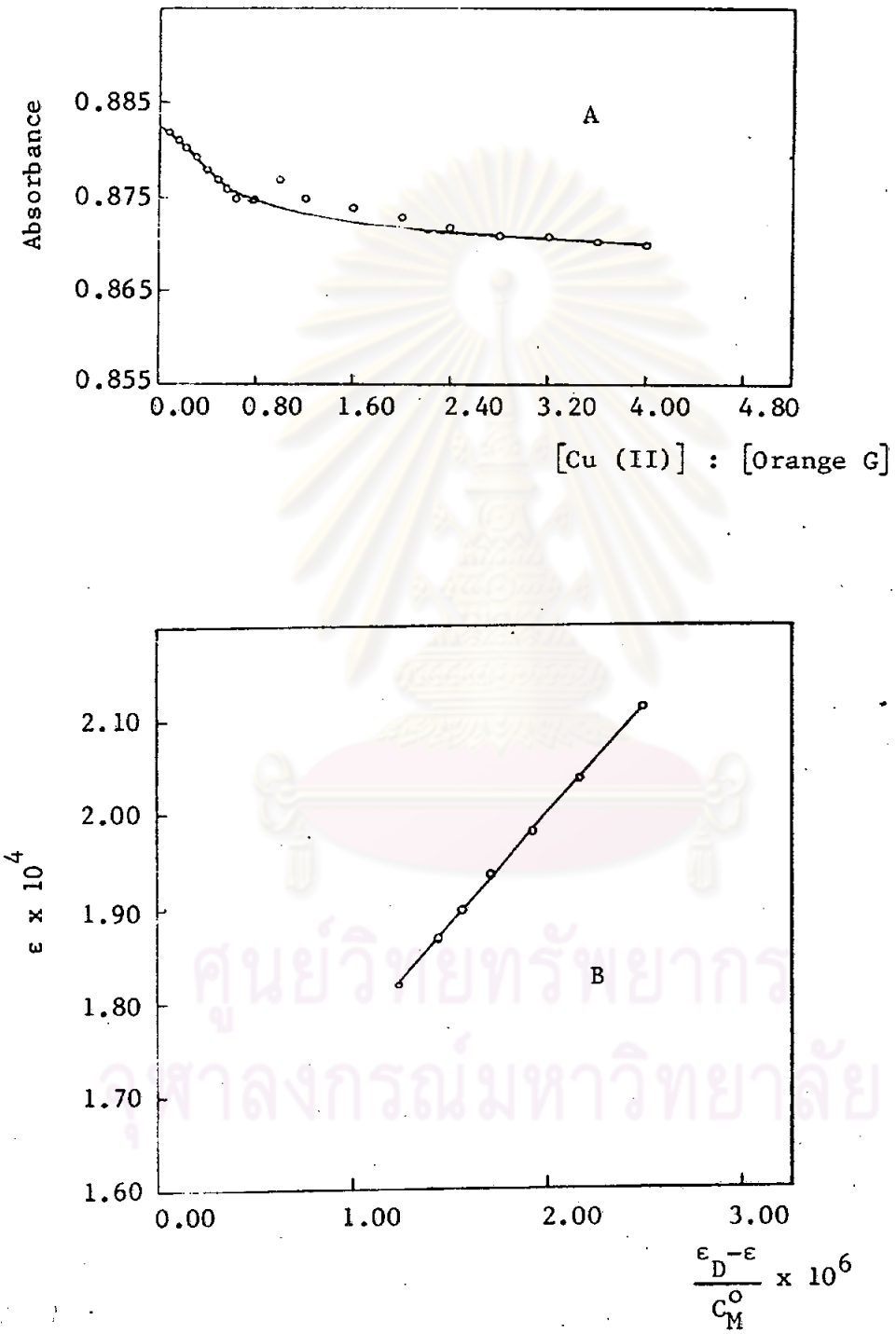

Figure 32 The Cu (II)-Orange G system at pH 4.00

A) Molar ratio plot for the solution contained 4.00×10^{-5} M Orange G and various concentrations of Cu (II) ion

B) plot of ε VS $\frac{\varepsilon_D - \varepsilon}{C_M^o}$ for the solution contained 4.00×10^{-5} M Orange G and various concentrations of Cu (II) ion

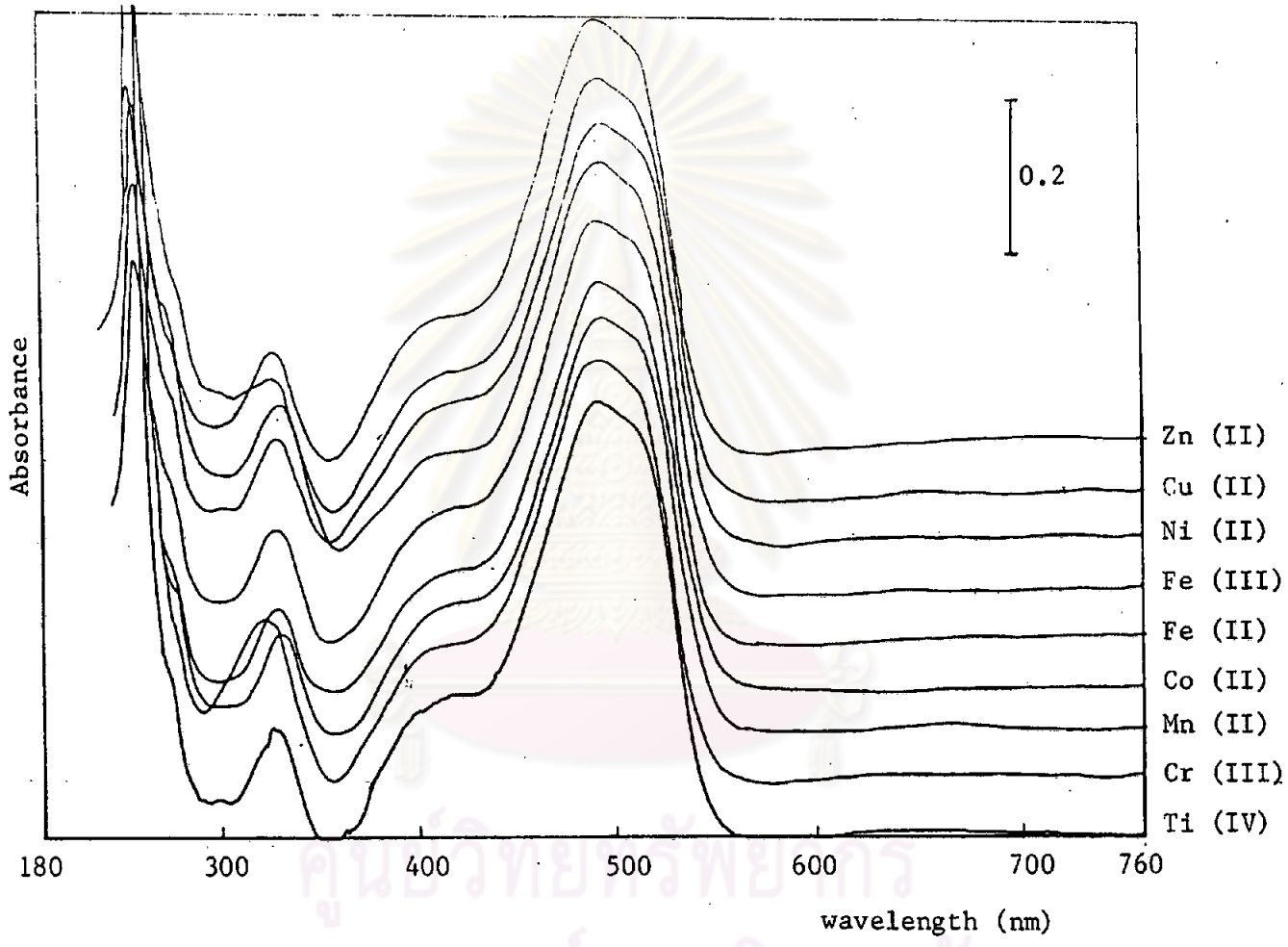

Figure 33A The UV-Visible absorption spectra of the mixture of Orange RN and metal ions in the acetic acid at pH 2.30.

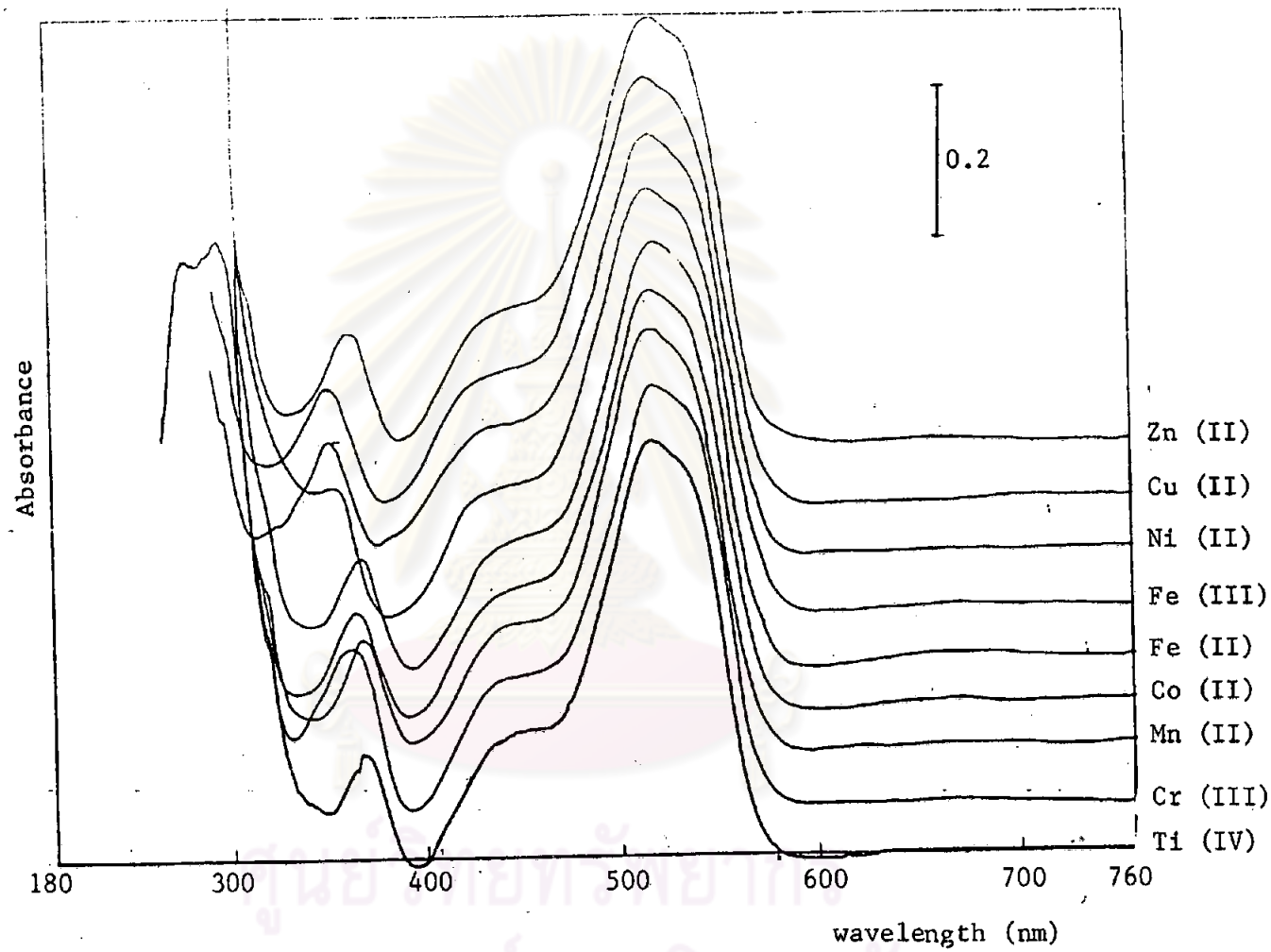

Figure 33B The UV-Visible absorption spectra of the mixture of Orange RN and metal ions in the phosphoric acid at pH 1.00.

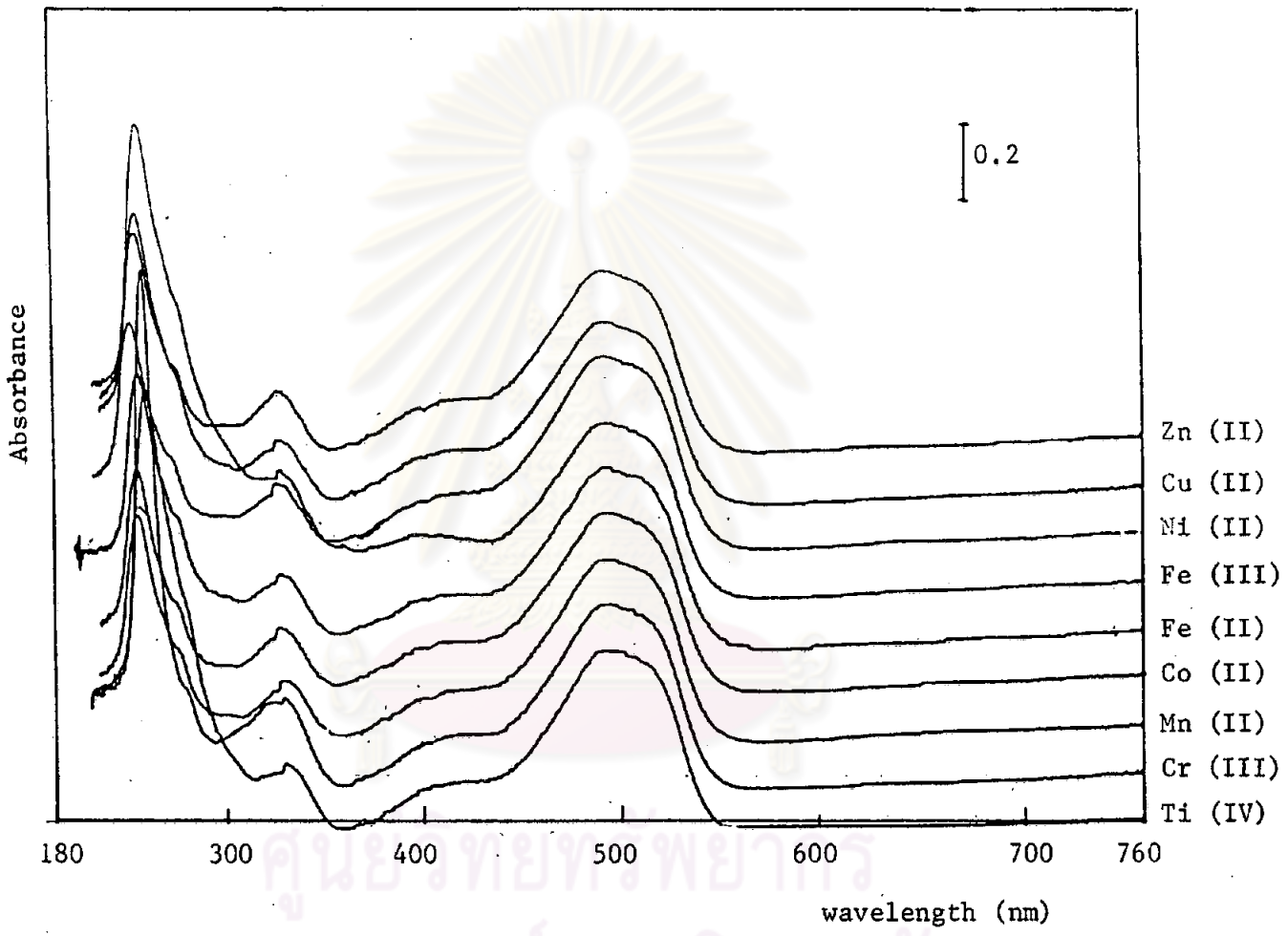

Figure 33C The UV-Visible absorption spectra of the mixture of Orange RN and metal ions in the McIlvaine buffer pH 3.10.

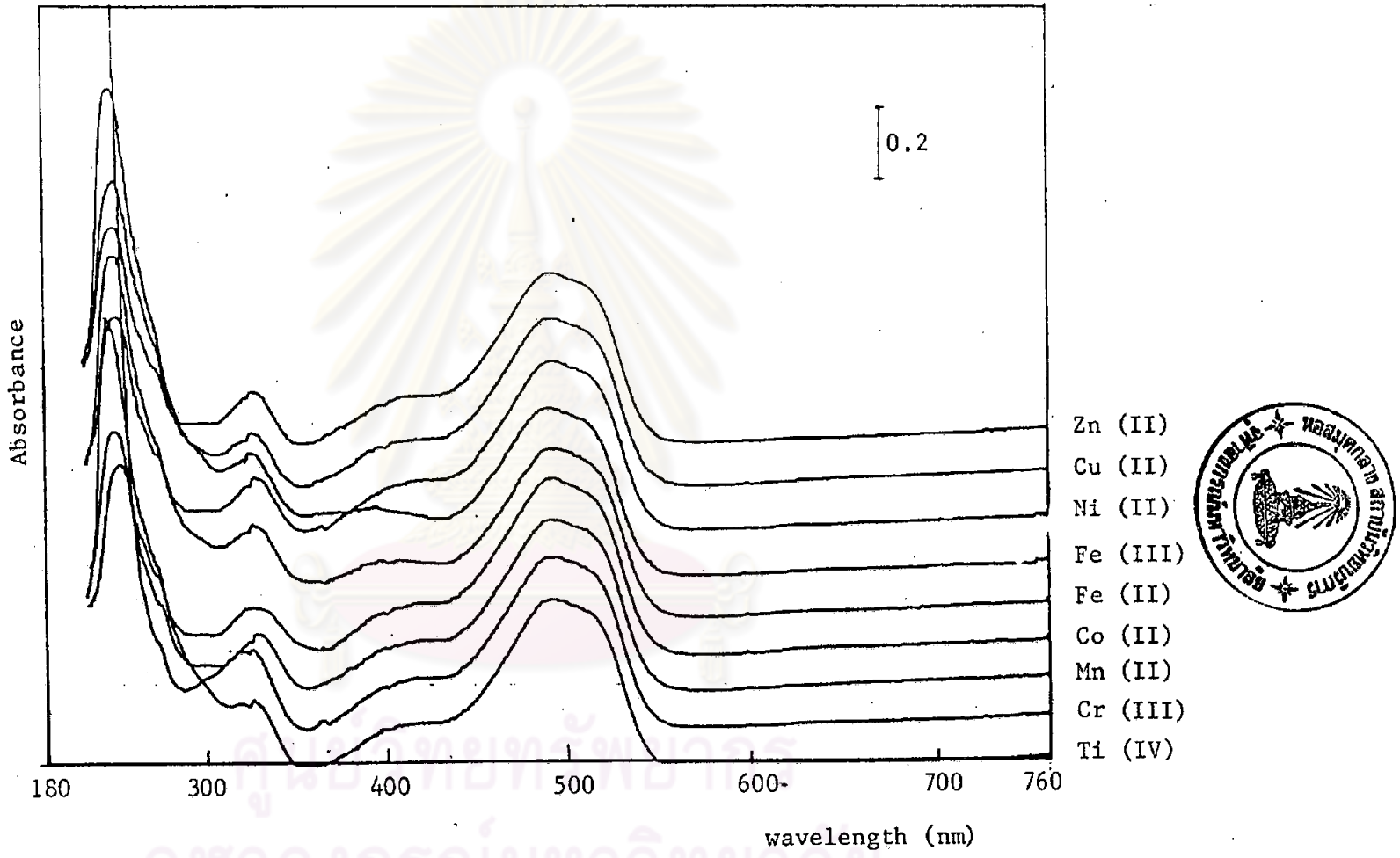

Figure 33D The UV-Visible absorption spectra of the mixture of Orange RN and metal ions in the McIlvaine buffer at pH 5.15.

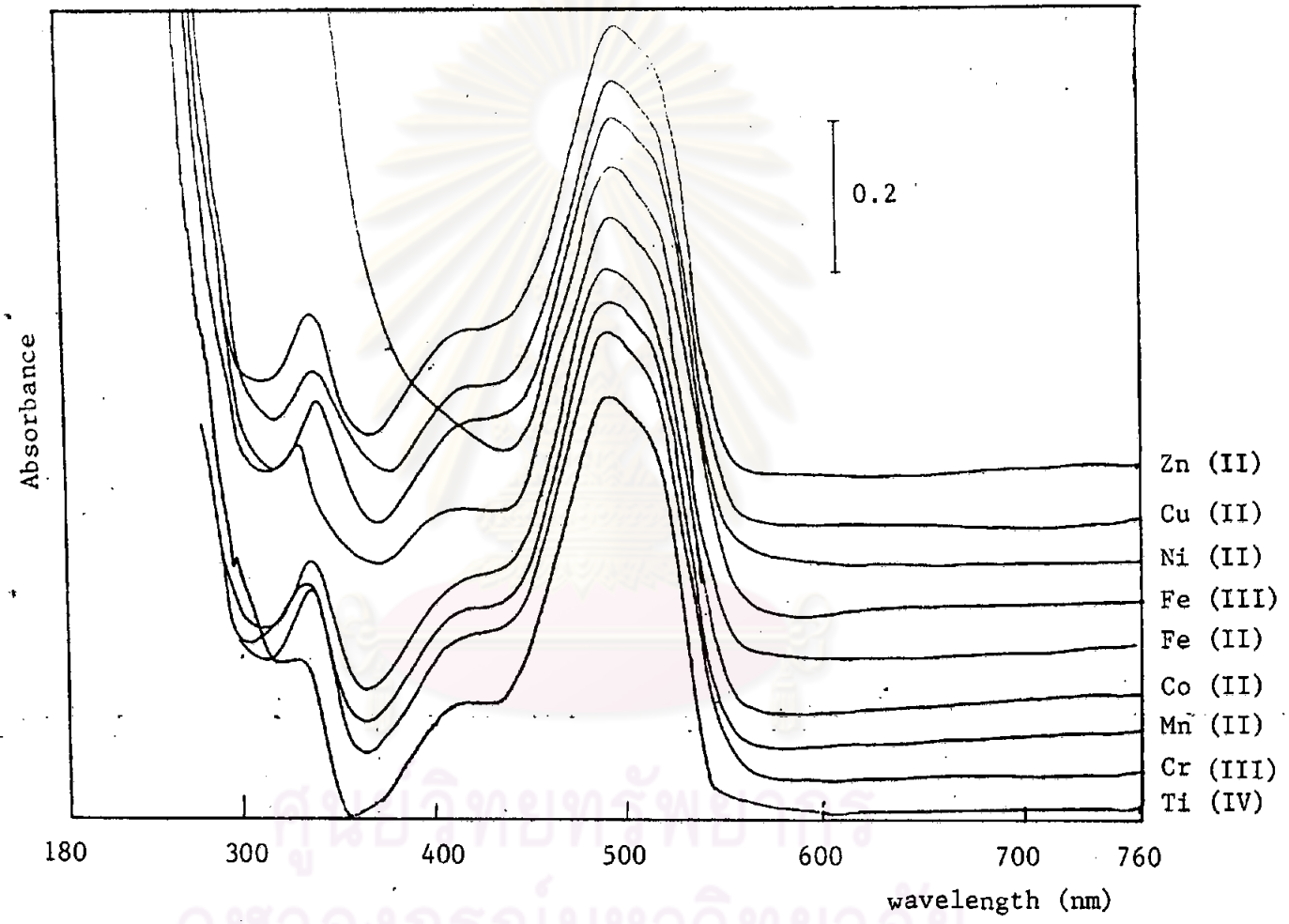

Figure 33E The UV-Visible absorption spectra of the mixture of Orange RN and metal ions in the McIlvaine buffer at pH 7.40.

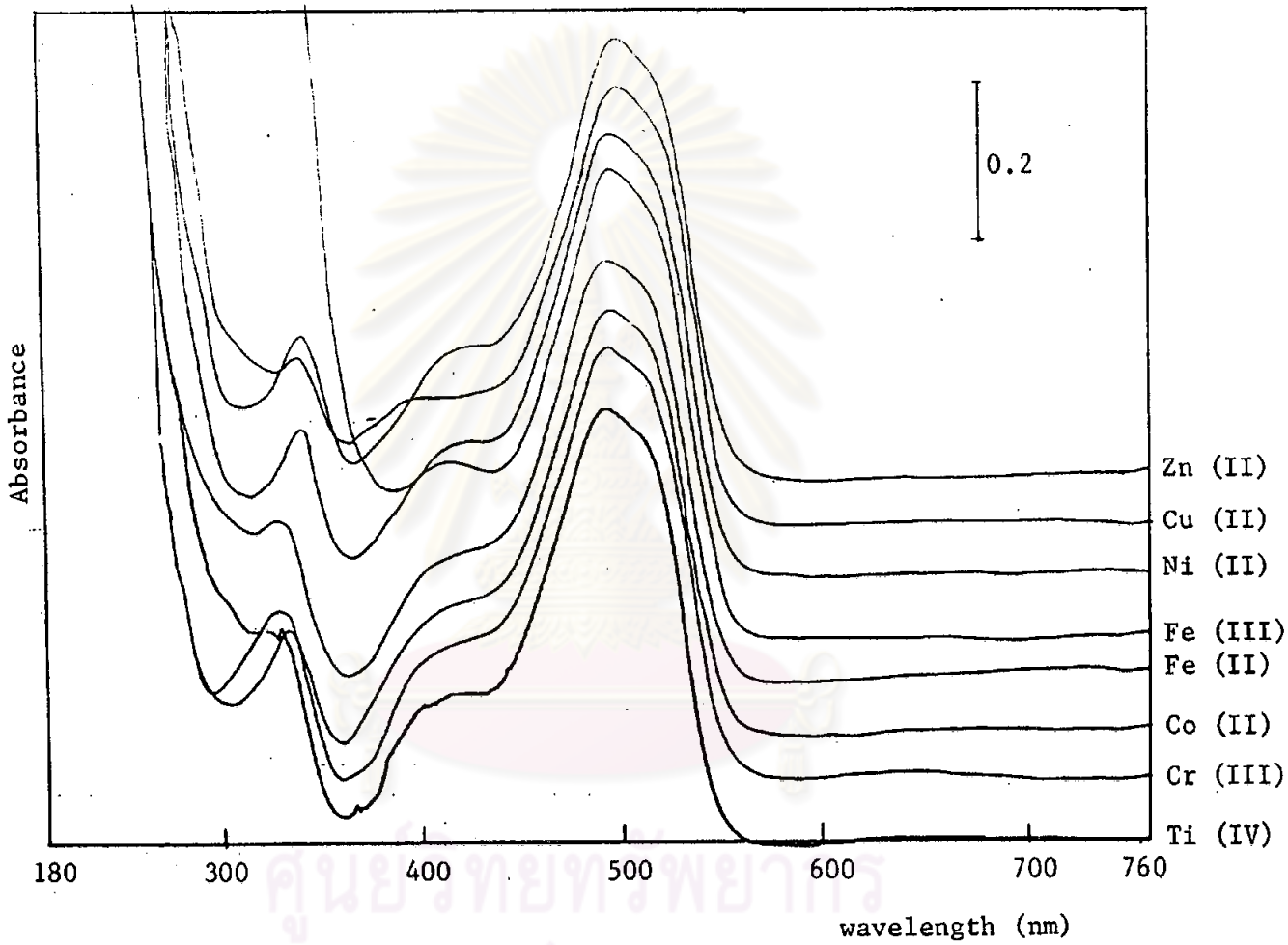

Figure 33F The UV-Visible absorption spectra of the mixture of Orange RN and metal ions in the phosphate buffer at pH 5.85.

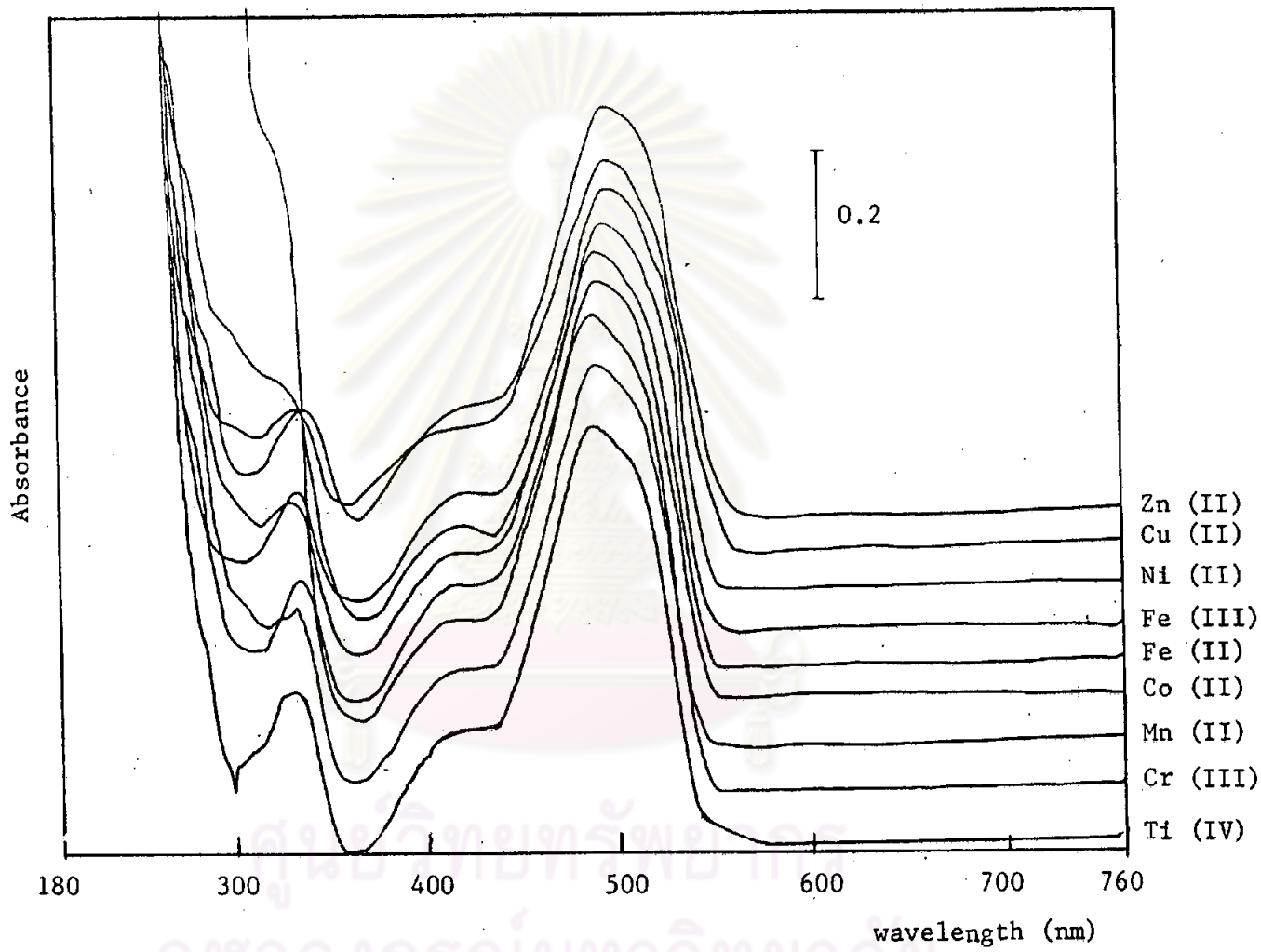

Figure 33G The UV-Visible absorption spectra of the mixture of Orange RN and metal ions in the phosphate buffer pH 7.00.

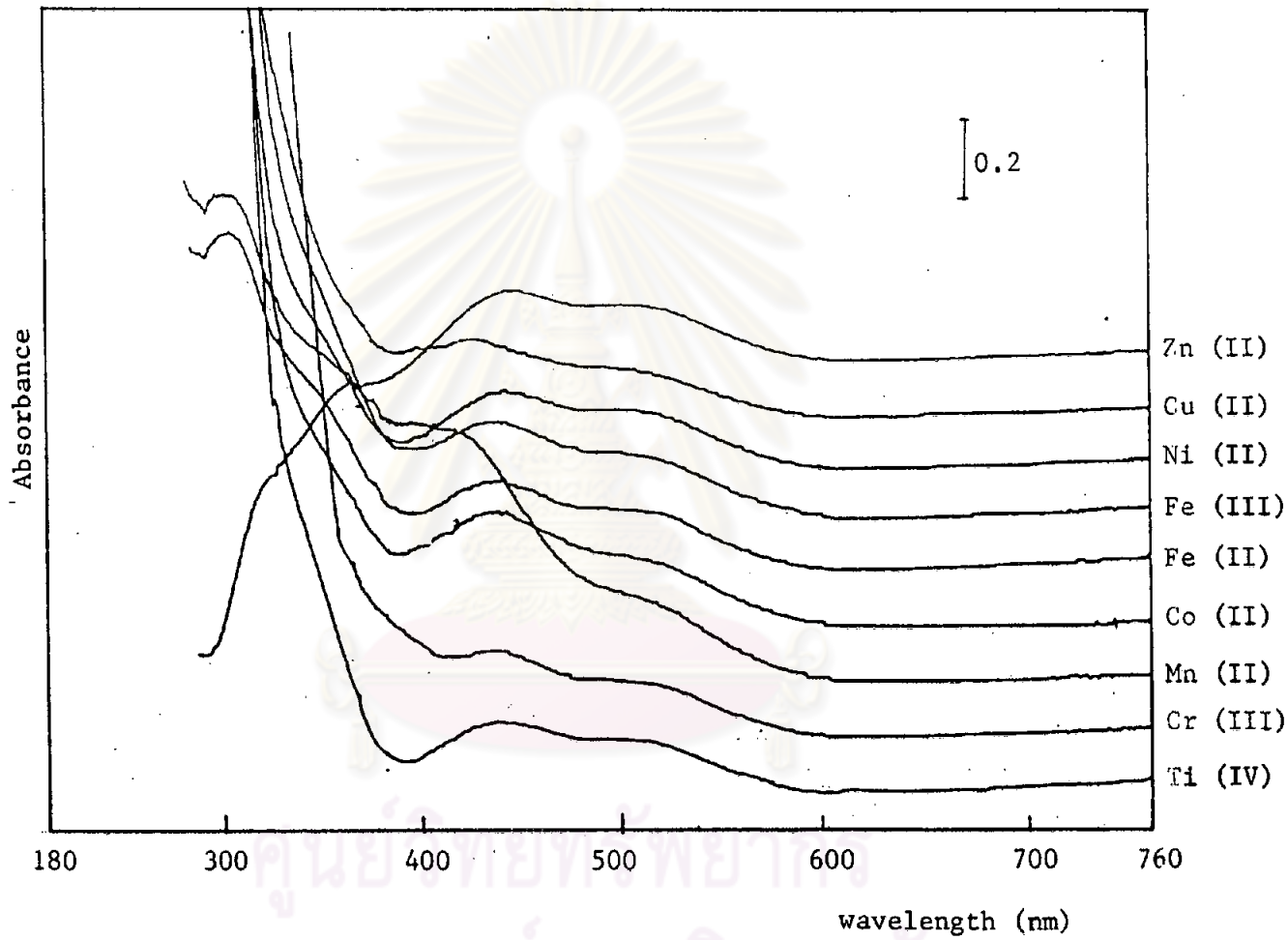

Figure 33H The UV-Visible absorption spectra of the mixture of Orange RN and metal ions in diethylamine at pH 12.50.

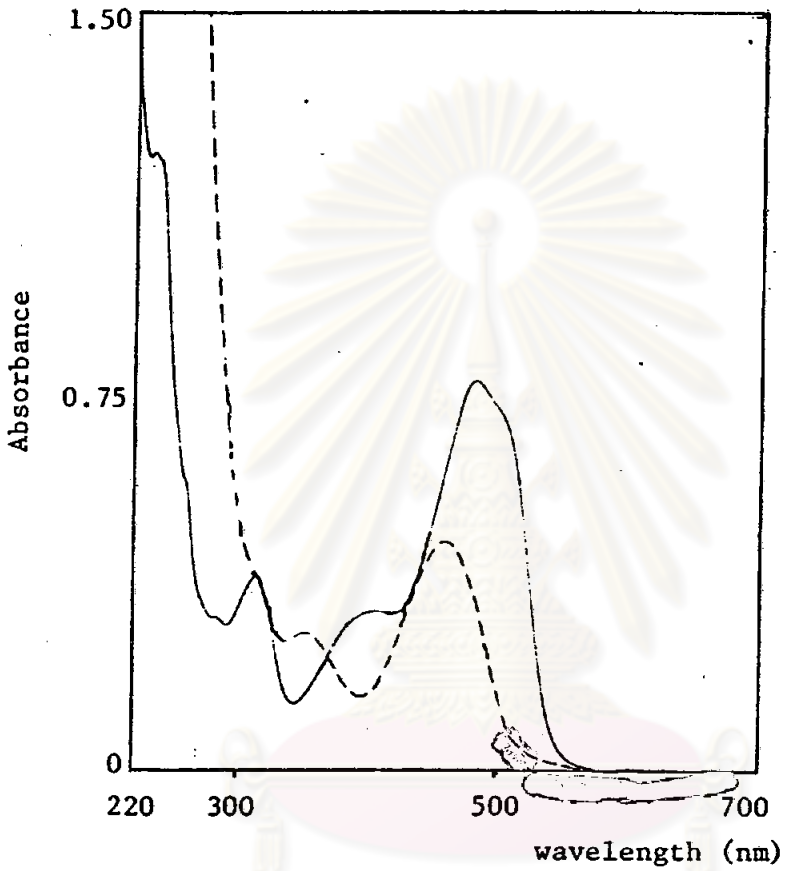

Figure 33I The UV-Visible absorption spectra of Orange RN and Cu (II) ion-Orange RN mixture in the acetate buffer at pH 6.10.

——— Orange RN

----- Cu (II)-Orange RN mixture

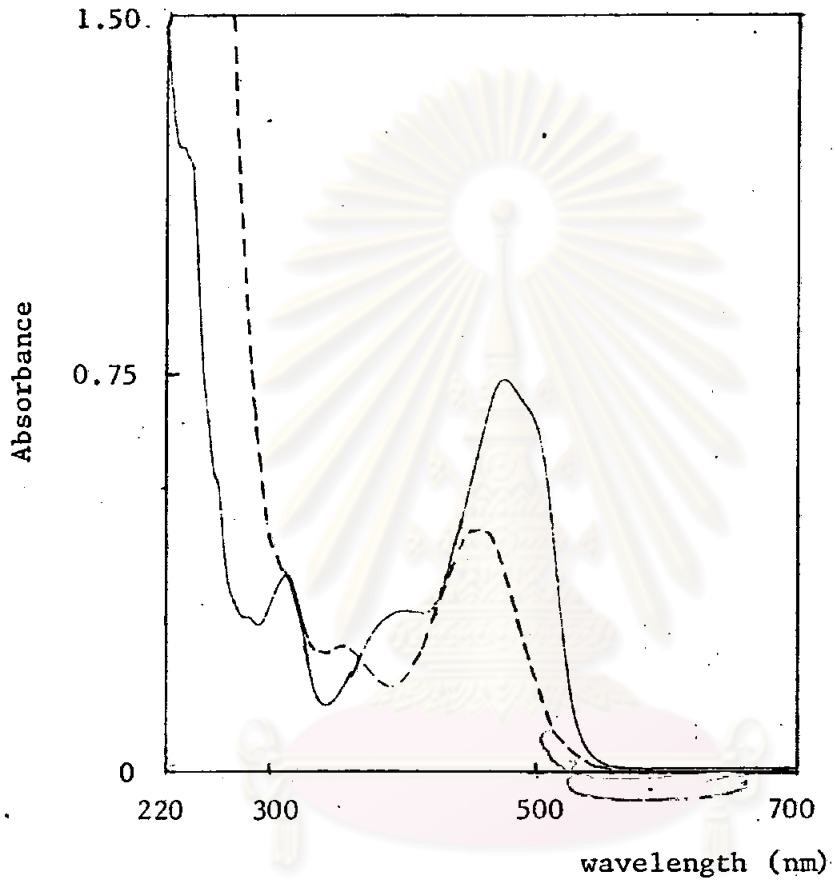

Figure 33J The VU-Visible absorption spectra of Orange RN and Cu (II) ion-Orange RN mixture in the acetate buffer at pH 5.10.

——— Orange RN

----- Cu (II)-Orange RN mixture

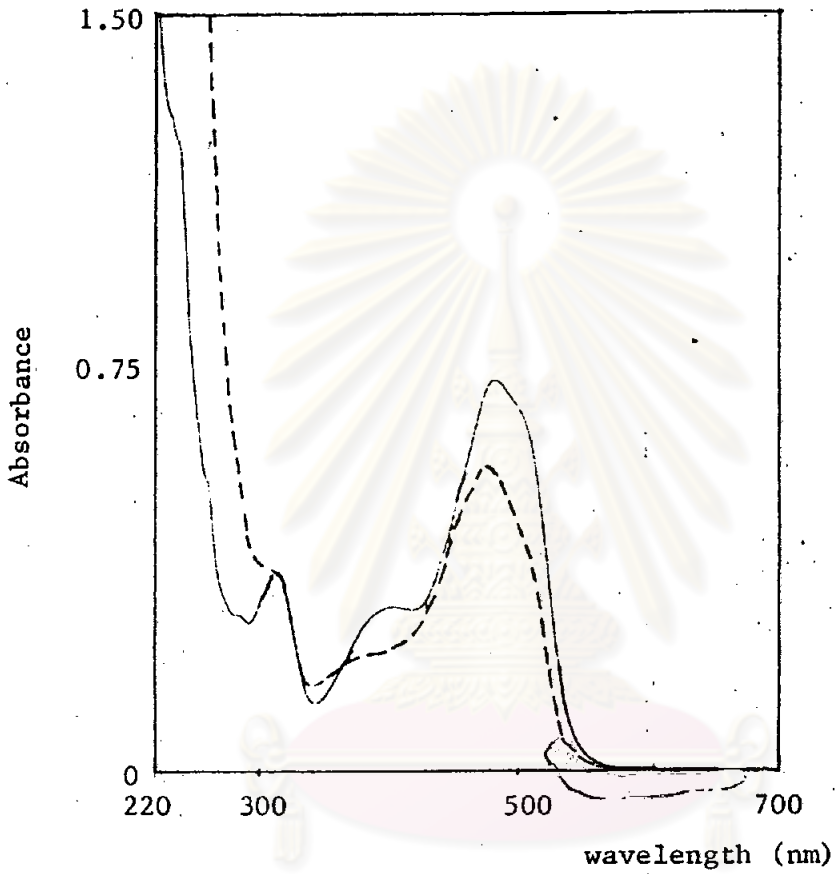

Figure 33K The UV-Visible absorption spectra of Orange RN and Cu (II) ion-Orange RN mixture in the acetate buffer at pH 4.00.

——— Orange RN

----- Cu (II)-Orange RN mixture

region and the absorption peak of Orange RN at 314 nm disappeared (see Figures 33I-33K).

3.7.8.2 The effect of pH on the absorption spectra of Cu (II) ion-Orange RN mixtures

Ultraviolet-visible spectra of Cu (II) ion-Orange RN mixtures at various pH values were shown in Figure 34. It was seen that the absorbance of Cu (II) ion-Orange RN mixture at 485 nm decreased when the pH of the solution increased and the wavelength at the maximum absorption of Cu (II) ion-Orange RN gradually shifted to the lower wavelength when the pH increased. At pH 6.10, the new absorption peak appeared at 350 nm but this absorption peak dissappeared when the pH was lower (see Table 24 and Figure 34). The absorption spectra of the mixture of Cu (II) ion and Orange RN in the acetate buffer pH 6.10, 5.10, 4.00 intersected each other at the same wavelength at 380 nm (isobestic point).

3.7.8.3 The influence of time on the color development

The influence of time on the absorbance of the Cu (II) ion-Orange RN mixture in the acetate buffer at 485 nm was shown in Table 25 and Figure 35. After the preparation, the absorbance of the mixture increased with time for 2 hours and after that the absorbance was time independence.

3.7.8.4 Composition of Cu (II)-Orange RN complex

The complex formation between Cu (II) ion and Orange RN was performed in the acetate buffer pH 6.10, 5.10 and 4.00. The absorbances of Cu (II) ion-Orange RN mixtures were measured at 485 nm, 2 hours after the preparation.

Because of the serious overlapping absorption bands between Orange RN and Cu (II) ion-Orange RN mixture the molar ratio method was used for determining the composition of the complex formed by plotting the absorbances of the mixture solution VS their molar ratios and plotting ε VS $\frac{\varepsilon_D - \varepsilon}{(C_M^o)^n}$

The absorbances of the mixture solutions which contained a constant concentration of Orange RN and a series of concentrations of Cu (II) ion were measured at 485 nm against the buffer solution the absorbances are listed in Table 26. The plot of the absorbance of mixture solutions VS their molar ratios are shown in Figures 36A-38A. By graphical method, the composition of the complex formed between Orange RN and Cu (II) ion is 1:1 in the acetate buffer pH 6.10, 5.10 or 4.00.

It was found that the plots of ε VS $\frac{\varepsilon_D - \varepsilon}{(C_M^o)^n}$ when $n = 1$ obeyed the reaction of type

$$Cu^{2+} + H_xD \rightleftharpoons [CuD]^{(2-x)} + xH^+$$

The results are shown in Tables 27A-27C and Figures 36B-38B. Therefore, the complex formed between Orange RN and Cu (II) ion is 1:1 in the acetate buffer pH 6.10, 5.10 or 4.00. The complex formation of 1:1 Cu (II)-Orange RN is expected to the replacement of the H atom of the OH group together with coordination by the azo-N atom as Cu (II)-Sunset Yellow FCF complex.

3.7.9 The mixtures of Tartrazine and Ti (IV), Cr (III), Mn (II), Co (II), Fe (II), Fe (III), Ni (II), Cu (II) or Zn (II)

The absorption spectra of the mixtures of Tartrazine and each metal ion in phosphoric acid, acetic acid, McIlvaine buffer, phos-

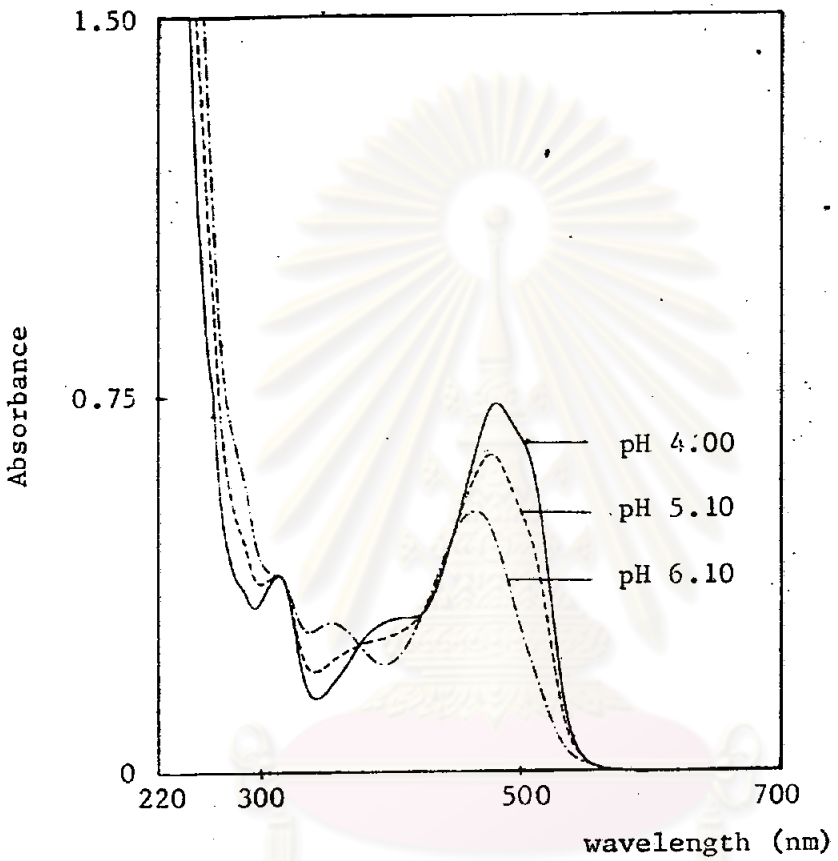

Figure 34 Effect of pH on the absorption spectra of Cu (II) ion-Orange RN mixture in the acetate buffer.

Table 24 Absorption characteristics of Orange RN and Cu (II) ion-Orange RN mixtures at various pH values in ultraviolet region.

pH	λmax in visible region, nm			λmax in ultraviolet region, nm		
	Orange RN	Cu (II) ion-Orange RN mixture	Δ λmax	Orange RN	Cu (II) ion-Orange RN mixture	Δ λmax
4.00	485	480	5	314	314	0
5.10	485	478	7	314	314	0
6.10	485	470	15	314	360	46

Table 25 Effect of time on the color development of the Cu (II) ion-Orange RN mixture in the acetate buffer.

Time	absorbance at λ 485 nm		
	pH 4.00	pH 5.10	pH 6.10
0 min.	0.722	0.585	0.426
5 min.	0.723	0.586	0.426
15 min.	0.723	0.587	0.427
30 min.	0.723	0.587	0.426
1 hr.	0.726	0.590	0.426
2 hr.	0.728	0.590	0.429
3 hr.	0.728	0.590	0.429
6 hr.	0.726	0.590	0.429
24 hr.	0.726	0.588	0.429

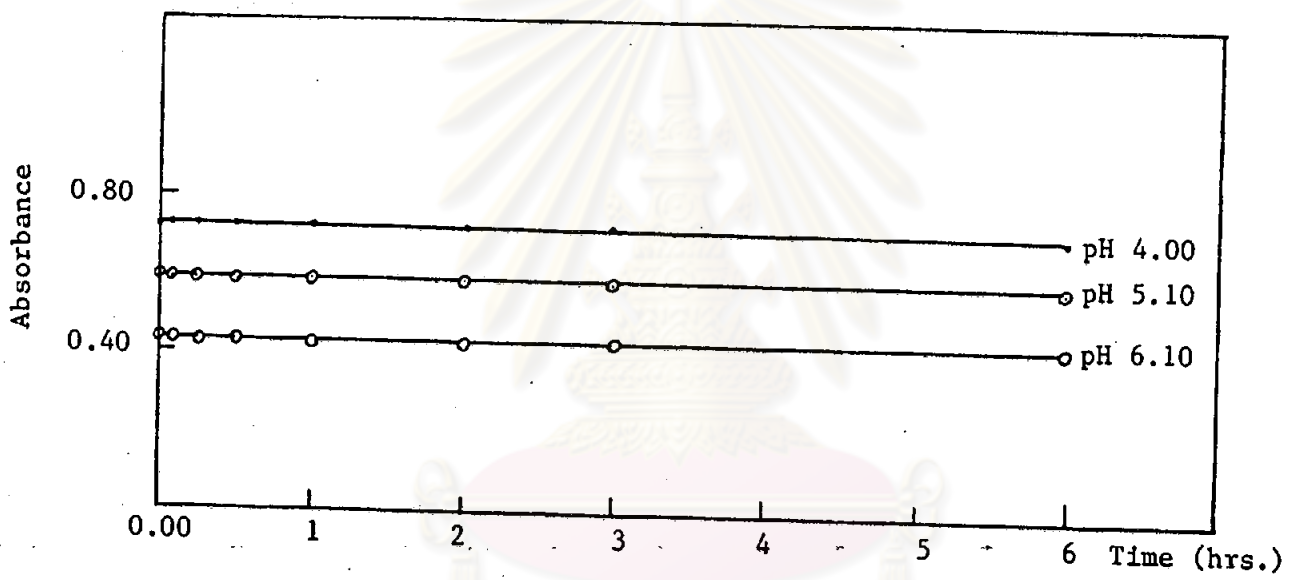

Figure 35 The influence of time on the absorbance of the Cu (II) ion-Orange RN mixture at various pH values.

Table 26 The molar ratio study of Orange RN and Cu (II) ion in the acetate buffer.

Molar ratio, Cu (II) : Orange RN	Absorbance 485 nm		
	pH 6.10	pH 5.10	pH 4.00
0.08	0.752	0.760	0.772
0.16	0.738	0.758	0.771
0.24	0.728	0.756	0.770
0.32	0.718	0.756	0.770
0.40	0.710	0.755	0.769
0.48	0.700	0.751	0.769
0.56	0.688	0.750	0.767
0.64	0.681	0.747	0.766
0.72	0.673	0.746	0.766
0.80	0.665	0.746	0.766
1.00	0.648	0.738	0.765
1.60	0.631	0.737	0.764
1.40	0.604	0.737	0.761
2.00	0.582	0.724	0.760
2.40	0.567	0.715	0.760
2.80	0.550	0.710	0.758
3.20	0.536	0.700	0.759
3.60	0.522	0.694	0.756
4.00	0.513	0.692	0.754

Table 27A Spectrophotometric data of the Cu (II)-Orange RN system in the acetate buffer pH 6.10, using 4.00×10^{-5} M Orange RN.

$10^3 \times C_M^o$	Absorbance at 485 nm	$\varepsilon \times 10^4$	$\frac{\varepsilon_D - \varepsilon}{C_M^o} \times 10^7$
0.00	0.766	1.9150	
0.40	0.418	1.0450	2.1750
0.80	0.392	0.9800	1.1688
1.20	0.382	0.9550	0.8000
1.60	0.378	0.9450	0.6063
2.00	0.374	0.9350	0.4900
2.40	0.371	0.9275	0.4115
3.20	0.369	0.9225	0.3102
4.00	0.367	0.9175	0.2494

Table 27B Spectrophotometric data of the Cu (II)-Orange RN System in the acetate buffer pH 5.10, using 4.00×10^{-5} M Orange RN.

$10^3 \times C_M^o$, M	Absorbance at 485 nm	$\varepsilon \times 10^4$	$\frac{\varepsilon_D - \varepsilon}{C_M^o} \times 10^7$
0.00	0.763	1.9075	
0.40	0.590	1.4750	1.0813
0.80	0.523	1.3075	0.7500
1.20	0.488	0.2200	0.5729
1.60	0.465	1.1625	0.4656
2.00	0.448	1.1200	0.3938
2.40	0.438	1.0950	0.3385
3.20	0.423	1.0575	0.2656
4.00	0.414	1.0350	0.2181

Table 27C. Spectrophotometric data of Cu (II)-Orange RN System in the acetate buffer pH 4.00, using 4.00×10^{-5} M Orange RN.

$10^3 \times C_M^o$, M	Absorbance at 485 nm	$\varepsilon \times 10^4$	$\frac{\varepsilon_D - \varepsilon}{C_M^o} \times 10^6$
0.00	0.767	1.9175	
0.40	0.722	1.8050	2.8125
0.80	0.690	1.7250	2.4063
1.20	0.665	1.6625	2.1250
1.60	0.645	1.6125	1.9063
2.00	0.628	1.5700	1.7375
2.40	0.615	1.5375	1.5833
3.20	0.593	1.4825	1.3594
4.00	0.577	1.4425	1.1875

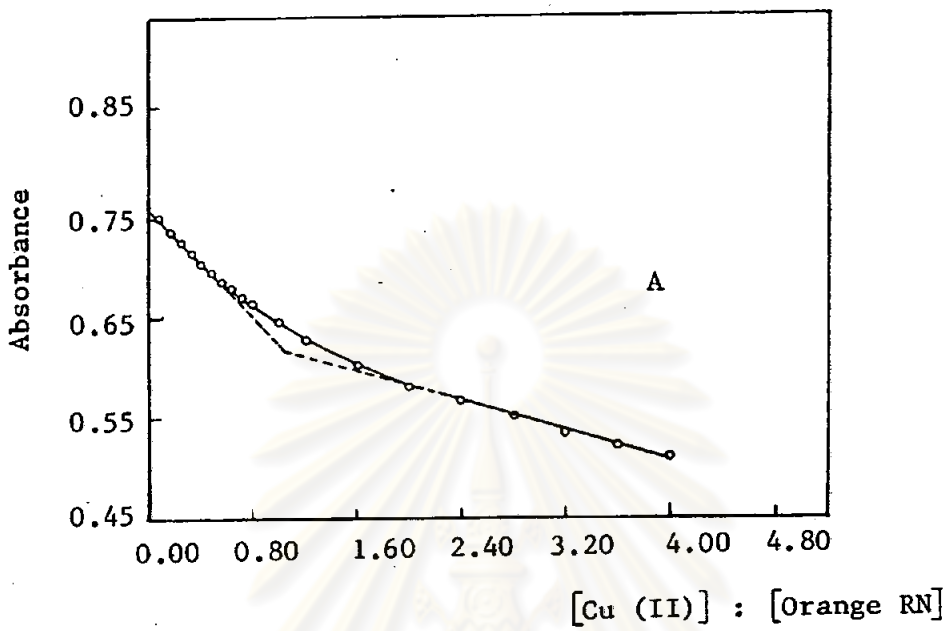

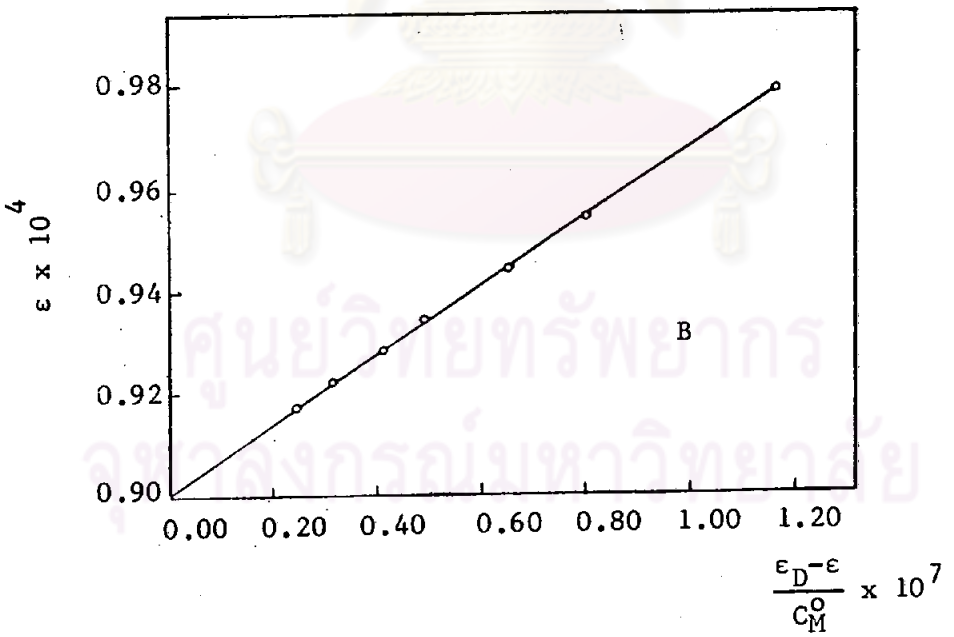

Figure 36 The Cu (II)-Orange RN system at pH 6.10
A) Molar ratio plot for the solution contained 4.00 x 10^{-5} M Orange RN and various concentrations of Cu (II) ion
B) plot of ε VS $\frac{\varepsilon_D-\varepsilon}{C_M^o}$ for the solution contained 4.00 x 10^{-5} M Orange RN and various concentrations of Cu (II) ion

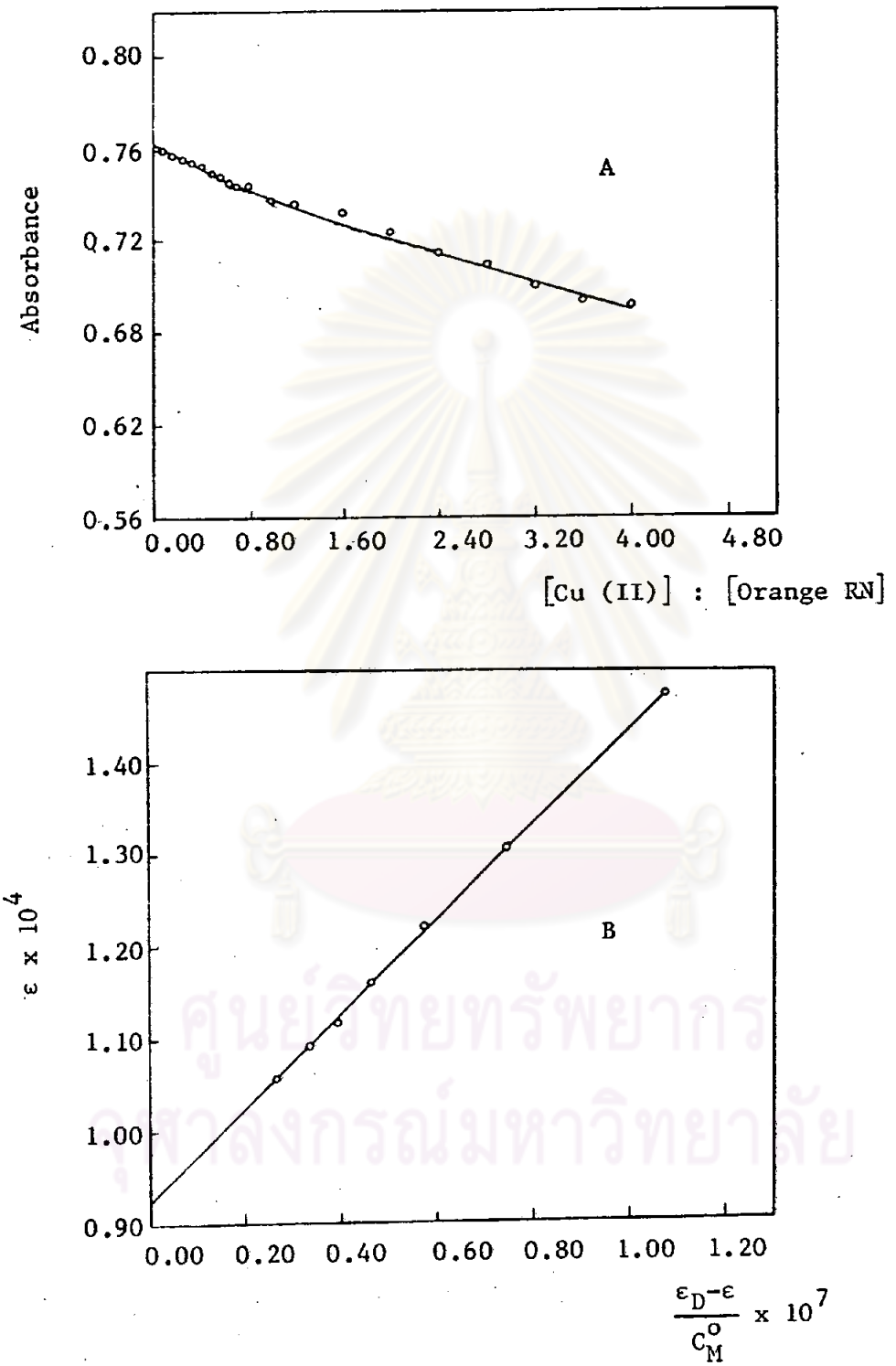

Figure 37 The Cu (II)-Orange RN system at pH 5.10
A) Molar ratio plot for the solution contained 4.00×10^{-5} M Orange RN and various concentrations of Cu (II) ion
B) plot of ε VS $\frac{\varepsilon_D-\varepsilon}{C_M^o}$ for the solution contained 4.00×10^{-5} M Orange RN and various concentrations of Cu (II) ion

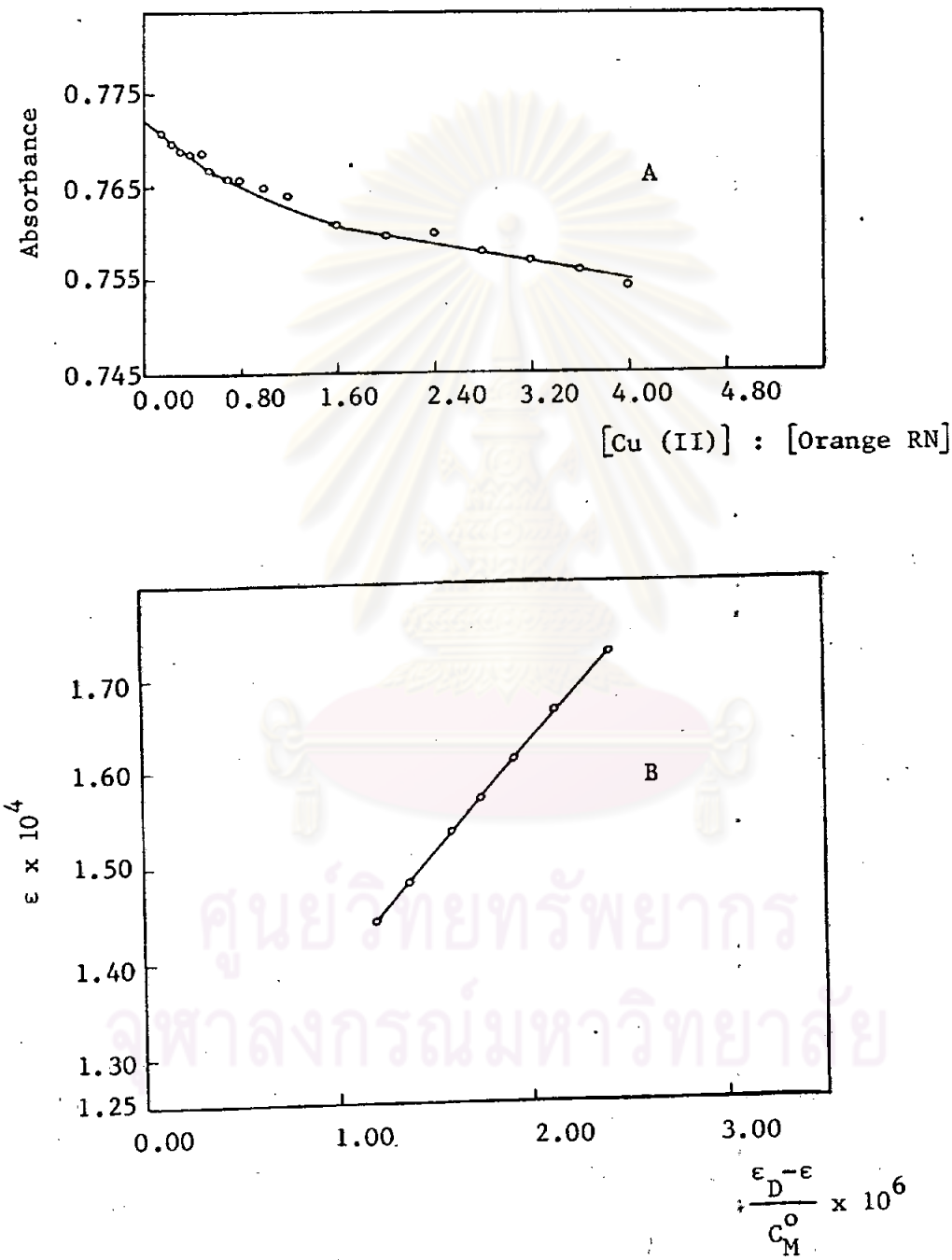

Figure 38 The Cu (II)-Orange RN system at pH 4.00
A) Molar ratio plot for the solution contained 4.00×10^{-5} M Orange RN and various concentrations of Cu (II) ion
B) plot of ε VS $\frac{\varepsilon_D - \varepsilon}{C_M^o}$ for the solution contained 4.00×10^{-5} M Orange RN and various concentrations of Cu (II) ion

phate buffer and diethylamine were shown in Figures 39A-39H. The absorption spectra of the metal ion-Tartrazine mixtures were not different from that of Tartrazine. In addition, no physical change in each mixture system was observed. This meant that no reaction between Tartrazine and Ti (IV), Cr (III), Mn (II), Co (II), Fe (II), Fe (III), Ni (II), Cu (II) or Zn (II) ion. Thus, no complex formed in the solution mixture of Tartrazine and Ti (IV), Cr (III), Mn (II), Co (II), Fe (II), Fe (III), Ni (II), Cu (II) or Zn (II) ion in all buffer systems used.

3.7.10 The mixtures of Green S and Ti (IV), Cr (III), Mn (II), Co (II), Fe (II), Fe (III), Ni (II), Cu (II) or Zn (II)

The absorption spectra of the mixtures of Green S and each metal ion in the buffer system such as phosphoric acid, acetic acid, McIlvaine buffer, phosphate buffer were shown in Figures 40A-40G. The same phenomena as mention in 3.7.9 were observed. Therefore, no complex formed between Green S and Ti (IV), Cr (III), Mn (II), Co (II), Fe (II), Fe (III), Ni (II), Cu (II) or Zn (II) ion in the buffer system mentioned above.

3.8 Stability constants of the complexes between the dye and Cu (II) ion

The stability constants of the Cu (II) ion-dye complexes under the condition studied as mention in 3.7 were evaluated. The results are shown in Tables 28A-28B. At pH 7.00, 5.85, in the phosphate buffer, the stability constants of the complexes were in the order of tenth and ninth respectively; and that of the acetate buffer pH 6.10, 5.10 were in the order of nineth and seventh, respectively. The stability constants of Cu (II)-Azorubine complex either in the phosphate buffer or the acetate buffer decreased when the pH of the solution decreased. This was due to the increment of the basic strength of Azorubine when the pH of the solu-

tion increased; the stronger complex formed in higher pH. The stability constants of Cu (II)-Sunset Yellow FCF, Cu (II) Orange G and Cu (II)-Orange RN complex at pH 5.10 or 4.00 were not determined since a small quantity of the complex formed. However, the stability constants of Cu (II)-Sunset Yellow FCF, Cu (II)-Orange G and Cu (II)-Orange RN complex at pH 6.10 was found in the order of seventh.

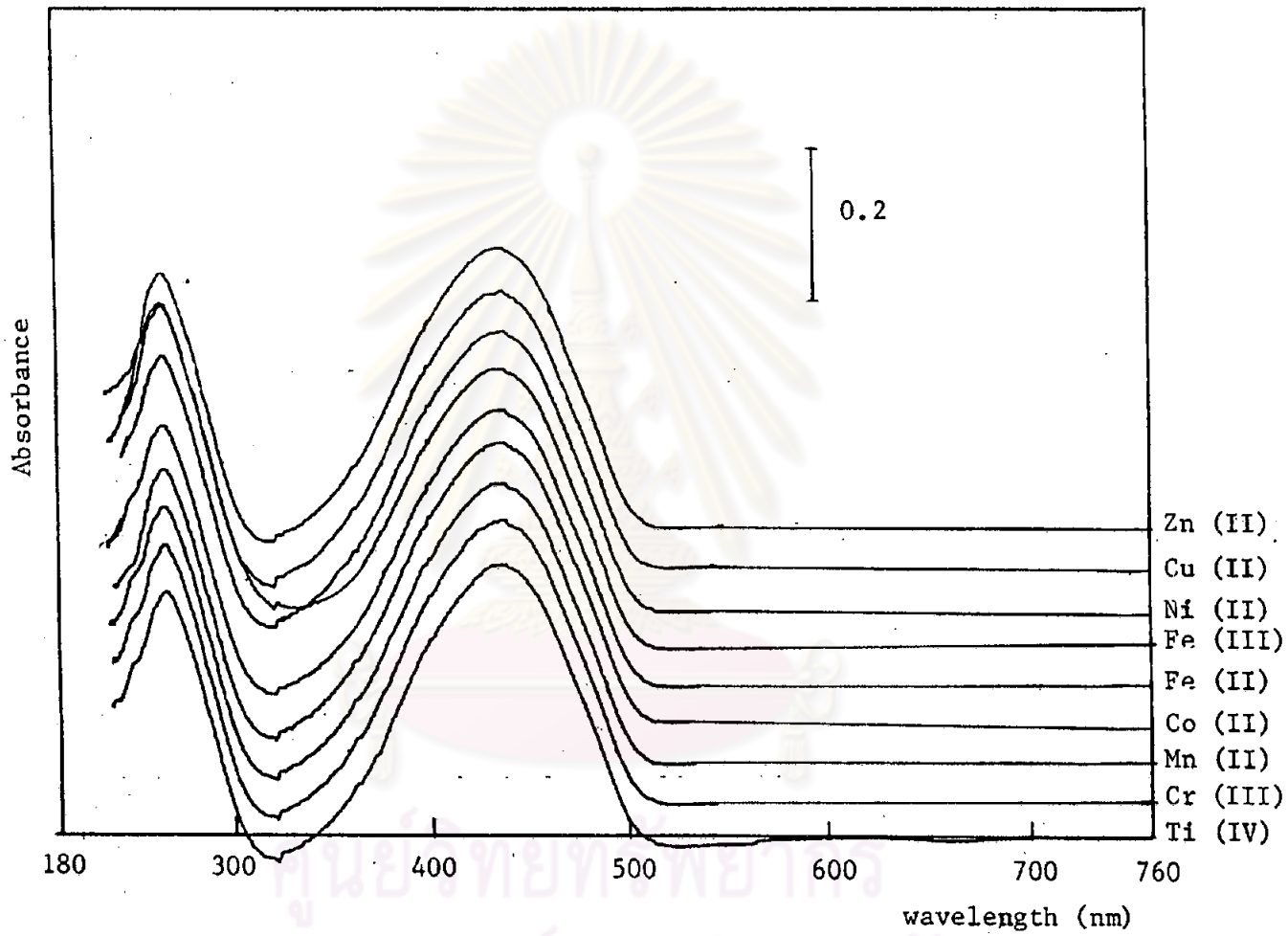

Figure 39A The UV-Visible absorption spectra of the mixture of Tartrazine and metal ions in the acetic acid pH 2.30.

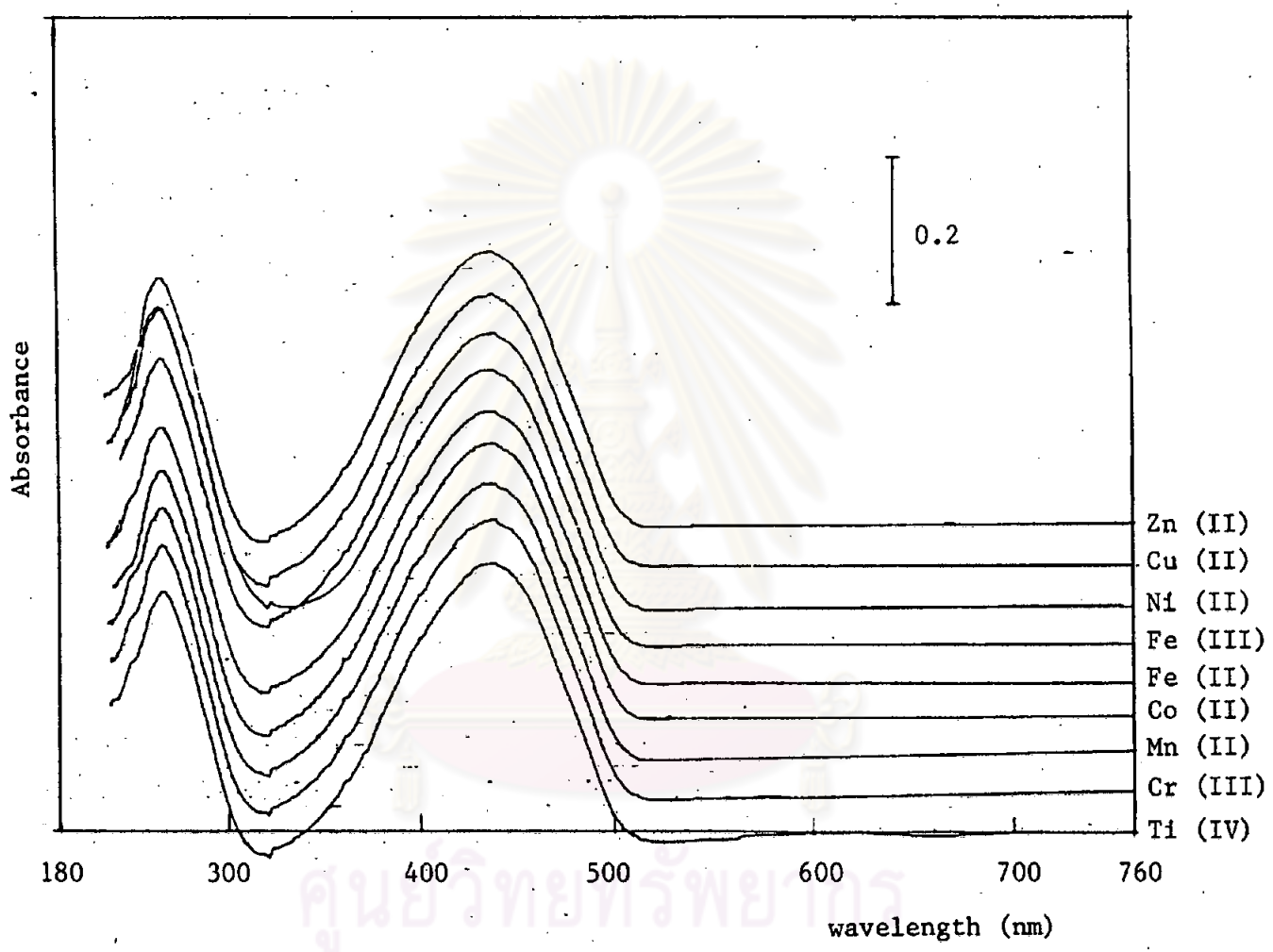

Figure 39B The UV-Visible absorption spectra of the mixture of Tartrazine and metal ions in the phosphoric acid at pH 1.00.

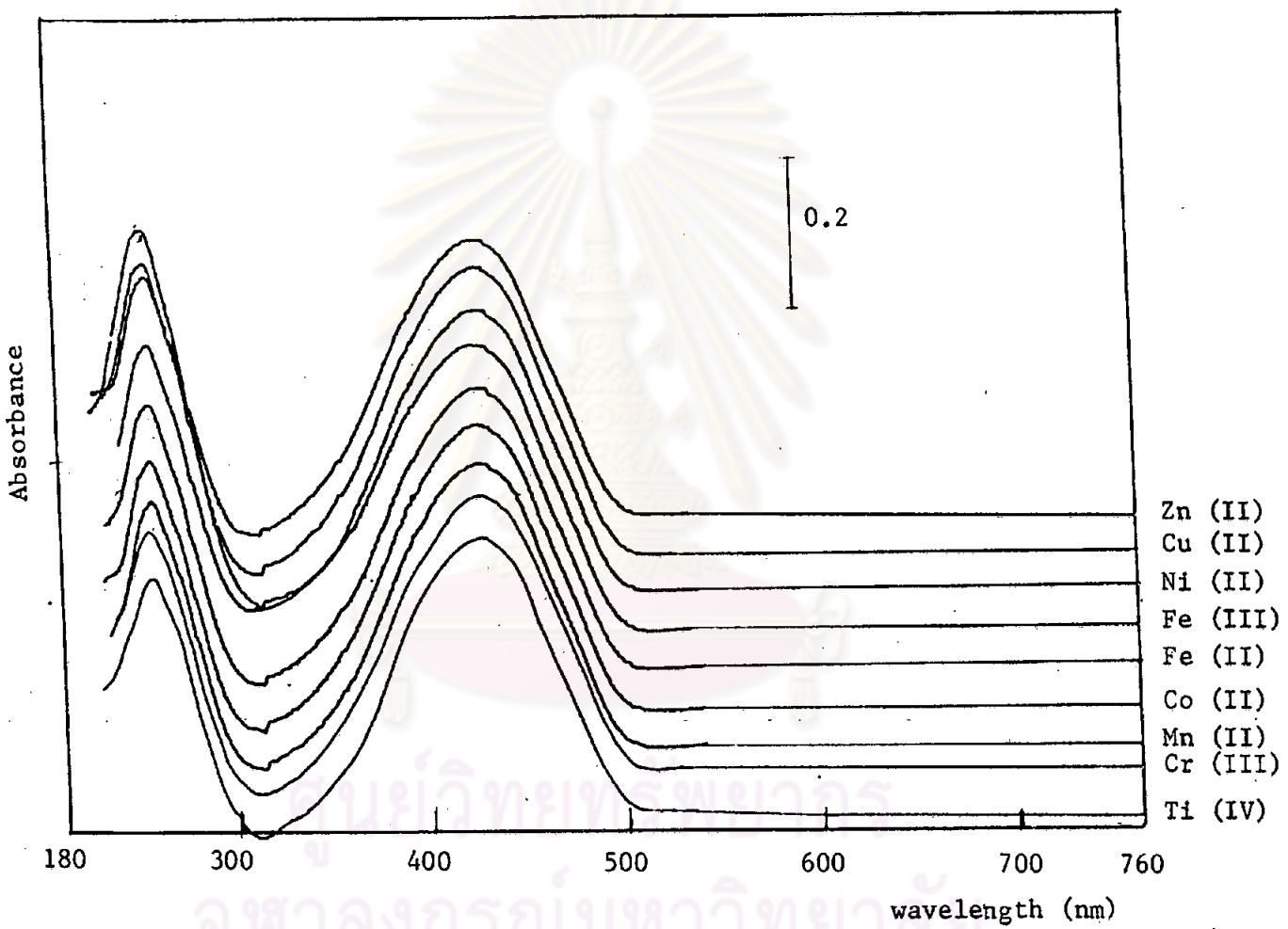

Figure 39C The UV-Visible absorption spectra of the mixture of Tartrazine and metal ions in the McIlvaine buffer at pH 3.10.

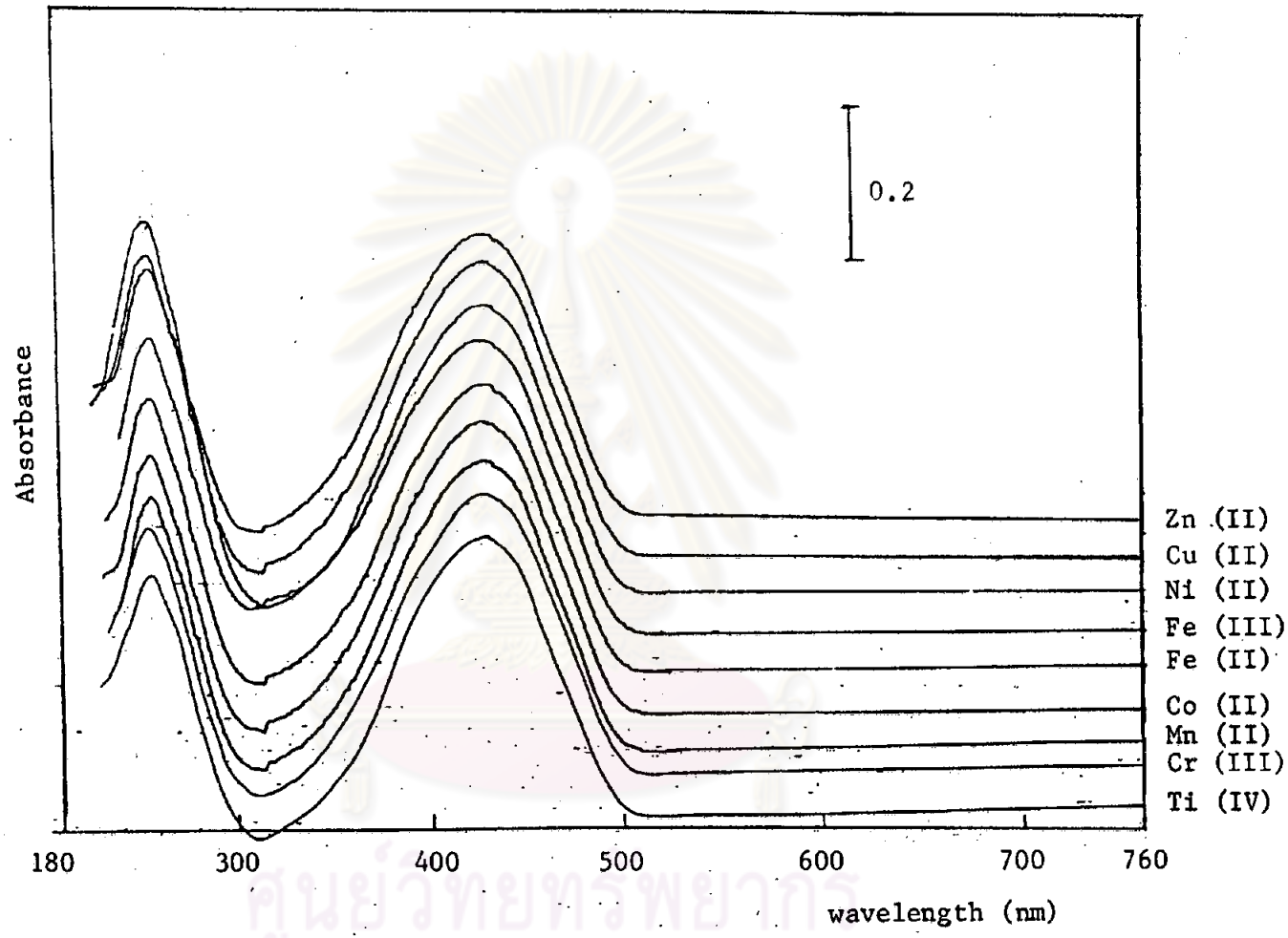

Figure 39D The UV-Visible absorption spectra of the mixture of Tartrazine and metal ions in the McIlvaine buffer pH 5.15.

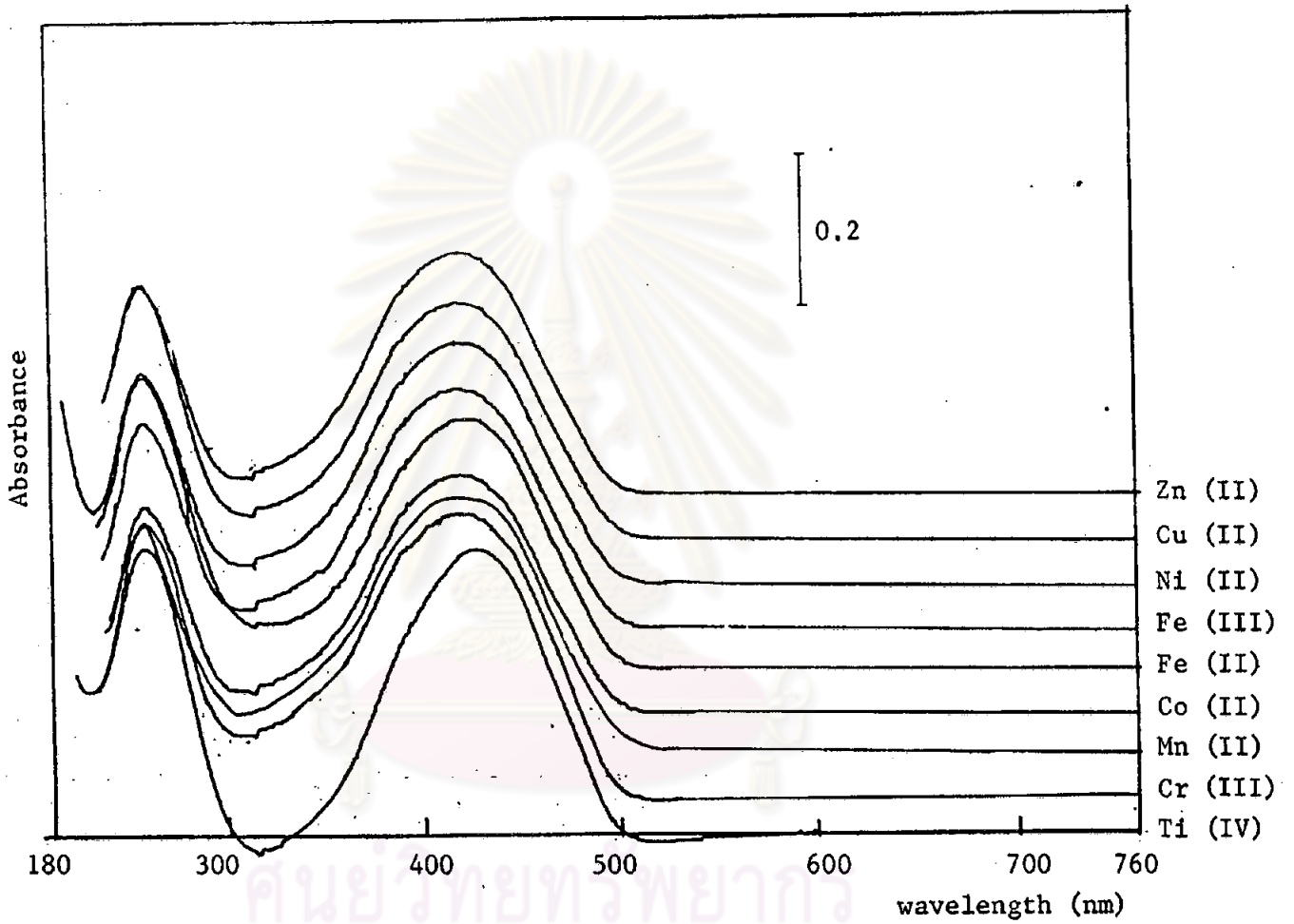

Figure 39E The UV-Visible absorption spectra of the mixture of Tartrazine and metal ions in the McIlvaine buffer at pH 7.40.

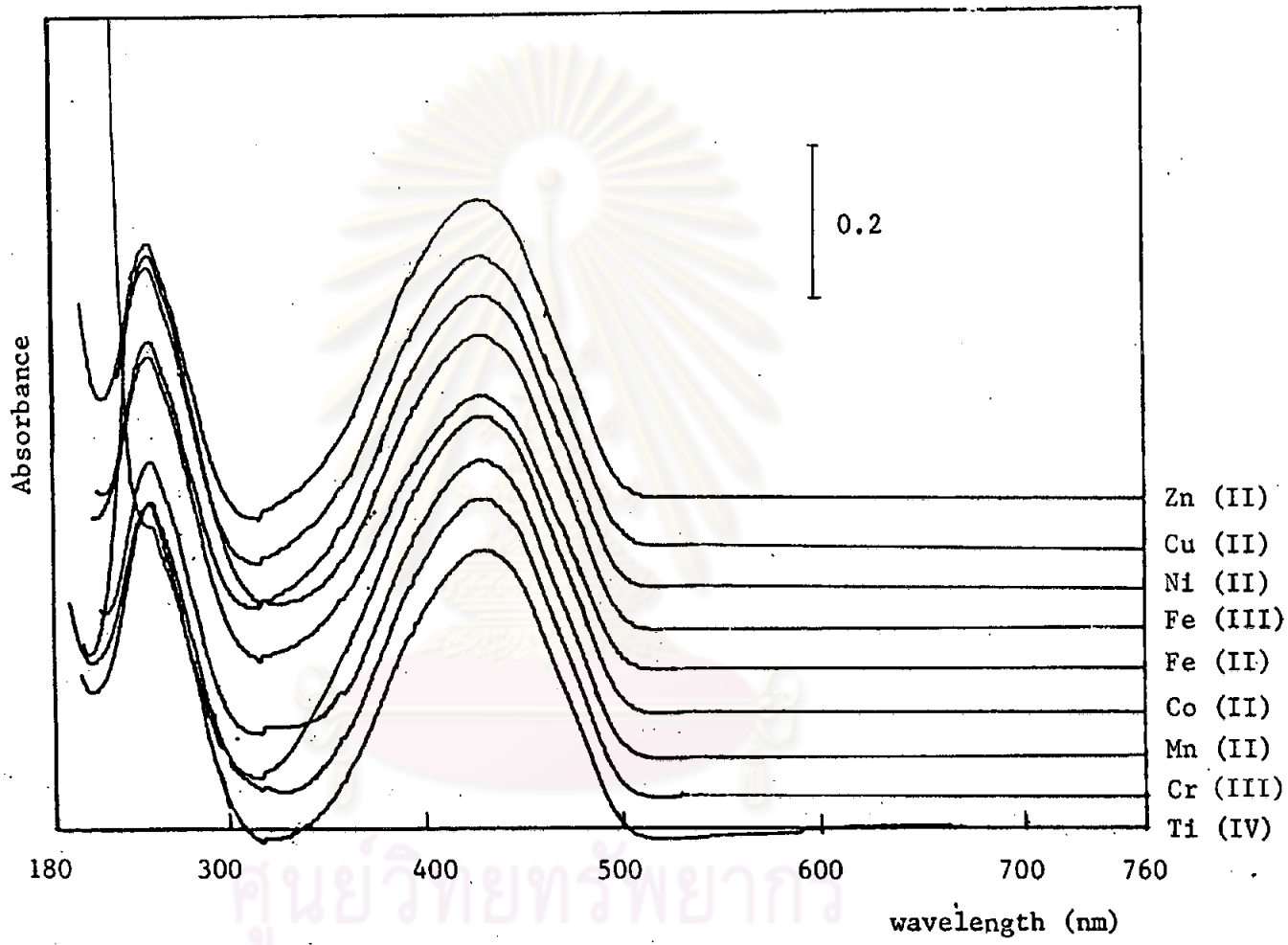

Figure 39F The UV-Visible absorption spectra of the mixture of Tartrazine and metal ions in the phosphate buffer at pH 5.85.

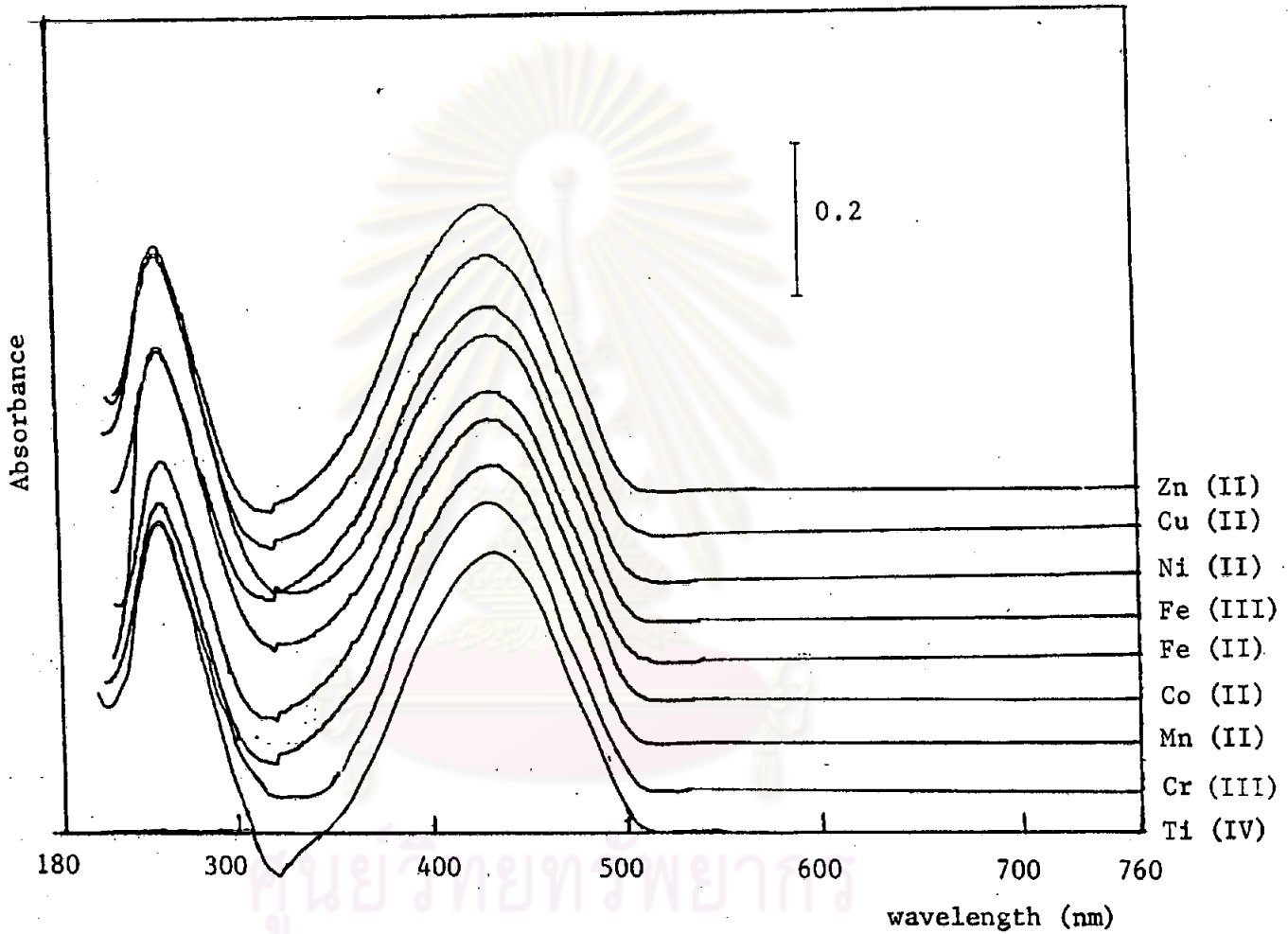

Figure 39G The UV-Visible absorption spectra of the mixture of Tartrazine and metal ions in the phosphate buffer at pH 7.00.

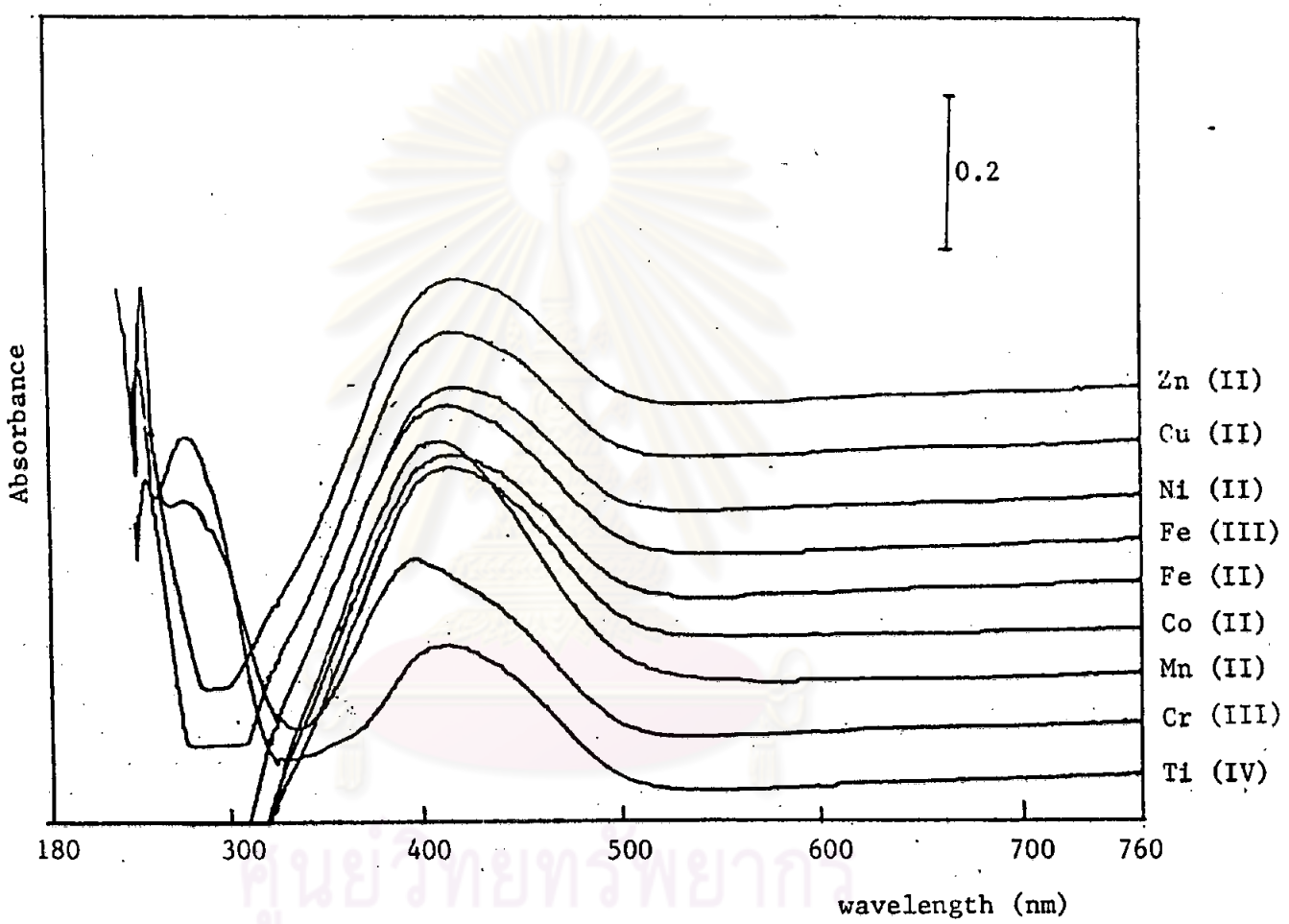

Figure 39H The UV-Visible absorption spectra of the mixture of Tartrazine and metal ions in diethylamine pH 12.50.

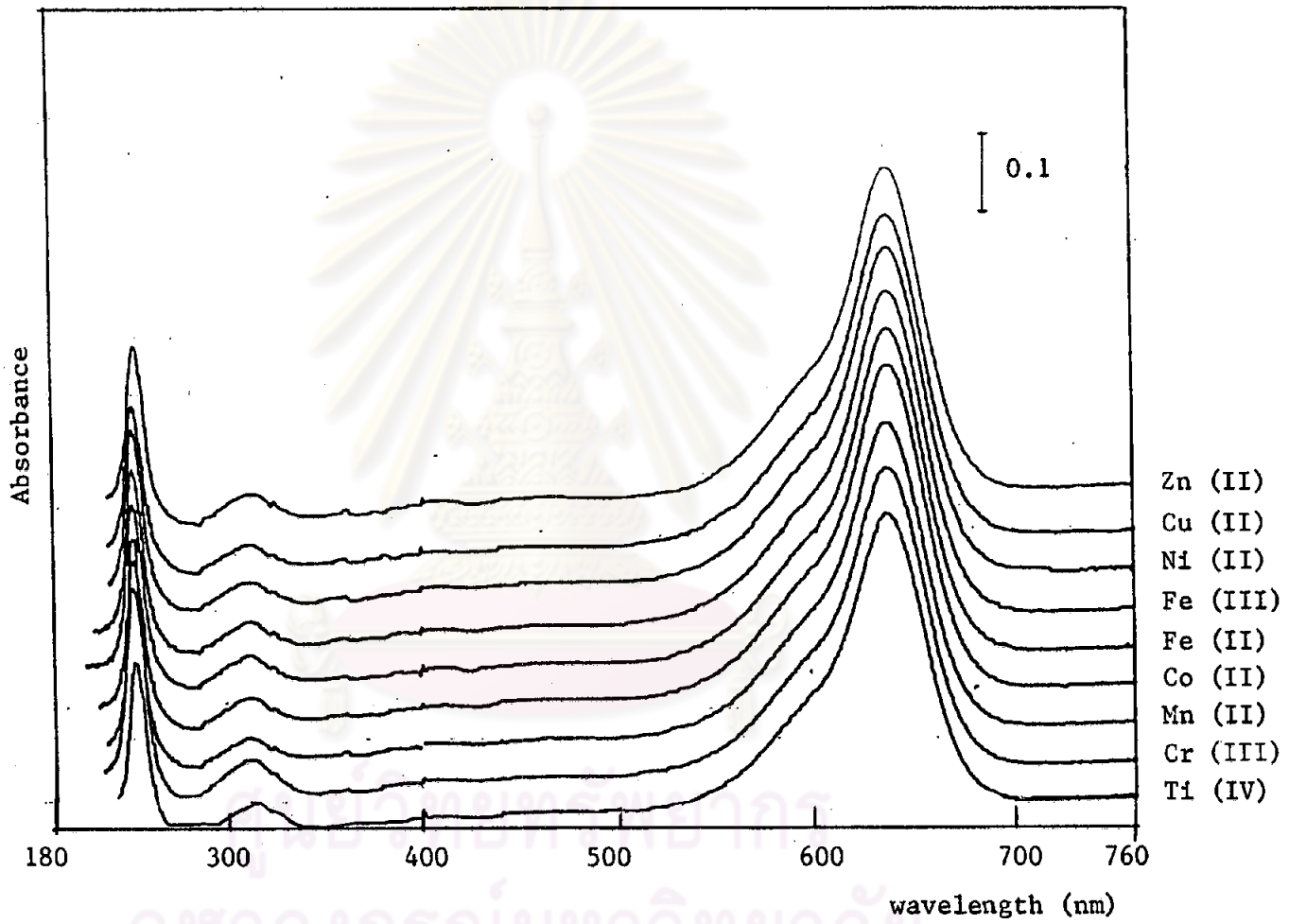

Figure 40A The UV-Visible absorption spectra of the mixture of Green S and metal ions in acetic acid pH 2.30.

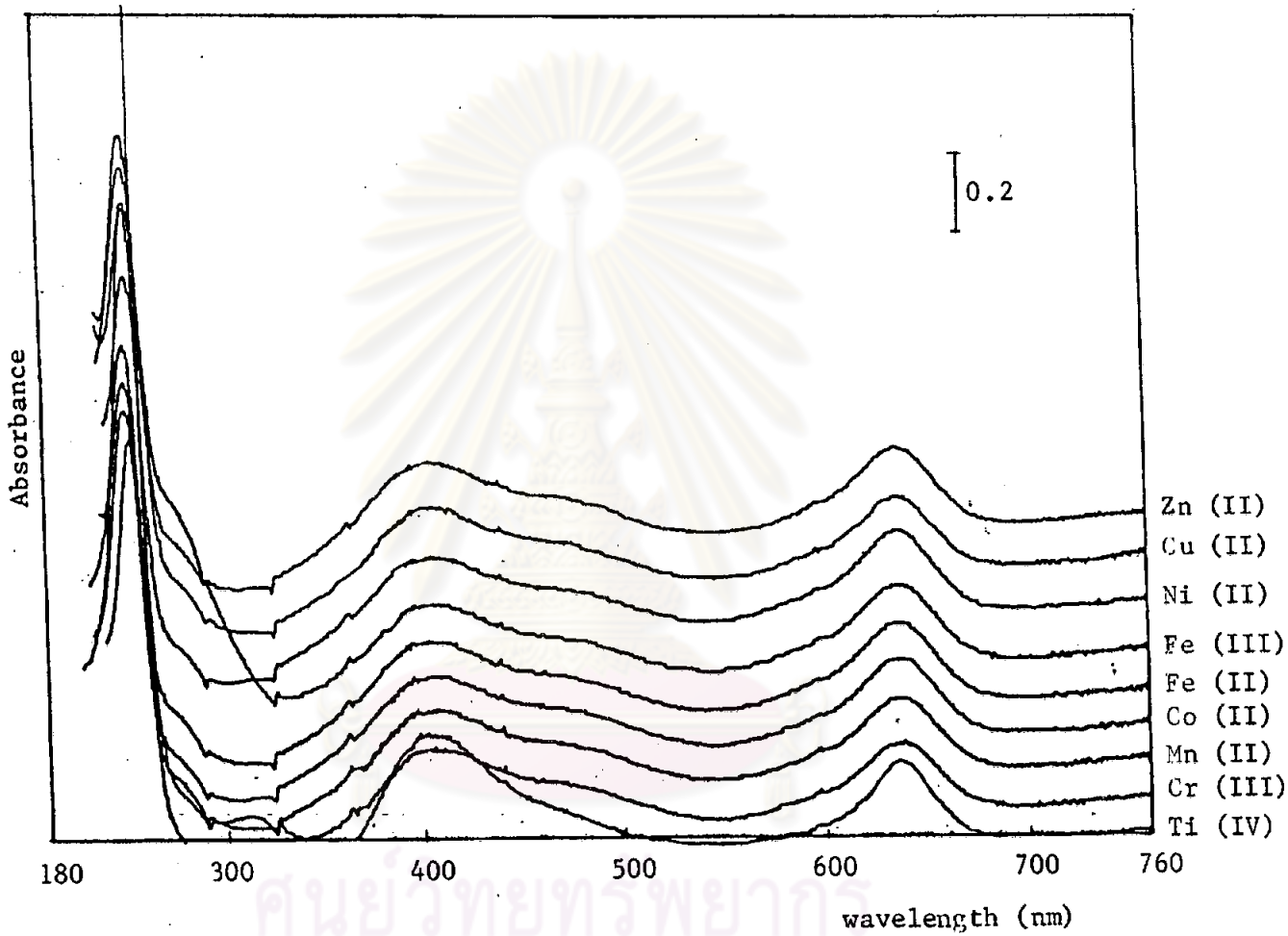

Figure 40B The UV-Visible absorption spectra of the mixture of Green S and metal ions in phosphoric acid pH 1.00.

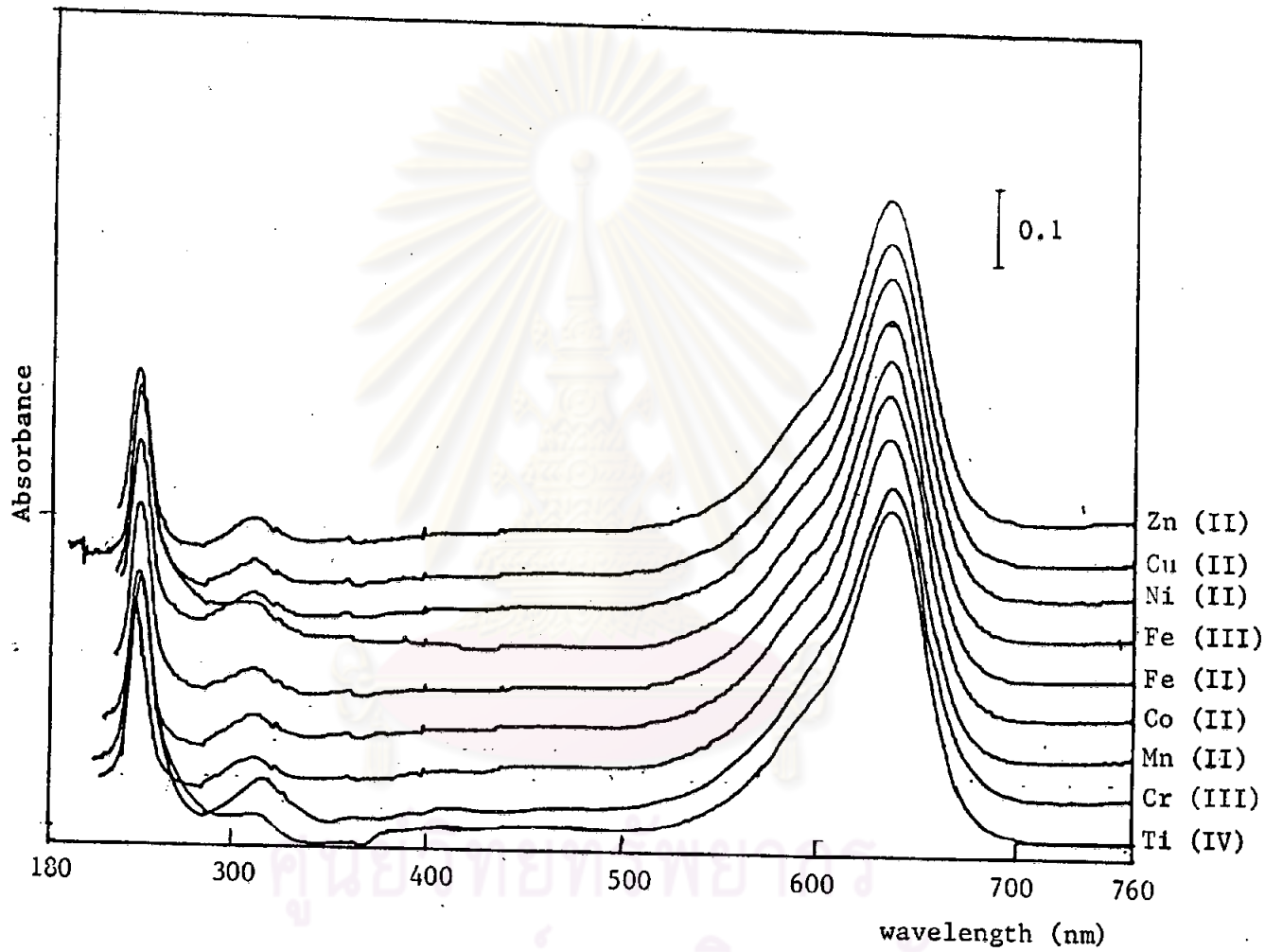

Figure 40C The UV-Visible absorption spectra of the mixture of Green S and metal ions in the McIlvaine buffer at pH 3.10.

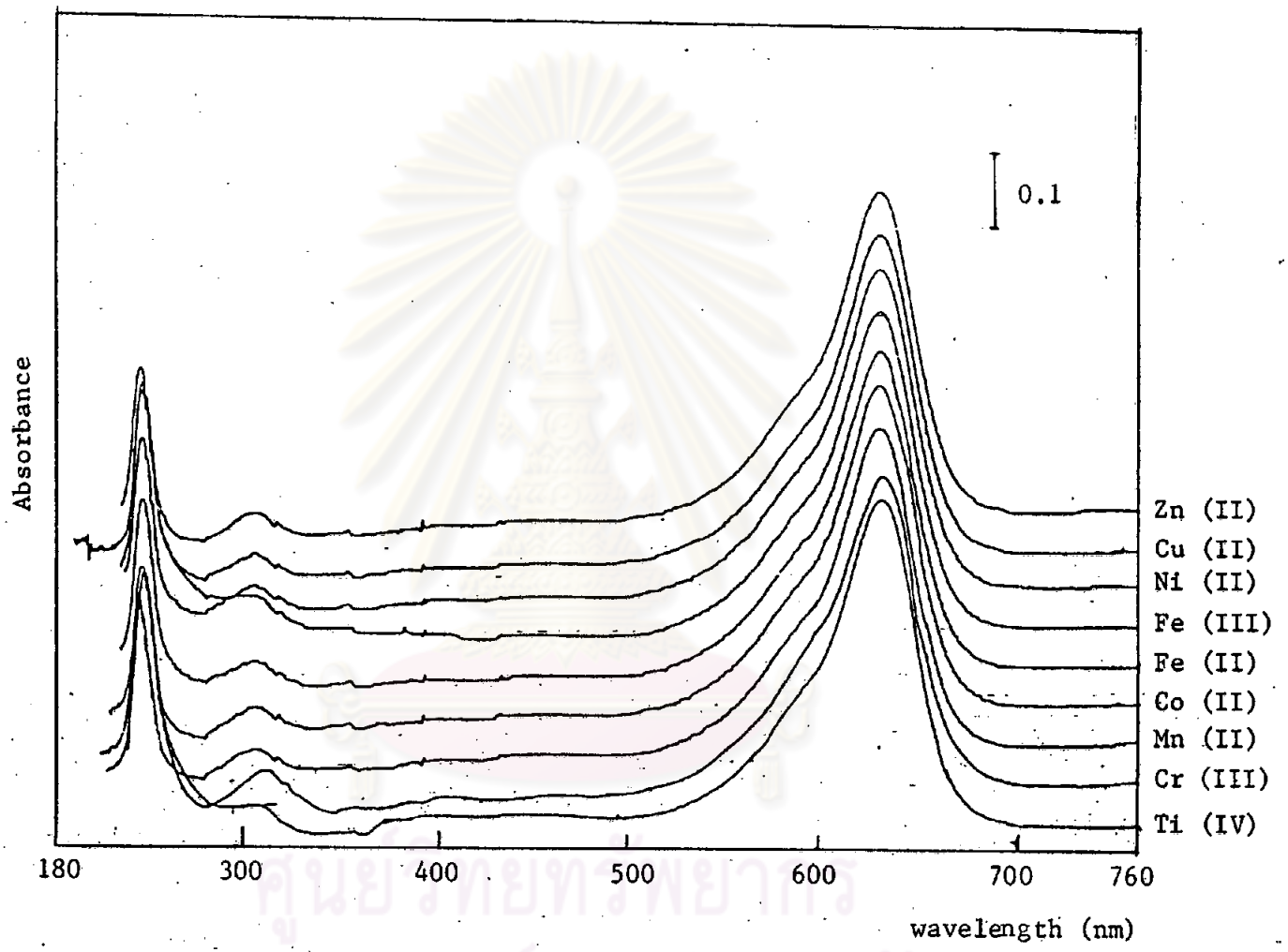

Figure 40D The UV-Visible absorption spectra of the mixture of Green S and metal ions in the McIlvaine buffer pH 5.15.

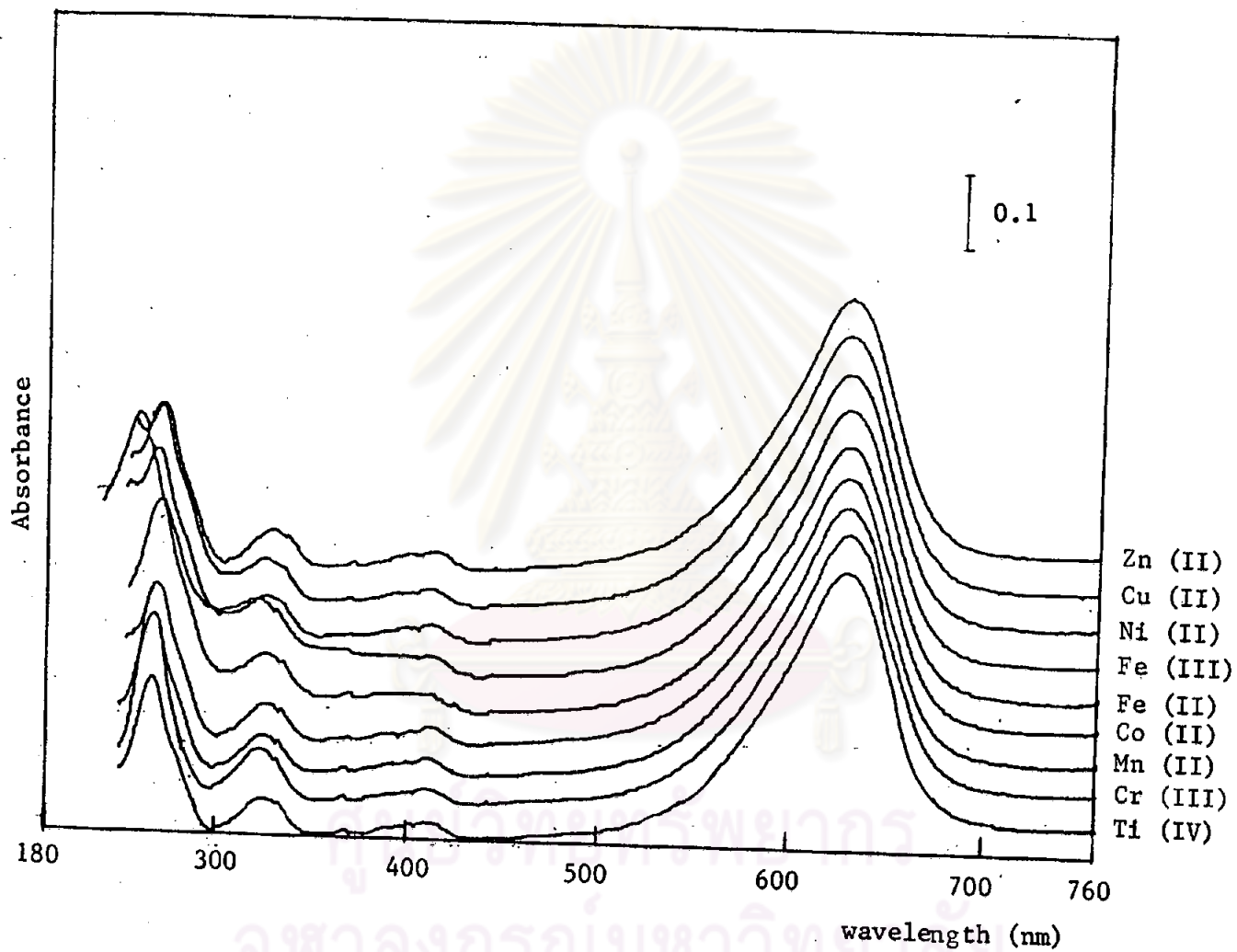

Figure 40E The UV-Visible absorption spectra of the mixture of Green S and metal ions in the Mellvaine buffer at pH 7.40.

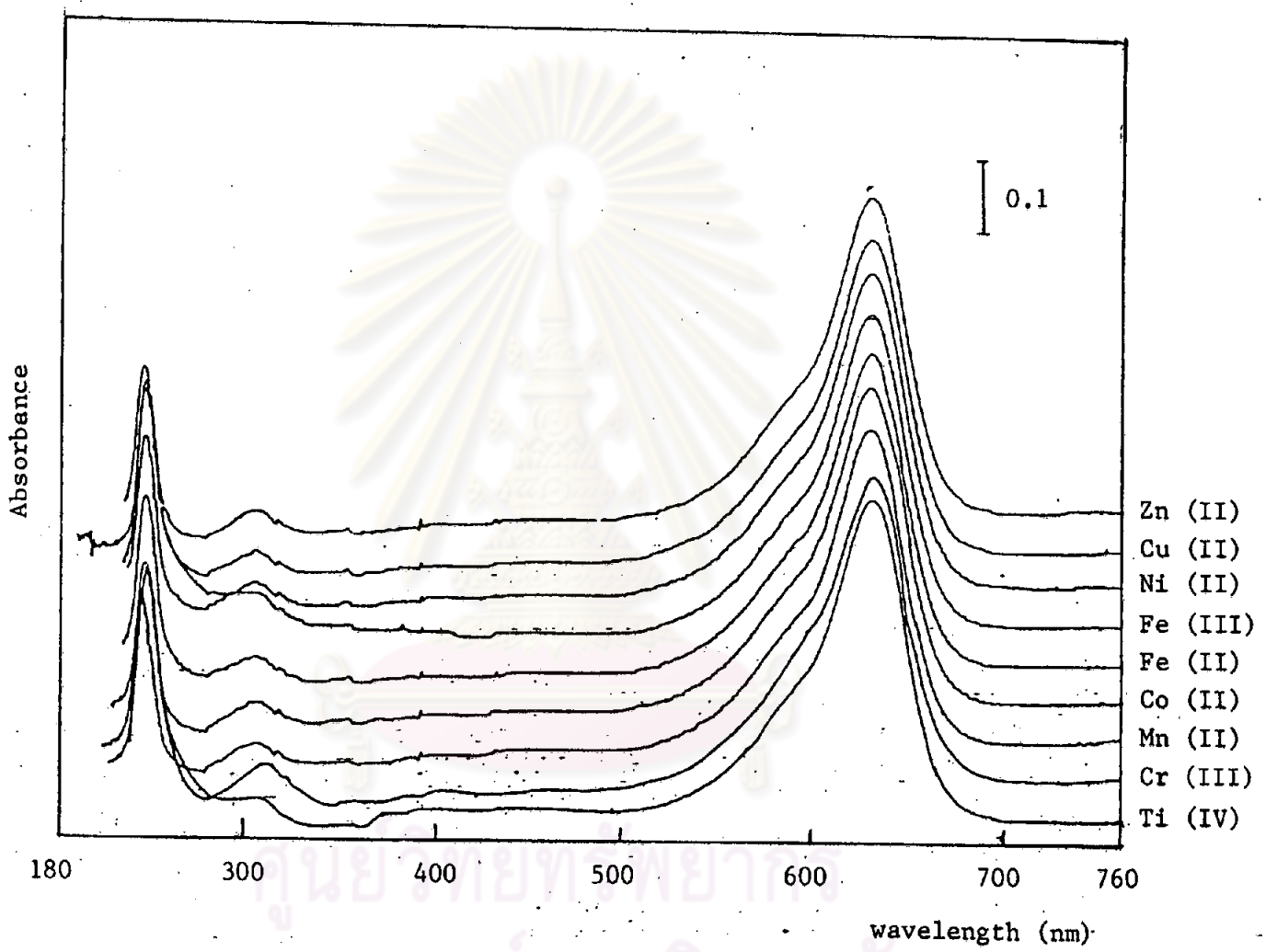

Figure 40F The UV-Visible absorption spectra of the mixture of Green S and metal ions in the phosphate buffer at pH 5.85.

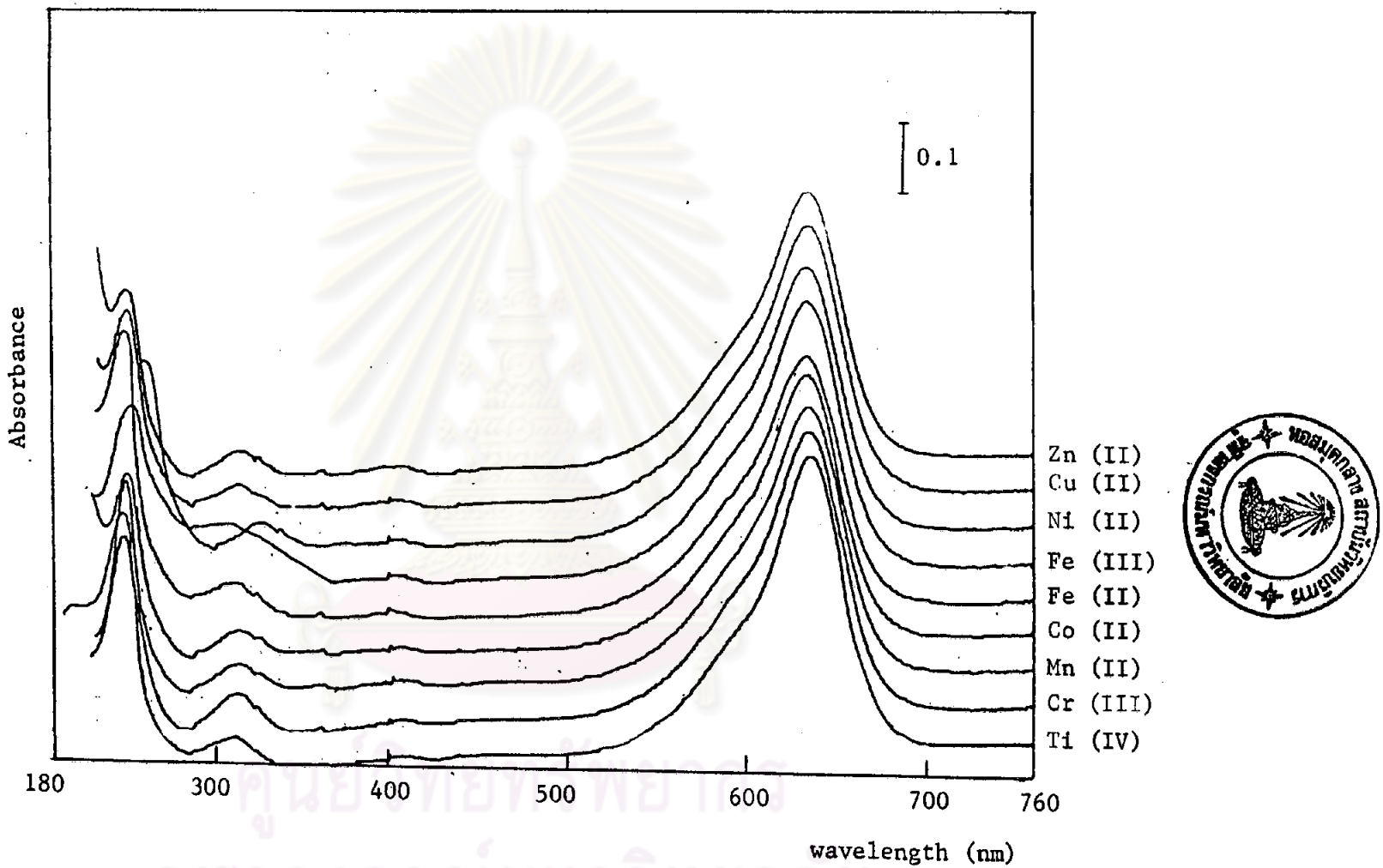

Figure 40G The UV-Visible absorption spectra of the mixture of Green S and metal ions in the phosphate buffer at pH 7.00.

Table 28A Stability constants of Cu (II) Azorubine in various buffers.

pH and buffer used	Stability constant	
	Continuous variation method	molar ratio method
7.00; phosphate	1.1×10^{10}	1.5×10^{10}
5.85; phosphate	6.1×10^{9}	9.7×10^{9}
6.10; acetate	4.8×10^{9}	6.9×10^{9}
5.10; acetate	1.2×10^{7}	1.2×10^{7}

Table 28B Stability constant of Cu (II)-dye in the acetate buffer at pH 6.10 by the molar ratio method.

Cu (II)-dye	Stability constant
Cu (II)-Sunset Yellow FCF	1.92×10^7
Cu (II)-Orange G	1.62×10^7
Cu (II)-Orange RN	1.05×10^7